ASRITE

Annual Symposium on Research and Industrial Training
of Department of Electronics

Proceedings of
8th Annual Symposium on Research and Industrial Training
of
Department of Electronics

24th & 25th, Sep 2021

Department of Electronics

Faculty of Applied Sciences

Wayamba University of Sri Lanka

Kuliyapitiya, 60200

Sri Lanka.

ASRITE

Annual Symposium on Research and Industrial Training of Department of Electronics

Proceedings of

8th Annual Symposium on Research and Industrial Training

of

Department of Electronics

24th and 25th September 2021

Department of Electronics

Faculty of Applied Sciences

Wayamba University of Sri Lanka

Kuliyapitiya, 60200

Sri Lanka

ISSN 2362 0560

Designing and Printing at department of Electronics,
Faculty of Applied Sciences, Wayamba University of Sri Lanka, Kuliyapitiya

Forward

It is with great pleasure, I send this message on the occasion of the 8th Annual Symposium on Research and Industrial Training of the Department of Electronics (ASRITE) 2021 at the Faculty of Applied Sciences, Wayamba University of Sri Lanka. Indeed, this is a very special occasion, as we are hosting ASRITE 2021 as an online conference for the first time.

The COVID-19 pandemic has changed the nature of the human activity, revealing gaps in human knowledge, systems, processes, and technologies. The new circumstance emphasizes the necessity of new knowledge creation and distribution. In this context, Information and Knowledge Dissemination becomes extremely important. I firmly believe that the ASRITE 2021 would provide a fruitful platform for undergraduates of the Department of Electronics to share their research findings gained during their final year research and six-month Industrial Training, where they produce optimal solutions for practical research problems in their training industries.

The symposium represents the effort of many people, and I would like to express my gratitude to Prof. Jagath C. Edirisinghe, the Acting Vice-Chancellor of the Wayamba University of Sri Lanka, and Prof. L.D.R.D Perera, Dean of the Faculty of Applied Sciences for their guidance and support. Moreover, I should thank Ms. U.A.D.N Anuradha, Coordinator of ASRITE-2021, Snr. Prof. K.P Vidanapathirana, Research Coordinator, and Dr. P.M. Senadeera, Industrial Training Coordinator of the Department for their hard work. I also would like to express my gratitude to all the academic staff members of the Department for supervision and revising papers for the proceeding.

Finally, I wish all participants and panelists to have a pleasant and productive experience in attending the online ASRITE 2021.

Dr. M.A.A. Karunarathna
Head - Department of Electronics

CONTENTS

Individual Research Papers

Proc. Annual Symposium on Research & Industrial Training, 08(2021) 1-8
Department of Electronics – Wayamba University of Sri Lanka

POINT-OF-CARE DEVICE FOR DIAGNOSIS OF BLADDER AND PROSTATE CANCERS

S.R.L. Gunawardhana*, W.A.S. Wijesinghe

Department of Electronics, Wayamba University of Sri Lanka, Kuliyapitiya, Sri Lanka

*lakshara94@gmail.com

ABSTRACT

Human cells normally expand and multiply to generate new cells as needed by the body. Cancer is a type of disease in which some cells in the body grow out of control and spread to other parts of the body. Bladder and Prostate cancers are among the top most common cancers over different forms of cancers. These cancers could be cured if they can be detected in the early stage. More importantly, the early cancer identification considerably improves the possibilities of successful treatment. However, people have a lack of awareness on the signs and symptoms of cancers in the early stage. Further, the diagnosis path is long, time consuming, expensive and not straightforward. This paper describes development of a fast, accurate, simple, disposable, non-invasive, sensitive and user friendly self-diagnostic tool. The proposed Point-Of-Care (POC) cancer detection device measures the luminous intensity and processes the data to diagnose the state of the bladder and prostate cancers. This sensing platform detects the state of the cancer through extracted data from the sample and the test results are conveyed to the user via a mobile application. The functionality and the accuracy of the device have been validated by using synthetic samples. Use of the proposed device will be helpful to increase the patient survival rate.

Keywords: Early cancer diagnosis, Point-of-care testing, Rapid testing

1.0 INTRODUCTION

Human cells normally expand and multiply (via a process known as cell division) to generate new cells as needed by the body. Cells die as they become old or injured, and new cells replace them. Cancer is a type of disease in which some cells in the body grow out of control and spread to other parts of the body. Cancer can begin practically anywhere in the trillions of cells that make up the human body. There are over 100 different forms of cancers. Cancers are frequently called after the organs or tissues in which they develop [1]. Bladder cancers and Prostate cancers are in the top most common cancers over different forms of cancers [2]. These cancers could be cured if they can be detected at early stage [3, 4].

Early stage cancer identification considerably improves the possibilities of a successful treatment. Early diagnosis (or down staging) and screening are the two components of cancer early stage detection. Early diagnosis focuses on finding symptomatic patients as soon as possible, whereas screening involves testing healthy people to detect cancers before symptoms arise. Early stage detection programs aim to reduce the number of individuals who are diagnosed late stages in their condition.

According to studies, for the detection of a cancer, the patients should undergo with a procedure called a transrectal biopsy. These biopsies have some risk and it is very uncomfortable for the patient. Magnetic Resonance Imaging (MRI) scans can also use for

the diagnosis. Since this MRI is not designed for this specific task, it can miss cancerous tumors and these tests cost much higher and limited in availability [5].

Patients rarely take the services available to them due to the high cost, time commitment, and invasive nature of many of the present methods [6]. The common drawbacks for the existing diagnosis methods are; high cost, path for the detection is not straight forward, takes long time period to proceed, have to do several tests for single result, accuracy of the results is less, False positive/negative results may occur [7].

Considering previous studies, Bryony Hayes and team developed a POC diagnostic technology but it was not portable and this was a microscopy-based approach, hence it is complex into some extend to do the test [8]. Keren Haney and team also developed a method for this case but they used complex ultra-sound method for the diagnosis [9].
The main objective of this work is to develop a fast, accurate, simple, disposable, noninvasive, sensitive and user friendly, self-diagnostic tool for more frequent monitoring of the bladder and prostate cancer and hence diagnose at a very early stage to increase the patient survival rate.

This study is mainly focused on designing of a diagnosis equipment to achieve the above-mentioned objectives. The introduction part of this paper gives a summary of the literature survey done on cancers, cancer diagnosis and the drawbacks in the existing diagnosis methods. To overcome those drawbacks, a new testing kit with effective diagnosis method is proposed here. The hardware architecture and the detection tools introduced for this study and the detection criteria is discussed in the materials and methods. The achieved results are discussed in the later part of this paper. The summery with the further improvements and developments for this study is discussed in the conclusion.

2.0 MATERIALS AND METHODS

Point-of-care (POC) devices were created to allow to conduct medical tests at or near the point of service. The field of POC diagnostics entices with the prospect of providing rapid diagnostic results outside the laboratory. To facilitate remote monitoring of patients' health, easy-to-use, network-connected diagnostic tools for self-testing are required. This system was designed to satisfy and overcome all those facts. The POC device discussed here can be used at home by the patient/user themselves or the test could be performed at a testing lab by a known medical professional. This POC testing allows for faster clinical decision-making in the areas of diagnosis, treatment selection, prognosis and monitoring as well as operational decision-making and resource usage.

The testing kit mainly consists of three (03) components; testing strip, testing equipment and the mobile application “DetectC”. Testing strip basically gives a unique colour about the state of the cancer according to the sample. Testing equipment is developed to detect the unique color of the strip, do the necessary processing and upload the processed data to the real-time database. The mobile application “DetectC” take those uploaded data from the database and analyze them with pre-defined constraints and output the result to the user.
The testing strip used for this diagnosis is designed to detect the above-mentioned types of cancers with a sample of a urine drop. This strip is based on the nanotechnology enhanced bioluminescent based lateral flow assay which further combined with data science for customer centered noninvasive Bladder Cancers (BC) and Prostate Cancers

(PC) assay. This assay is basically containing bioluminescent which uses the properties of dyes and Nano carbon material. Once the sample is added, the strip gets a unique colour. The luminescent intensity varies with the stage of the cancer and that can be used for further decisions [10].

2.1 Hardware Architecture

The eyes and brains of humans' work together to convert light into colour. The signal is transmitted to the brain via light receptors in our eyes. The colour is then recognized by our brain. As the brain in human body, the detection equipment in this project is acting like the brain of the system.

Colour information plays an important role in this detection path. In this pitch real-time colour image segmentation is introduced, which is based on colour similarity in RGB colour space.

The detection equipment is used to capture the luminescent intensity of the strip. When the sample is added to the strip, it gets a unique colour. When the strip is placed in the identification bay in the detection equipment, it captures the colour of the strip and analyze it according to the colour map. The dominant colour is chosen first, based on colour and intensity information in RGB colour space, and then the RGB values were calculated according to the colour-class map. Apart from that the detection equipment will communicate with an online real-time database. The calculated RGB values are uploaded to the real-time database along with the captured sample. Then it can be used by the mobile application.

The following figure 2.1 shows the block diagram of the equipment that is designed to detect the colour of the strip described above.

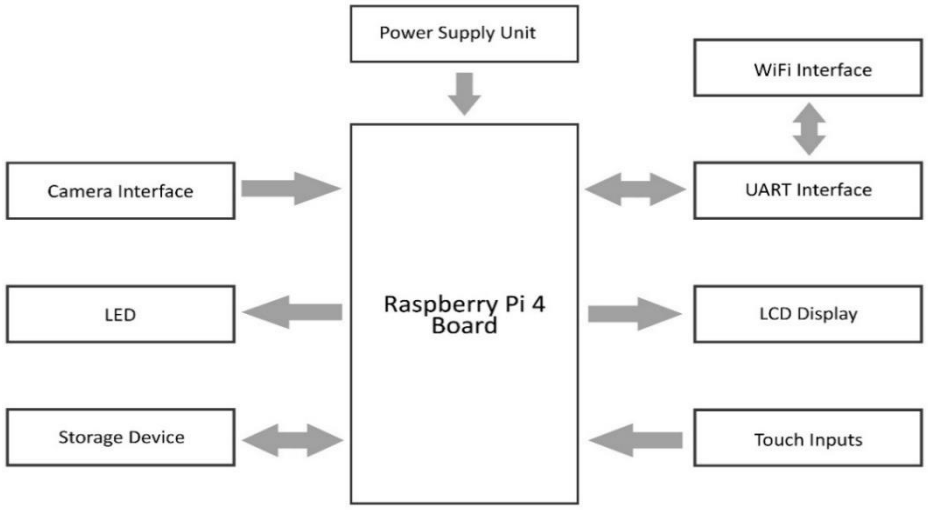

Figure 2.1: Block diagram of the proposed detection equipment

The equipment design is based on the main board of Raspberry Pi 4. For the identification of the colours, a camera module is used and a LED is used as the illumination source of the identification bay. This device is designed with a touch screen LCD display for the user-friendliness. The communication between the real time database and the mobile application is established through the Wi-Fi module.

2.2 Mobile application

The diagnosis kit is designed with a user friendly mobile application named as "DetectC". The detection procedure goes through this mobile application that provides graphical and touch-sensitive interfaces through the mobile device, such as a smartphone or tablet that allows the user to interact with the features, content, and functionalities of the detection path.

This mobile application is originally designed specifically for this detection device; hence it can be also customized and optimize accordingly. This application contains five (05) user interfaces. They are;

1. Loading interface
2. Main interface
3. Analysis interface
4. Constraint assigning interface
5. Test result interface

The following figure 2.2 shows the block diagram of the designed mobile application "DetectC";

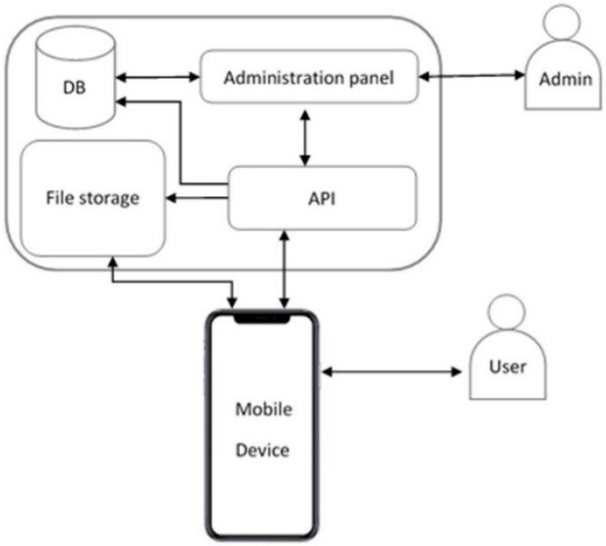

Figure 2.2: Block diagram of the designed mobile application "DetectC"

2.4 Detection criteria

The detection criteria is based on several steps. The sample collection should be done in a medically accepted manner. It should follow medical standards [11]. Those steps are performed by two ends; by the equipment end and by the mobile application end. The whole detection path steps can be listed as follows;

- By the equipment
  - Image capturing
  - Process the captured image
  - Colour detection
  - Uploading the detected constraints to real-time database
- By the mobile app
  - Downloading sample image and constraints from real-time database
  - Analyzing those constraints from the app
  - Decision making using analyzed values

- Presenting final results to the user
-

The detection part performed by the equipment can be fetch into the following figure 2.3;

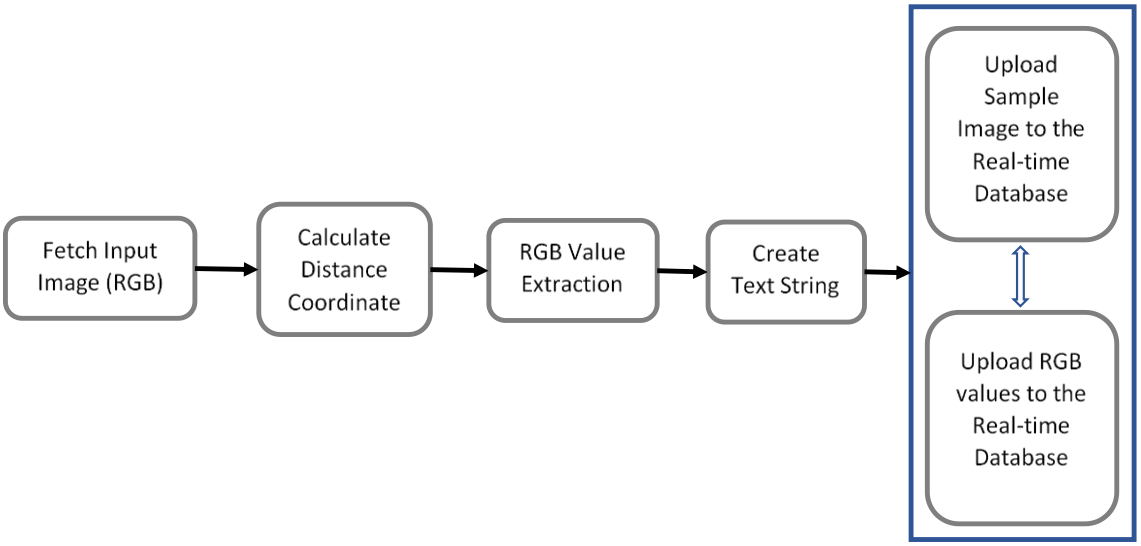

Figure 2.3: Performance path of the equipment

As shown in the figure 2.3, the captured image in the local storage would load to the algorithm in the equipment. The then the parameters from the fetched image will map with the colour map and then the RGB value string is created. Finally, the string is uploaded to the real-time database with the sample image.
The detection part performed by the mobile application can be fetch into the following figure 2.4;

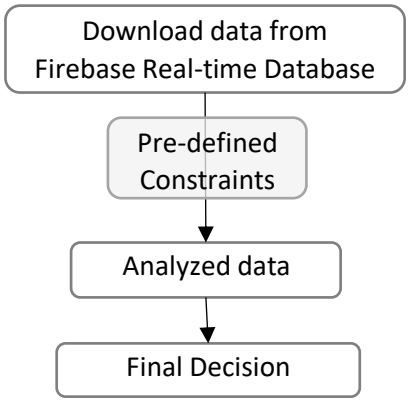

Figure 2.4: Performance path of the mobile application

Final result should follow certain standards to ensure the correct decision is conveyed to the patient. The detection procedure also should undergo with certain set of guidelines [12]. As above figure 2.4 shows, the data in the real-time database are downloaded to the mobile application. That data will be analyzed by the mobile application using pre-defined constraints. After the data are analyzed, the final decision will be displayed with an image of the sample.

3.0 RESULTS AND DISCUSSION

The designed equipment was tested with many synthetic samples. Synthetic samples were used to test the reader because there were certain limitations in collecting actual samples due to the Covid-19 pandemic. Those synthetic samples were created by printing various colour strips with known RGB values. According to the trials performed, the synthetic samples were tested and the observed results can be compared in terms of primary colours as shown below in figure 3.1 (Red), figure 3.2 (Green) and figure 3.3 (Blue).

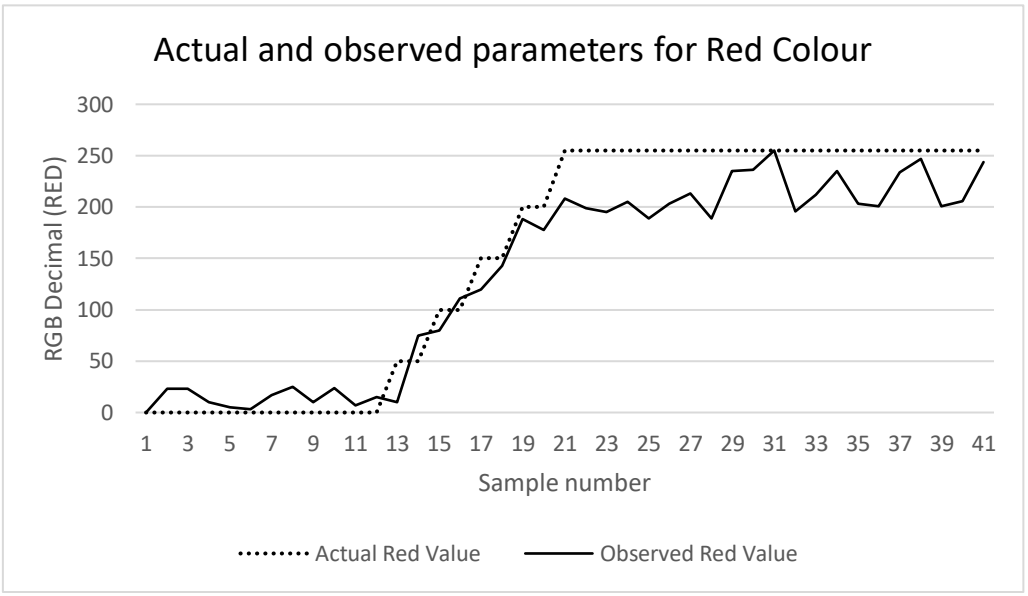

Figure 3.1: Graph of actual and observed parameters for Red Colour

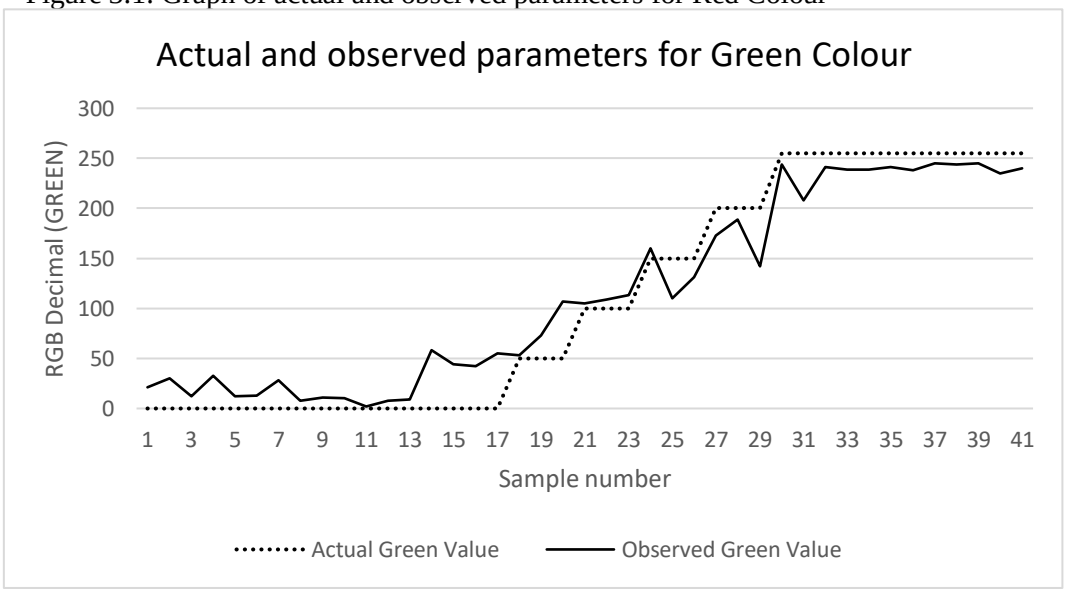

Figure 3.2: Graph of actual and observed parameters for Green Colour

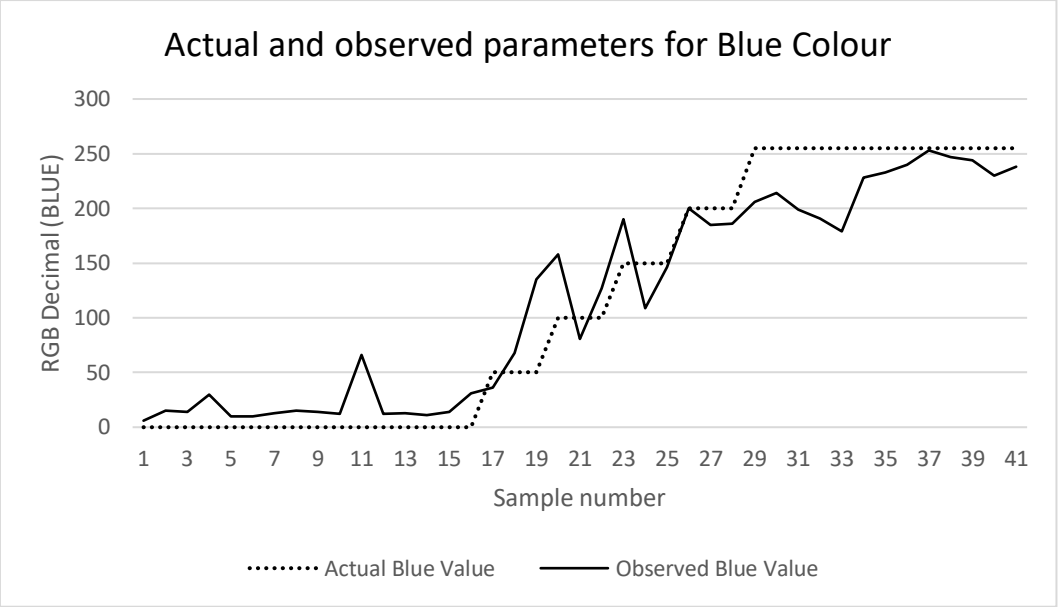

Figure 3.3: Graph of actual and observed parameters for Blue Colour

As stated under detection criteria, by comparing and analyzing the observed RGB values of the sample with the database, the state of the cancer could have been determined through the pre-defined constraints. However, due to the limitation in collecting actual sample, the calibration process was not completed. The system functions have been developed so that the administrator can use real sample data and calibrate it easily. Once calibrated, the system will produce outputs for new samples so that the user can easily recognize the results.

The POC device discussed here can be used at home by the patient/user themselves or the test could be performed at a testing lab by a known medical professional. This POC testing allows for faster clinical decision-making in the areas of diagnosis, treatment selection, prognosis and monitoring as well as operational decision-making and resource usage. According to the results obtained, the detection can be performed by this device in high accuracy as shown in figures 3.1, 3.2 and 3.3. There were some deviations observed in the results with respect to the actual values. That deviations would occur due to; poor picture quality of the camera and quality of the lighting source. To overcome these issues a high-quality camera with adaptive light can be used. By the usage of such a camera with adaptive light, a higher quality picture of the sample can be taken and that will help in recognizing the true colour. To enhance the accuracy of this device furthermore, a development of a large data pool is necessary. By this data pool, the accuracy of the pre-defined constraints can be increased.

For the detection of cancers efficiently this rapid, low-cost, sensitive and reliable self-diagnostic point-of-care cancer detection device has been developed as mentioned above. This was carried out using the latest nanofabrication and microfabrication-based technologies combined with various sensors and platforms. This diagnosis kit can be used to diagnose cancers at a very early stage to increase the patient survival rate.

4.0 CONCLUSION

In the field of cancer diagnosis, POC diagnostic devices are becoming more popular and has increasing demand.
In this paper, we proposed a design of Immunoassay reader for POC diagnosis of bladder and prostate cancers. The design consists of colour recognition mechanism of testing strips and IoT platform. The calibration of the system was unable to verify due to limitations in collecting real samples. However, the system was tested with synthetic strips and the results indicate potential applications in cancer diagnosis. We intend to verify the results with clinical specimens with different case scenarios, which impose design of different constraints on all aspects of the POC diagnostics device.
As further studies, this research can be extended with machine learning technique to detect accurately not only cancers but also any specimen-based tests in medical and chemical fields.

REFERENCES

[1]. Strategic Information Management (SIM) Unit, National Cancer Control Programme, Ministry of Health, *National Cancer Incidence and Mortality Data Sri Lanka 2015*, 17th Publication, National Cancer Control Programme, Ministry of Health, 2021, E-book.
[2]. National Cancer Institute, Epidemiology and End Result Program, Cancer Stat Facts: Prostate Cancer", https://seer.cancer.gov/statfacts/html/prost.html (Accessed 2021.03.21).
[3]. American Cancer Society, about bladder cancer, 2021, https://www.cancer.org/cancer/bladder-cancer/about/what-is-bladder-cancer.html (Accessed 2021.03.21).
[4]. American Cancer Society, about prostate cancer, 2021, https://www.cancer.org/cancer/prostate-cancer/about/what-is-prostate-cancer.html (Accessed 2021.03.21).
[5]. Ian Demsky, Study: New Prostate Cancer Test Could Avoid Unnecessary Biopsies, Health Tech, 2021, https://labblog.uofmhealth.org/health-tech/study-new-prostate-cancer-test-could-avoid-unnecessary-biopsies (Accessed 2021.04.05).
[6]. Lotan Y, Kamat AM, Porter MP, *Key concerns about the current state of bladder cancer: a position paper from the Bladder Cancer Think Tank*, the Bladder Cancer Advocacy Network, and the Society of Urologic Oncology, 2009, E-book.
[7]. Bernd J. Schmitz-Dräger, Michael Droller, Vinata B. Lokeshwar, Yves Fradet, George P. Hemstreet, Per-Uno Malmstrom, Osamu Ogawa, Pierre I. Karakiewicz, Shahrokh F. Shariat, *Molecular Markers for Bladder Cancer Screening, Early Diagnosis, and Surveillance*: The HO/ICUD Consensus, Urologia Internationalis, 2014, https://www.karger.com/Article/FullText/369357 (Accessed 2021.04.07).
[8]. Bryony Hayes, Caroline Murphy and Richard O'Kennedy, *Developments in Point-of-Care Diagnostic Technology for Cancer Detection*, US National Library of Medicine, 2018
[9]. Keren Haney, Pushpa Tandon, Ro Divi, Houston Baker and Paul C.Pearlman, *The Role of Affordable, Point-of-Care Technologies for Cancer Care in Low- and Middle-Income Countries* IEEE Journal of Translational Engineering in Health and Medice, 2017, https://www.ncbi.nlm.nih.gov/pmc/articles/PMC5706528/ (Accessed 2021.04.07).
[10]. U.S. Provisional Patent No. 62/931,944 For: a biosensor and system for detecting an analyte in a bodily fluid sample for at-home point-of-care diagnosis.
[11]. PHSA Laboratories, *CWPC_UDIP_0130 Urine Dipstick Patient Test Procedure*, Version 1.2, 2016, E-book
[12]. Chiawei Lim, Sehui Han, Chansung Jung, and Whoi-Yul Kim, *Smartphone-Based Point-of-Care Urinalysis Under Variable Illumination*, IEEE Journal of Translational Engineering in Health and Medice, 2018, https://www.ncbi.nlm.nih.gov/pmc/articles/PMC5764119/ (Accessed 2021.04.07).

FABRICATION OF POLYANILINE/EXFOLIATED GRAPHITE BASED SUPERCAPACITOR FOR LOW POWER APPLICATIONS

I.G.P.N. Karunaseena*, K.P. Vidanapathirana

Department of Electronics, Wayamba University of Sri Lanka, Kuliyapitiya, Sri Lanka.

*karunasena.neel@gmail.com

ABSTRACT

With the advancement in technology, researchers are now focusing on storing the energy produced and efficiently use later. Among them, supercapacitor (SC) is being tested with more focus. This is because SC can be used to store more energy than conventional capacitors and to reduce the gap between batteries and capacitors. In this study, hybrid SC has been fabricated using exfoliated graphite (EG) and polyaniline (PANI) electrodes. Gel polymer electrolyte (GPE) was used as the electrolyte and the hot press method was used to produce the GPE. Fluorine-doped tin oxide (FTO) glasses were used to make the EG/PANI electrode. The doctor blade method was used to apply EG on FTO glasses. Polymerization process of aniline was performed using a charge density of 1200 $mCcm^{-2}$. SCs were fabricated with EG/PANI electrode sandwiching between GPE. They were characterized using cyclic voltammetry (CV), electrochemical impedance spectroscopy (EIS) and Galvanostatic charge discharge test (GCD). CV test was performed within a potential window of -1.2 V to 1.2 V with a scan rate of 5 $mAcm^{-2}$, CV results showed a single electrode specific capacity (C_{sc}) value of 94.86 Fg^{-1}. The GCD test was performed for 10000 cycles and it produced, single electrode specific discharge capacitance (C_d) value of 23.21 Fg^{-1} for the first cycle. A capacitor bank was built using supercapacitors and a circuit was designed to charge it. A brushless motor was operated using the capacitor bank.

Keywords: Supercapacitor, Exfoliated graphite-polyaniline electrode, Low power application

1.0 INTRODUCTION

Capacitors are a common component of many everyday electronic devices. The main problem with these typical capacitors is their smaller capacitance. SC is a high-capacity capacitor with a capacitance value much higher than conventional capacitors. SCs can be divided into three main types: electrochemical double-layer capacitor (EDLC), pseudocapacitor or redox capacitor, and hybrid capacitor. Hybrid capacitors can also be divided into three types as asymmetric, symmetric, and battery-type [1]. Here the same type of electrodes are used to make symmetric type. Hybrid SCs use oxidation (or doping) and reduction (or de-doping) to charge and discharge.

Carbon materials and conducting polymers (CPs) are used to make hybrid electrodes. Carbon materials can be used in different forms such as exfoliated-graphite (EG), activated carbon, carbon aerogels, and carbon nanotubes, while polyaniline (PANI), polypyrrole (PPy) can be used as the CP. The main advantages of using a CP are its good intrinsic conductivity, mechanical flexibility, chemical stability, and relatively cheapness [2]. The use of PANI as electrode material in particular is due to the low self-discharge capability of PANIs compared to other CPs [3]. PANI's higher environmental stability, controllable electrical conductivity, and easier processability are the other factors that led to the use of PANI for electrode fabrication [3]. Polyacrylonitrile based GPE was used as the electrolyte in SC fabrication. The advantage of using a GPE is that the electrolyte does not have a leaking problem. In this study, SC fabrication was performed mainly using EG-PANI as the electrode. SCs were characterized with three different methods to investigate their performance. A circuit was designed to charge the SCs and a brushless motor was operated using those SCs.

2.0 EXPERIMENTAL

2.1 Fabrication of Hybrid Supercapacitor

2.1.1 Preparation of Exfoliated Graphite

Graphite (was obtained from Bogala Graphite Lanka Ltd, Bogala, Sri Lanka.) was mixed with Sodium dodecylbenzene sulphonate (SDBS) (5 $mgml^{-1}$) solution and exfoliate in an ultrasonic homogenizer (Athena ATP 150) for 10 hours. The resultant mixture was centrifuged using a universal centrifuge (rate of 1500 rpm for 90 minutes). The mixture obtained after centrifugation was filtered through vacuum suction and dried to obtained EG powder [4].

2.1.2 Preparation of Electrodes

2.1.2.1 EG electrodes

First, EG was mixed with 1-methyl-2-pyrrolidinone (NMP) and coated to FTO glasses using the doctor blade method or spraying using Master Airbrush (Brand-Model 79). The EG coated FTO glasses were then thoroughly dried at 100 ^{0}C for 5 h.

2.1.2.2 EG/PANI electrodes

EG electrodes were used to deposit PANI using electrochemical polymerization with aniline concentration of 0.4 M and 0.5 M H_2SO_4 (0.6 ml). A three-electrode setup was used for this process. In polymerization, platinum (Pt) electrode was used as counter electrodes, Ag/AgCl electrode was used as reference electrodes and FTO plate was used as the working electrode. After polymerization EG/PANI electrodes were washed with distilled water and dried.

2.1.3 Preparation of gel polymer electrolyte

Polyacrylonitrile (PAN) (ALDRICH, MW 150000), ethylene carbonate (EC) (ALDRICH, 98%), propylene carbonate (PC) (ALDRICH, 99%) and magnesium chloride ($MgCl_2$) (ALDRICH, 99%) were mixed in weight ratios of 1: 4: 4: 1.25 respectively. The mixture was heated to 120 ^{0}C in a glass tube for 45 min. The mixture was then made into a GPE using the hot press method.

2.1.4 Fabrication of SC

Sandwich-type symmetric hybrid SC was fabricated using two EG/PANI electrodes and the GPE. The structure of the hybrid SC was in the form of EG-PANI / PAN: EC: PC: $MgCl_2$ / EG-PANI. Fabricated SC was then sealed with a parafilm to avoid it exposing to the external environment.

2.2 Characterization

2.2.1 Cyclic Voltammetry (CV) test

For the CV test, a three electrode setup was used where one electrode of the SC was used as the working electrode and the other one as the reference and counter electrodes. The CV test was performed for 500 cycles in the potential window of -1.2 V to 1.2 V using a scan rate of 5 mVs^{-1}. The data was obtained by a computer-controlled potentiostat (Metrohm Autolab 101). Single electrode capacitance (C_{sc}) was calculated using the following equation.

$$C_{sc} = \frac{2\int_{V_1}^{V_v} i \, dV}{ms\,\Delta V} \quad (01)$$

Where; $\int_{V_1}^{V_v} i \, dV$ is the integrated area of the CV curve, s is the scan rate (mVs^{-1}), ΔV is the voltage window, m is the electrode mass (g)

2.2.2 Electrochemical Impedance Spectroscopy (EIS) test

Impedance measurements were carried out for frequencies range from 400 KHz to 0.0005 Hz. From the impedance data, Nyquist plots were drawn. Further, bode plots were drawn for the real part of the complex capacitance (C') and the imaginary part of the complex capacitance (C'') which were calculated using the following equations.

$$C'(\omega) = \frac{-z''(\omega)}{\omega[z(\omega)^2]} \quad (02)$$

$$C''(\omega) = \frac{z\prime(\omega)}{\omega[z(\omega)^2]} \quad (03)$$

Where; $Z''(\omega)$ is the imaginary part of complex impedance, $Z'(\omega)$ is the real part of complex impedance, and $Z(\omega)$ is the complex impedance

2.2.3 Galvanostatic Charge-Discharge (GCD) test

GCD test was performed with charging and discharging cut off voltages of 1 V to 0.1 V with a battery analyzer under a constant current of 0.2 A. Single electrode-specific discharge capacitance (C_d) values were calculated using the following equation.

$$C_d = \frac{I}{m(\frac{dV}{dt})} \quad (04)$$

Where I is the constant current, m is the mass of a single electrode, dV/dt is the rate of drop of potential excluding IR drop during discharging.

2.3 Fabrication and testing of capacitor bank

A capacitor bank was fabricated by connecting SCs series and a circuit was designed to charge the SC bank. SC bank was used to drive a brushless motor as an application of the SCs.

3.0 RESULTS AND DISCUSSION

3.1 Cyclic Voltammetry (CV) test

In this case, the potential window from -1 V to 1 V received a high value of C_{sc} approximately 102.40 Fg^{-1}, but that potential window was not selected for further studies. Instead, a potential window ranging from -1.2 V to 1.2 V with a C_{sc} of 94.85 Fg^{-1} was selected. This is because it was possible to observe two symmetric peaks in a potential window from -1.2 V to 1.2 V. Table 01 is a summary of calculated C_{sc} values for different potential windows and the cyclic voltammograms for each of those potential windows is shown in figure 3.1.

Table 2.1: Calculated single electrode specific capacitance (C_{sc}) values in different potential windows

lower voltage (V)	upper voltage (V)	ΔV (V)	scan rate (mVs^{-1})	mass (mg)	area	C_{sc} (Fg^{-1})
-0.2	0.2	0.4	5	2.3	8.98E-05	39.06
-0.5	0.5	1.0	5	2.3	4.04E-04	70.31
-1.0	1.0	2.0	5	2.3	1.18E-03	102.41
-1.2	1.2	2.4	5	2.3	1.31E-03	94.86
-1.5	1.5	3.0	5	2.3	1.37E-03	79.47
2.0	2.0	4.0	5	2.3	1.61E-03	70.16

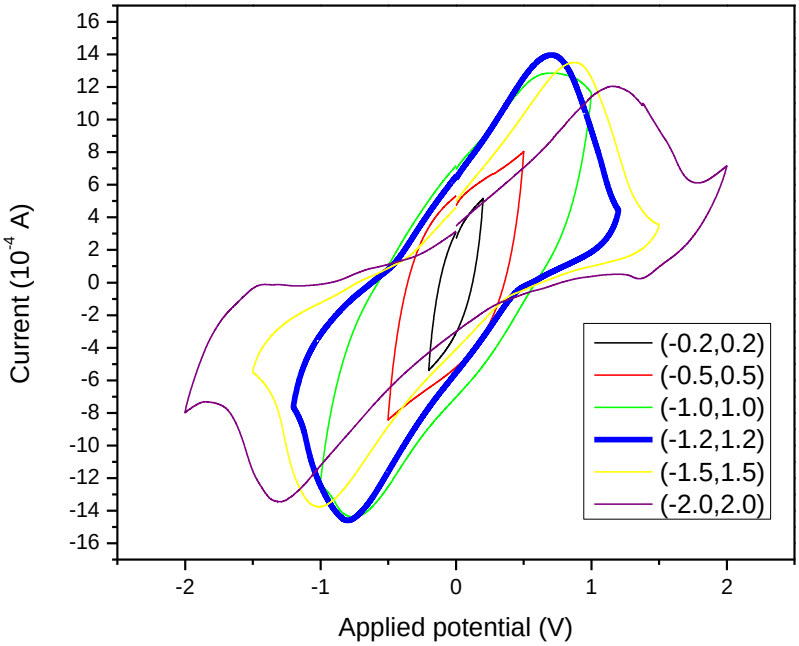

Figure 3.1: Cyclic voltammograms of the SC in the configuration of EG-PANI/1 PAN: 4 EC: 4 PC: 1.25 $MgCl_2$/EG-PANI for different potential window variation at 5 mVs^{-1} scan rate

Figure 3.2 shows the cyclic voltammograms obtained with continuous cycling of the SC for 500 cycles.

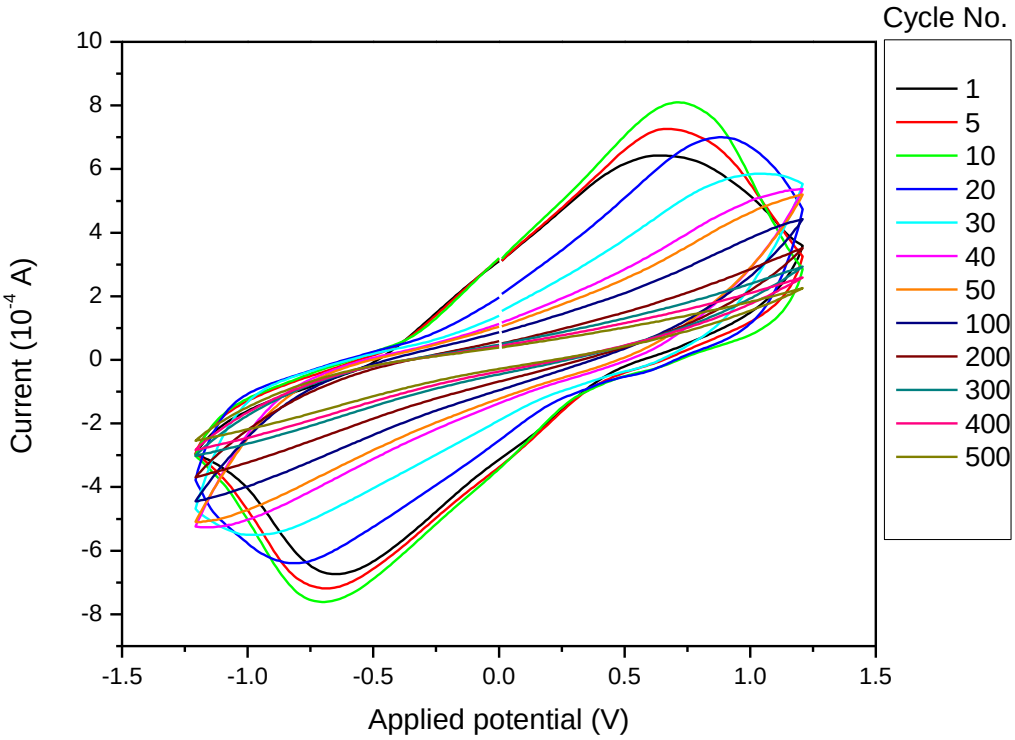

Figure 3.2: Cyclic voltammograms of the SC in the configuration of EG-PANI/1 PAN: 4 EC: 4 PC: 1.25 $MgCl_2$/EG-PANI for 500 continuous cycles. Scan rate at 5 $mAcm^{-2}$

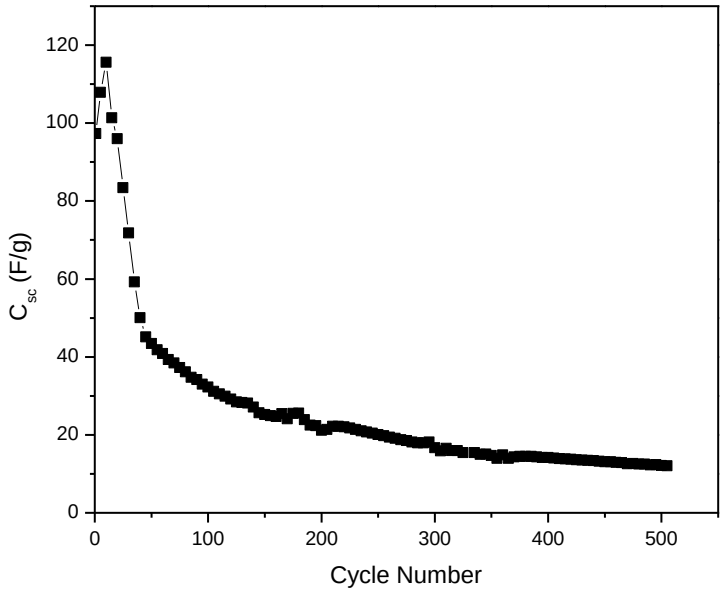

Figure 3.3: Single electrode specific capacitance variation with the cycle number for SC in the configuration of EG-PANI/1 PAN: 4 EC: 4 PC: 1.25 $MgCl_2$/EG-PANI

According to figure 3.2, a comparison between the first cycle and the 100th cycle shows that the maximum current in the 100th cycle is reduced and the peaks are missing compared to the first cycle. Variation of the C_{sc} with the cycle number is depicted in figure 3.3. Figure 3.3 shows a 65% decrease in the C_{sc} value between the first and the 100th cycle. This may be due to the physical deformation of the EG/PANI electrodes. This physical deformation can have a direct impact on the cycle life of the SC.

3.2 Electrochemical Impedance Spectroscopy (EIS) test

The Nyquist plot obtained from the impedance measurements between 400 kHz – 0.0005 Hz is given in figure 3.4. In the low frequency region, it shows a semi vertical line which represents the capacitive behavior of the SC. The corresponding bode plots were drawn after calculating the *C'* and *C''* values. The best set of graphs could be obtained in the frequency range 400 kHz – 0.0005 Hz and are shown in figure 3.4 and figure 3.5.

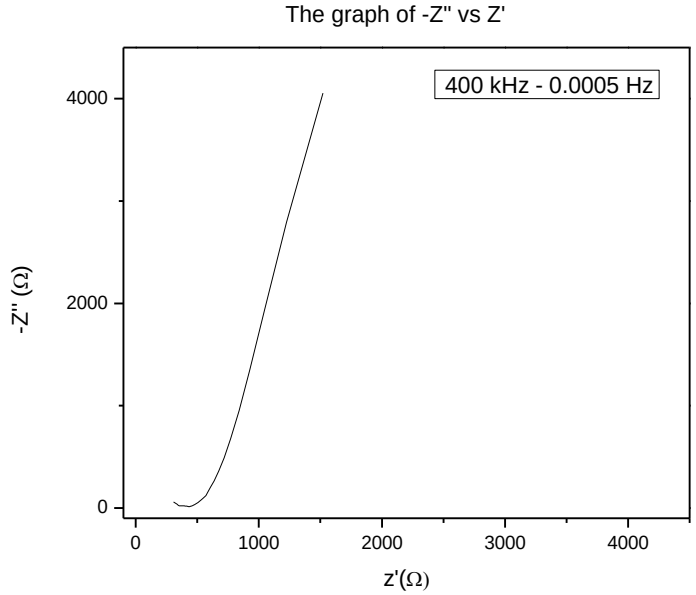

Figure 3.4: Nyquist plot of the SC in the configuration of EG-PANI/1 PAN: 4 EC: 4 PC: 1.25 $MgCl_2$/EG-PANI in the frequency range 400 kHz – 0.0005 Hz.

Ideally, it should be parallel to the Z" axis but due to the imperfections between the electrodes and the interfaces this type of inclination results.

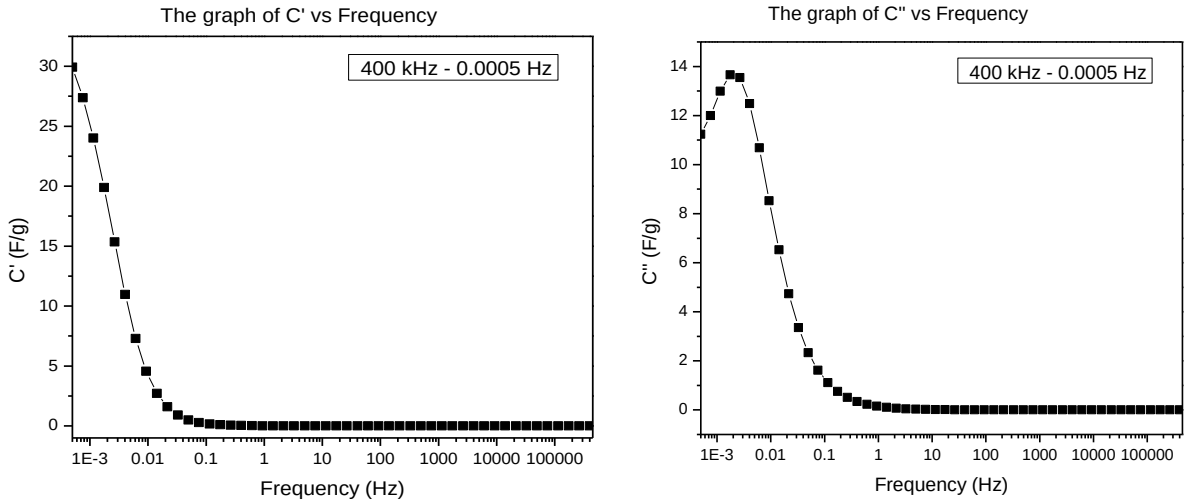

(a): C' vs log (frequency) (b): C" vs log (frequency)

Figure 3.5: Bode plots from 400 kHz to 0.0005 Hz frequency range of the SC

The value of *C'* is inversely proportional to the frequency. The maximum value of C_{sc} is obtained from the highest point of the graph (maximum value of C') shown in Figure 04(a). According to this frequency, it gives C_{sc} of 29.92 Fg^{-1}.

3.3 Galvanostatic Charge Discharge (GCD) test

GCD cycles obtained for the EG/PANI base SC is shown in figure 3.6. The GCD test was performed for 10,000 cycles and a graph was plotted the variation of C_d with the cycle numbers, figure 3.7.

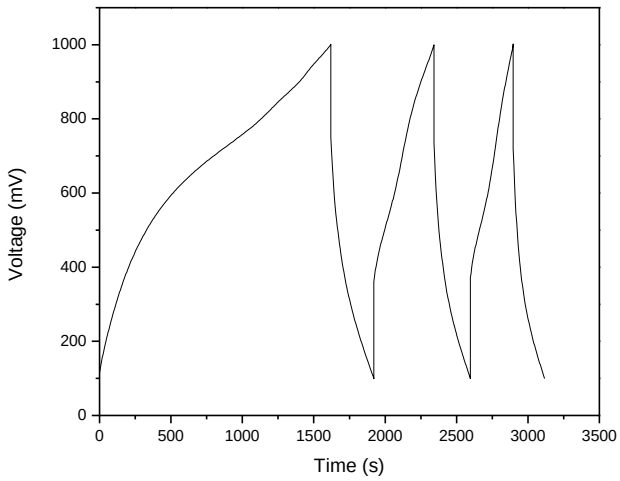

Figure 3.6: Galvanostatic charge discharge obtained for the EG-PANI/ 1 PAN: 4 EC: 4 PC: 1.25 $MgCl_2$/ EG-PANI

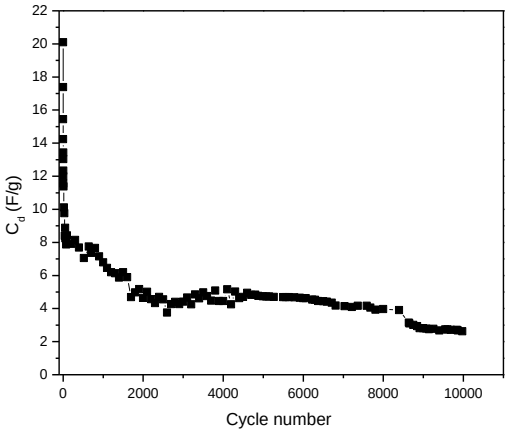

Figure 3.7: The variation of single electrode specific discharge capacitance with cycle number

In addition, Figure 3.7 indicates that the C_d value for the first cycle was 23.21 Fg^{-1} and it was decreased to 7.32 Fg^{-1} at the end of 1000 cycles. The graph further shows that the C_d value quickly drops during the first few cycles and this may be due to the reactions that take place within the interfaces. After 2000 cycles the rate of the capacity decay is slower than at the beginning. This may have resulted as the capacitor get matured with the long cycling.

3.4 Fabrication and testing of capacitor bank

The capacitor bank was fabricated by connecting several SCs in series. A circuit was designed (shown in figure 3.8) to charge this capacitor bank and the relevant PCB design according to the Copper and 3D design are given the figure 3.9 and figure 3.10 respectively.

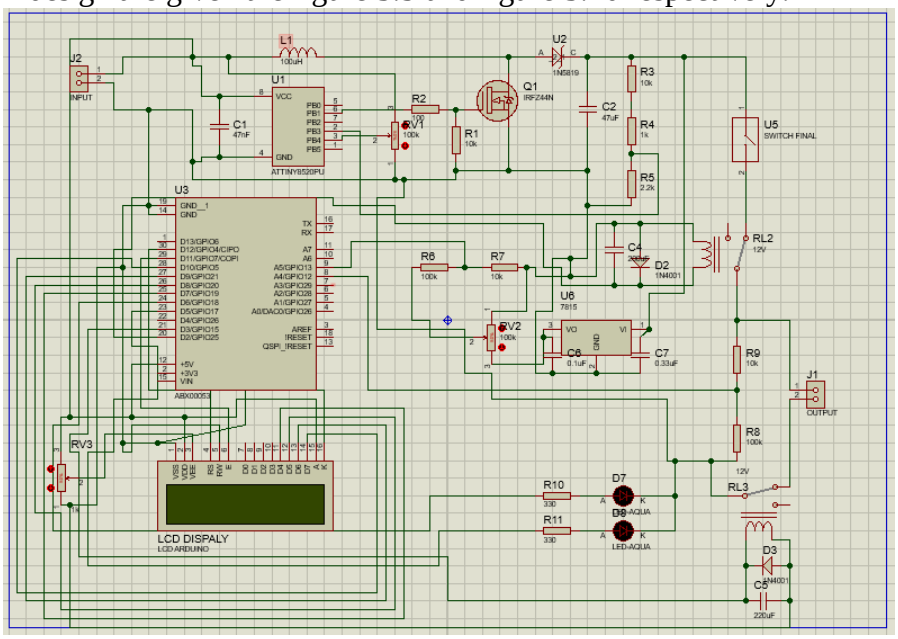

Figure 3.8: Designed circuit diagram for the charging circuit

The brushless motor was rotated using a capacitor bank, which provided the starting power needed to rotate the motor.

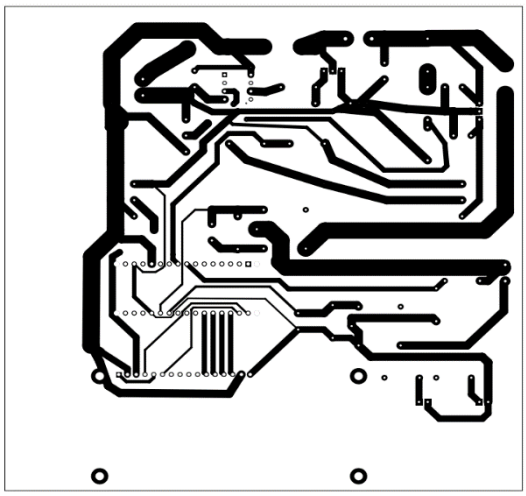
Figure 3.9: Bottom copper layer PCB design for the charging circuit

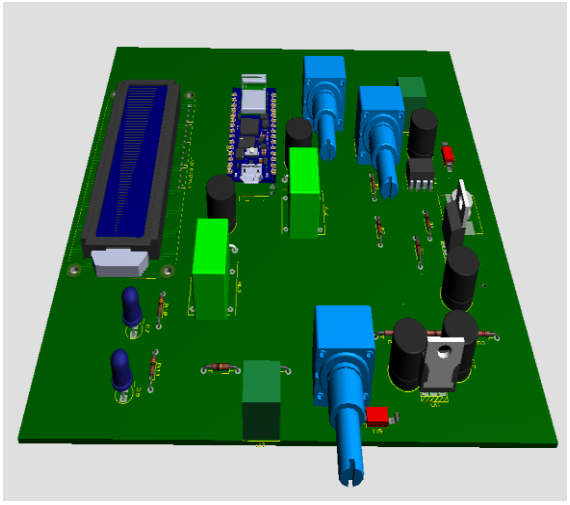
Figure 3.10: 3D layout of the charging circuit

4.0 CONCLUSION

In this study, attempts were made to fabricate EG/PANI-based SC. CV, EIS, and GCD tests were performed to characterize SC. The first cycle of the CV test received a C_{sc} value of 97.27 Fg^{-1}. With the EIS test conducted in the frequency range of 400 kHz to 0.0005 Hz, the value of C_{sc} was calculated as 29.92 Fg^{-1}. The GCD test for 10000 showed C_d value of 23.21 Fg^{-1} for the first cycle. Furthermore, a capacitor bank was created using SCs and a circuit was developed to charge the

capacitor bank. A brushless motor was successfully operated using this capacitor bank. This study confirmed that these SCs can be used for low-power applications.

ACKNOWLEDGEMENT

Special thanks to Ms. Dinithi S. K. Rajaguru, Mrs. H.G.N. Rajapaksha, Mr. Lasitha Rathnayake, and other members of the Polymer Electronics Research Group (PERG) at the Wayamba University of Sri Lanka. Also Bogala Graphite Lanka Ltd, Bogala, Sri Lanka is highly acknowledged for providing natural graphite samples.

REFERENCES:

[1]. Raza, W., Ali, F., Raza, N., Luo, Y., Kim, K. H., Yang, J., Kumar, S., Mehmood, A., and Kwon, E. E., Recent advancements in supercapacitor technology, *Nano Energy*, 52,(2018), pp. 441–473, doi: 10.1016/j.nanoen.2018.08.013.

[2]. Weerasinghe, W. A. D. S. S., Vidanapathirana, K. P., Perera, K. S., Effect of monomer concentration on the performance of Polyaniline based redox capacitors, *Ceylon J. Sci.*, 46, (2017), p. 31, doi: 10.4038/cjs.v46i3.7440.

[3]. Eftekhari, A., Li, L. and Yang, Y., Polyaniline supercapacitors, *J. Power Sources*, 347,(2017), pp. 86–107, doi: 10.1016/j.jpowsour.2017.02.054.

[4]. Rajaguru, D. S. K., Vidanapathirana, K. P., Perera, K. S., Dependence of capacitive properties of an EDLC on exfoliation time of graphite electrodes, *Res. Sq.*, (2021), pp. 99–117.

Proc. Annual Symposium on Research & Industrial Training, 08(2021) 17-24
Department of Electronics – Wayamba University of Sri Lanka

FABRICATION OF NATURAL RUBBER/ MgTF ELECTROLYTE BASED SUPERCAPACITORS FOR SOLAR ENERGY STORAGE

M.P.N.T. Meghapathirana*, G.A.K.S. Perera

Department of Electronics, Wayamba University of Sri Lanka, Kuliyapitiya, Sri Lanka

*nt.meghapathirana@gmail.com

ABSTRACT

Nowadays supercapacitors are a preferred choice for energy storage due to their high specific power, fast charge/discharge capability, and long cycling stability as compared to batteries and conventional capacitors. As a result, supercapacitors may become an attractive power solution for an increasing number of applications. This study was carried out to fabricate an electrochemical double-layer capacitor (EDLC) with natural rubber (NR) based solid polymer electrolyte (SPE). Modified natural rubber, magnesium trifluoromethanesulfonate ($Mg(CF_3SO_3)_2$ – MgTF) were used to prepare the SPE while a combination of natural graphite, activated charcoal and polyvinylidene fluoride (PVDF) were used as electrode materials. The fabricated device had better performance within the 0.005 - 0.5 V potential window at 10 mVs^{-1} scan rate in cyclic voltammetry (CV) test. The EDLC was confirmed a longer life cycle by keeping the specific capacitance (C_{SC}) value more or less constant even after 500 cycles. It was possible to observe the potential of the supercapacitor to store solar energy.

Keywords: Electrochemical double layer capacitor, Natural rubber, Specific capacitance

1.0 INTRODUCTION

Supercapacitors are one of electrochemical energy storage (EES) devices and they have high specific power fast charge/discharge capability and long cycling stability as compared to batteries and conventional capacitors. With the unending demand for uninterrupted power as well as due to endangering state of fossil fuels, there is a great necessity to move towards renewable energy sources. For that purpose, supercapacitors are now receiving considerable attention due to their fascinating features which are well-matched with basic needs in present-day society.
Electrochemical double-layer capacitors (EDLCs) are one type of supercapacitors with carbon-based electrodes [1]. Even though solid-state electrolytes-based EDLCs have several advantages over liquid-based EDLCs, they have low conductivity. Therefore, solid polymer electrolytes (SPEs) have received a noticeable interest as they are more conductive, lighter, and flexible [2, 3].

Many polymers used for the preparation of SPEs are not safe for flora and fauna. This has highlighted the necessity to seek friendly polymers for SPEs. Intense research done on this issue has discovered the suitability of natural rubber (NR) to be used for SPEs. NR is obtained by the latex tapped from the tree *hevea brasiliensis* and this latex is a polymer made from isoprene units with a small percentage of impurities in it [4,5]. NR is naturally an insulator and hence, several modifications are done to transform the material to be a polymer candidate. Methyl grafted NR (MGNR) is one of the modified NR that has better mechanical and thermal properties [6, 7].

This research is based on the fabrication of an EDLC based on an NR SPE with the objective of storing solar energy.

2.0 EXPERIMENTAL

2.1 Preparation of electrolyte

Methyl grafted natural rubber (MGNR) and magnesiumtrifluoromethanesulphonate ($Mg(CF_3SO_3)_2$ - MgTF) were dissolved separately in a solvent well in advance. The two solutions were mixed and stirred for 24 hours. The mixture was poured into a petry dish and kept for film formation. This film was used as the electrolyte to fabricate EDLC.

2.2 Preparation of electrodes and fabrication of EDLCs

Polyvinylidenefluoride (PVDF) was mixed in acetone first. Then, activated charcoal (AC) and natural graphite (NG) were added. The whole mixture was sonicated for 2 hours using an ultrasonic probe sonicator. The resulting slurry was coated on fluorine-based tin oxide (FTO) glass plates to be used as the electrodes. The electrode composition was 10% PVDF: X% AC: Y% NG by weight. X and Y values were altered and the optimized composition was selected. A prepared NR SPE film was sandwiched in between two electrodes and sealed with sealing tape. The area of an electrode was 1 cm^2 and the weight of the electrode was 1.4 mg.

2.3 Characterization of EDLCs

A computer-controlled frequency response analyzer was used to do EIS tests. The measurements were taken in different frequency ranges. Observations were analyzed by using Nyquist plots and bode plots. A time-based EIS test was carried for the chosen EDLC which has the optimized electrode composition. CV tests were completed for the EDLC under different scan rates and potential windows. The scan rate was varied from 5 to 100 mVs^{-1} and the potential window was varied in the range between 0.005 V to 0.9 V. Next the continuous CV test was carried out. The EDLC was galvanostatically charged and instantly discharged under the GCD test using an eight-channel battery analyzer [8].

3.0 RESULTS AND DISCUSSION

3.1 Electrochemical impedance spectroscopy (EIS)

Table 1 shows the highest values of single electrode specific capacitance (C_{sc}) and calculated relaxation times (τ_0) of EDLCs having electrodes of different graphite compositions (weight %). The complex capacitance $C(\omega)$ can be calculated by using real $Z'(\omega)$ and imaginary part $Z''(\omega)$ of the complex impedance $Z(\omega)$, by using equations proposed by Tey et al [9].

Table 3.1: C_{SC} and relaxation times of different electrode compositions

Graphite: AC composition (Weight %)	**Specific Capacitance C_{sc} ($F\ g^{-1}$)**	**Relaxation time τ_0 (s)**
70 : 20	2.37	0.07
75 : 15	7.59	0.37
80 : 10	2.05	2.79
85 : 05	1.26	1.63
90 : 00	0.39	0.78

Accordingly, the electrode composition which has 75% graphite has gained the highest specific capacitance. This confirms the fact that only the combination of graphite: AC at 75: 25 accommodates the maximum charge storage. Minimum relaxation time is one of the characteristics of an EDLC which has better performance. The lowest τ_0 is available with the lowest amount of graphite. This might be due to the assistance given by AC to expedite charge-discharge reactions. However, results point out that there is no direct correlation between the capacitance and the reaction rate. Though the reaction rate is slow, capacitance can be maximum. Figure 1 and 2 show the resulting Nyquist plot and bode plots of optimized EDLC.

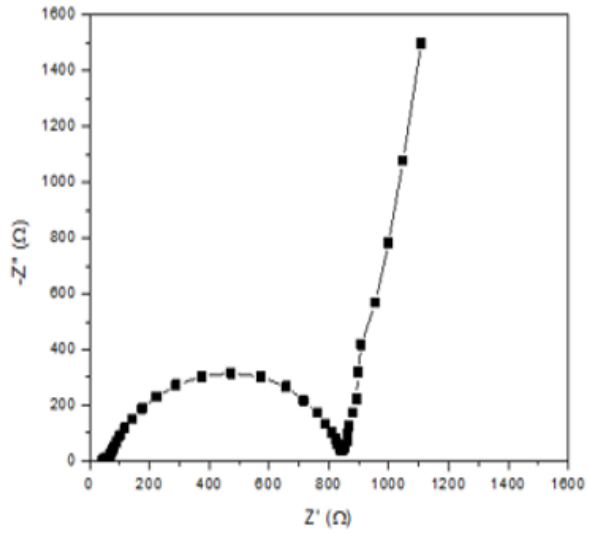

Figure 3.1: Resulting Nyquist plot frequency range at 0.01 – 40 000 Hz

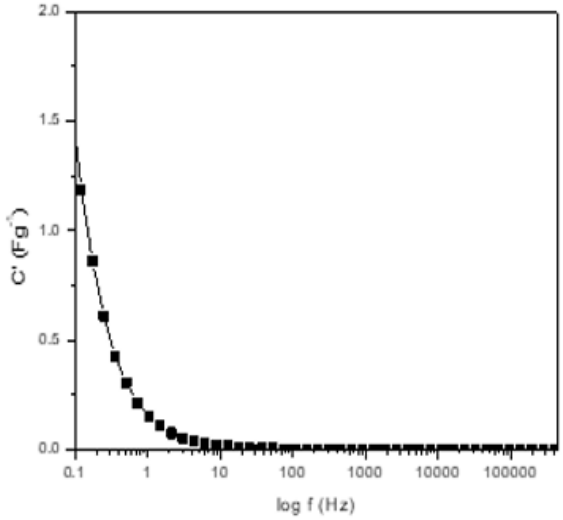

Figure 3.2: Real part of capacitance variation with the log frequency in the

As shown in Figure 3.1, the obtained Nyquist plot has only one circle in mid-range frequencies and the lowest frequency region represents capacitive features. The C′ value had decreased with increasing frequency. The maximum point of the curve associates with C_{sc} as shown in Figure 3.2. Figure 3.3 shows the bulk electrolyte resistance variation with time

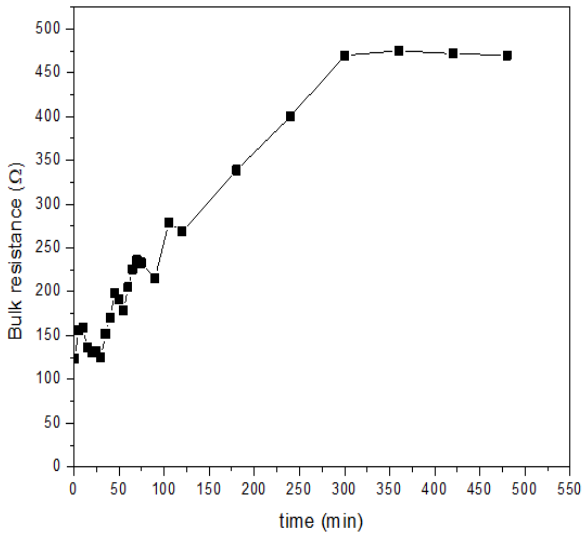

Figure 3.3: Time based EIS results

At the beginning (0 min), the bulk resistance value was 124 Ω. With the time, it has increased and became stable at 450 – 500 Ω range. At the initial stage, the contacts between the electrolyte

and the electrode may not be well-formed. So, the initial resistance can be small. With the time, when contacts become mature, resistance can be increased. Reaching a constant value is a proof for showcasing the stable nature of the electrolyte. If the electrolyte was degraded, it would not be possible to observe such a constant state. Instead, its resistance would increase further. The increase of R_b with time is a common drawback that has been noticed for many SPEs. Results confirm the suitability of the electrolyte to be used for applications.

3.2 Cyclic voltammetry (CV)

3.2.1 Scan rate variation test

Figure 3.4 shows the obtained cyclic voltammogrammes when varying the potential window and Table 3.2 exhibited the resulted values.
All curves showed near rectangular shapes, especially for the lower scan rates.
By using equation (01), the single electrode specific capacitance (C_{sc}) was calculated.

$$C_{sc} = \frac{2.\int I\, dv}{S.m.\Delta V} \quad \text{----------01}$$

where ∫I dv is the area of the cyclic voltammograms, S is the scan rate, m is the mass of a single electrode, ΔV is the width of the potential window.

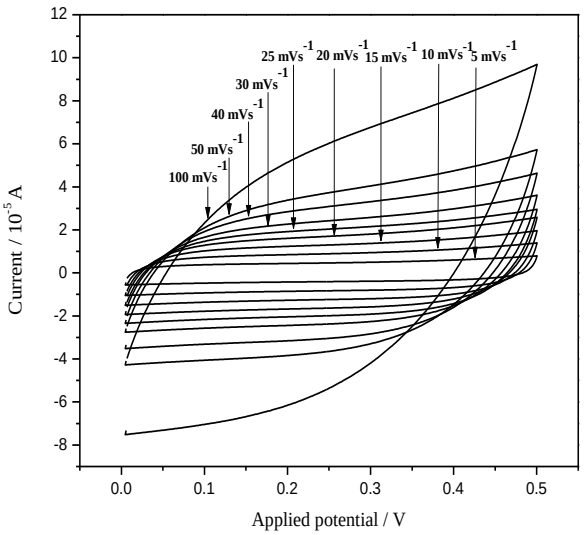

Figure 3.4: The voltammogram graphs in different scan rates

Table 3.2: Calculated specific capacitance values in different scan rates

Scan rate ($mV\ s^{-1}$)	**C_{sc} ($F\ g^{-1}$)**
5	15.35
10	14.70
15	14.03
20	13.53
25	12.77
30	12.43
40	11.52
50	10.80
100	7.91

At lower scan rates, the capacitance values were higher than the higher scan rates, and the voltammogram was taken near parallelograms shape [10,11]. Theoretically, the C_{sc} value decreases with increasing scan rate because the scan rate is inversely proportional to the C_{sc} (Equation (01)). In practice, it could be due to insufficient time for the electrolyte ions to complete the electrochemical reaction on the electrode surface at higher scan rates [12]. 10 mVs^{-1} value was selected as optimized scan rate which has a relatively high specific capacitance.

3.2.2 Potential window variation test

Figure 3.5 shows the potential window variation graphs at 10 mVs^{-1} and as per equation (01), calculated C_{sc} values in different potential windows exhibits in Table 3.3.

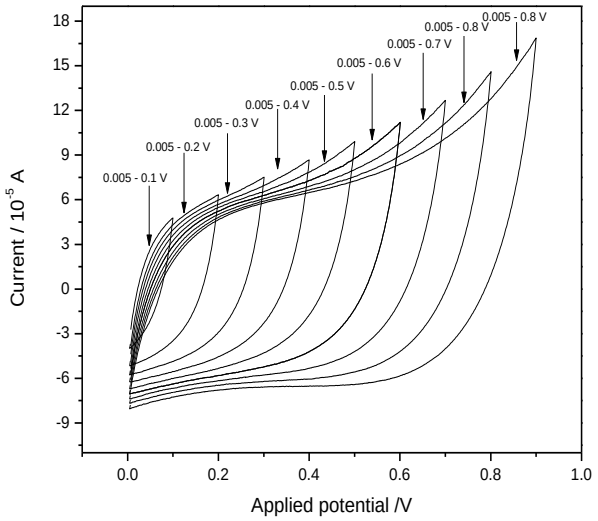

Figure 3.5: The graphs of potential window variation at 10 mVs^{-1} scan rate

Table 3.3: Calculated single electrode specific capacitance (Csc) values

Potential window / V	**C_{sc} ($F\ g^{-1}$)**
0.005-0.1	3.14
0.005-0.2	5.35
0.005-0.3	6.62
0.005-0.4	7.45
0.005-0.5	8.12
0.005-0.6	8.73
0.005-0.7	9.27
0.005-0.8	9.88
0.005-0.9	10.51

The EDLC exhibited a relatively high specific capacitance value and better performance within the 0.005 - 0.5 V potential window. In this potential window, the cyclic voltammograms have the proper shape that belongs to an EDLC. Reversibility reaction requires fast enough electron transfer kinetics to maintain the surface concentrations of charges on the electrode/electrolyte interface. The charges are moving only when they are reached to the required potential for charge mobility. Hence, the optimum C_{sc} occurs only within a specific potential window [15]. Figure 3.6 confirms that the device has a better reversible, electron transfer process until it reaches 0.5 V. Beyond that, the shape of cyclic voltammograms started to distort. It indicates that after 0.5 V the capacitive properties of EDLC were beginning to be destroyed. An occurrence of an irreversible reaction could be an effect of this distortion. Therefore 0.005-0.5 V potential window was selected for further study.

3.2.3 Continuous cyclic voltammetry

Continuous cyclic voltammetry test (for 500 cycles) was completed within the potential window, 0.005 – 0.5 V, and at the scan rate of 10 mVs^{-1}. The obtained results were shown in Figure 6.

The designed EDLC was stable in the potential window,0.005 to 0.5 V, and at the scan rate of 10 mVs^{-1}. As shown in Figure 3.7, it was able to continue nearly the same specific capacitance during the additional cycle numbers. Initial C_{sc} was 10.42 Fg^{-1} and it had been decreased to 10.20 Fg^{-1} after 500 cycles. Potential reasons for the observed slight C_{sc} drop could be the loss of contacts between the electrodes / SPE interfaces, degradation of SPE, and the degradation of electrodes [16].

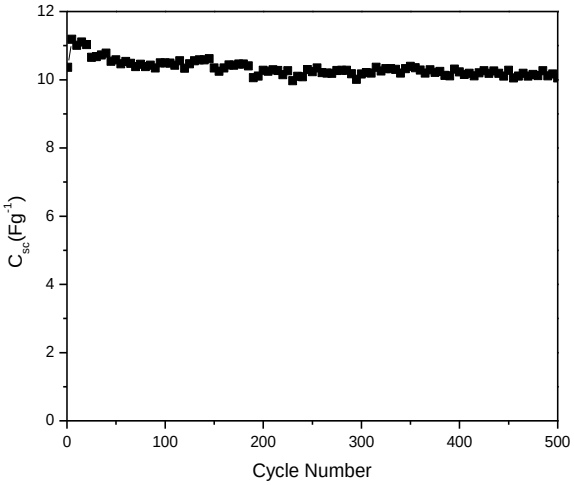

Figure 3.6: The graphs of C_{sc} vs cycle number

3.3 Galvanostatic charge-discharge test (GCD)

A longer life cycle with better charging and discharging performance of the fabricated EDLC was shown when it was in the potential window between the 0 and 0.5 V under 0.05 mA current.
Figure 3.7 and 3.8 illustrate the results of GCD test.

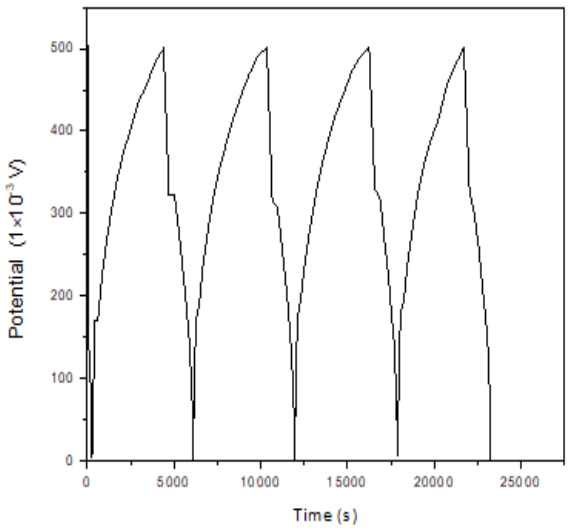

Figure 3.7: Some initial GCD curves

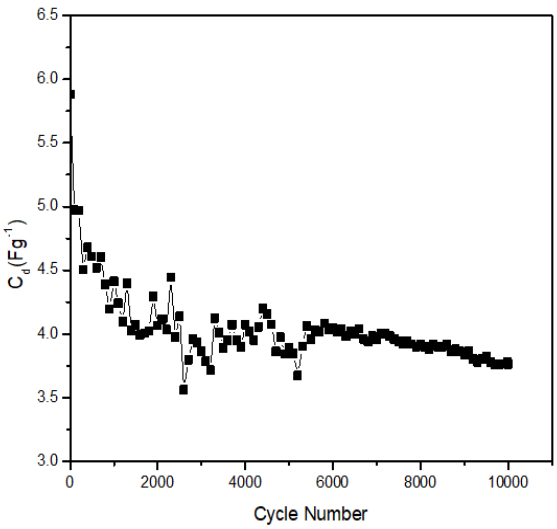

Figure 3.8: The graph of C_d vs cycle number

The device has a single electrode discharge capacitance, C_{sd} between 3.5 – 6 Fg^{-1}. Discharge curve behavior evidences the presence of a non-faradic capacitive charge storage mechanism. Equilateral triangle shapes symbolize good reversibility during charge/discharge cycles of an EDLC. The resulted charge-discharge shapes are having a triangular shape to some extent but they are not perfect equilateral triangles. Due to the possible problems in the structure of SPE as well as the graphite electrodes, unique ion movement may not take place. As a result, reversibility problems may arise [16].

3.4 Application

It was possible to charge the fabricated EDLC under a voltage of 0.5 V and a current of 50 μA using a charger circuit, which was powered by a solar cell.

4.0 CONCLUSION

NR-based electrolyte could be used successfully for an EDLC. The electrode combination of graphite: AC at 75: 25 accommodates the maximum charge storage. Results of EIS, CV, and GCD tests prove the capacitive behavior of the fabricated device. The EDLC has gained a high specific capacitance value and better performance within the 0.005 -0.5 V potential window at a 10 mVs^{-1} scan rate. The device showed a long-life cycle with better charging and discharging performance under a 50 μA current. Solar energy could be stored in the EDLC through the photovoltaic cells. This study confirms that further improvement of NR-based electrolytes for supercapacitors would open the door for storing renewable energy.

ACKNOWLEDGEMENT

Heartfelt thanks for all the support of Ms. H.G.N. Rajapaksha and all members of the Polymer Electronics Research Group (PERG) at the Wayamba University of Sri Lanka. ASR Ltd, Kegalle, Sri Lanka and Bogala Graphite Lanka, Bogala, Sri Lanka are highly acknowledged for providing natural rubber and natural graphite samples.

REFERENCES

[1]. Rahman, S., Oni N. S., Quazi A.I.M., *Design of a Charge Controller Circuit with Maximum Power Point Tracker (MPPT) for Photovoltaic System*. B.Sc. diss., BRAC University, 2012

[2]. Samui, A.B, Sivaraman, P., Solid polymer electrolytes for supercapacitors. In *Polymer Electrolytes Fundamentals and Applications,* Sequeira C, Santos D. (eds), 3-61, India: Woodhead Publishing, 2010

[3]. Abu Bakar, M.H., Hana, K.F., *Advanced Engineering for Processes and Technologies*,1st Ed.,Malaysia, Springer Publication, 2019, E-book

[4]. Pal, B., Yang, S., Ramesh, S., Thangadurai, V., Jose R., Electrolyte selection for supercapacitive devices: a critical review, *Nanoscale Advances,* 1/10, (2019), 3807-383

[5]. Taer, E., Taslim, R., and Deraman, M., Preparation and characterizations of activated carbon monolith from rubber wood and its effect on supercapacitor performances, *Proc. AIP Conference Proceedings 1712, Jatinagor , Indonesia,* 2016, 1-5

[6]. Phinyocheep P., Chemical modification of natural rubber (NR) for improved performance. In *Chemistry, Manufacture and Application of Natural Rubber,* 68-118, India: Woodhead Publishing, 2014, doi: 10.1533/9780857096913.1.68

[7]. Saramolee P., Lopattananon N., Sahakaro K., Preparation and some properties of modified natural rubber bearing grafted poly(methyl methacrylate) and epoxide groups, *European Polymer Journal*, 56/1, (2014) ,1–10, doi:10.1016/j.eurpolymj.2014.04.008

[8]. Rajapaksa, H.G.N., Perera, K.S., Vidanapathirana K.P., A novel redox capacitor with a natural rubber-based solid polymer electrolyte for energy applications, *Ionics,* 27/2, (2021), 1-9, doi: https://doi.org/10.1007/s11581-021-03970-w

[9]. Tey, J. P., Careem, M. A., Yarmo, M. A., Arof, A. K., Durian shell-based activated carbon electrode for EDLCs, *Ionics*, 22/7, (2016), 1209–1216, doi: 10.1007/s11581-016-1640-2

[10]. Vaidyanathan, I.S., *Electrochemical Characteristics of Conductive Polymer Composite based Supercapacitors*, MSc diss., School of Energy and Materials Engineering, College of Engineering and Applied Science, 2012

[11]. Scibioh, M. A.,Viswanathan, B., Characterization methods for supercapacitors, *Materials for Supercapacitor Applications* , (2020), 315–372. doi:10.1016/b978-0-12-819858-2.00005-6

[12]. S. Alkahalaf, C.K. Ranaweera, P.K. Kahol, K. Saim, H. Adhikari, S.R. Mishra, F. Perez, B.K. Gupta, K. Ramasamy, R.K. Gupta, Elecrochemical energy storage performance of electrospun $CoMn_2O_4$ nanofibers, *Journal of Alloys and Compounds*, 692/C, (2017) ,59-66, doi: https://doi.org/10.1016/j.jallcom.2016.09.005

[13]. Sanjaya, N.A.A.K., Perera, K.S., Vidanapathirana, K.P., Applicability of natural rubber-based polymer electrolyte for electrochemical double-layer capacitors, *Sri Lankan Journal of Physics*, 20/ 17, (2019), 17-26, doi: http://DOI.org/ 10.4038/sljp.v20i0.8067s

[14]. Rajapaksa, H.G.N., Perera, K.S., Vidanapathirana, K.P., Fabrication and Characterization of Electrochemical Double-Layer Capacitors using a Natural Rubber Based Polymer Electrolyte. Proceedings of the Technical Sessions, Institute of Physics – Sri Lanka, 2020 ,49-56

Proc. Annual Symposium on Research & Industrial Training, 08(2021) 25-31
Department of Electronics – Wayamba University of Sri Lanka

SELF-BALANCING, PORTABLE, AND AUTOMATED CONDITION CONTROLLING SYSTEM FOR AN INFANT INCUBATOR

G.C.W. Thilakarathne*, P.M. Senadeera

Department of Electronics, Wayamba University of Sri Lanka, Kuliyapitiya, Sri Lanka

*gayathri.thilakarathne95@gmail.com

ABSTRACT

Premature babies cannot control their body temperature without any external aid. Most of the current incubators are operated by a manual process and under someone's supervision. In order to address this issue, an incubator is contained with an automated system to monitor and maintain the internal parameters of the incubator (temperature and humidity) and infant's conditions such as weight, postnatal age, abdominal temperature, and heart rate have been designed and implemented. The auto-balancing, parameters monitoring, and maintaining features of the incubator were mainly based on the Raspberry Pi 3 Model B+ which was programmed using Python. Sensors were connected to obtain the readings and conditions were controlled with the help of an external cooling system, heating system, and vaporizing system. As the designed incubator is portable, the maintaining the balance of the incubator during transportation was carried out with a gyroscope sensor and servo motor. Buzzer was used for the alert system and conditions of the baby and the incubator were displayed via 16x2 LCD. This automated system increases the accuracy, compared to a manual monitoring process and avoids the necessity of being observed by someone all the time. This proposed incubator system was developed with a specific feature of quick self-balancing to reduce the risk during transportation and the capability of providing immediate alerts during critical conditions of the baby.

Keywords: Automated condition controlling, Self-balancing, Portable infant incubator

1.0 INTRODUCTION

Nearly twenty million premature and low birth weight infants are born each year in developing countries and four million of them die within their first month. The infant mortality rate is an important key factor in measuring health development in developing countries. The current infant mortality rate of Sri Lanka in 2020 is 7.12 deaths per 1000 live births, a 3.09% decline from 2019. These deaths occur mainly due to the unavailability or unreliability of traditional incubators in providing basic care for infections and breathing difficulties [1,2].

A conventional incubator should be always operated by well-trained nurses or medical staff and accurate information about the infant are required to keep the infant healthy and safe. As the condition setting up is a manual process, the incubator should be always kept under someone's supervision [3]. The most significant case during the transportation is to maintain the stability of the incubator table on the y-axis without moving up and down. As these babies are not grown properly and due to the weak status of their organs, they have a high risk of damage even from a small leaning of the incubator.

The main objective of the automated system is to increase the accuracy compared to the manual monitoring process and to avoid the necessity of being observed by someone all the time with human errors.

The proposed incubator was provided with the artificial interior conditions for the premature baby (a baby born before the 37th week of 40 weeks of pregnancy period) which match with the conditions inside the mother's womb. This automated system may provide immediate alerts if the baby is in a critical condition.

2.0 EXPERIMENTAL

The implemented system consists of three main processes; automated interior condition checking, controlling, and self-balancing, and notifying the critical conditions of the baby.

2.1 Automated interior condition checking and controlling

The interior conditions of the incubator were controlled based on the birth weight and the postnatal age of the baby. The weight was read by using the load cell combined with an HX711 module. The postnatal age of the baby was fed as input data on the first-day baby was kept in the incubator. Hereafter, the age was calculated and displayed automatically in the system. The calibration of the scale should be done at the start of the system. The calibration was done by using a known weight and a touch display. The postnatal age of the baby was input into the system using a keypad. The reference conditions were checked and set according to the input weight and the postnatal age.

Interior humidity levels and temperature were measured using a DHT11 sensor. The interior humidity and the temperature of the incubator were maintained from A/C (air conditioning), heater, and vaporizer which were connected through relays. The heater was designed by fixing the heating side of a Peltier module to a heat sink. The cooling system was designed by fixing the cooling side of a Peltier module to a thick aluminium plate (heat sink) which was fixed at the backside of a fan. A wide plastic tunnel was fixed in front of the fan. The humidifier was designed with the ultrasonic mist maker module. A hose was set up from the mist maker to the fan tunnel.

2.2 Monitoring baby's conditions

The pulse sensor was interfaced via ADS 1115 (for microcontrollers without an analogue-to-digital converter or when want a higher-precision ADC, the ADS 1115 provides 16-bit precision at 860 samples/second over I^2C). The DS18B20 was interfaced to measure the abdominal temperature of the baby. A vibration sensor was interfaced to identify whether the baby shows an unusual vibration. A buzzer was connected to inform whether the baby is in a critical condition. A 16 x 2 LCD was interfaced with the Raspberry Pi to monitor the current conditions of the baby and the incubator. The LCD was set up in four-bit mode to display the baby's condition.

2.3 Self-balancing (motion)

The motion (balance) of the incubator was tracked using an MPU 6050 gyroscope sensor. The incubator was kept balanced parallel to the x-axis. An MG 995 servo motor was interfaced to do liftings up and down. The servo motor was powered by an external power supply.
The prototype was designed using Perspex sheets. The main purpose of using Perspex sheets was to reduce the weight of the structure and to avoid heat and electrical conductivity.

3.0 RESULTS AND DISCUSSION

The prototype of the implemented design is shown in figure 3.1.

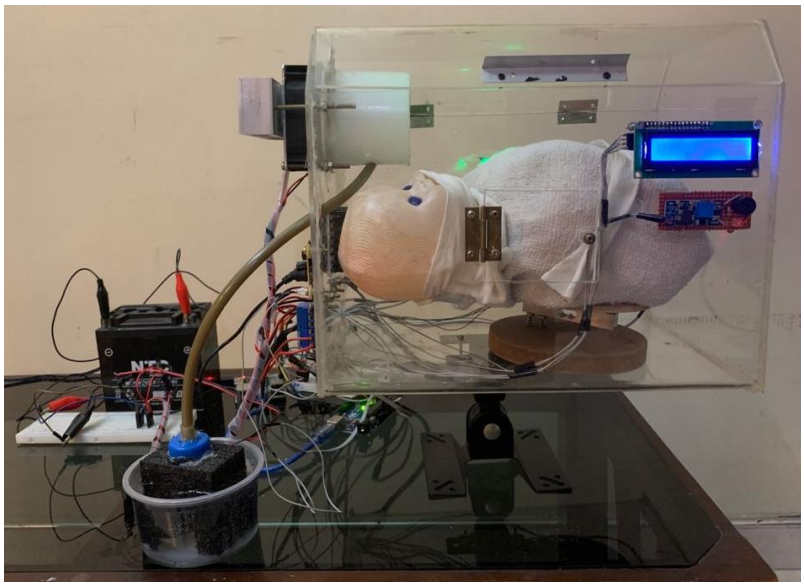

Figure 3.1: Proposed Prototype of the incubator.

3.1 Interior conditions controlling

The interior conditions depend on the infant's postnatal age and birth weight. The system scale was calibrated with a known weight by following the system instructions. When the system displayed as 'Keep baby >>> Press Enter' the system started to read the baby's initial details. The postnatal age of the baby in days and weeks were requested from the system and the details were input via a keypad on the first time when the system was started.
The reference values were stored in the system as comma-separated values (CSV) files as shown in figure 3.2. As the system and process were not dependent on the past records and no need of connecting databases analysis parts to make the procedure complex. The reference data was simply attached as CSVs and the easy updating. The matching row and reference data were found by the system according to the age and the birth weight of the baby.

id	weight	values
1	1000	10:35-11:34-14:33
2	1500	10:35-11:34-14:33
3	2000	10:34-18:35-14:33
4	2500	2:34-19:33
5	3000	2:33

Figure 3.2: CSV file contains the data storage

The 'id' is the key for the matching row. The values were stored in a format of 'duration (in days): reference value – next duration: reference value' etc.

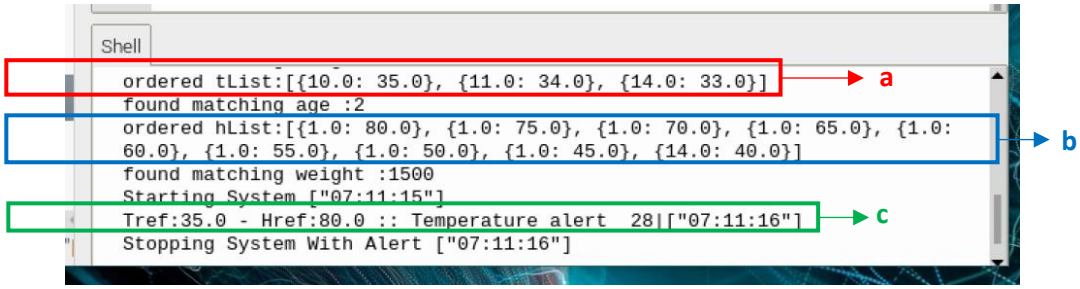

Figure 3.3: CSV file contains the reading of the birth weight of the baby, the reference values, and the duration.

First, The matching row, duration, and reference values were obtained. The matching temperatures and duration were shown in the array in box (a), and the matching humidity values and duration were shown in the array in box (b). As shown in box (c) it was alerted as the reference temperature (Tref = 35.0) was not matched with the current temperature (28).
These steps were completed within less than five minutes and the time was saved compared to the manual process as the operator should do set-ups after checking out the textbooks, etc. Due to the automation, there was no need to take out the baby several times to measure weight when needed. The heater was turned on to increase the temperature within the incubator as shown in figure 3.4 (a). The cooling system was turned ON when the current temperature was higher than the reference temperature as shown in figure 3.4 (b).

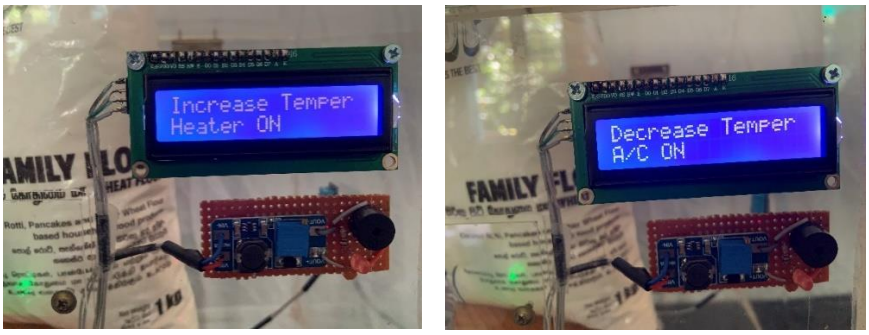

(a) (b)

Figure 3.4: (a) The heater was turned ON. (b)The Peltier and the fan were turned ON.

Then the system was set up according to the retrieved values. If the current values do not match with the retrieved data, the system fixes it automatically. The interior humidity level was controlled by the mist maker module and the cooling fan. If the current humidity level was lower than the reference level, the humidity level was increased by the mist maker as shown in figure 3.5.

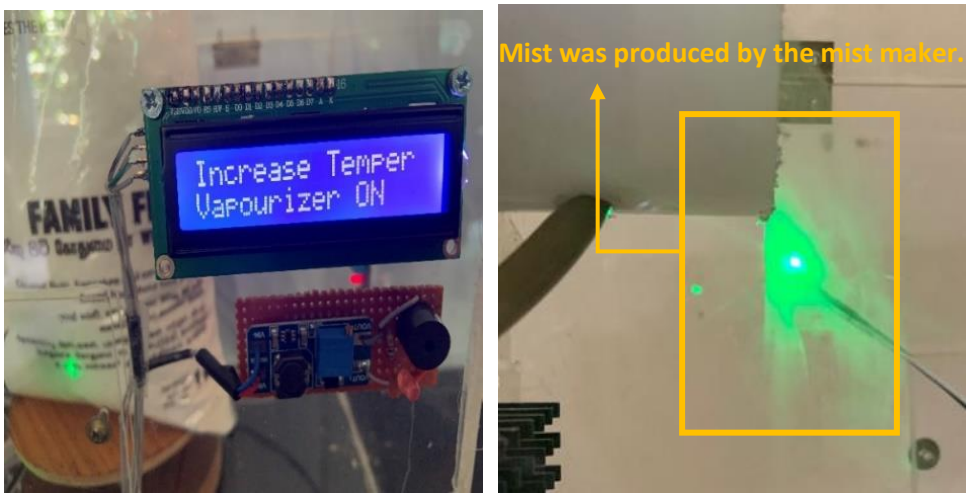

Figure 3.5: Mist maker was turned ON.

The current interior conditions of the incubator were displayed on the LCD. The current postnatal age and the current weight of the baby were also displayed as shown in figure 3.6.

Figure 3.6: The incubator parameters and the baby's conditions were displayed.

The implemented system could be operated easily by any authorized person without any specific training or practice. The proposed incubator was maintained with the aid of the system without being manually observed all the time.

3.2 Baby's conditions

The baby's conditions were checked continuously. The set-up was included with a temperature sensor (DS18B20), a pulse rate sensor, and a vibration sensor. DS18B20 sensor was worn around the baby's abdominal by using a wrapper around belt. The baby's body was touched by the sensor with care since the belt and the sensor give the approximately accurate value. The Baby's temperature was displayed using an LCD screen. If the abdominal temperature did not match with the reference value, it was indicated that the baby is not healthy and immediate treatments were needed.

The pulse rate of a healthy baby was continued between the BPM (Beats Per Minute) values 120 to 160. If the baby's heartbeat was not within this range, it was considered that the baby is in a danger. The rise of the baby's BPM was the only option to identify the seizure condition in modern incubators. But the implemented design was consisted of a motion detector too to identify the unusual movements of the baby. The critical conditions were notified by using a buzzer. Otherwise, the seizure conditions needed to be identified manually. Sometimes the incubator was covered up for some lighting conditions. This type of automated systems are very advantageous in a situation like when an incubator needed to be kept fully covered due to some medical reasons.

Because the seizure conditions and other main critical conditions could be identified without being watched.

Several weeks were taken for the actual interior condition checking and for the maintaining process. It was difficult to show the process with real duration. Therefore, the system was programmed with the assumption, a scale of one second equals one day. The duration variable in the program can be adjusted to a suitable scale.

3.3 Self-balancing

The implementation of the self-balancing option was implemented by using a simple structure. When the bottom plate was in an unbalanced position, it was identified by a gyroscope sensor and the upper plate was always kept parallel to the ground with the help of a servo motor. The upper plate was self-balanced when the bottom plate was unbalanced. Self-balancing for both sides was implemented as shown in figure 3.7.

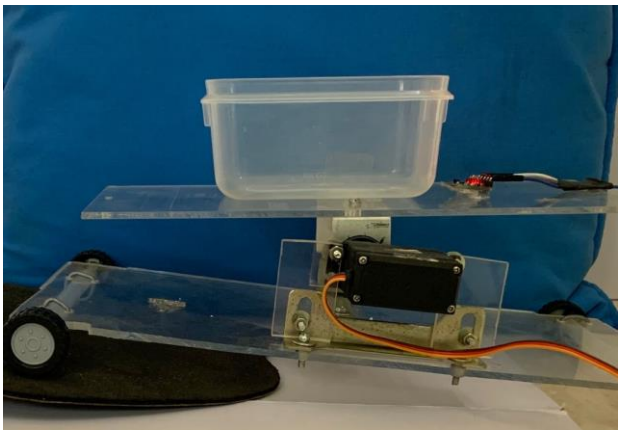

Figure 3.7: Self-balancing of the upper plate when the bottom plate was moved to an angle.

The self-balancing technique is helpful during quick transportation as the baby's bed can stay well-balanced parallel to the x-axis without causing any unnecessary movements of the baby. Therefore, there is no need of making the baby uneasy by tightening with the use of belts. As the implemented incubator is portable, there is no need for extra preparation for transportation. Immediate transportation is possible when needed.

4.0 CONCLUSION

The implemented design consisted of a self-balancing option, an automated conditional controlling system, and a critical condition notifying system. The balancing of the baby's bed along the x-axis was maintained by the self-balancing option when the incubator supporter was not moving on a flat surface. The risky movements of the baby during transportation of the incubator were protected due to this technique. The interior conditions were maintained by the automated condition controlling system depending on the baby's weight and postnatal age. Without using external scales, it was able to measure the weight of the baby inside the incubator allowing baby to be protected from the higher probability of getting infected from germs. Due to the automated interior condition setup, time and manpower can be saved compared to manual setups through logs or textbooks. The unusual conditions and the movements that occurred, they were notified via an emergency buzzer. The probability of identifying critical conditions of the

baby was increased by the automated notification system. Therefore, the users can direct the baby to immediate treatments without risking the baby's life.

All the components including Peltiers, fan, and mist maker module which were used to control the interior conditions were operated with a 12 V battery. The implemented system can be made portable due to this low voltage consumption and less number of power suppliers. The current study can be further developed to improve the efficiency allowing practical application and commercialization. In that regard, self-balancing can be improved by concerning all three axes which will make it more comfortable for the baby, especially during transportation. Moreover, developing a mobile application will make it easier to observe and maintain the interior conditions manually. The proposed automated incubator system will be efficient and be more accurate than a manual process.

Even though this proposed study has proven to be very fruitful and timely, it is important for this system to be further studied before applying it in an actual setting. When using with infants to improve and verify the system's reliability, more experiments can be conducted with varying conditions such as changing ambient conditions, stability of the instrument in actual transportation situations, and implementing a UV sterilizing unit. Advancement of this initial study, will lead to betterment of society.

ACKNOWLEDGEMENT

Authors would like to express sincere gratitude and appreciation to Dr.Vindya Subasinghe for the guidance and support provided. Authors would also like thank Academic Staff of Faculty of Applied Sciences, Wayamba University of Sri Lanka for their expert advise.

REFERENCES

[1]. Shaib, M, Rashid, M., A., Hamawy, L., Arnout, M., Majzoub, I., E., Zaylaa, A., J., Advanced portable preterm baby incubator, *Proc. Fourth International Conference on Advances in Biomedical Engineering (ICABME), Beirut, Lebanon*, 2017, 5836.

[2]. Sri Lanka Infant Mortality Rate 1950 – 2020, *Macrotrends*, (2020), https://www.macrotrends.net/countries/LKA/sri-lanka/infant-mortality-rate, (Accessed 10. 05.2021).

[3]. Subramanian, M., Sheela, T., Srividya, K., Aruselvam, D., Security and health monitoring system of the baby in incubator, *International Journal of Engineering and Advanced Technology (IJEAT)* 8/6, (2019), 3582, DOI: 10.35940/ijeat.F9353.088619.

Proc. Annual Symposium on Research & Industrial Training, 08(2021) 32-39
Department of Electronics – Wayamba University of Sri Lanka

LOW-COST LIQUID DENSITY SENSOR SOLUTION TO AUTOMATE THE PHOSPHORIC ACID RECOVERY PROCESS OF ACTIVE CARBON

K.A.S. Dilshan*, Y.A.A. Kumarayapa

Department of Electronics, Wayamba University of Sri Lanka, Kuliyapitiya, Sri Lanka

*dilshan162185@wyb.ac.lk

ABSTRACT

Haycarb (PLC) is one of the world's largest coconut shell-derived activated carbon manufacturers accounting for approximately 17% of the global production. In Haycarb (PLC) activation process, 85% of the used acid is recovered and reused to meet the expected cost of production. The acid recovery process which is used in Haycarb (PLC) is currently done manually by operators and the degree of recovery is dependent on the work skills. Therefore, many errors can be occurred and, it consumes more time. This acid recovery system operates based on the density of phosphoric acid. Although density sensors can be used to automate this system, the existing density sensors in the industry are very expensive. As a solution to the above problems, a low-cost sensor and a microcontroller-based automation system were successfully simulated to measure the density of phosphoric acid, which is important for automating the acid recovery process. Two methods were studied to determine the density of phosphoric acid, based on the angle of deviation and absorbance. In the angle of deviation-based method, it was observed that the angle of deviation of the laser beam through the prism was increased, when the density of phosphoric acid was at 5 Baume(B^0), $10B^0$, $20B^0$, $30B^0$, $35B^0$, $45B^0$, $55B^0$, and $60B^0$, respectively. The drawback of this method is the system size is not suitable for an industrial density sensor unit. Therefore, the second method (absorbance) was further studied. In the second method, a significant change in absorbance was observed at above different density points. Currently, the second method can be used to determine the density of an unknown phosphoric acid sample in the density range $0B^0$ to $60B^0$. This system can be used to measure approximately $\pm 2B^0$change in the density. Then microcontroller based automation system was developed to automate the recovery process with density feedback.

Keywords: Automated acid recovery, Density sensors, Angle of deviation - absorbance techniques

1.0 INTRODUCTION

The carbon activation industry is one of the rapidly growing research-based industries in the world. Activated carbon is used widely in water treatment, food and beverage, healthcare, automotive industries, and industrial processing. The carbon activation process is the most important in the activated carbon production. In this activation process, expensive activation agents such as phosphoric acid and zinc chloride are used as catalyzers. So, at the end of this activation process, the used activation agent can be recovered. This important process is called the acid recovery process in the activated carbon industry [1,2,3].

Haycarb (PLC) is a world's leading manufacturer and marketer of coconut shell activated carbon. Accounting for over 17% of the global market share, the company has an annual capacity of over 50,000 metric tons of activated carbon. Haycarb manufactures a complete range of standard, washed and impregnated granular activated carbon, powder activated carbon and extruded pellet activated carbon [4]. In the Haycarb activation process, phosphoric acid is

used as an activating agent to produce activated carbon. However, this acid is not consumed during the activation process. Therefore, the used acid in the activation process can be recovered. According to the research and development of Haycarb, 85% of the used acid needs to be recovered and re-used to meet the expected cost of production [4]. In the Haycarb acid recovery process, currently operates manually by the laborers. This causes some delays and reduces the efficiency of the acid recovery process, and it affects their expected cost of production. Therefore, these problems can be minimized by automating the acid recovery system. This acid recovery system operates using different density levels of phosphoric acid. Although density sensors can be used to get important density feedbacks to automate this system, the existing density sensors in the industry are more expensive price range of $800-$1300, but involve human laber with errors. To solve the above problems, this study was carried out for designing a low-cost sensor solution for measuring the density of phosphoric acid, which is important for automating the acid recovery process.

2.0 EXPERIMENTAL

Two methods were studied to determine the density of phosphoric acid, based on the angle of deviation and absorbance.

2.1 Angle of deviation measurements

2.1.1 Preparation of Samples

The 'Baume' scale is a pair of hydrometer scales used to measure the density of liquids in the industry. The 'Baume' unit (B^0) of measurement was used instead of the standard unit used to measure the solvent density. Samples of $5B^0$, $10B^0$, $20B^0$, $30B^0$, $35B^0$, $45B^0$, $55B^0$ and, $60B^0$ were prepared at 25 ^{0}C temperature by mixing pure phosphoric acid with distilled water.

2.1.2 Experimental Setup

A hollow prism and a 650 nm wavelength laser source were used as the tools of this setup. As shown in Figure 2.1, the angle of deviation caused by the (semi) transparent liquid can be measured by introducing the liquid into a hollow prism.

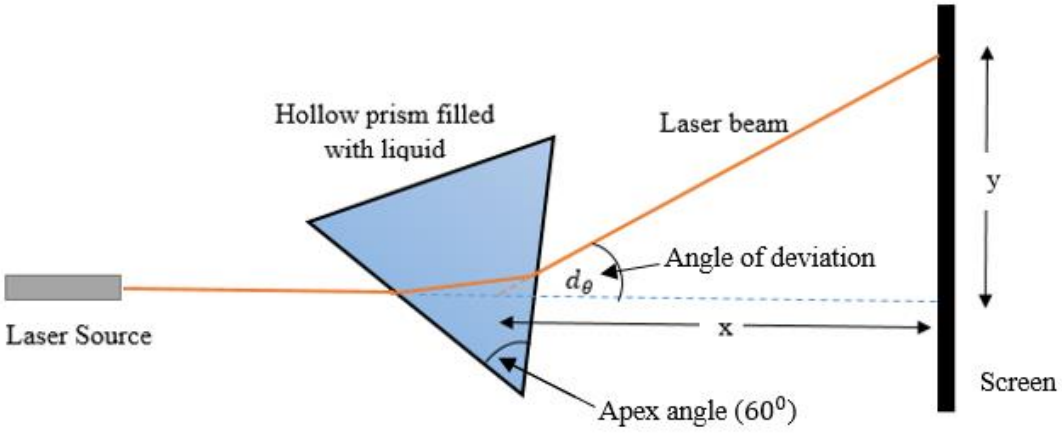

Figure 2.1:Top view of the experimental setup for measuring deviation angle of liquid acid samples

Initially, the laser beam was recorded on the screen while the prism was empty. The 5 B^0 phosphoric acid samples were filled into the prism and the deviation of the laser beam was recorded. Similarly, 10 B^0, 20 B^0, $30B^0$, $35B^0$, $45B^0$, $55B^0$ and, $60B^0$ samples were separately filled into the prism and the laser beam deviation was recorded.

2.2 Absorbance measurements

2.2.1 Preparation of samples

The phosphoric samples with the densities of 5 B^0, 10 B^0, 20 B^0, 30 B^0, 45 B^0, and 60 B^0 were prepared at 25 ℃ temperature by mixing pure phosphoric acid with distilled water. UV spectrometer measurements were obtained for each prepared sample.

A 50 ml equivalent volume of each prepared sample of phosphoric acid were added to 6 beakers separately. Six equal quantities of 100 mg of carbon were measured by a chemical scale. The measured equal amounts of carbon were mixed into the six beakers containing phosphoric acid samples simultaneously and separately. After six hours, samples were filtered by using 0.45 µm different font type size filter paper to remove carbon. The UV spectrometer measurements were obtained for each filtered 6 samples (5 B^0, 10 B^0, 20 B^0, 30 B^0, 45 B^0 and 60 B^0). The reason for obtaining a spectrum for samples of phosphoric acid mixed with carbon was to determine whether there is a change in the chemical properties of the phosphoric acid after forming the carbon solution.

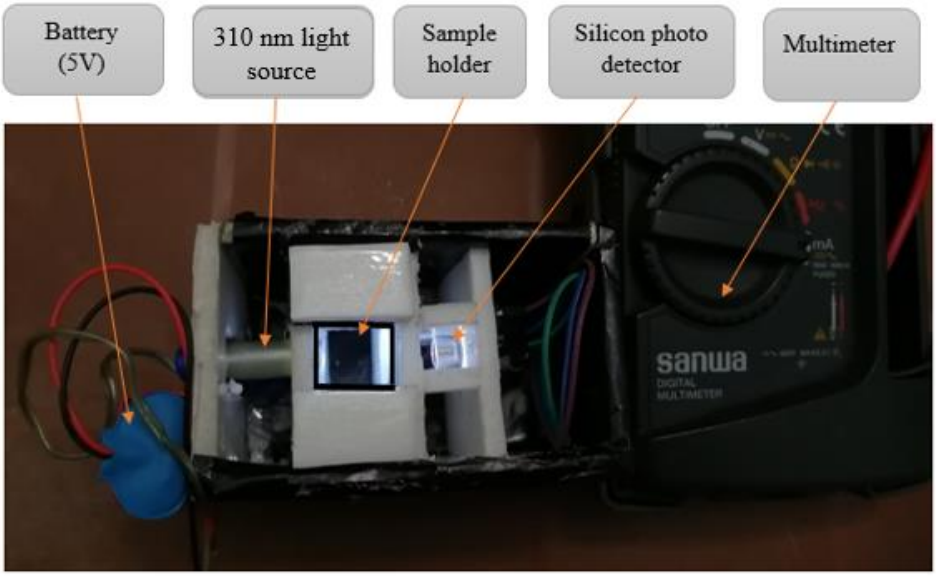

Figure 2.2: Experimental setup for optical measurements taken under darkroom conditions

Initially, the photodetector reading was obtained when the cuvette holder was empty. The photodetector current was obtained by adding distilled water as a reference sample to the cuvette holder. The prepared 5B^0 the sample was placed into the cuvette holder and the photodetector current was measured. Likewise, photodetector currents were measured for other prepared 10 B^0, 20 B^0, 30 B^0,45 B^0, and 60 B^0 samples. All these readings were performed at a constant temperature of 25 ℃ and fully covered the dark mode system. The transmission and absorbance readings were calculated for each sample data. The baseline for calculated transmission and corresponding density were plotted.

2.3 Automation of the acid recovery system

The automation circuit was successfully designed by using Proteus simulation software for the acid recovery process. The atmega328 microcontroller was used as the controlling unit. A Liquid-crystal display (LCD) was interfaced to the microcontroller for monitoring the liquid density variation from the beginning to the end of the process while monitoring each stage of the process taking place at that moment. A potentiometer was used instead of the density sensor

to get density feedback for the automation. LEDs were used to represent the output signals at different density levels.

3.0 RESULTS AND DISCUSSION

3.1 Angle of Deviation Measurement

The laser beam deviations caused by phosphoric acid samples of different densities in this experiment are shown in Figure 3.1 and Figure 3.2 below. Figure 3.1 shows the observed laser beam deviation data when the prism was empty and the 5 Baume sample was in the prism (first point). Figure 3.2 shows observed changes in the deviation of the laser beam (from the first point) at each phosphoric acid density sample.

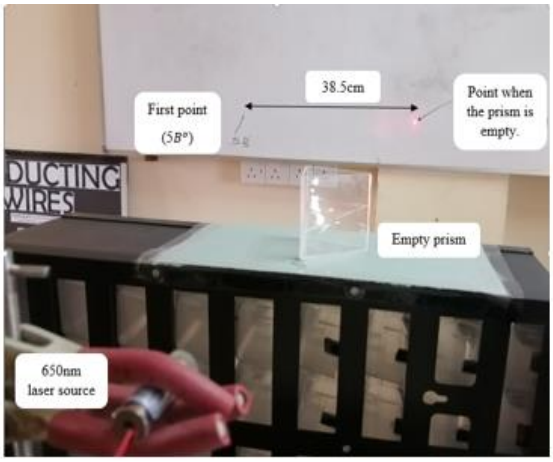

Figure 3.1: Observed laser beam deviation data when the prism was empty and the 5 Baume sample was in the prism.

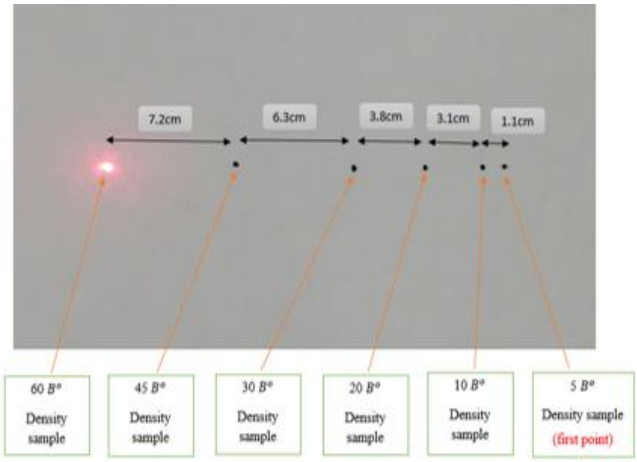

Figure 3.2: Observed changes in the deviation of the laser beam at each phosphoric acid density sample.

When the prism was empty, the point at which the laser beam pointed on the screen was taken as the reference value. That point is marked in Figure 3.1. After placing the 5 B^o phosphoric acid sample in the prism, the laser beam deviated 38.5 cm from the reference value. After placing the $10B^o$ phosphoric acid sample in the prism, the laser beam deviated linearly 1.1 cm above the deviation point of the 5 B^o sample. Similarly, the refracted laser beam of the 20 B^o, 30 B^o, 35 B^o, 45 B^o, 55 B^o and 60 B^o phosphoric acid samples were deviated from the refracted point of the previous sample linearly and respectively as shown in Figure 3.2.

The deviation angle data of the laser beam due to different densities of phosphoric acid samples are given in Table 3.1 below. The graph drawn for this data is illustrated in Figure 3.3 below.

.

Table 3.1: Calculated angle of deviation and standard deviation of errors for different phosphoric acid densities.

Phosphoric acid density (B^0)	Angle of deviation (d_θ)	Standard deviation (1×10^{-3})
5	15.974^0	$\pm 22^0$
10	16.405^0	$\pm 18^0$
20	17.613^0	$\pm 25^0$
30	19.072^0	$\pm 12^0$
35	20.130^0	$\pm 31^0$
45	21.433^0	$\pm 35^0$
55	22.423^0	$\pm 29^0$
60	24.041^0	$\pm 33^0$

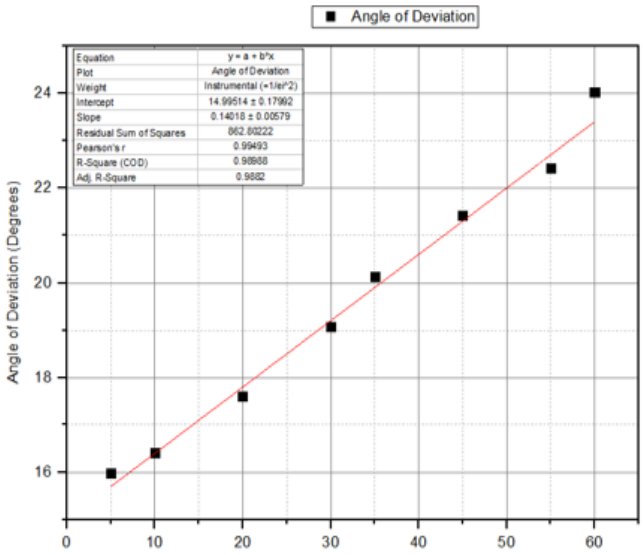

Figure 3.3: The graph of deviation angle (Degrees) vs density (B^0) of the different

The above graph shows a directly proportional relationship between the angles of deviation with the phosphoric acid density. The following equation was derived by using the experimental data plotted in the graph, Figure 3.3. The intercept and gradient values of the derived equation were obtained by using the origin software.

$$Y = (0.140 \pm 0.006)X + (14.995 \pm 0.180) \ldots\ldots\ldots\ldots\ldots (1)$$

where, Y = Angle of deviation
X = Density of liquid phosphoric acid

As the density of liquid phosphoric acid increased, the angle of deviation of the laser beam through the prism was increased. This is well illustrated by Figure 3.3 above. If it is known the angle of deviation of an unknown phosphoric acid sample, the density can be found by using this relationship. The drawback of the angle of deviation-based method was the system size is not suitable for an industrial density sensor unit. A very small phosphoric acid density differences were difficult to measure properly due to the deviated angle was too small. It was able to gain a measurable angle of deviation for relatively a small density difference by increasing the radius of the angle circle (In Figure 2.1 the distance between the prism and screen). Therefore, the space of the experimental setup is needed to increase and the size is not suitable for an industrial density sensor unit. Since it is shown a better deviation with the density, a device for measuring fluid density can be successfully developed using the angle of deviation method.

3.2 Absorbance measurements

The UV spectrum analysis was done for several prepared phosphoric acid density samples without mixing carbon and then for phosphoric acid samples mixed with the carbon and after filtering. Then, using several UV spectrum analysis graphs, it could be observed that the peaks for both types of samples were occurred around 310 nm wavelength. Further, a large absorption band corresponding to the different densities of phosphoric acid is observed around 310 nm. Moreover, it is observed that a small absorption band around 300 nm increases with

increasing the phosphoric acid density. Hence, a light source with a wavelength of 310 nm and a 530 nm peak response photodetector were selected for carrying out the research study.
The reason to above similar variation of absorption can be explained as follows. Phosphoric acid promotes bond cleavage reactions and a reactant in the formation of crosslinks via processes, such as cyclization and condensation [3,10]. That is, the chemical properties of phosphoric acid do not change significantly after carbon mixing.

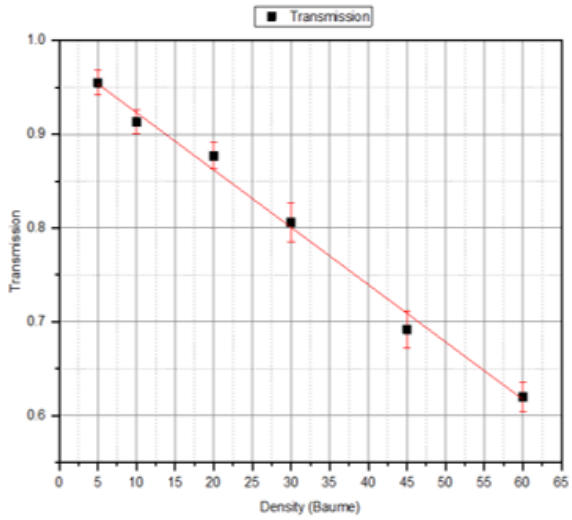

Figure 3.4: The graph of transmission vs density (B^0) of phosphoric acid samples.

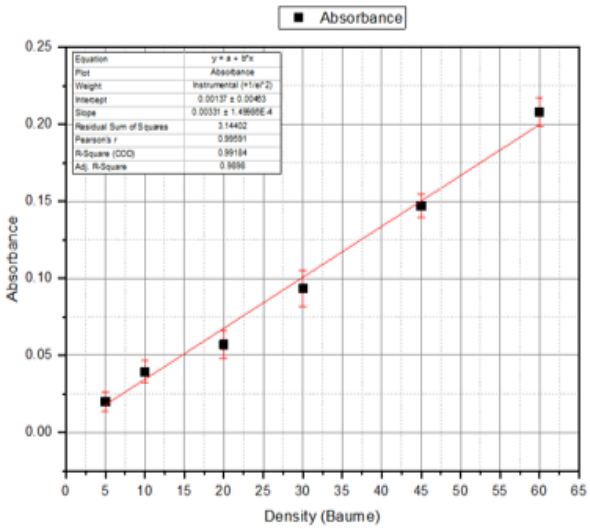

Figure 3.5: The graph of absorbance vs density (B^0) of phosphoric acid samples.

Figure 3.4 above shows the relationship between the density of phosphoric acid and the corresponding calculated transmission values. An inversely proportional relationship between phosphoric acid density and transmission was observed. The results obtained were agreed with the standard results obtained with the experimental setup in [5]. The attenuation of light occurs either as a result of distance through a solution or increasing concentration. In our study, the distance through the solution is constant due to the use of the same sample holder for obtaining observations. Therefore, light attenuation only depends on the concentration of the solution. And concentration is proportional to the density of the sample [5]. So, the transmission is decreased with the increasing density of the solution.

As shown in Figure 3.5, a directly proportional relationship was obtained between the absorbance with respect to the phosphoric acid density as reported by many other researchers [5, 6]. One factor that influences the absorbance of a sample is concentration. When concentration goes up, it is affected to increase the attenuation. It is caused to absorbe more radiation. Therefore, the absorbance is directly proportional to the concentration [7, 9]. The equation of the graph drawn for the obtained experimental data is as follows.

$$Y = (33.1 \times 10^{-4} \pm 1.5 \times 10^{-4})X + (13.7 \times 10^{-4} \pm 46.3 \times 10^{-4}) \ldots (2)$$

where, Y = Absorbance
X = Density of liquid phosphoric acid

This relationship between density and absorbance can be used to determine the density of an unknown phosphoric acid sample. Currently, this system can be used to determine the density

of an unknown phosphoric acid sample in the range of $0B^0$ density to $60B^0$ density and it can accurately measure a change in the density of approximately $\pm 2B^0$. However, successfully developing this method further, a device for measuring fluid density can be developed.
The current density sensors on the market are in the price range of $800-$1300. A density sensor can be designed at the cost of approximately $300-$600 by developing this method and using the more qualitative device components. This will be highly profitable for density sensors which are required industry.

3.3 Automation System
Our proposed automation system could be successfully designed and simulated by using Proteus simulation. The operation of the basic and important output signals were studied according to the input signals in the automation of the acid recovery process. This system can be further improved and applied for acid recovery system automation. Following Figure 3.6 shows the Proteus simulation circuit diagram for the proposed automation system.

Currently, Programmable Logic Controllers (PLCs) are mainly used for industrial automation and, they will cost more. But this acid recovery system can be successfully automated using microcontrollers. Therefore, the cost of using PLCs can be greatly reduced by using microcontrollers.

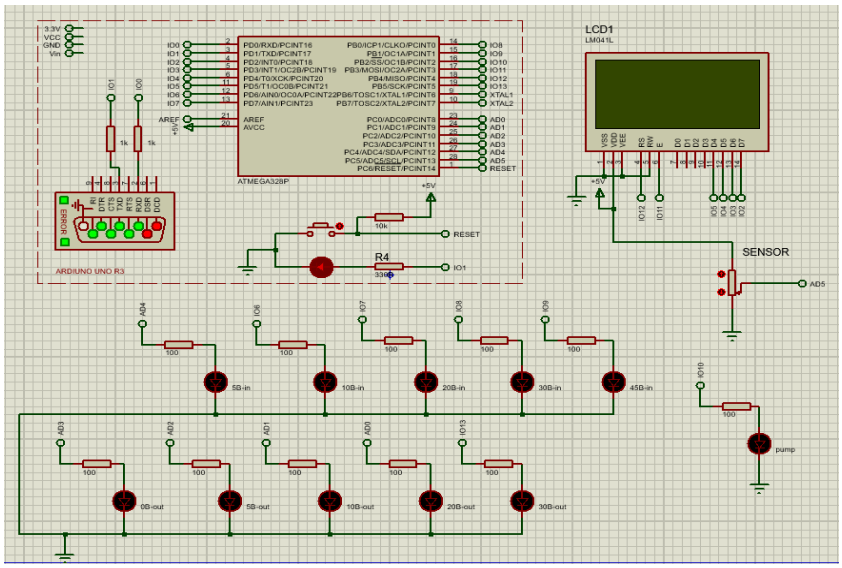

Figure 3.6: The simulation circuit diagram for illustrating the prototype of acid recovery process

4.0 CONCLUSION

A low-cost sensor implementation technique and a microcontroller-based automation system were proposed and experimentally studied to measure the density of phosphoric acid, which is important for automating the acid recovery process, in the production of activated carbon. Two techniques were proposed and the systems were designed to determine the density of phosphoric acid, based on the angle of deviation and absorbance. Although there was a good variation in the angle of deviation with acid density, the problem with its implementations were studied in practice. Because very small phosphoric acid density differences were difficult to measure properly due to the deviated angle was too small. Therefore, the second method was used for further study due to its accuracy for determining the density of phosphoric acid more practically than the first technique. In the second method, a significant change in absorbance

was observed at 5 B^0, 10 B^0, 20 B^0, 45 B^0, and 60 B^0, which are the important density points of the acid recovery process. Currently, this system can be used to determine the density of an unknown phosphoric acid sample in the range of 0 B^0 density to 60 B^0 density. This system can be measured approximately $\pm 2B^0$change in the density. The accuracy of our proposed experimental technique can be further enhanced by using a photodetector with a suitable peak response such as 310 nm, instead of the photodetector available at present. A microcontroller-based automation system was developed to automate the acid recovery system using density feedback. Our second method based on absorbance can be further developed and used to obtain significant density feedbacks required to automate the acid recovery process.

ACKNOWLEDGMETNS

It is a pleasure to acknowledge Prof. C.A.N. Fernando, Dr. Murthi S.Kandanapitiye and, Dr. R.D.A.A. Rajapaksha of the Department of Nano- Technology, Wayamba University of Sri Lanka for their research guidance. Haycarb (PLC), Sri Lanka is highly acknowledged for providing research problem with necessary material solution samples. Also, our thanks were given to all the members of Electronics Laboratory, Wayamba University of Sri Lanka.

REFERENCES

[1]. Van Oss, C.J., Bansal, R.C., Donnet, J.B., Stoeckli F., Dekker, M., A Review of: 'Active Carbon.', *Journal of Dispersion Science and Technology*, 11/3, (1990), 323, doi:10.1080/01932699008943255.

[2]. Yakout, S. M., El-Deen, G. S., Characterization of Activated Carbon Prepared by Phosphoric Acid Activation of Olive Stones, *Arabian Journal of Chemistry*, 9, (2016), S1155–62, doi:10.1016/j.arabjc.2011.12.002.

[3]. Rodríguez-Reinoso, F., Sepúlveda-Escribano, A., Porous Carbons In Adsorption And Catalysis, *Handbook of Surfaces and Interfaces of Materials*, 9, (2001), 309-311, doi: 10.1016/b978-012513910-6/50066-9.

[4]. Haycarb (PLC), Activated Carbon Resources & Library | Haycarb PLC, https://www.haycarb.com /document-library, (Accessed 2020-09-21).

[5]. Edinburgh Instruments Ltd, Beer Lambert Law | Transmittance & Absorbance, Edinburgh Instruments, (2021), www.edinst.com/blog/the-beer-lambert-law, (Accessed: 2021-01-18).

[6]. Mayerhöfer, T. G., Pipa, A. V., Popp, J., Beer's Law-Why Integrated Absorbance Depends Linearly on Concentration, *ChemPhysChem*, 20/21, (2019), 2748–53, doi:10.1002/cphc.201900787.

[7]. Kittipanyangam, S., Abe, K., Eguchi, K., Design of a Measurement Device Explaining the Relationship between the Concentration of Solution and the Light Absorbance for Chemical Education, *2016 13th International Conference on Electrical Engineering/Electronics, Computer, Telecommunications and Information Technology (ECTI-CON)*, (2016)., doi:10.1109/ecticon.2016.7561271.

[8]. Mäthger, L.M., Hanlon, R.T., Malleable Skin Coloration in Cephalopods: Selective Reflectance, Transmission and Absorbance of Light by Chromatophores and Iridophores, *Cell and Tissue Research - SCI journal*, 329/1, (2007), 179–86, doi:10.1007/s00441-007-0384-8.

[9]. Yu, S.J., Ha, S.R., Cheon, S.U., Hwang, J.Y., Relationship Between Allochthonous Doc Concentration And A Specific Uv254 Absorbance (SUVA) At A Meso-Stratified Reservoir, *Journal of Water and Environment Technology*, 1/1, (2003), 111-117, doi:10.2965/jwet.2003.111.

[10]. Baghel, A., Singh, B., Pandey. P., Gutch, P.K., Preparation and Characterization of Active Carbon Spheres Prepared by Chemical Activation, *Carbon*, 49/14, (2011), 4739-4744, doi:10.1016/j.carbon.2011.06.080.

Proc. Annual Symposium on Research & Industrial Training, 08(2021) 40-46
Department of Electronics – Wayamba University of Sri Lanka

ELECTRONIC CHEST PROTECTOR SYSTEM FOR TAEKWONDO

W.A.A. Dilshan*, P.M. Senadeera

Department of Electronics, Wayamba University of Sri Lanka, Kuliyapitiya, Sri Lanka

*arunadilshanfernando@gmail.com

ABSTRACT

Taekwondo is the most popular martial art in Sri Lanka as well as in other countries. This martial art has two parts; namely poomsae and sparring. Only the sparring parts are considered for this project. There are two players and four referees in the sparring section, and the points are awarded to the athletes under the supervision of the referees. The two players are dressed in blue and red trunk protectors, and players are awarded points based on the power and sound of the layer hitting of the protector. But sometimes, referees may not able to award points accurately because of the attacking speed of the players. So in that case, it is a disadvantage for the players. Hence, the protector should use digital technology.At present, it is used only for international or national competitions, because of its high price. Therefore, if the players want to participate for those competitions, they have to be trained from the expensive system. This highlights the necessity of a low cost electronic chest protector system to solve this problem. This proposed system automatically scores points on the computer screen for a player's attack. Final system was mounted on the player's protector and the correct kick was detected according to the attacking force of the interlocutor. Final results of the system, consisted of the attacker's kicks were detected by the opponent's protector. The corresponding marks were displayed on the computer screen. As a result, taekwondo players in the taekwondo institution could get proper training through this proposed electronic chest protector system.

Keywords: Taekwondo, Chest, Protector

1.0 INTRODUCTION

Taekwondo is the art of self-defense that originated in Korea. The name is selected for its appropriate description of the art: Tae (foot), Kwon (hand), and Do (art) [1]. In taekwondo competitions, the target is to land kicks and punches upon the scoring zones of your opponent. They are torso and head. Both kicks and punches must be accurate and powerful, because the light tapping kicks are not counted by scorers (or electronic scoring system in major competitions). At the end of the third round of the match, the player with the highest points is declared as the winner, but the match can be over early by one player knocking out the other player [2]. The same basic principles from SooBak and Won Kang's teachings are the foundation for the modern taekwondo. As the name implies, taekwondo focuses on hand and foot techniques centered around kicking, punching or striking, and blocking. However, the taekwondo philosophy also embraces principles such as integrity, respect, and self-control. While each taekwondo school varies slightly on curriculum, students generally learn Sparring, Poomsae, and Breaking techniques. These techniques were introduced to demonstrate power and skill [2]. Sparring technique was considered for this project.

In Taekwondo competitions, fighters of same sex compete each other. They are grouped into weight categories to ensure that fights are evenly matched as much as possible. In junior competitions, there may be age categories too. The white taekwondo uniform is often called a gi, but technically the Japanese name for a martial arts uniform and the proper Korean term is a dobok. A colored belt is tied round the middle of the dobok and the color signifies the grade of the practitioner. The belt system goes from white for beginners through to yellow, green, blue,

red and then black for more experienced practitioners. Black belts receive their 'dan' grades as they progress further with their experience and expertise. In a Taekwondo match, each competitor wears several pieces of protective equipment and they are Head guard, Chest (trunk) protector, Groin guard, Forearm guards, Hand protectors, Shin guards and Mouth guard [2].

- Trunk: The blue or red colored area of the trunk protector
- Head: The entire head above the bottom line of the head protector

Point(s) would be awarded when a permitted technique is delivered to the scoring areas of the trunk with a proper level of impact. Point(s) would be awarded when a permitted technique is delivered to the scoring areas of the head. The determination of the validity of the technique, level of impact, and/or valid contact to the scoring area would be made by the electronic scoring system except for the fist techniques. These electronic Protector Scoring System (PSS) determinations would not be subjected to Instant Video Replay. The WTF(World Taekwondo Federation) Technical Committee would determine the required level of impact and sensitivity of the PSS, using different scales such as weight category, gender, and age groups. In certain circumstances it is deemed necessary the Technical Delegate recalibrate the valid level of impact.

- The valid points
  - One (1) point for a valid punch to the trunk protector
  - Two (2) points for a valid kick to the trunk protector
  - Four (4) points for a valid turning kick to the trunk protector
  - Three (3) points for a valid kick to the head
  - Five (5) points for a valid turning kick to the head
  - One (1) point awarded for everyone "Gam-jeom" given to the opponent contestant

Match score would be the sum of points of the three rounds. The following prohibited act(s) give Invalidation of point(s).

1. Kicking below the waist
2. Attacking the opponent after "Kal-yeo"
3. Hitting the opponent's head with the hand
4. Butting or attacking with the knee
5. Attacking the fallen opponent
6. Attacking trunk PSS with the side or bottom of the foot having the knee pointed out in clinch position
7. Grabbing or pushing the opponent while kicking

When a contestant records points if prohibited act was followed by point(s), the referee would declare the penalty for the prohibited act and invalidation of the point(s) [2].

This game is very fast because it takes only one and half, two or three minutes. When players attack very fast at the same time, the referees will fail to score each attack. Therefore, electronic scoring systems have been developed using new technology to maintain the quality of the game. However the shortcomings of these devices have been reported. The most well-known and famous protector scoring systems available today were developed by KPNP and DAE DO companies. Their accessories were similar to each other and they include electronic chest protectors, electronic head gears, receivers, transmitters, electronic socks, judge boxes and software. The problems in these system were high cost [4-5]. Therefore a novel system was designed in this project to solve above problem. This application is not only a new scoring system but also provides a low cost solution for small clubs. The system was created to help

popularization of taekwondo martial art among the trainers, and to resolve the issues in the taekwondo clubs. Due to the above reasons, a low cost electronic trunk (chest) protector and electronic pair of socks were suggested for the domestic clubs. In this system, kicks are identified when a kick is attacked to the trunk (chest) protector. When a kick is made to the trunk protector, the corresponding marks are automatically marked on a computer display.

2.0 **EXPERIMENTAL**

The Figure 2.1 illustrate the components in transmitter side and how they work.

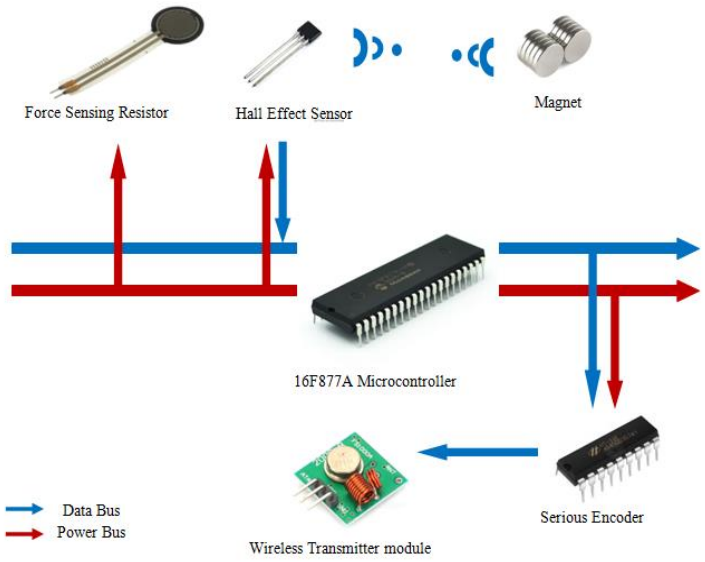

Figure 2.1: Block diagram of the transmitter side

The Figure 2.2 illustrate the components of the receiver side and how they work.

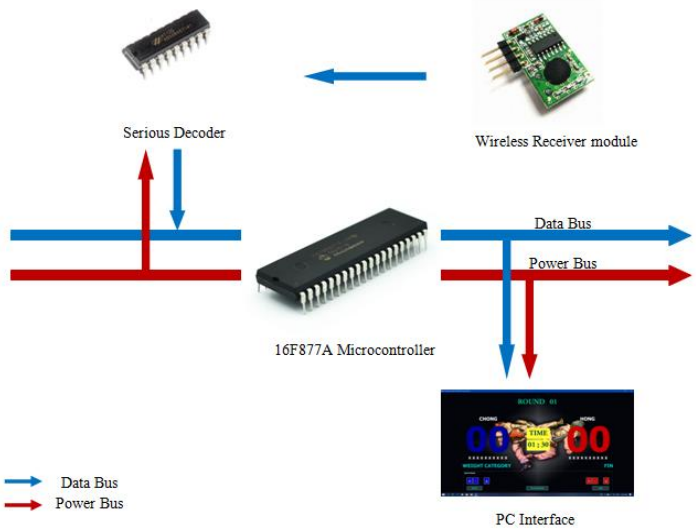

Figure 2.2: Block diagram of the receiver side

The electronic chest protector system consisted of two parts, the transmitter section and receiver section. The microcontroller in transmitter side identifies the kicks which are detected by the Hall Effect Sensor and FSR sensor. If it is a correct kick, a signal will be sent to the wireless transmitter through the series encoder. The transmitter section was mounted in the player's trunk

protector. The data which was transmitted by the wireless transmitter was received by the wireless receiver. After that the data was sent to the microcontroller through the series decoder. Then according to the received data, the points were increased on the computer screen. Computer software was designed to record player's scores, number of rounds played and time of the match.

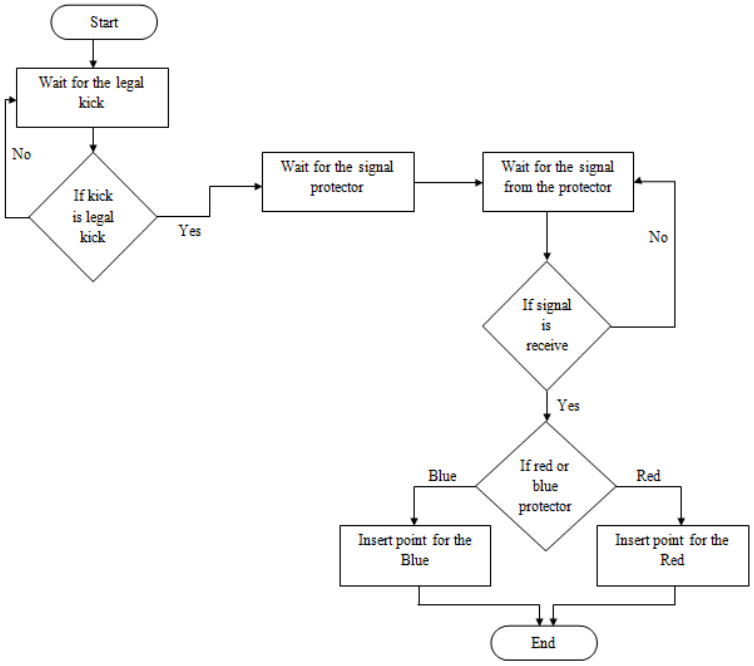

Figure 2.3: Flow chart for the System

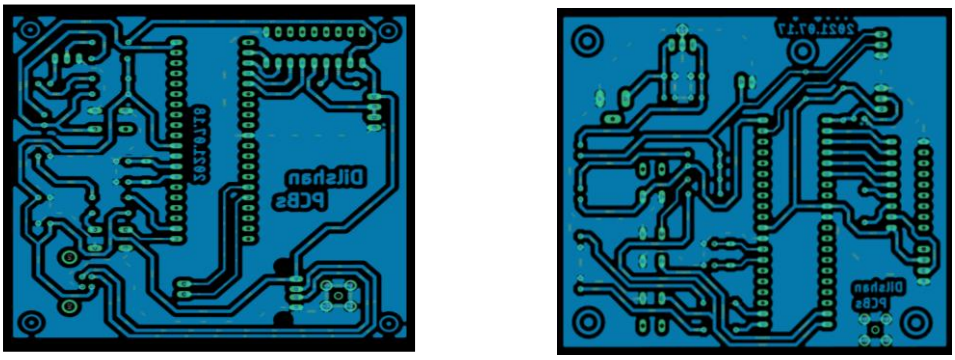

(a) (b)

Figure 2.4: PCB layout of the receiver circuit(a) and transmitter circuit(b)

Also this electronic trunk protector system contain a software to process and display the score. This software was created especially for this system and it was also a part of this system. In addition updating the details according to the data that obtained through the serial communication protocol was a main feature of this system. This software contains 4 panels called Startup Panel, Communication Setting Panel, Game Setting Panel and Score Panel. The Communication Panel and the Game Setting Panel have been linked to the Startup Panel. At first using the Communication Setting Panel, communication between microcontroller and the software must be established. After that, using Game Setting Panel, Score Panel must be linked through it. Also all the points related to a match was shown on this Score Panel. Also at the end of every match, the Startup Panel must be accessed before going to a new match. Otherwise it

cannot be started. There can be more software like this but this software has its own indigenous design. The whole software was designed on NetBeans IDE using Java language. The Java codes that used to implement some functions on Net Beans and its interfaces were shown below.

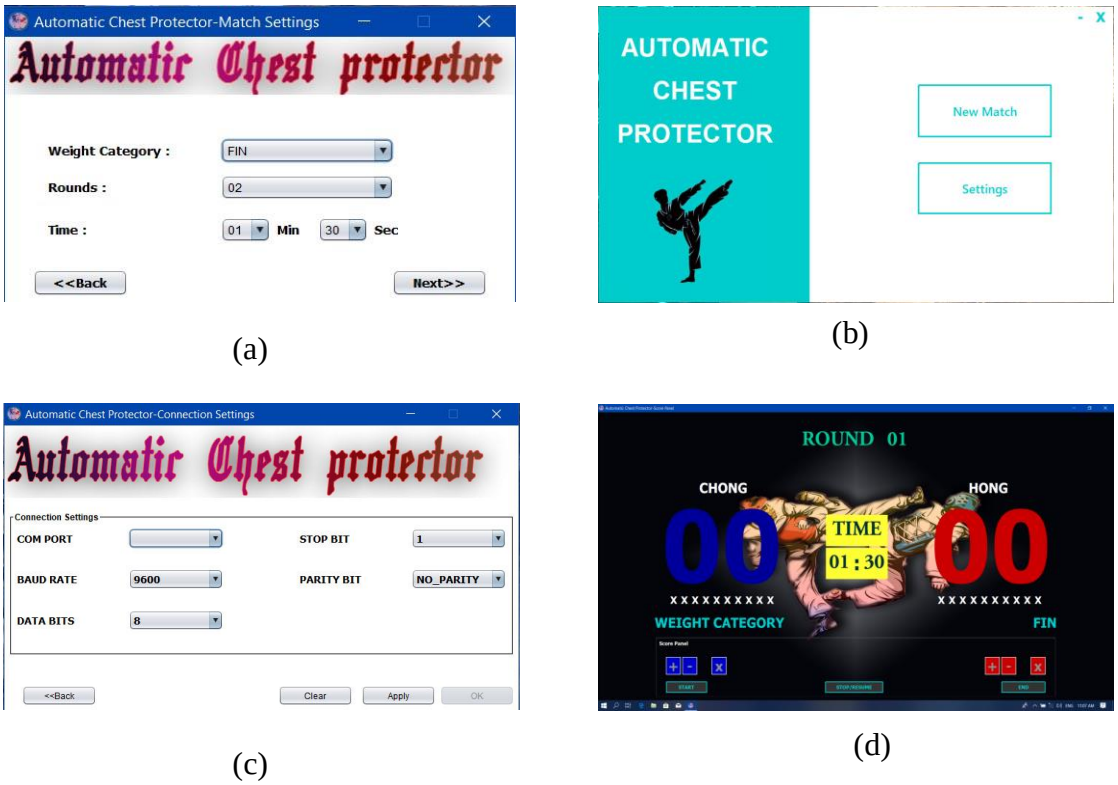

Figure 2.5: Interface of the Match settings(a), Interface of the Open match(b), Interface of the connection settings(c) and Interface of the Score panel(d)

The Figure 2.5 (c) shows serial communication connection between the microcontroller and the software. This window must be changed according to the communication port. A java code was used to develop Serial communication between MC and software,

```
public void serialConn(){
String[] portList = SerialPortList.getPortNames();
try{
serialPort = new jssc.SerialPort(portList[port]);
serialPort.openPort();
serialPort.setParams(BR,DB,SB,PB);
if(serialPort.isOpened()){
T.start();
JOptionPane.showMessageDialog(this, "Automatic Chest Protector System Has Been Connected Succesfully...!");
```

Window of the score panel shows the player's scores, weight category, time duration of the match, and match round. The match can be started, stopped, resumed and ended depending on the match situation. The matches were started when the START button was pressed and the

matches were stopped and resumed when the END and RESUME buttons were pressed respectively. Following java code was used for the point calculation.

```
public class Calculation {
 public String ScoreIncreaseByOne(String x){
 int a,b;
 String score="";
 a = Integer.parseInt(x);
 b=a+1;

 if(b>=10){score = Integer.toString(b);}

 if(b<10){score = "0"+Integer.toString(b);}

return score;    }
public String ScoreDecreaseByOne(String x){
 int a,b;
 String score="";
 a = Integer.parseInt(x);
 if(a>0){
 b=a-1;

 if(b>=10){score = Integer.toString(b);}
 if(b<10){score = "0"+Integer.toString(b);} }
 else{score = "00";}

return score;      }
public String ScoreIncreaseByTwo(String x){
 int a,b;
 String score="";
 a = Integer.parseInt(x);
 b=a+2;
 if(b>=10){score = Integer.toString(b);}
 if(b<10){score = "0"+Integer.toString(b);}
return score;    }
```

3.0 **RESULTS AND DISCUSSION**

In the proposed system, number of problems were encountered during its development and most of the problems were solved successfully. The main problem was the difficulty of obtaining the components needed to build the system. It was planned to use the NRF 24 module in the proposed system for wireless communication, instead RF module was used. Because of this reason additional serious decoder and serious encoder were used and transmitting distance reduced. The players' scores were recorded on the computer screen.
The software was created for this system. Creating this software was a difficult task because the data received by the players had to be sent serially to the Netbeans interface. But that task was successful and a high level software was eventually created. Also the cost of this system is nearly about 25 000.00 rupees.

This electronic chest protector system has many advantages which are,

- Ability to get the training for Taekwondo players who were participating in international competitions.
- Fixing the problem caused by players of not getting points for their kicks.
- Ability for players to view the relevant scores and the time remaining while playing.
- Cost effective.
- Efficient.

4.0 **CONCLUSION**

This system was an electronic trunk protector system for the Taekwondo and also included a built-in software. Such systems are very expensive in the market. Therefore a low cost system is highly essential. This proposed system can be used for Taekwondo training institutes. Points were scored automatically when players play and Gam-jeoms can be recorded according to the referee's command. In this proposed system, electronic chest protector and the pair of electronic socks was created, kicks that attack to the chest protector with enough power were identified and the software to connect system to the computer were exposed. This proposed system is very useful for players participating in international competitions to receive training through their training institutes.

ACKNOWLEDGEMENT

Authors would like to thank all the staff of Deartment of Electronics, Faculty of Applied science, Wayamba University of Sri Lanka.

REFERENCES

[1]. AN INTRODUCTION TO TAEKWONDO, *Bytomic Martial Arts & Fitness*, (2020), https://bytomic.com/blog/an-introduction-to-taekwondo/ , (Accessed 30- Aug- 2020).
[2]. E. Watta, Know your sport: Olympic Taekwondo rules, scoring and equipment, *Olympicchannel*, (2020), https://www.olympicchannel.com/en/stories/features/detail/know-your-sport- taekwondo-rules-scoring-equipment/, (Accessed 30- Aug- 2020).
[3]. Taekwondo , *Ministry of Youth and Sports*, (2020), https://mos.gov.lk/our-sports-inner/173/ , (Accessed 25- June- 2021).
[4]. J.Y. Lee, KNP PSS user guide, *Sliedshare.net*, https://www.slideshare.net/JangkyuLee3 kpnp-pss-user-guide.pdf, (2017), (Accessed 17- Sep- 2020).
[5]. R.C.W.Lunn, Dae Do user guide, *studentsrepo*, (2020) http://studentsrepo.um.edu.my/9352/2/Ryan_Chong_Wy_Lunn_-_Thesis.pdf, (Accessed 17- Sep- 2020).

Proc. Annual Symposium on Research & Industrial Training, 08(2021) 47-53
Department of Electronics – Wayamba University of Sri Lanka

AUTOMATED HUMAN FOLLOWING SHOPPING TROLLEY WITH SMART SYSTEM

A.C.R. Jayathilaka*, U.A.D.N. Anuradha

Department of Electronics, Wayamba University of Sri Lanka, Kuliyapitiya, Sri Lanka

*arjcharitha@gmail.com

ABSTRACT

As a part of automation and smart living, smart shopping also plays a key role in enhancing the lives of people in modern life. Customers who need to purchase different products in supermarkets need lots of time and patience in coordinating among themselves for successful shopping. The congestion in shopping malls makes it difficult to search the desired product in the whole supermarket one by one and there are also spent time in long queues to pay bills by using the barcode reader. The main purpose involved in this research is to implement a smart shopping cart in terms of shopping in individuals and helping to the less time-consuming shopping experience. In this project the words "smart shopping trolley system" depicts an auto bill generating, item localization, and will follow the footsteps of the consumer. This trolley is capable of following the customer automatically without human effort while assists the customers by showing the catalog of products, locations, and their respective costs. This will make shopping more relaxed, comfortable, and systematic for the customers as well as improving the administrative nature of entrepreneurship. Therefore, doesn't require the extra staff to handle the customers, so profit margins can be increased for owners. Further this multifunctional trolley, which will be largely helpful in the Medicare sector, childcare, luggage handling (airport), and also in the area of material handling in industries. The scope of this work is beyond the barriers of trade and commerce.

Keywords: RFID, GPS, Automation

1.0 INTRODUCTION

Malls and markets are big corners for customers who buy everyday necessities such as branded foods, snacks, fabrics, and electrical and electronic equipment [1]. The people were in demand and spent more time in the shopping malls. After the total purchase, one should need to approach the counter for billing. The cashier uses a barcode reader to create the invoice, which is a time-consuming process [2]. Barcodes can only be read and cannot be written again. The scanner can read one bar code at a time, and the bar code contains very little information. This printed barcode can easily be damaged by harsh climatic conditions [3].

Customers are not always offered an assistant for better shopping; therefore, it takes longer to search for items. The desired things to purchase may be in the store, but the customer may be unable to locate them. Shopping malls must expand the number of billing counters to manage crowds during great offers, weekends, Sinhalese New Year, Christmas, and Ramadan. Customers who need to buy a variety of products in supermarkets need a lot of time and patience to coordinate between them in order to make a successful purchase.

The navigation of a human following robot is a problem that needs to be studied in depth in order to discover the best solution. There are numerous approaches for following a target in the present scenario [4]. Ultrasonic sensors, various tags, and other types of technologies such as accelerometers and gyroscopes are examples of this. However, it was discovered during the

research of these cases that none of the above technologies are totally accurate, are not suitable to shopping malls, and cannot effectively satisfy the needs of customers.
This article describes the design and development of a smart shopping cart to address these issues, which the user can use while shopping and which includes an automatic bill production capability. In addition, an Android application is created to make it even easier for customers to identify the details and location of each product. With the human following functions and an automated billing system, the major goal of this project is to build a smart shopping cart for assisting individuals in shopping and a less time-consuming shopping experience.

2.0 EXPERIMENTAL

Figure 2.1 depicts a block diagram of the proposed system. By installing this system, the ordinary trolley was converted into a smart trolley. Arduino microcontroller was used as the electronic platform used for controlling the whole process of navigation and other features.

2.1 Hardware Requirements

RC522 RFID Module
The Radio Frequency Identification (RFID) reader was selected for this project is RC522 RFID model. It operates at a frequency of 12.95 MHz to 13.56 MHz. It runs at a voltage range of 3.5V-5V, with an output power range of 0dbm-26dbm. The reading range is 10cm-3m, depending on the tag, antenna, and implementation.

16x2 LCD Display
When the RFID scans the data from each tag, a liquid crystal display (LCD) was used to display the data that came from the microcontroller. It has 16 pins, with 8 pins assigned to data communication, read, write, enable, and brightness control, and 4 pins dedicated to power supply. On the back of the LCD screen, there was an I2C module that could be readily connected to the Arduino board via serial communication.

NEO-6M GPS module
It can monitor up to 22 satellites on 50 channels and achieves the industry's highest level of sensitivity i.e., -161 dB tracking. The Global Positioning System (GPS) provides information about where the device is, but does not provide the information of speed and direction for the application [5]. This is used here to detect the trolley's self-positioning against the customer's location and retrieved the result from the longitude and latitude position.

HC-05 Bluetooth Module
The Bluetooth device was used as a communicator between the mobile phone and the trolley system. This module communicates with the help of USART (Universal Synchronous/ Asynchronous Receiver/ Transmitter) at 9600 baud rates between any microcontroller devices which supports Bluetooth functionality at the operating volage of 4V -6V. This can be used for communication up to a range of 100m [6].

HMC5883L Compass Sensor
This is a multichip module that behaves as a digital compass IC to find the direction and measures the magnitude and direction of the magnetic field along the X, Y, and Z-axis. This allows for an easy I2C (Inter-Integrated Circuit) serial interface and the maximum data output rate: 160Hz [7]. This was used to calculate the exact direction; the cart should be turned in relation to the Earth's north and south magnetic poles.

12V Metal Geared Motors

A gear motor is the combination of a motor and a gearbox. Two gear motors were added to two wheels to alter the speed of the application and in addition, is to increase torque. Both the speed and rotation direction of two DC motors were controlled by L298 D Motor Drive

L298 D Motor Drive

L293D consist of two H-bridge designed using 4 transistor circuit that helps to reverse the direction of rotation and to control the speed of the DC motor. L293D motor driver was used here for interfacing the gear motors with Arduino.

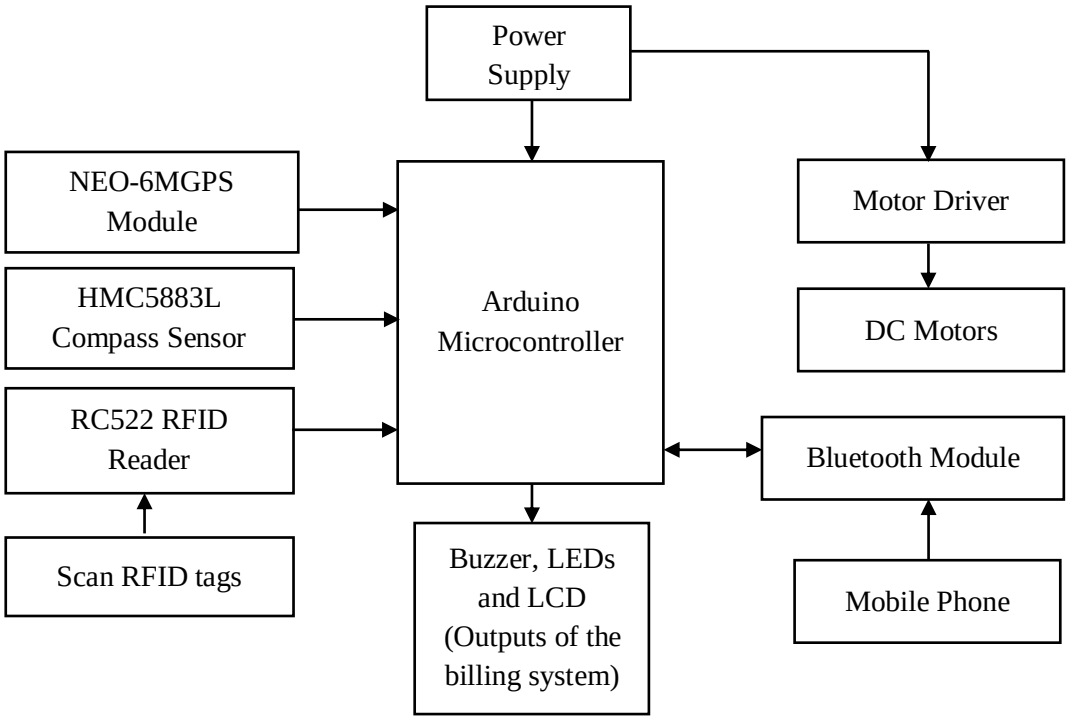

Figure 2.1: Block diagram of the proposed system

2.2 Software Requirements

Arduino IDE

Arduino consists of both a physical programmable circuit board and a piece of software that runs on the computer. For writing and compiling the code into the Arduino development board, the Arduino Integrated Development Environment (IDE) open-source software is used. Arduino reads these signals and sends commands to the driver circuit to drive the motors.

The Blynk IoT platform

Blynk is a platform with iOS and Android apps to control Arduino, Raspberry Pi over the Internet. It's a digital dashboard where can build a graphic interface for the project by simply dragging and dropping widgets like buttons, displays, sliders, etc. Using these widgets, users can control hardware remotely and can monitor the sensor data on the phone screen.

Visual Studio

Visual Studio is an IDE platform from Microsoft. It functions as a code editor which supporting the code completion components and code refactoring. This is generally used to develop computer programs, as well as websites, web apps, web services, and mobile apps. This platform was used to develop the android application with react native open-source framework.

2.3 Project Design

Every cart is connected with an RFID reader and an LCD screen. When the customer starts dropping products into the trolley, RFID tags will be read by the reader and send the information to the microcontroller. It notifies the customer via Piezo buzzer. Then the cost of that product will be displayed on the LCD screen for the user.

The customer connects with the trolley via Bluetooth technology [5] and then the trolley tracks the customer's location with the navigation of GPS technology [6]. At the same time, with the help of the compass sensor determines the angle of rotation with respect to the North and South magnetic poles of the earth. Then the microcontroller drives the motor and the cart is moved towards the customer. This continues until the customer stops moving.

The developed smart shopping mobile interface is including the feature of the location of products on a map. This allows users to easily find items in the supermarket thus helping them to organize their shopping journey better.

3.0 RESULTS AND DISCUSION

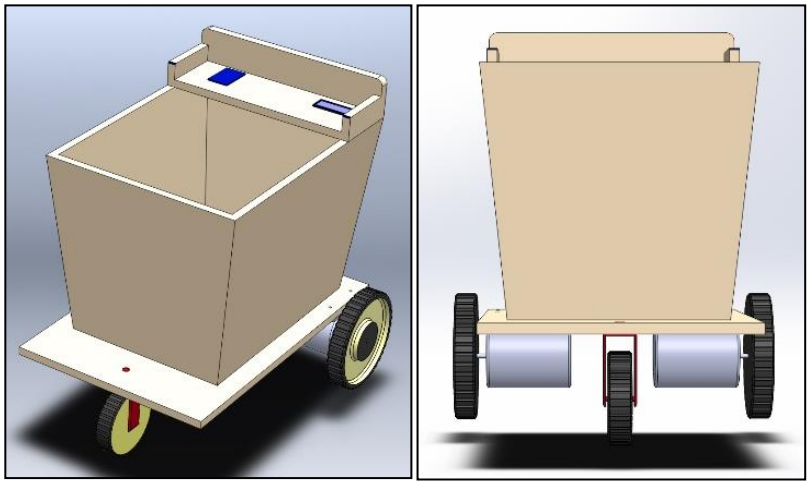

Figure 3.1: Perspective and back view of the designed trolley

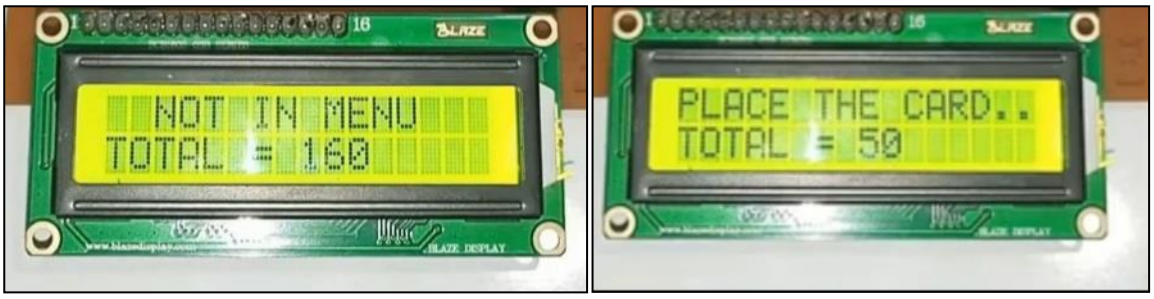

Figure 3.2: Output results of the LCD during the billing process

Figure 3.2 shows how to RFID tags are read and products are displayed on an LCD screen. Figure 3.3 shows the created mobile application's user interfaces.

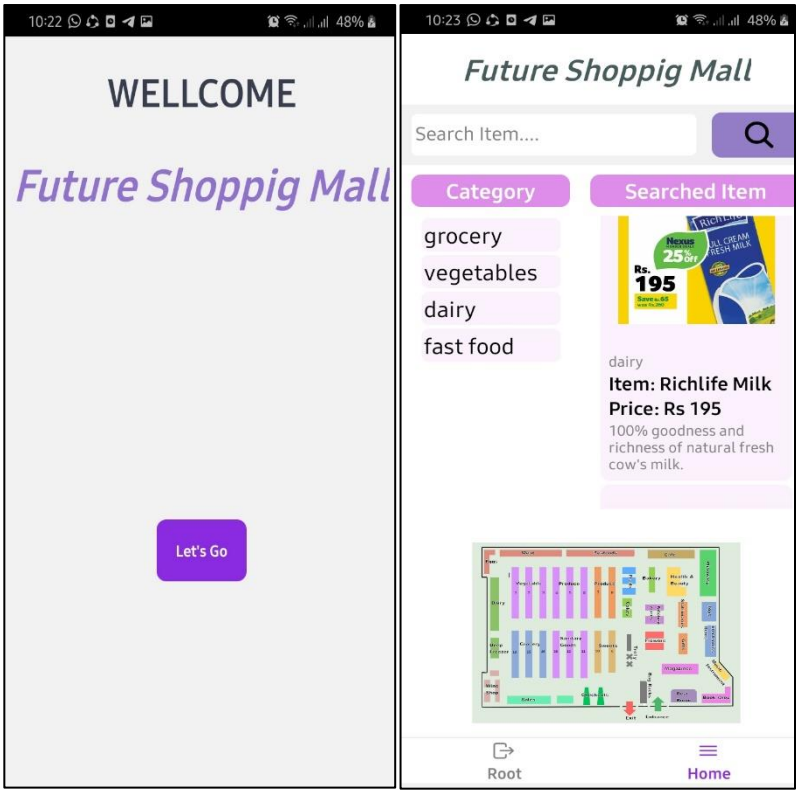

Figure 3.3: User interfaces of mobile application

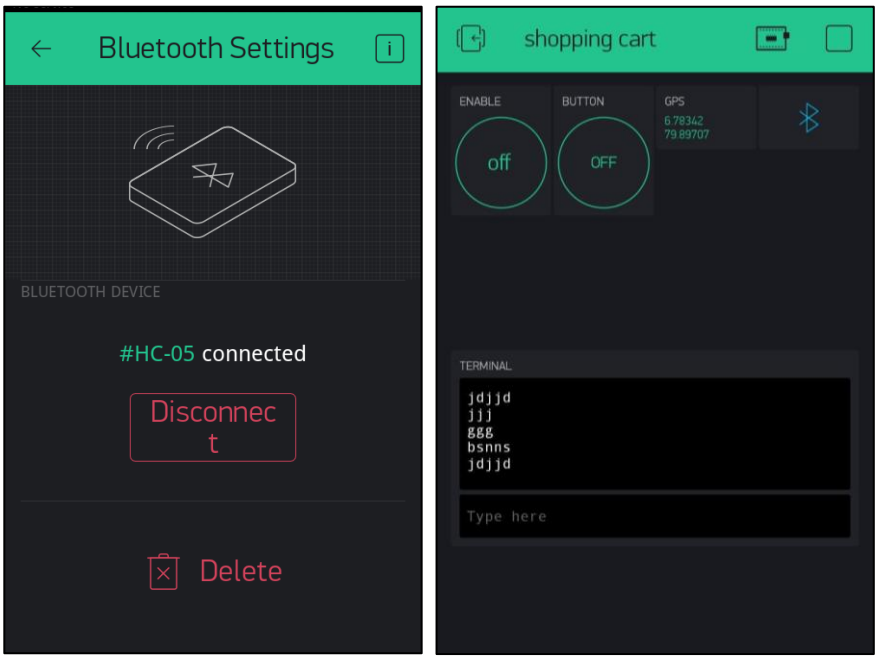

Figure 3.4: Blink App testing result with Bluetooth and GPS module

3.1 Features of the Smart Trolley

This shopping cart is user-friendly, reliable, and very convenient for the customer. A person who is unable to read or find the product price printed on the product does not need to seek assistance from anyone in order to obtain this information. Different variables like item cost and item name are continuously displayed on LCD attached to the trolley by simply scan tags on the reader. The mobile application allows users to access the location of items that plan to purchase in supermarkets.

Using GPS technology to activate a human following system is very easy and attractive for both sellers and customers. The human following system has the ability to simply be activated. The user can activate the human following feature by connecting the Bluetooth module ID of the trolley to the mobile phone.

3.2 Future Scope and Limitation

This application was activated in a building, and it could not able to track the mobile GPS data properly all the time. Although the Blink app showed that the phone and the trolley were connected when it was inside the building, the trackers did not have enough GPS data to find the direction and it was not enough to move the trolley correctly to the mobile phone. It functioned well in the outdoor area.

There are some rooms for further improvement of the project. With connecting to Supermarket's centralized shopping server, the current system will be able expand to a fully automated shopping application. Then it is possible to upgrade the payment facility to the system to get a more efficient output. It also allows the system to be upgraded to many areas, and to include more precise and secure tools in the system to prevent unauthorized actions such as theft of goods. Furthermore, if possible, the tracing facilities of the trolley should also be developed for the efficient tracking of the trolley inside the market. With the implementation of this work and integrating the same with automatic stores, it will be changing the whole scenario of shopping.

4.0 CONCLUSION

Hypothesis of this work was to design a user-friendly shopping cart that would enhance the shopping experience in shopping malls for assisting customers by saving a lot of time in buying commodities. The objective was effectively attained in the prototype model developed. The developed product is of low cost, amiable to use, and does not require any specific practice. Human following smart trolley is a good alternative when compared to the conventional shopping trolleys which are being used currently in the supermarkets. Huge amount of work, time and money could be saved by the implementation of the concept. The technologies similar to the ones implemented in the work could be used in other sectors such as in Medicare field as a nurse following robot, in childcare or material handling in manufacturing industries.

ACKNOWLEDGEMENTS

Authors would like to thank all the staff of Department of Electronics, Faculty of Applied Sciences, Wayamba University of Sri Lanka, and others who have supported to make this research a success.

REFERENCES

[1]. Jadhav J.D., Gaddime S., Hiware K., Khadtsar N., Tanya Smart Trolley: A Fast and Smart Shopping Experience Using Android and Cloud, *International Journal of Innovative Research and Advanced Studies (IJIRAS)*,3, (2016), 192 -193.

[2]. Mane M. R., Amane N. G., Patil S. D., Lakesar A. L., Electronic Shopping Using Barcode Scanner *Int. Res. J. Eng. Technol*. (2016), 2395 - 56.

[3]. Lalith K., Ismail M., Gurumurthy S., Tejaswi A., Design of an intelligent shopping basket using IoT, *Int. J. Pure Appl. Math.* (2017), 114, 141–147.

[4]. Moriok, K., Lee J.H., Hashimoto H., Human-following mobile robot in a distributed intelligent sensor network, *IEEE Transactions on Industrial Electronics*, (2004), 51, 229-237, doi: 10.1109/TIE.2003.821894.

[5]. Ershad A., *Global Positioning System (GPS): Definition, Principles, Errors, Applications & DGPS*, University of North Bengal,(2020).

[6]. Budiharto W., Gunawan S. A.A., Irwansyah E., Suroso J.S., Android-Based Wireless Controller for Military Robot Using Bluetooth Technology, *2019 The 2nd World Symposium on Communication Engineering*, 2019, 215, doi:10.1109/WSCE49000.2019.9040985.

[7]. Ladetto, Q., Gabaglio, V., Merminod, B., Combining Gyroscopes, Magnetic Compass and GPS for Pedestrian Navigation, *Proceedings of the International Symposium on Kinematic Systems in Geodesy, Geomatics, and Navigation*. (2001), 205-212.

Proc. Annual Symposium on Research & Industrial Training, 08(2021) 54-61
Department of Electronics – Wayamba University of Sri Lanka

ENERGY HARVESTING AND POWER MONITORING SYSTEM FOR GYM USING WASTED HUMAN POWER

T.G.S. Lakshith*, Y.A.A. Kumarayapa

Department of Electronics, Wayamba University of Sri Lanka, Kuliyapitiya, Sri Lanka

*Sahanlakshithgamage1995@gmail.com

ABSTRACT

The demand of electricity for industrial purposes and other appliances is increasing day by day even for a gym. Therefore, the generation of electricity are more important to fulfill the large energy demands. Conversion of wasted energy into electrical energy is an alternative method for minimizing energy crisis. Different methods are proposed already for power generation using non-conventional energy sources are solar energy, wind energy, biomass energy, geothermal energy and human power. Human power can be obtained by a power produced from gym exercise machines. Human power is another renewable source of energy. The intention of this project is to design a system based on renewable energy source at the gym. This project is focused on the harvesting of the energy by using wasted human power at the gym. In the power converting part, motor was rotated parallelly with a gym bicycle. The generating current was stored in a 12V DC battery. The generator shaft was guided by the gym bicycle and variable DC power was generated. Then the battery was fed by the power of charging circuit with proper controlling. When the battery was fully charged, the power supply of the battery was cut off by the charging circuit. Then the charged 12V DC power was driven through an inverter circuit and then step it up into 230V AC power. It can be used to get some appreciable power. In this project, a schematic design for DC power generator with battery bank by using wasted kinetic energy was simulated, where a dynamo motor to generate dc supply, hand prime mover as a prototype and universal battery was modeled. All the components which used in this project were supposed to be parasitic, and a step-up transformer was used at the output as well as 12V/ 7A battery used as the input source. The simulation results show that system operated outcomes are 50W/230V/50Hz.

Key words: Electrical energy generation, Gym exercise bicycle, Human energy harvesting

1.0. INTRODUCTION

1.1. Overview

The world is going through an energy crisis. It is known that the contribution of fossil fuels is limited and their utilization as energy sources. So, the effect of a steady replacement of fossil fuels with renewable energy source is vital consideration for the most situations [8]. As the population of the world is continuously being increasing with their living standard, uses of electric equipment go on increasing day by day. To produce this electricity, large conventional methods are being employed like power plants run by coal, hydro power plants run by water, nuclear power plants [7]. As well conversion of wasted energy into electrical energy is an alternative method to fulfill the large energy demands. The electricity generated by gym bicycle converted from mechanical energy to electrical energy using motor as generator will be helpful for solving energy crisis at the gym [10].

Our research study focuses on how to harvest electrical energy through wasted human power at the gym by considering the gym bicycle. According to the project, the system is divided into few subsystems for design properly. Each of every subsystem were designed individually as

prime mover, DC generator, charging circuit, battery, DC-AC inverter, transformer and power output. The generator to generate DC supply with the help of the prime mover that as stationary prime mover of gym equipment. But here, hand prime mover used as a prototype. Thereby, it can produce approximately 40watt of 230V AC power.

The 24V motor which is powered by a gym bicycle used as a generator. A motor is connected to gym bicycle used for the circular rotation of the front wheel rotates the motor shaft. The resulting direct current is converted into different usable DC voltages levels. It will useful to power light bulbs, laptop and mobile charging and other appliances at the gym. This will reduce the energy demand at the gym by using wasted human power.

1.2.Research Objective

When considering a gym, the human energy generated in typical workout is usually wasted. Conversion of this wasting energy to AC or DC power through power converting mechanism will be utilized as generated electricity at gym for day-to-day usage. It causes to generate electricity from wasted human power generated. Generated electricity is important to power lights, fans, air conditioners, phone chargers used at the gym [5]. Thereby, electrical demand at the gym can be minimized by utilizing the wasted power generated from human. It leads to save money and get a profit from the gym by avoiding unnecessary expenditures for the gym owner.

1.3. Literature Review

Mechanical kinetic energy is the key point to drive and improve the life cycle. The generation and utilization of energy is directly proportional to the progress of mankind. The field of energy conservation is becoming an increasing notable subject of research among the scientific community today [1]. Here, the gym exercise bicycle used for a gym used as an energy generator system for converting mechanical energy from a workout to electricity. As energy usage across the world continues to rise, there is need to develop new sources for electricity generation that have less environmental impact [1]. Human power is an alternative method for energy generation. In addition to that, human power is easily accessible through human exercises at the gym.

The idea of first sustainable gyms was carried out by Italian inventor Lucien Gambarota. He invented it with the involvement of the entrepreneur Doug Woodring and Hong Kong-based company California Fitness open the world's first such gym in 2008. It was named as "The Green Gym" by fitness instructor Adam Boesel in Portland, Oregon. The goal of Bosel is to complete sustainability.

2.0. EXPERIMENTAL

2.1.Theories

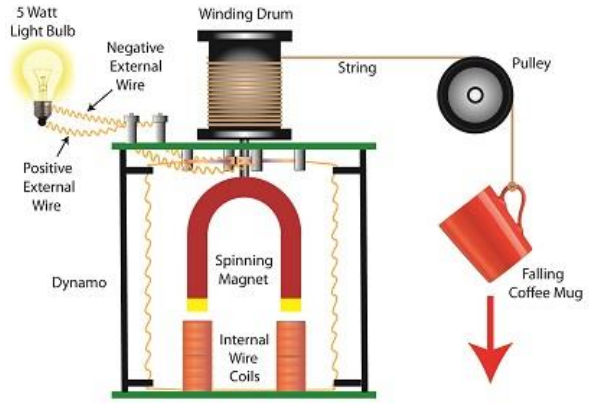

Figure 2.1. Diagram for converting kinetic energy into electrical energy [7].

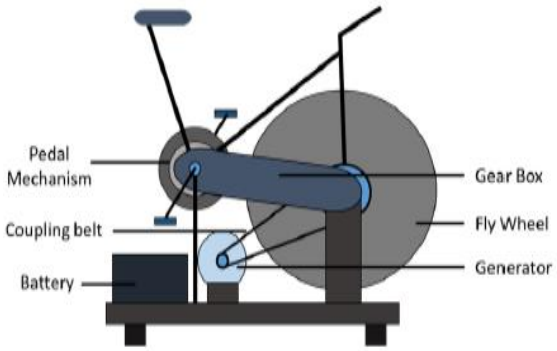

Figure 2.2. Diagram of gym exercise machine [8].

According to the Figure 2.1. it shows how kinetic energy converts into electrical energy. In this study concentrates on how electrical energy can be generated from gym equipment.

In this system, the group of researchers have conducted tests on exercise bicycle and found that an average rider could generate up to 75W of power in the span of one hour. They also found that it was possible to reach 200W at 25 kph for short periods, and 750W under extreme load for about a second. As a result, the research suggests that it is feasible to exploit mechanical energy generated from pedaling and store the electrical energy in battery banks, which in turn can run small appliances in the gym. The paper considered a fitness club and made measurements to test their proposed prototype. The system assumes the total energy consumption in 295 days is 7 4800kWh, with every exercise bike working at least 6 hours a day at an average speed of 20 kph also flywheel of 40 cm diameter and 10 kg. Thus, the kinetic energy is,

$$w = \frac{1}{2}\, mr^2 w^2 \qquad (1)$$

With: ω = 264 rpm, the energy produced by a single bicycle in one hour is calculated by substituting w. Consequently, the energy of one cycle or 6 hours is 1.38kWh [8].

2.2. **Procedure**

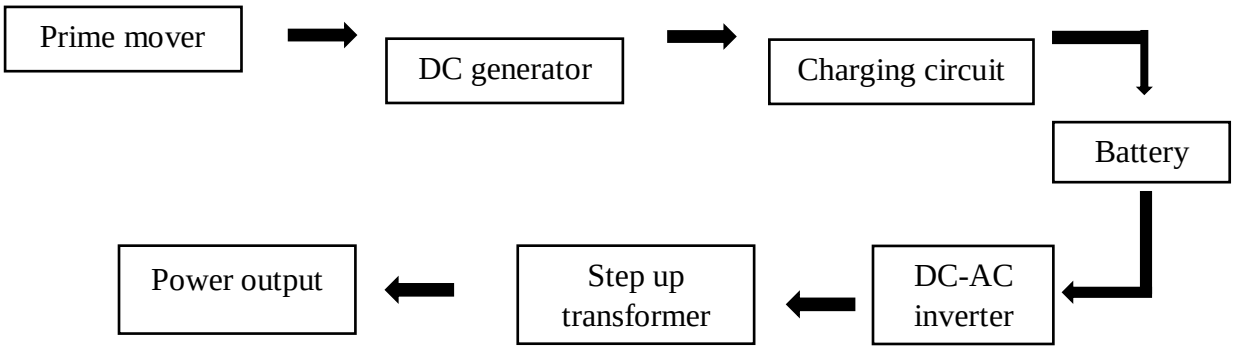

Figure 2.3. Proposed system for electrical energy generation

Power monitoring part was designed according to the figure 2.3. The system was divided into few subsystems for designing properly. The generator shaft was guided by the gym bicycle and then variable DC power was generated. And then the battery was fed by the power of charging circuit with proper controlling. When the battery was fully charged, the supply of the battery was cut off by the charging circuit. It causes to protect the battery from over charging and heating.

Then the charged 12V DC power was driven through an inverter circuit and then step it up into 230V AC power. It can be used to get some appreciable power. The generator was used to generate DC supply with the help of the prime mover that as stationary prime mover of gym equipment. But here, hand prime mover was used as a prototype. It causes to produce approximately 40watt of 230V AC power. In this project, a DC permanent magnet motor was used according to the requirement. Also, it should be a 12V dynamo motor.

2.2.1. Charging circuit

Charging circuit is a subsystem of this whole circuit and it shows in figure 2.4. This battery charger automatically shut off the charging process once the battery attains full charge. This prevents overcharging of the battery and save the battery. If the terminal voltage of the battery reduces below the set level, the circuit automatically turns on to the charge mode.

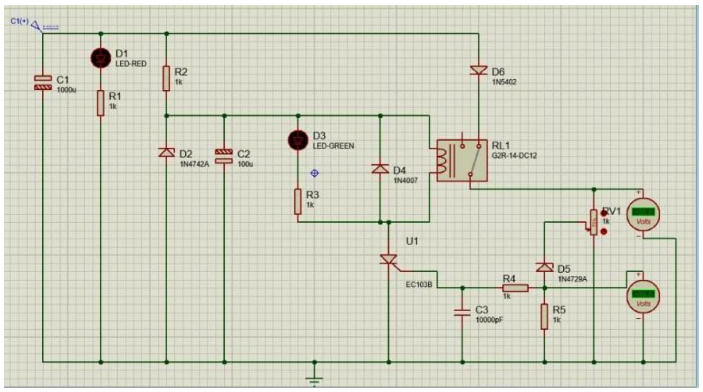

Figure 2.4. The proposed diagram of the charging circuit

The main two methods used to charge batteries are constant current charging and constant voltage charging. Here, used methods mainly depend on the features of the battery. The charger voltage is constant due to the constant voltage charging. The amount of current drown by the battery will be depend on its state of charge. When the battery becomes charged, it will draw less current, and it affects to the battery voltage to increase slightly. Due to the constant current charging, the current to the battery is held constant. Thereby, the voltage is allowed to fluctuate.

Figure 2.5. Proposed charging circuit

2.2.2. Inverter circuit

Inverter circuit is important for converting DC voltage to AC voltage. The figure 6 shows inverter circuit diagram. The transformer used here to step up the voltage to 230 V. The load can be bulbs, laptop charger, mobile charger, musical system used at the gym [4].

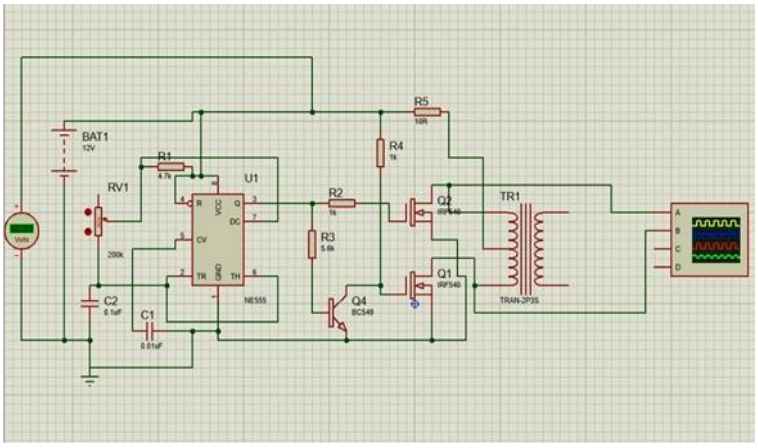

Figure 2.6. The proposed diagram of the inverter circuit

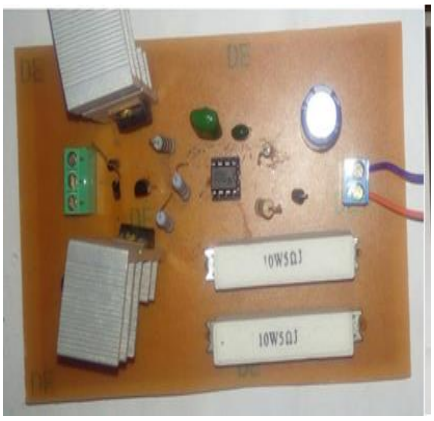

Figure 2.7. Proposed inverter circuit

3.0. RESULTS AND DICUSSION

According to the results, a high voltage can be obtained from inverter that can be used for everyday use at lower voltage. Here 12V-18V used as a voltage approximately as the input because the way gym equipment operates varies from person to person and hoped to get this low voltage from a gym to take advantage of the wasted energy loss. For this a belt can be used to the cycling machine in the gym. It can be connected to 12Vdc dynamic motor and the battery 12V/7Ah through a charging circuit so that the wasted energy can be stored properly. It has the ability to provide the power needed for low voltage bulbs, mobile phones charging, laptops charging etc. The outcome of the proposed charging circuit is shown in Figure 3.1.

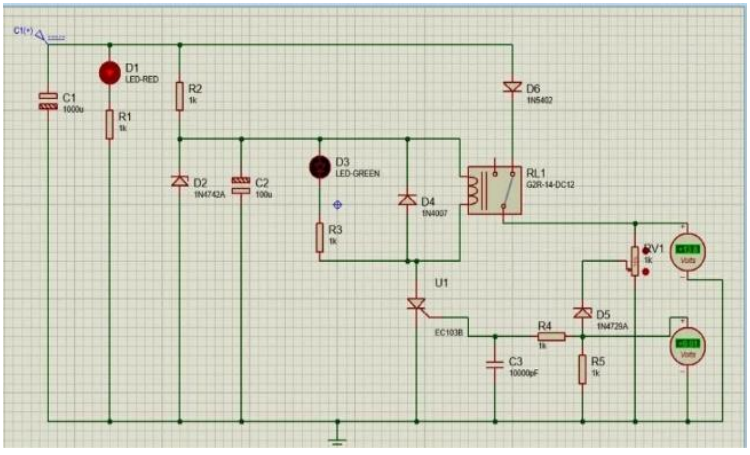

Figure 3.1. Outcome of proposed charging circuit

Actually, the output of the inverter circuit should come as a sine wave. According to the below simulation results of figure 3.2, this wave is not similar to the sine wave. It may be happened due to the failure of using compatible components to design those systems.

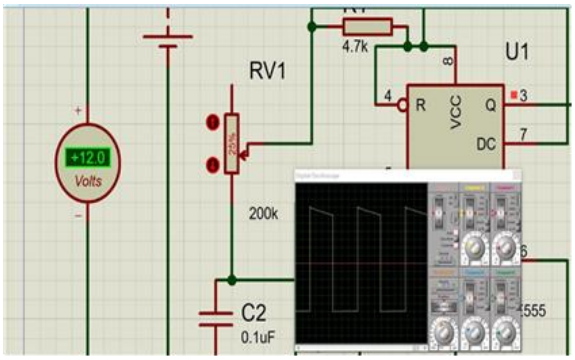

Figure 3.2. Outcome of proposed inverter circuit

Figure 3.3. Current generating mode

Figure 3.4. Battery charging mode

Figure 3.5. The non-charging mode

Figure 3.6. Battery overcharging mode

The power generator dynamo motor was used to generate DC supply with the help of the prime mover that as stationary prime mover of gym equipment. But here, hand prime mover and 12v motor were used as prototype. It causes to produce approximately 40watt of 230V AC power. This process shows in Figure 3.3. as a current generating mode.

Here 12V-18V used as a voltage approximately as the input because the way gym equipment operates varies from person to person and hoped to get this low voltage from a gym to take advantage of the wasted energy loss. For this a belt can be used to the cycling machine in the gym. It can be connected to a motor (12Vdc Motor) and the battery 12V/7Ah through a charging circuit so that the wasted energy can be stored properly. Figure 3.4. shows the usage of output current that stored in the battery to charge a mobile phone. Figure 3.5. shows as the stage of battery is not charging but stored current in the battery can be used properly. Figure 3.6. shows the overcharging mode of the battery and the generator shaft was guided by the gym bicycle and then variable DC power was generated. And then the battery was fed by the power of charging circuit with proper controlling. When the battery was fully charged, the supply of

the battery was cut off by the charging circuit. It causes to protect the battery from over charging and heating. Overcharging mode is prevented by using a relay.

4.0. CONCLUSION

We have investigated for an alternate renewable energy resource with the use of gym bicycle in this research study. This project causes to convert human wasted kinetic energy at the gym using a gym bicycle into electrical power by implementation of DC power generator. It can be used as a sub system for different human energy wasting technologies like exercise machines such as gym bicycle. The wheel rotational energy of gym bicycle can be used to operate small power devices. Both dynamo and alternator can be used in various power generation situations such as the rotation with gym bicycle etc. In this project, a schematic design for DC power generator with battery bank by using waste energy is interpreted and simulated using prototype system. Here, a dynamo motor was use to generate dc supply and then a step-up transformer is used at the output. Therefore, this project can implement for small industry purposes. The final outcome of this project is to harvest the energy by using wasted human power at the gym. Hence, by using proposed system, small power can be generated. This can be used for several appliances such as bulbs, phones used at the gym for charging effectively from the generated electrical power of the proposed system. It caused to earn a profit for the gym owner by avoiding unnecessary expenditures for electrical power. On the other hand, it influences to face the energy crisis in the future with individual contributions for the energy generated at such gyms as combined effect. The future studies will be carried out by developing a remote monitoring system to get data of producing and consuming current by motor and battery for such energy harvesting systems.

ACKNOWLEDGEMENTS

The authors wish to express their gratitude to all Lecturers and laboratory staff of Department of Electronics, Faculty of Applied Sciences, Wayamba University of Sri Lanka.

REFERENCES

[1]. Rajneesh, S., Mahesh, C.K., Krishna, K.S. and Abhishek, S. Generation of electrical power using bicycle pedal, *International Journal of Recent Research and Review*, 2014, Volume VIII.

[2]. Rocky, K.M. and Murali, P. The Pedal Power Generation, *International Journal of Engineering and Science*, 2012, Volume 7.

[3]. Suhalka, R., Khandewal, M.C., Sharma, K.K. and Sanghi. A. Generation of electrical power using bicycle pedal, *International Journal of Recent Research and Review*, 2014, vol. VIII.

[4]. Negi, K., Anam, R. and Gautam, S. Development and Analysis of Gym Bicycle with Comfort Facilities and Power Generation, *International Journal of Science Technology & Engineering*, 2016, Volume 2., ISSN (online): 2349-784X.

[5]. Bhattacharjee, C.R. Wanted an Aggressive Outlook of Renewable Energy, *Electrical India*, 2005, Volume 4., pp. 112-116.

[6]. Human –powered Gyms: For a Healthier You-and a Healthier Earth Friday, 17 February, Written by Victoria Cho Article.

[7]. Philip., J. and Keefe., O. (2009), Engineering expert witness blog. Available: http://www.engineeringexpert.net/Engineering-Expert-Witness-Blog/converting-kinetic-energy-to-electrical-energy (Accessed 2021-08-20)

[8]. Dmini, M. A., Darhmaoui, H., & Sheikh, N. N. (2020). Viability of gym machines in electricity generation.
[9]. Khaleel., 2014, Available: http://www.circuitsgallery.com/2014/01/sg3525- inverter-circuit-pwm.html (Accessed 2020-11-07)

ECONOMICAL TENNIS BOWLING MACHINE CONTROLS MULTIPLE THROWING ANGLES

S.M.K.J. Subhasinghe*, M.A.A. Karunarathne

Department of Electronics, Wayamba University of Sri Lanka, Kuliyapitiya, Sri Lanka

*subhasinghe1995@gmail.com

ABSTRACT

Unlike many other sports, competitive tennis athletes need a mixture of anaerobic skills, such as speed, agility, and power, combined with capabilities to quickly turn and run-in different directions. In order to achieve these performances and efficient planning and training, unique physical aspects are required for the sport. This paper presents details of a tennis ball throwing machine for use in the tennis practices. This proposed machine has the capability of controlling the delivery of tennis balls to a player's forehand and backhand at various speeds with spins when playing the game. This machine has a pair of wheels which are independently and controllably driven to throw a tennis ball delivered between an automatic ball feed mechanism at a speed and with an angle determined by the position of the frame which is attached to the two wheels. This machine transfers the kinetic energy to the ball by frictional gripping of the ball between the two rotating wheels. The base is supported on a loose assembly, which is mounted on a bracket frame in a way that the required angular adjustment of the rotational plane of the wheel about an axis parallel to the direction of delivery of the ball. The perpendicular axis is also possible for delivering the ball. Electronic motor controls are provided for controlling the speed of rotation of the wheel and angle. These adjustments of relative rotational speeds and plane of rotation of the wheels afford wide variations in the bowling speed, spin, and direction while accessing the control with mobile application.

Keywords: Bowling machine, Tennis, Practice

1.0 INTRODUCTION

Tennis is a racket sport that can be played individually against a single opponent (singles) or between two teams of two players each (doubles). The player who is unable to return the ball will not get a point, while the opposite player does win [1]. Throughout matches and practice sessions, tennis players need to be able to perform repeated dynamic movements involving acceleration, deceleration, multi-directional agility, and explosive jumps [2], all in a reactive environment [3]. Also, they should be able to attack and face different styles of shots specific to tennis sports such as ground stroke, volley, lob, overhead, drop shot, and serve [4]. These capabilities of movements and the need to continuously respond to situations, require the coach to spend time and develop a tennis-specific motion training program for improving the athlete's game style, strategy, and strengths of movement [5].

There are a number of developed balls throwing devices available. Machines that rely on pneumatic pressure to propel the ball [6-8], machines that employ a spring-actuated mechanism or elastic member to throw the ball [9-11] and machines that employ at least one rotating wheel to throw the ball. It identified some of the limitations that were with these machines such as occupying more space, high manufacturing cost, inability to throw with different angles and not being portable. Especially the spring or elastic mechanism machines are incapable of fully simulating the flight characteristics of a pitched ball. Therefore, there is a need for an indigenous tennis-bowling machine that is capable of throwing a ball accurately and adjustably to a specific, predetermined location.

Tennis practice machines that are available for purchase in the market are very expensive. Cost is a major issue with this product. Some players want to train their own, but they miss out because of the high cost of purchasing these products. In today's world, it has become an essential part of manufacturing to handle all the technological work and electronic devices handled through the mobile phone. But a mobile phone app does not seem to have improved with the existing machines. In that case, the players can use these machines to train whenever they want to train even when they are without opponents. Also, training with skillful and offensive opponents is a key factor in a tennis player's improvement. But players cannot be expected to be able to play with good partners all the time when they train.

This paper presents the design and development of a machine capable of producing a tennis ball that throws at various speeds with a change of direction in predetermined line and length and adjustable frequency, with the number of balls that can be thrown out of the machine in a given time. The design of the machine also aims to develop a cost-effective (economic) and compact tennis bowling machine that provides provision for using various patterns of style such as ground stroke, volley, drop shot, and lob, etc. This also has a manual and automatic control approach with the mobile application. The tennis bowling machine will provide accurate and consistent practice for players of all standards, professional, amateur, school level, and club level players for becoming a good player as well as eliminating flaws in their playing without the necessity of an opponent.

2.0 EXPERIMENTAL

The entire mechanism is mounted on a cart-like assembly for easy moving, with an alternate embodiment to provide remote control by a mobile application of ball speeds, spins and direction of delivery. It also includes a random variation (auto mode) in the height of the delivery. The machine (Figure 2.1) consists of wheel mounting, two wooden wheels, motors, an electronic control panel, and a stand with a swing (outer frame).

The machine of the present invention is characterized by a rectangular body supported on a frame assembly having a pair of wheels, a bearing between said inner and outer frame assemblies for allowing relative oscillation. They are mounted approximately in a vertical axis (figure 2.1). The pair of adjacent ball ejecting wheels, each provided with a concave surface formed in a body of wooden material which are independently controlled by two dc motors driven in opposite direction to throw a tennis ball delivered with a speed and with spinning. It was determined by the speed of the wheels. These wheels are mounted on a base for axial rotation in a common plane, the spacing between the wheels is less than the diameter of a ball to be thrown and the rotational speed of both wheels are adjustable.

AT89S52, is a low-power, high-performance dual core 32-bit microcontroller with 34 GPIOs (General Purpose Input/Output). The C program was embedded inside the microcontroller. The power supply (Analog to digital converter was used) should be +5V, with maximum allowable transients of 10mv to the microcontroller. A 12V AC supply was provided to motor drivers for operating the stepper motors. Two stepper motors (1 and 2 see Figure 2.1) were used to rotate the inner frame and outer frame vertically and horizontally respectively.

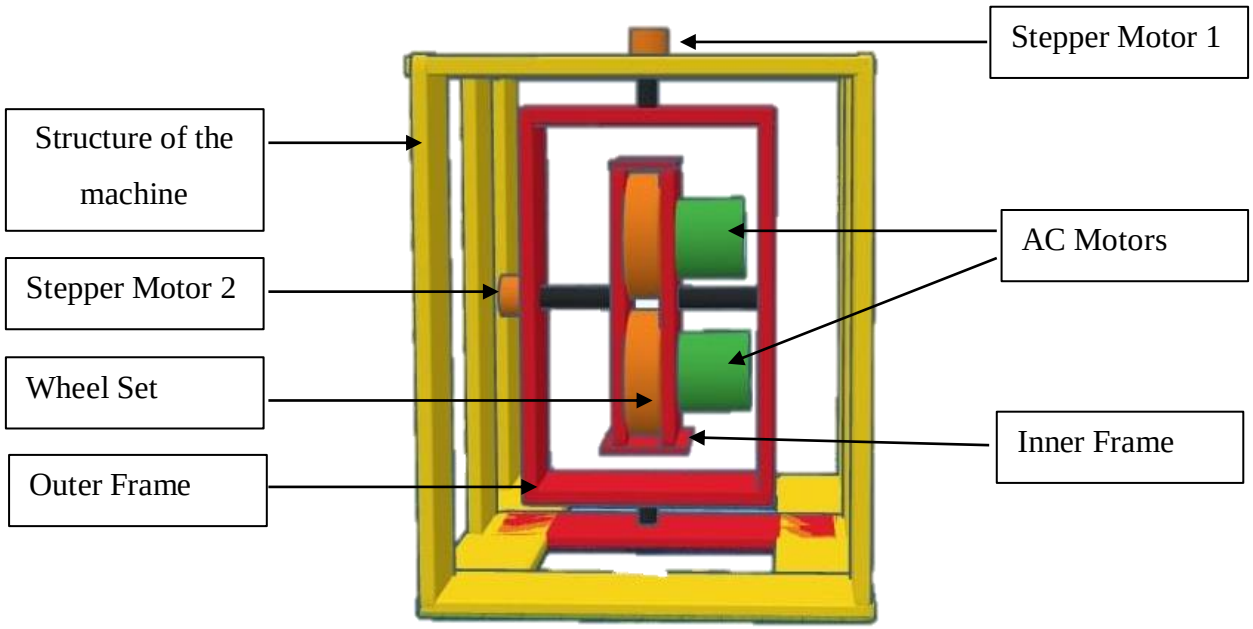

Figure 2.1: Perspective of the tennis ball throwing machine of the present invention.

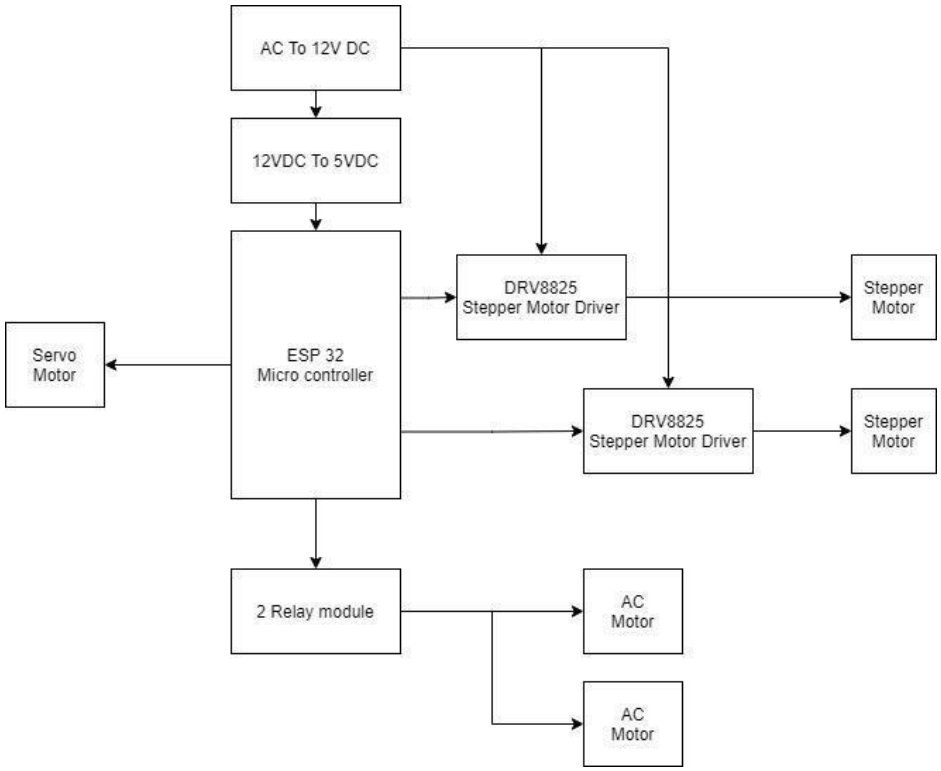

Figure 2.2: Block Diagram of the control scheme

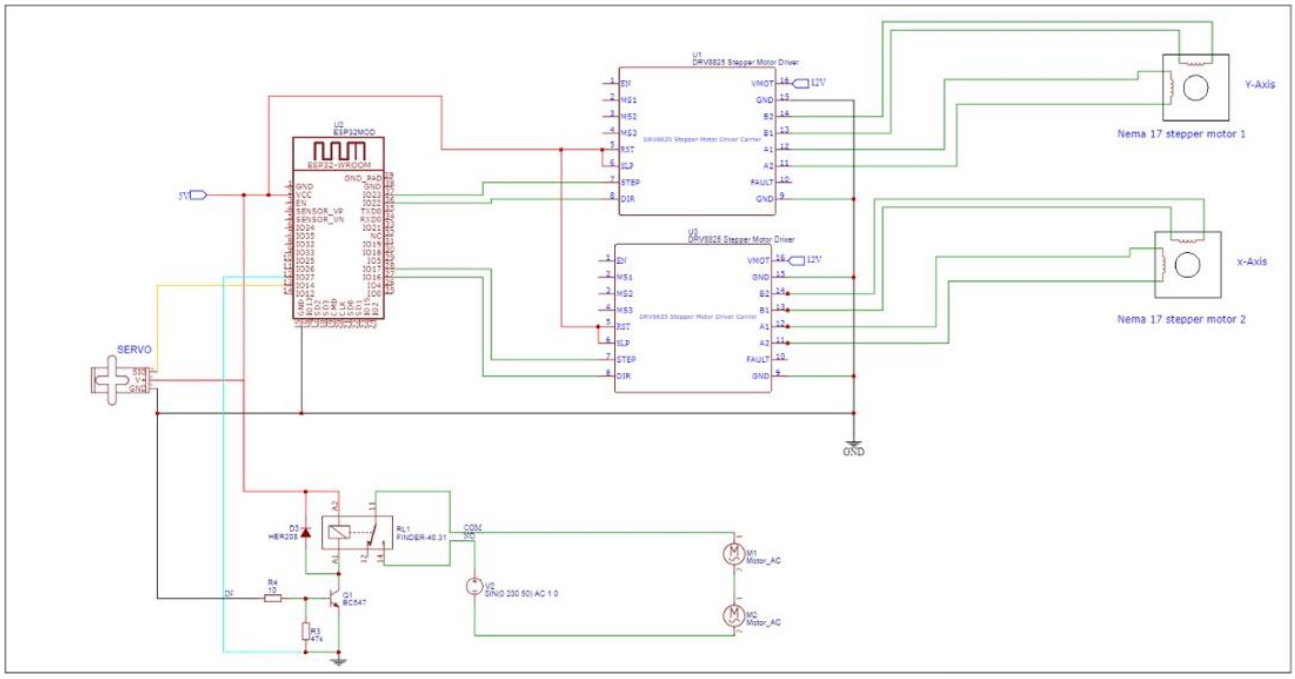

Figure 2.3: Schematic diagram of the control system.

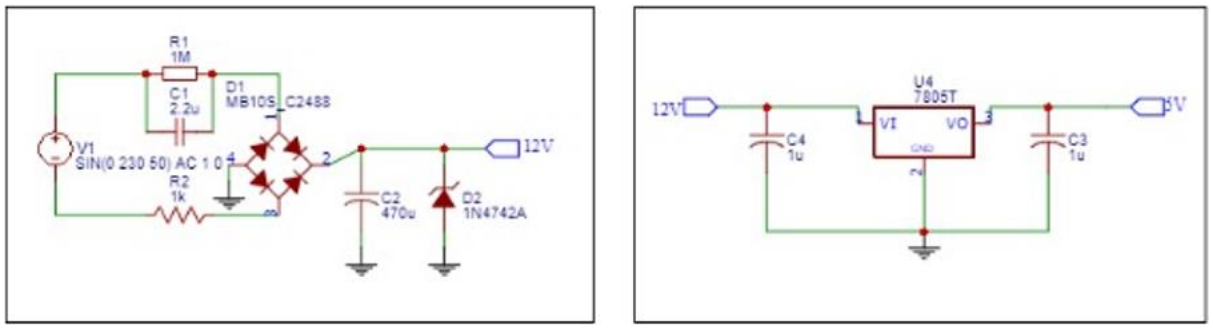

Figure 2.4: Block Diagram of the power circuit

3.0 RESULTS AND DISCUSSION

A prototype of the bowling machine (figure 2.1) was designed. The key features of the developed machine were i) Adjustable bowling speed in 2 km/h increments from 70-160 km/h; ii) Weight of the machine, 25 kg; iii) Height of the delivery point of the machine, 35 cm; iv) Developmental cost of the machine, Rs. 30,000; v) Range of diameter of the ball to be thrown, 65-75 mm; vi) The maximum vertical height of throwing was 3.9 m; vii) The minimum vertical height of throwing was 3.2 m; and viii) angular range of the throwing was 60^0.

- In the normal functioning of the machine, the ball comes to the space between the two wheels, and is thrown straight towards the practicing player.
- In the case of the swing of the ball, a differential speed was maintained on the two wheels.
- To create a twist on the ball of different kinds, a differential speed was maintained between two wheels and at the same time, the outer frame platform was either inclined towards the left or towards the right with respect to the fixed frame, according to the kind of spin.
- To control the length of the bowling, the inner frame was inclined upward or downward.

Figure 3.1: Minimum and Maximum vertical height of the throwing

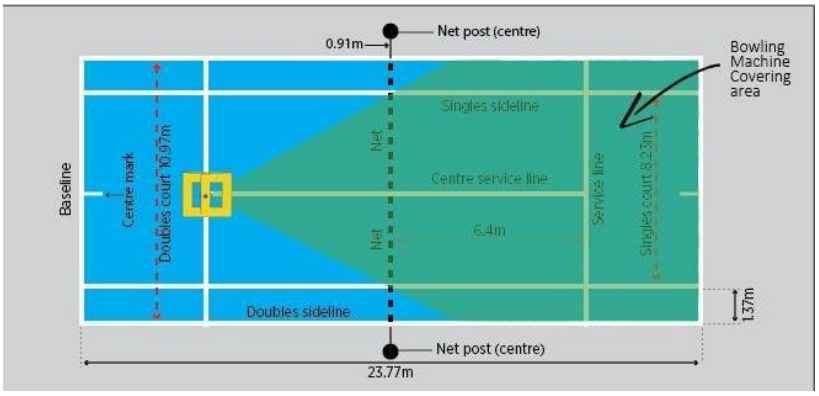

Figure 3.2: Maximum angular range of throwing

The control system manual has features that can be manually adjusted for speed, horizontal and vertical inclination. The automatic mode has an on/off switch. When the mode was on, balls were randomly thrown from the machine, because it has the feature of adjusting the number of balls thrown per minute from the machine.

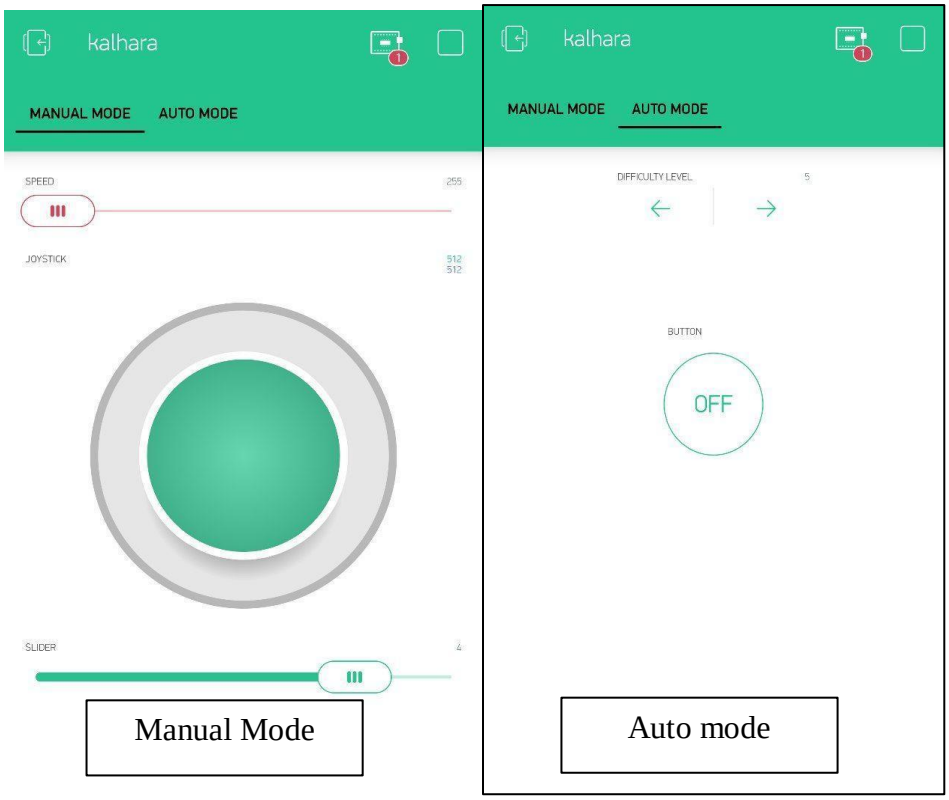

Figure 3.3: Control interface of the mobile application

4.0 CONCLUSION

The bowling machine of the present work, by imparting rotation to the ball, causes the flight characteristics of the throwing ball to simulate those of a pitched ball thus making the machine suitable for use in batting and keeping practice. The proposed bowling machine has the following advantages, the bowling speed was variable, positive adjustment of line and length of bowling was possible with repeatability, Different varieties of bowling like good length, slice serve, kick serve, flat serve, etc. were possible, and the machine was portable and low cost. Further work was proposed to develop this system for the bowling machine that detects the movement of the player and automatically throws the ball from the player to the opposite area. This will help in more efficient training.

ACKNOWLEDGEMENT

The author wishes to extend her gratitude for the assistance given by the Department of Electronics at the Wayamba University of Sri Lanka, the staff of Sri Lanka Telecom - OPMC Kegalle, and others who have supported to make this research a success.

REFERENCES

[1]. https://en.wikipedia.org/wiki/Tennis (Accessed 17-09-2020).
[2]. Kovacs, M., Tennis physiology: training the competitive athlete. Sports medicine (Auckland, N.Z.). 37, (2007), 189-98.
[3]. Kovacs, M.S., Tennis physiology: Training the competitive athlete. *Sports Med* 37: 1– 11, (2007).
[4]. https://tenniscompanion.org/how-to-play-tennis/#the-court,(Accessed 17-09-2020).

[5]. Kovacs, M., Movement for Tennis: The Importance of Lateral Training. *Strength & Conditioning Journal*. 31,(2009), 77-85. Doi:10.1519/SSC.0b013e3181afe806.
[6]. Castelli J.T., Forrester J.J., *Ball throwing machine*, Kamphaeng Phet Rajabhat University, (1978).
[7]. Stokes, G.A., Tennis ball throwing machine with continuously rotatable barrel having friction strip on one side only of inner wall, 18 February 1986. https://patents.justia.com/patent/4570607,(Accessed 21-08-2021).
[8]. Horvath, T., Automatic ball thrower, *US Pat 3584614*, 15 June 1971. https://patentimages.storage.googleapis.com/11/3b/67/abbace9fd92686/US3584614.pdf. (Accessed 21-08-2020).
[9]. Thakur T., Srinivasa C.K., Syed I., Integrated Novel Multi-Game Ball Throwing Machine, Design and Fabrication. *International Journal of Scientific and Engineering Research*. 10, (2019), 493-505.
[10]. Winchester, D., A., Portable spring type impact ball pitching device, 2 November 1999.https://patentimages.storage.googleapis.com/ca/b1/03/f688c14e319dc5/US4237851.pdf,(Accessed 21-08-2020).
[11]. Paulson, J.K., Ball throwing device,*US Pat 4080950*, 28 March 1978. https://patents.justia.com/inventor/john-k-paulson (Accessed 21-08-2020).

Proc. Annual Symposium on Research & Industrial Training, 08(2021) 69-73
Department of Electronics – Wayamba University of Sri Lanka

AUTOMATIC ROTATING STAND FOR MEASURE THE ANGLE FOR SPECIFIC TASKS

T.A.R.N. Thenuwara*, M.A.A. Karunarathne

Department of Electronics, Wayamba University of Sri Lanka, Kuliyapitiya, Sri Lanka

*rnisansalathenuwara@gmail.com

ABSTRACT

Although there are several ways to measure angles, the most commonly used method is the protractor. The international unit of the measurements of angle is the degrees and radians and revolutions are also used to measure degrees. However, in this project only degrees are considered. Usually an object has to be rotated at some angles in the different experiments. It is essential to rotate angles for antenna experiments, robotics, photography and geography etc. By rotating the antenna to different angles, it can get the best angles for data which can be received, and an object can be photographed from different angles. But in such cases, it is not possible to measure the angle accurately. Considering these factors, when the angle required for rotation is entered into the system, the antenna or objects rotates accordingly. Observers can obtain results and experiments can be done accurately, because the instruments can be rotated according to any input angle. Also any degrees of angle with three digits can be inserted, however the stand is not rotated for the some angles which are made up with fraction numbers. The final goal of this project is that any degrees of angle can be inserted and the stand is rotated accordingly. So not only this Automatic Rotating Stand was used to rotate a number of objects but also for antenna experimentation.

Keywords: Rotating, Stand, Measurement of angle

1.0 INTRODUCTION

Angle measure techniques are required in various precision engineering applications. Examples are manufacturing robotics, antennas, etc. There are three types of units to represent the magnitude of an angle: revolutions, degrees and radians. In trigonometry, radians are used most often, but it is important to be able to convert between any of the three units [1]. However the most important angle representing units is the degrees for this Automation system.

Sometimes it is necessary to rotate instruments to a given number of degrees. It is usually hard to figure out how much the device is spinning. Some cases a device has to be rotated to any angle and the protractor cannot be used for this. In some experiments the device had been rotated manually until it got the correct results. But during such experiments it is difficult to rotate the instrument manually and it is not practical and not suitable for accurate experiments. Therefore it is necessary to measure the angle of rotation automatically while conducting the experiment. Also experiment instruments or devices must be rotated to the given number of degrees. Then it is easy to measure how many rotors are needed and it is also easy to record those measurements. Several rotating systems have been developed to rotate the number of instruments or devices, but some of the systems have been identified as faulty.

In a current system, the motor is rotated to the same size as the input degrees in the “UPG SCR Shaft Motor Step by Step Angle Rotation Control " system and the GLCD screen indicates that number of degrees. But this System has the problem of rotating at the desired angle and then returning to the zero degree position. Sometimes this can lead to inaccurate measurements for the experiments. [2]. “The Arduino PIC DC Motor Position Control Close Loop System" is also one

of the existing automatic protractor systems. In this case, input degrees are entered from an android app. However, the system cost is more to design the system [3].

Based on these facts, it is necessary to create a low cost automatic rotating stand to measure the angle of the device and rotate the devices according to the input degrees. This makes it easy to take required measurements and perform tests efficiently as the system can rotate a given angle. In this automated system, angles of the instruments or devices were shown. Instruments were rotated according to the given angle which is input from the keypad. Outputs were measured while instruments were rotated. Output angle was shown on the screen. Output angle should be equal to the angle which is given by the keypad.

2.0 METHODOLOGY

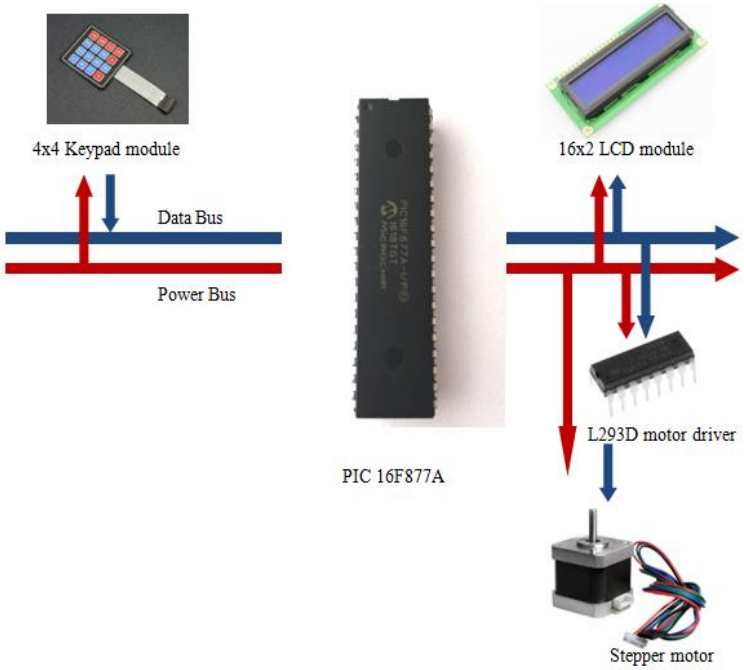

Figure 2.1: Block diagram for the system

The object must be rotated according to the value of the angle entered in a stand or antenna experiments. Here the value of the angle required to rotate is entered by the 4x4 matrix keypad. The value entered by the keypad is displayed on the 16x2 LCD module. Because of this reason the value of the entry angle and the number of the digits of the angle can be seen accurately. So the stepper motor was rotated according to the value of the input angle, which causes the stand or antenna mounted on the motor to rotate. The stepper motor requires 12V voltage and 1A current, but the microcontroller generates 3.3V to 5V voltage and 25mA current, so the stepper motor is controlled through a L293D motor driver because it cannot be directly controlled by the microcontroller.

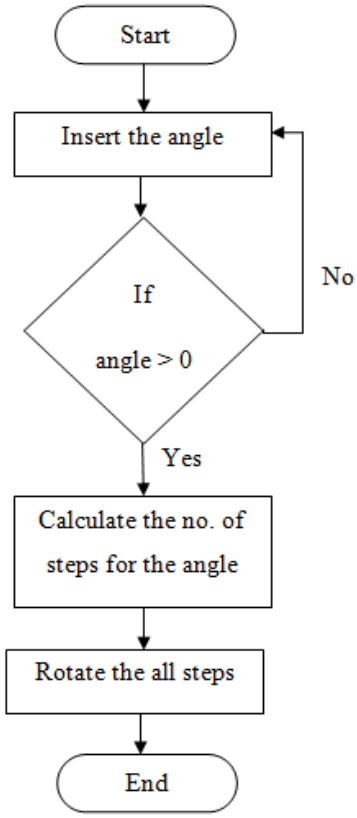

Figure 2.2: Flow chart of the system

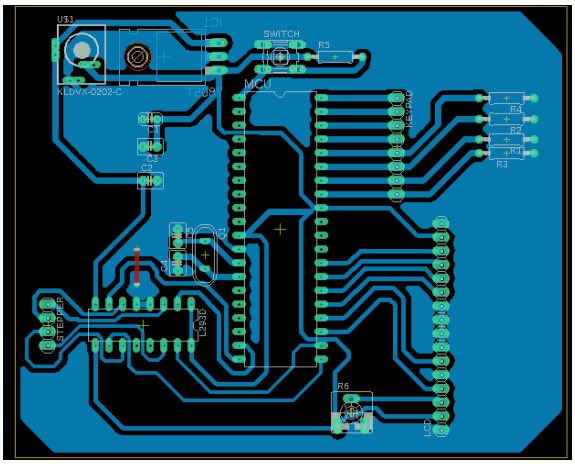

Figure 2.3: PCB layout of the System-Bottom view

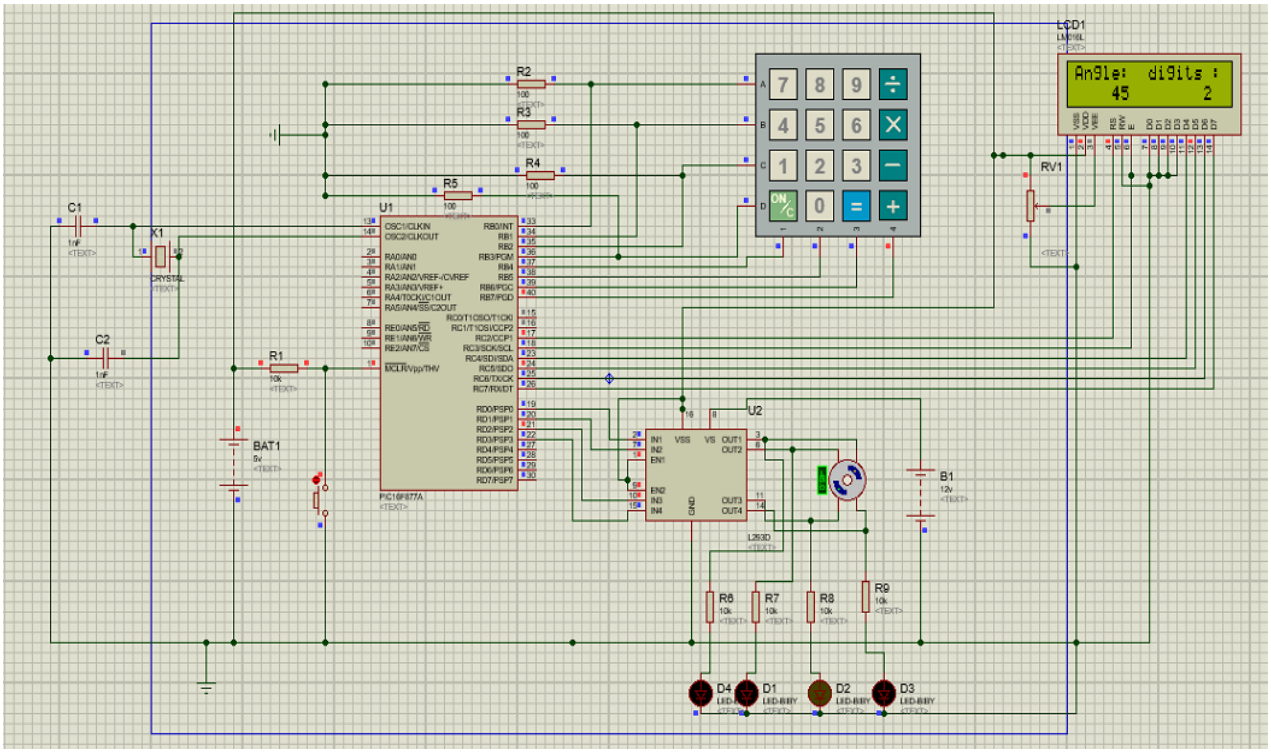

Figure 2.4: Simulation of the Rotating system

3.0 RESULTS AND DISCUSSION

The stepper motor was rotated according to the half wave drive mode and in this case the motor rotated in 08 parts. The motor was rotated by 0.9^0 when the value was given by the keypad. So, 0.9^0 degrees to degrees was rotated because the step angle of the stepper motor is 1.8^0. As a result, several problems occurred and those could be successfully resolved.

The stepper motor has a rotating mechanism. When a value is given by the keypad, it first checks the number of steps.

$$number\ of\ steps = (input\ angle \times 2)/(step\ angle) \quad (1)$$

If an angle was entered by the keypad, the motor was rotated according to the two sections. For example, input angle 18^0 degrees for the rotation.

$$number\ of\ steps = (18 \times 2)/1.8 = 20$$

$$number\ of\ roate\ full\ cycles = \frac{20}{8} = 2\ and\ remain = 4$$

According to the above example, the stepper motor has used 04 steps and half-wave drive twice to rotate the rotary of the stepper motor. Therefore the stepper motor has used 08 steps for each half-wave drive. But there is a sequence of using the above mentioned sections. It means if the entered angle value is 18^0 it has 20 steps to rotate. Here the number of half cycles must be rotated first and after that remaining parts must be rotated. Suppose 9^0 degrees is rotated again.

$$number\ of\ steps = (9 \times 2)/1.8 = 10$$

$$number\ of\ roate\ half\ cycles = \frac{10}{8} = 1\ and\ remain = 2$$

But in the previous 18^0 degree rotation it rotates 02 half cycles and 04 steps. So it needs 04 more steps to complete the half cycle. Therefore the required steps which need to complete the half cycle were obtained from the next initial input angle. Because of this reason 04 steps from the next initial input angle were rotated first and the remaining 06 parts were rotated by considering a new angle. The reason to follow the above procedure when a new angle is inserted is this system is always looking for the initial state before starting the rotation. So it is important to get rotary to the next initial point. However there are a number of initial states in this system. It can be obtained by dividing 360 from (step angle*4). In the given example, $18^0 + 9^0 = 27^0$, but if the system does not follow the above procedure the rotation of the system is only 23.4^0. This is an error in the system however after following the above procedure the value resolved properly.

Also, since the stepper motor rotates in eight parts of 0.90 each for a half cycle, it shows an error of 0.10 when rotated one degree. This error had to be corrected by the use of cogs, which could not be created in the corona pandemic situation.

4.0 CONCLUSION

This project proposes an automatic rotating stand for rotating devices for certain angles. Also it displays the rotating angle. Also this system can be useful for antenna measurements, robot technologies and photography. So it is easy to test and rotate many objects for different angles through this automatic system. Any 03 digits number can be entered into this system as not only the object of this system but also many devices were automatically rotated according to the given angle. Therefore this automatic rotating stand can be used in any rotation experiment.

ACKNOWLEDGEMENT

Authors would like to thank all the staff of the Department of Electronics, Faculty of Applied science, Wayamba University of Sri Lanka.

REFERENCES

[1]. Trigonometry: angle, *Spark notes*, https://www.sparknotes.com/math/trigonometry/angles /section2/, (Accessed-2021. 06. 28)
[2]. Madalina U., Fanel V., UPG SCR shaft motor step by step angle rotation control, *Angular positioning using a step by step motor*, (2018), https://youtu.be/fHcGXHbp6hE, (Accessed: 30- Aug- 2020)
[3]. Sandeep, Arduino PID DC motor position control close loop system, *Electric DIY lab*, (2019), https://electricdiylab.com/arduino-pid-dc-motor-position-control-close-loop-system, (Accessed: 30- Aug- 2020)

Proc. Annual Symposium on Research & Industrial Training, 08(2021) 74-79
Department of Electronics – Wayamba University of Sri Lanka

DESIGN OF AN AUTOMATIC AIR CONDITION CONTROL SYSTEM BY DETECTING THE NUMBER OF OCCUPANTS.

G.S.A.Fernando*, J.M.J.W. Jayasinghe

Department of Electronics, Wayamba University of Sri Lanka, Kuliyapitiya, Sri Lanka.

*thushariakalanka@gmail.com

ABSTRACT

Temperature control refers to the processes, which aim at maintaining the temperature in a given area at a given value or within a certain range. Recently, globalization and industrialization have further necessitated the need for temperature control applications in various daily activities, especially with the advent of the greenhouse effect. The air conditioner (AC), which is used for temperature control, is one of the most used electrical appliances nowadays. However, the energy consumption for AC units is quite high. The main objective of the proposed automatic AC control system is to optimize the utilization of electricity. The proposed system provides automatic control of the temperature inside a building based on occupancy. The system continuously detects the entry and exit of people by using Infrared (IR) sensors and identifies the number of occupants available in the hall. The automatic control system of the AC units operates based on the signals provided by the IR sensor system. The control system switches ON and OFF the AC units automatically, keeping only the minimum number of AC units switched ON based on the occupancy.

Keywords: Air Conditioner, Digital bidirectional visitor counter, Arduino Microcontroller.

1.0 INTRODUCTION

1.1 Overview

An air conditioner is an appliance, system, or mechanism designed to extract heat from an area using a refrigeration cycle. In construction, a complete system of Heating, Ventilation, and Air Conditioning is referred to as HVAC. The purpose of the AC is to provide comfort during hot days and nights. In a thermodynamically closed system, any energy input into the system that is being maintained at a set temperature (which is a standard mode of operation for modern air conditioners) requires that the energy removal rate from the air conditioner increase. This increase affects that each unit of energy input into the system requires the air conditioner to remove that energy. To do that the air conditioner must increase its consumption by the inverse of its efficiency times the input unit of energy.

In the United States, the efficiency of AC units is often (but not always) rated by the Seasonal Energy Efficiency Ratio (SEER). The higher the SEER rating, the more energy-efficient is the air conditioner. The SEER rating is the BTU of cooling output during its normal annual usage divided by the total electric energy input in watt-hours (W.h) during the same period. So when we use the air conditioner, we need to pay more bills.

1.2 Research Objective

In the present society with the increase of atmospheric temperature, people tend to use air conditioner units at the office as well as at home. However, its electrical consumption and related expenses are very high. The main aim of this project is to build up a system that

automatically operates based on the number of occupants inside the room. In the proposed system, an AC unit automatically starts to operate when a person enters the room. When the number of occupants increases, the number of operating AC machines increases accordingly, and vice versa. When all the occupants inside the room are gone out, all the AC machines automatically get switched OFF. Through this process, energy consumption can be reduced.

1.3 Literature Review

Air conditioning systems are major electrical loads in houses, auditorium halls, indoor stadiums, and other such buildings. Conventional air conditioners consume constant wattage when they are operating. When the desired temperature reaches, the outside unit is turned OFF. There are two states of operation; either ON or OFF. The operating states can be increased using fuzzy logic for reducing the consumption of electricity without affecting the air conditioning process [5]. In fuzzy logic, the output of the system is evaluated based on the system's input/inputs. The inputs are fuzzified using a triangular membership function. Based on these values fuzzified output is produced using fuzzy rules. The fuzzified output is converted to crisp output by the 'center average using a singleton value' defuzzification method [04]. The air conditioning process can be controlled using various methods. Some of these methods are ON/OFF control, neural network control, fuzzy control, robust control, and many more. A detailed review of these control methods is given by Afram et al [5]. In 2016, Winfred Adjardjah proposed the design and construction of a Digital Bidirectional Visitor Counter (DBVC). The DBVC is a reliable circuit that takes over the task of counting the number of persons/visitors in the room very accurately the total number of persons inside the room is also displayed on the Liquid Crystal Display (LCD) [7].

2.0 EXPERIMENTAL

2.1 Theories

The British thermal unit (BTU or Btu) is a unit of heat; it is defined as the amount of heat required to raise the temperature of one pound of water by one degree Fahrenheit.Every AC has a BTU value. The BTU value represents the number of occupants obtain cooling from a single AC in the AC system. BTU value per person is 600 BTU. The following table provides the BTU values for each type of AC according to the square feet.

Table 2.1: Air Conditioner BTU Calculation Table

Area To Be Cooled (square feet)	Capacity Needed (BTUs per hour)
100 to 150	5000
150 to 250	6000
250 to 300	7000
300 to 350	8000
350 to 400	9000
400 to 450	10000
450 to 550	12000
550 to 700	14000
700 to 1000	18000

In the proposed system; an Arduino microcontroller was worked as a counter controller. Two IR sensors, IR_1 and IR_2 were used on a single door in this system. IR_1 was used for counting

entry persons and IR_2 was used for exit persons. The emitter was passed an infrared beam which is detected by an IR receiver (phototransistor). The beam is broken when a person walks by the beam. Upon this event, infrared light no longer could detect by the phototransistor and another event is triggered (door opens).An infrared LED has consisted of the transmitter and it was associated with the circuitry as well as the receiver [6].

The LCD is used to display the count. A TSOP sensor is an IR Receiver that could be used to decode the signal coming from the remote. The Receiver was interfaced in between Arduino to signal for each button and an IR Led was used with Arduino to mimic the signal whenever required. In this way, the AC was gained under control by using an Arduino [3].The power supply block has consisted of the following units: Step down transformer; Bridge Rectifier Circuit, Input Filter, and Voltage Regulator [1].

2.2 Procedure

The circuit shown in Figure 2.1 was designed to count the occupants. A 5V potential was supplied to the circuit. The LCD was connected to an Arduino board to display the count of the occupants. Two IR sensors (IR_1 and IR_2) were connected to A_0 and A_1 pins of the Arduino board to receive the signals from the IR sensors which sense the entry and exit of the occupants. The count of occupants who entered the room was detected when someone pass the IR_1 sensor first and then the IR_2 sensor. Similarly, the count of occupants who exit from the room was detected when the IR_2 sensor is passed first and then the IR_1 sensor. The code was written to count people and display it on the LCD and the code was uploaded to the Arduino board. This circuit was installed at the entrance of the room to counts the number of people who enter and exit.

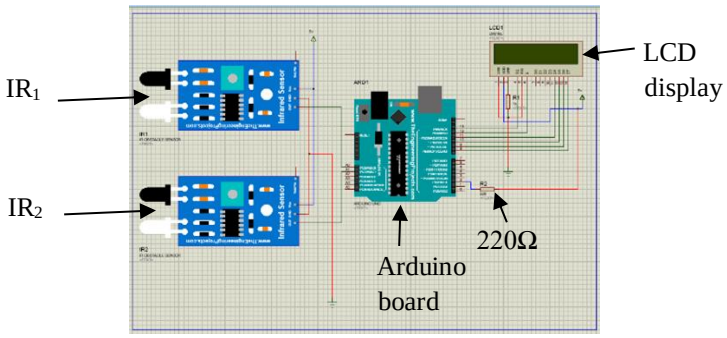

Figure 2.1: The circuit diagram of the people counter.

The circuit in Figure 2.2 was designed by connecting the TSOP sensor to Arduino. It was designed to automatically switch ON/OFF the AC unit by retrieving the data provided by the remote controller to the serial monitor instead of a switched ON/OFF the AC unit with the remote controller. The Arduino code was uploaded and open the Serial Monitor. The remote controller was placed in front of the TSOP sensor and pressed the switched ON or switched OFF button on the AC unit. Then, data were displayed on a serial monitor.

An IR LED was connected as shown in Figure 2.3. IR LED is the one that passed the signal to the AC unit instead of the remote controller. When the people entered the room, the total count should be increased and the count should be decreased when people leave. It can be checked by the LCD. The code was implemented by using the details in Figure 2.2 and switch to the Arduino board as the AC unit should be turned ON when the count shows 1 and should be turned OFF when the count is 0.

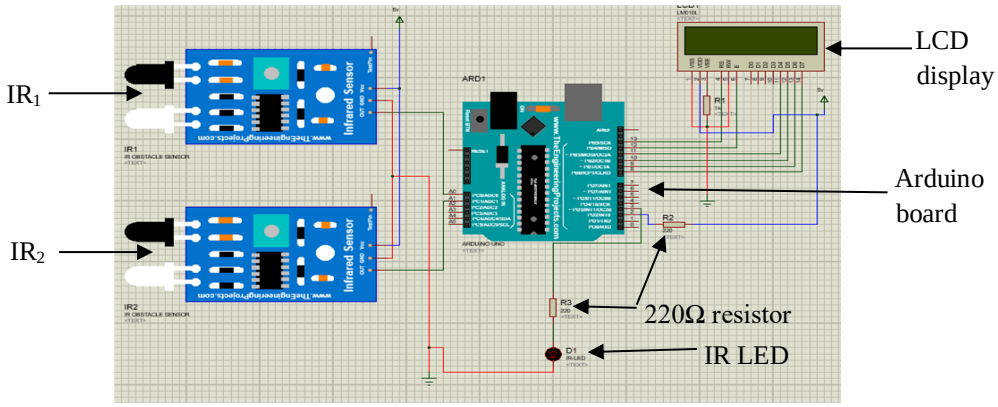

Figure 2.2: Circuit diagram for automatic ON/OFF the AC system.

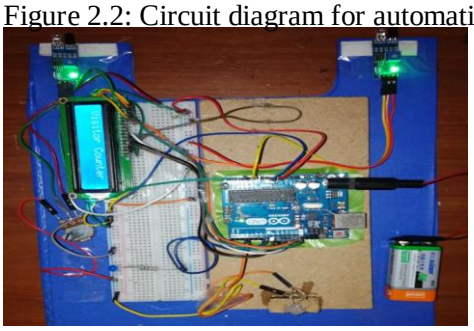

Figure 2.3:Control circuit.

Figure 2.4: Circuit with of 4 bulbs.

Figure 2.2 shows the circuit of automatic on/off of a single AC unit. To test the functionality of the circuits, four bulbs were used instead of four AC units. The AC units/bulbs are named B1, B2, B3, and B4 respectively (Figure 2.4 left to right). A TSOP sensor has placed as shown in Figure 2.5 since the TSOP sensor has contained an AC unit. The reason for that is to take the signal which is taken from the circuit shown in Figure 2.3 and switch ON/OFF the bulbs automatically.

The Arduino code was uploaded to the Arduino board and placed the TSOP sensor in front of the remote controller. The buttons were pressed in 1 to 8 orders respectively. The signal was decoded through the serial monitor. The value of the signal was equated to the number of the AC units which was in ON and OFF state. According to the number of AC units that were in switched ON and OFF states, table 2.2 was arranged.

Table 2.2: Assign pin numbers for Switch ON/OFF buttons of AC units

AC unit	PINs of switch ON buttons	PINs of switch OFF buttons
B_1	1	8
B_2	2	7
B_3	3	6
B_4	4	5

A step-down transistor was connected as shown in Figure 2.5 to reduce the 230V AC voltage to the exact 12V AC voltage. Further, four diodes were connected to convert an Alternating Current (AC) to a Direct Current (DC). An electrolyte capacitor was connected to smooth the current. The 7812 voltage regulator was connected to take the exact 12V DC voltage. Four

capacitors were used to cut the frequencies from 7812 and 7805 voltage regulators due to detecting the remote control frequency properly.

Four-channel relay module was used as a switch and a 230v was controlled AC unit by using 5v. The automatic AC system was fully completed as a combination of Figure 2.3 and Figure 2.6 circuitries. The code which is included the decoded values from 1 to 8 buttons was uploaded to the circuit shown in Figure 2.3. The count of people and the BTU value were decided the number of AC units that needed to light up as shown below.

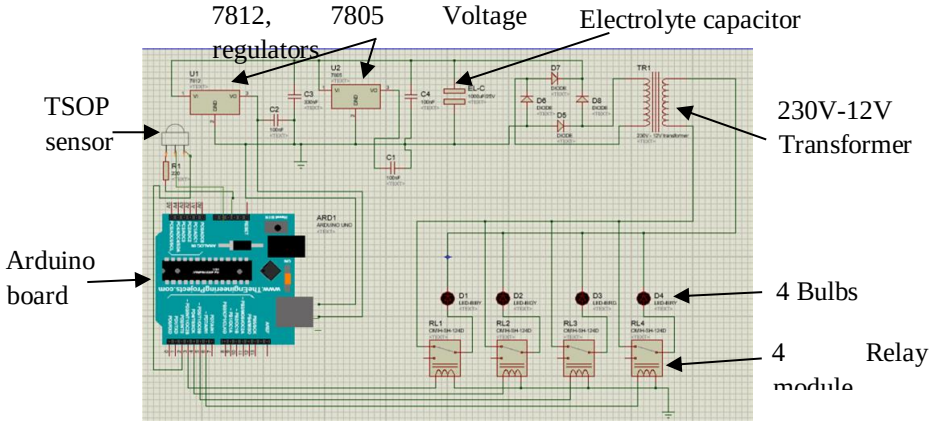

Figure 2.3: Circuit diagram of 4 bulbs (suppose that these bulbs as 4 AC

AC machines that have a BTU value of about 48000 used for the proposing system.
The BTU value of AC unit = 48000
Per person necessary BTU value = 600
Number of occupant one AC can be cooled = 48000/600 = 80
Number of AC in the room = 4
The minimum number of occupants required to operate the AC_1 air conditioner automatically was one. Accordingly, 81 of the minimum occupants were required to activate AC_2 automatically. A minimum number of 161 and 241 occupants were required to activate AC_3 and AC_4 respectively. Similarly, the number of occupants must be 240 for inactivated the AC_4. AC_3, AC_2, and AC_1 were inactivated when the number of residents was 160, 80, and 0 respectively.

3.0 RESULTS AND DISCUSSION

The count on the LCD display was 0 initially and increases gradually when people enter the room passing IR_1 and IR_2 respectively. The count decreases when the people leave the room passing IR_2 and IR_1 respectively.

When a person passes IR_1 and IR_2 respectively, the count becomes 1 and the AC_1 is turned ON automatically. Similarly, when the number of counts reaches 81, the AC_2 turns ON automatically with no difference to the status of AC_1. Likewise, AC_3 and AC_4 turn ON automatically when the count becomes 161 and 241 respectively. To check the operation of 4 AC units, a circuit arrangement with 4 bulbs was used. Similarly, the number of counts decreased as people leave the room and the automatic switching OFF process takes place. Hence, the status of the AC units (switch ON or OFF) depends on the number of people in the room or building.

4.0 CONCLUSION

In this paper, a method capable of optimizing the cooling of a room automatically is demonstrated. Thus, an automatic AC unit control system would make a pleasant work environment without the need to constantly switching the AC unit switched ON and OFF. The IR sensors count the number of people entering and leaving the room and send it to the microcontroller. The number of active AC units is decided by the Arduino microcontroller based on the number of occupants available in the room. The hardware implementation of the proposed system has been done and confirmed that it works properly. The number of occupants is detected correctly and the AC units are switched ON and OFF accordingly. This system is helpful to save the consumption of electricity in a building.

REFERENCES

[1]. Adjardjah W., Design and Construction of a Bidirectional Digital Visitor Counter Computer, *Department of Electricals and Electronics, Takoradi Polytechnic,*7, (2016).
[2]. Gole, R., Sangale, K., Ramesh, R., Ravale. U., Smart Air-conditioning Control System, *International Journal of Information and Computing Science*, 6, (2019), 633.
[3]. Aswinth Raj, Automatic AC Temperature Controller using Arduino, DHT11 and IR Blaster, https://circuitdigest.com/microcontroller-projects/arduino-automatic-ac-temperature-control, (Accessed 2020-09-16)
[4]. Abdul A., Sharifi F. J., Theory and applications of HVAC control systems–A review of model predictive control (MPC), *Building and Environment ,72*,(2014), 343-355.
[5]. Saha S., Saha S. K., Iqbal I. S., Kundu A. K., Khan M. T. H., Pramanik S. K., Designing of an air-conditioning system using fuzzy logic with advantage of energy saving, *2014 International Conference on Informatics, Electronics & Vision (ICIEV), Dhaka*,(2014),1-6, doi:10.1109/ICIEV.2014.6850757.
[6]. Kumar V, Kumar S., Kansal H., Fuzzy logic controller based operating room air condition control system, *International Journal of Innovative Research in Electrical, Electronics, Instrumentation and Control Engineering*, (2014).
[7]. Effah E., Aryeh F. L. Kehinde W. K., GSM Based Home Appliances Control System (HACS) for Domestic Power Users in Ghana, *4th UMaT Biennial International Mining and Mineral Conference, Tarkwa, Ghana, (*2016), 58-64.

Proc. Annual Symposium on Research & Industrial Training, 08(2021) 80-87
Department of Electronics – Wayamba University of Sri Lanka

USER FRIENDLY AUTOMATED SYSTEM TO WATER CHENA CULTIVATION

H.W.E. Madushani*, K.P. Vidanapathirana

Department of Electronics, Wayamba University of Sri Lanka, Kuliyapitiya, Sri Lanka

*erangimadhushani@gmail.com

ABSTRACT

In daily operations related to farming, watering is the most important labour – intensive task. People are unable to water the plants when they go on vacations, in an emergency or regularly fail to remember to water the plants, which results in damaging the plants. As a solution, the proposed system was developed to reduce the human effort in watering the cultivation. This system is based on Node MCU. In this system, soil moisture sensor checks the moisture level in the soil and if the moisture content is below the threshold value then water pump will automatically turn ON via the relay to provide water to the plants. It will automatically get switched OFF when the system detects required moisture level in the soil. Usually, farmers do not have a clear idea about the amount of water in the well for watering the plants for coming days. This system will also provide an update to the farmer about the amount of water in the well for watering for coming days. Therefore, this system will be very useful for them to plan the watering. This system is also convenient for people who are engaged in other duties with farming. Due to low cost, any individual can implement this system into their cultivation.

Keywords: Automated watering system, Node MCU, Weather API

1.0 INTRODUCTION

Fertilizer, sunlight as well as water are the most important factors for healthy plant growth. Usually the plants should be watered twice a day. In addition to rainfall, groundwater is an important natural resource for watering plants. As weather changes, the amount of groundwater in the wells decreases during the periods of low rainfall.

Today, farmers face major problems in irrigating their crops due to their busy schedules of daily life. Sometimes if they have to go for a long vacation or in an emergency, they are unable to attend to water the plants. As a result, plants can be destroyed. Usually farmers do not have a clear idea about the amount of water in the well for watering the plants for coming days. But if the farmers get updates of available water amount, it is very useful for them to plan the watering.

1.1 Literature review

Several systems have been developed for watering using different ways and ideas. In 2015 Vidadala *et al*., implemented an agricultural automation system using WEB and GSM technologies. Optimum usage of water was the main objective of that system. It used a soil moisture sensor and a temperature sensor to detect the water quantity present in the soil and water level sensor for detecting water level in the tank. In this system status of the sensors was monitored through WEB and GSM technologies. Here temperature, soil moisture and water level can be monitored on a web page through micro controller and information will be sent to the user by SMS [01].

In 2017, an automatic irrigation system was reported which is based on microcontroller ATMEGA328. In this system temperature and soil moisture sensors are placed in the field. Sensors sense the moisture content of the soil and give the information to farmer through GSM [02].
The existing systems used GSM module to give the information to the farmer by SMS. But for the operations involvement of the farmer is essential. Therefore, it is necessary to create a user friendly system for farmers. Current systems do not inform the farmer about the total water consumption for a day and how many days watering can be done with the existing amount of water considering future weather predictions. It is necessary for them to plan the watering. Considering all above, the proposed system was developed and implemented having such features via an android app.

1.2 Objective of the study
The present system was developed with the aim to reduce human effort in watering the cultivation. It is not only meant for watering plants but also with a user friendly android app. This will update the farmer with a daily report including the current moisture level of soil, total water consumption of a day, how many days watering can be done with remaining water considering future weather prediction data.

2.0 EXPERIMENTAL

This automated system sense the moisture level in the soil and according to that value, water pump will be automatically switched ON and watering will take place. When moisture value exceeds the given value, the motor will be automatically switched OFF. The water pump is controlled through a relay module. Weather data will be updated every day and the time interval is given by RTC module. Ultrasonic sensor detects the water level in the well and a value is used to calculate the remaining water in the well.

By using water flow sensor, amount of water used per day will be measured. Microcontroller collects that data and sends those data into the database (Firebase). Those will be generated as a report and sent to the farmer using an android app. Farmer can check the report at any time by clicking on the App. Figure 1 shows the block diagram of the system.

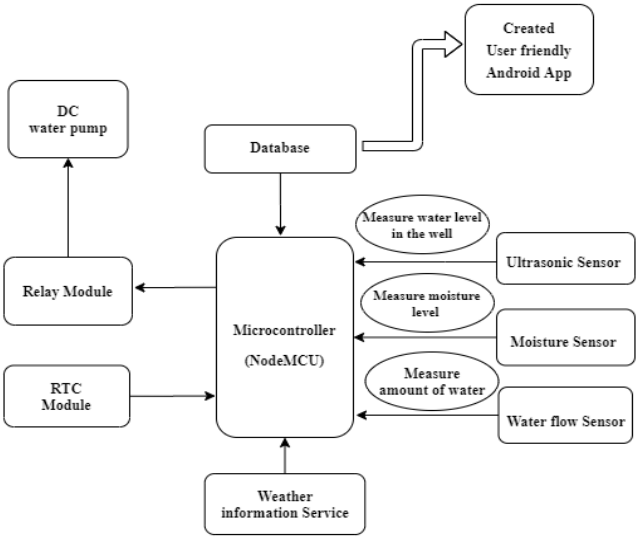

Figure 2.1: Block diagram of the design

The system will also update the farmer about how many days watering can be done by considering future weather predictions and amount of water available in the well. The Node MCU board is getting weather information service data as shown in the block diagram. After comparing all data, results will be sent to the user friendly mobile android app via database. Weather data is updated every day for the next 7 days from open weather map. Figure 2 shows the flow chart of the system.

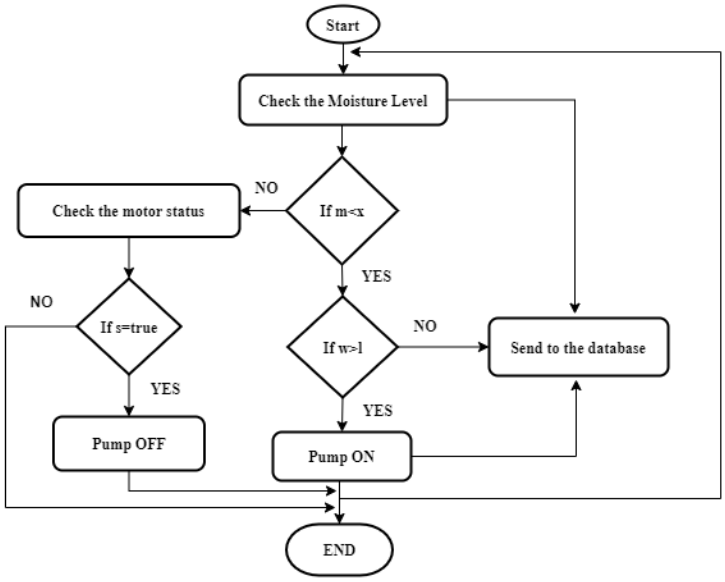

Figure 1.2: Flow chart of the system

Where; m- the moisture level of the soil, s- motor state, x- desired moisture level of the soil, w- water level in the well, l- water low level in the well.

The modules, components and software used to develop the system are explained in the next sections.

2.1 Node MCU (ESP8266)

ESP 8266 is a Wi-Fi module that is more and more popular among hardware developers. In addition, the price is very affordable. This is a versatile Wi-Fi module coming as SOC (System on Chip), which can be programmed directly to ESP8266 without requiring an additional microcontroller [03].

2.2 REES52 - Soil Moisture Sensor

Soil moisture sensor is used to determine the moisture present in the soil. The moisture of soil depends upon various factors such as types of soil, whether it is sandy, clay, loam, and salts present in soil such as iron, manganese, calcium, phosphorus, nitrogen, etc [04].

2.3 HC-SR04 Ultrasonic Sensor

Ultrasonic sensor is an electronic device that measures the distance of a target object by emitting ultrasonic sound waves, and converts the reflected sound wave into an electrical signal. Ultrasonic wave travel faster than the speed of audible sound (i.e the sound that humans can hear) [05].

2.4 YF-S401 Water Flow Sensor

The YF-S401 water flow sensor consists of a plastic valve body, flow rotor and hall-effect sensor. It is usually used at the inlet end to detect the amount of flow. This sensor sits in line with the water line and contains a pinwheel sensor to measure how much water has moved through it [06].

2.5 DS 3231- RTC Module

A Real-Time Clock (*RTC),* is an integrated circuit that keeps track of time. It uses a back-up battery to maintain the time in the event that the main power source is removed. The RTC keeps track of seconds, minutes, hours, day, date, month, and year data [07].

2.6 LM2596 Buck Converter Module

Basically a DC-DC buck converter consists of power switches such as MOSFET or BJT that will act as switches to control pulses. In buck convertor, the output voltage is always lower than the input voltage [08].

2.7 JQC-3FF-S-Z Relay Module

Relay is a switch which is operated by an electrical signal and is an electromechanical component consisting of two main parts: electromagnetic coil and a mechanical switch. Relays use electromagnetic principle to move switch with low power voltage to conduct high voltage [09].

2.8 DC Water Pump

Smaller electric water pumps, usually have small DC motors. The DC motor is contained in a sealed case attached to the impeller and powers it through a simple gear drive. The center of the motor consists with a rotor with coils around it [10].

2.9 Android Application

MIT (Massachusetts Institute of Technology) application (App) inventor is an online platform. It provides a web-based "What you see is What you get" (WYSIWYG) editor for building mobile phone application targeting the android and iOS operating systems. MIT app inventor, uses code application behavior using a block-based programming language. Its user interface includes two main editors: the design editor and the blocks editor [11].

2.10 Firebase

Firebase is a cloud-hosted, NoSQL database that uses a document-model. It can be horizontally scaled while letting storing and synchronizing data in real-time among users [12].

2.11 Weather API

Open weather platform is a set of elegant and widely recognizable APIs powered by convolutional machine learning solutions. It is capable of delivering all the weather information necessary for decision-making for any location on the globe.

3.0 RESULTS AND DISCUSSION

The picture of the overall complete system is illustrated in figure 3 (a), (b) and figure 4 (a), (b), (c). All the components of the system were connected to the Node MCU via PCB. According to soil moisture and water level in the well, water pumping motor will turn ON or OFF via the relay automatically.

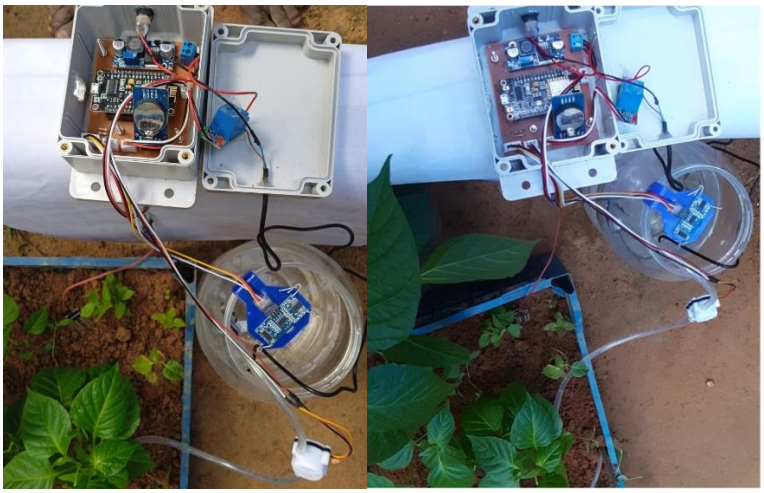

(a) (b)

Figure 2.1 (a), (b): Top view of the System

Node MCU is the main component of the system, all other sensors and modules are connected to it to provide a serial communication among each other and real time data to the user.

This system is powered by a 12V power supply. A buck converter is used in this system that can be supplied any voltage between 5V to 30V. The output of the buck converter is 5V. Node MCU, ultrasonic sensor, soil moisture sensor and relay module of the system work at 5V. RTC module and water flow senser are operating at 3.3V which is supplied by Node MCU board. This system was built inside a project box to protect it during rainy days.

(a) (b) (c)

Figure 3.2 (a), (b), (c): Pictures representing the entire system

Figure 3.3 shows the result of uploaded data on real time database in firebase.

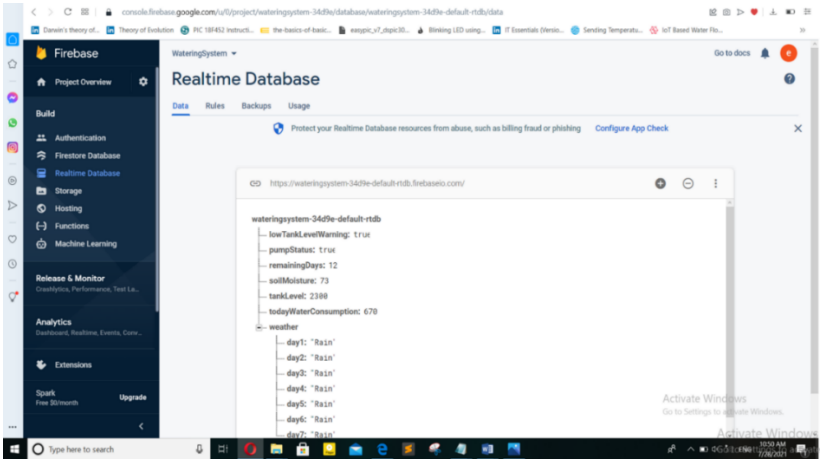

Figure 3.3: The screenshot of the real time database of the system

Open weather platform provides weather data for coming seven days. If there is a rainy day, the amount of water required for cultivation on that day is received from the rain. The important part of the system is after the watering, famer can see a report by clicking on user friendly android app at any time. The report includes the current moisture level of soil, total water consumption on a day and how many days watering can be done as shown in Figure 3.4(a), (b).

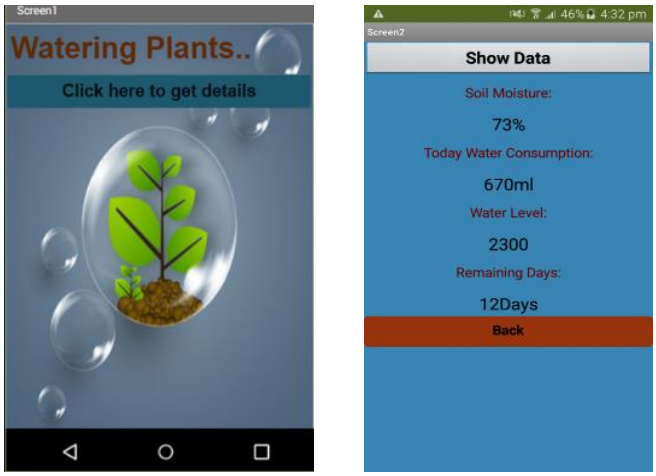

(a) (b)

Figure 3.4 : The screenshots of the screen1 (a) and screen 2 (b) of the app

When clicking on "show data", farmers can get updates about the atmosphere around the cultivation as shown in Figures 3.4(a) and (b). This system will be very useful for farmers, who are involved with chena/small scale cultivation to plan the watering. It can also be developed for any kind of cultivation and for people who are engaged in other duties with farming.
This system requires a Wi-Fi connection for getting updates to the database. 12V power supply is used for this system. But it is better to have a rechargeable battery for the system to avoid the power issues. The operating voltage for some components of this system is 5V. But since output voltage of the Node MCU board is 3.3V, the required voltage had to be supplied to those components using a buck converter. It was not easy to write the software for the system and upload it in Node MCU to run the water pump and getting weather data and uploading the data into firebase, but with the help of Arduino library, the program was completed with perfect results.

4.0 CONCLUSION

This "User Friendly Automated System to Water Chena Cultivation" was designed and tested using Node MCU successfully. The main objective of this project is to help the farmers who do not have enough time to water their cultivation. And also to update the farmer about the availability of water for the remaining days to water the plants considering weather data using a user friendly android app. Therefore, this system will be very useful for farmers to plan the watering. As future work, this system can be developed to be powered using renewable energy such as solar power instead of batteries to reduce cost. Also, this system can be further developed to control the amount of watering to different sections of the field by using solenoid valves.

ACKNOWLEDGEMENTS

The authors would like to express their sincere gratitude to everyone who helped to carry out this project successfully.

REFERENCES

[1]. Vidadala S., Bala Mur.ali P. K., Implementation of agriculture automation system using web & GSM technologies, *International Journal of Engineering & Science Research*, 5, (2015), 1201-1202.
[2]. Bishnu D. K. , Prach S., Reetika A., Vany T., Microcontroller Based Automatic Plant Irrigation System, *International Research Journal of Engineering and Technology(IRJET)*, 4, (2017), 1436.
[3]. R., Widodo A., Romadhon A.D., Hudha M.S., Saputra P.P., Lestari N.A., The prototype of infant incubator monitoring system based on the internet of things using NodeMCU ESP8266, *Journal of Physics*, (2019), 4.
[4]. Neha K., Gurmohan S., Jain D.K,, Manjit K., Design and development of soil moisture sensor and response monitoring system, *International Journal of Latest Research in Science and Technology*, 3, (2014), 142.
[5]. Danny J., What is an Ultrasonic sensor, *Fierce Electronic*, (2020), https://www.fierceelectronics.com /sensors/what-ultrasonic-sensor, (Accessed 2021-07-14)
[6]. Hareendran T.K., Working with water flow sensor & Arduino, *Circuit Basics*, (2020), https://www.electroschematics.com/working-with-water -flow-sensors-arduino/, (Accessed 2021-07-14)
[7]. Mallari J., How to use Real -Time clock module with the Arduino, *Circuit Basics*, (2020), https://www.circuitbasics.com/how-to-use-a-real-time-clock-module-with-the-arduino/, Accessed 2021-07-14)
[8]. Bharudin N.H., Manusar T.M.N.T., Hamid F.A., Ali R., Misrun M.I., Performance Analysis of DC-DC Buck Converter for Renewable Energy Application, *Journal of physics*,1, (2020), 2.
[9]. Nanang S., Marliana S., Busye S., Smart home Using Android Smartphone, Arduino uno Microcontroller and Relay Module, *Journal of physics*, 1, (2018), 3.
[10]. Isaiah D., How an Electric Water Pump Works, *Hunker*, https://www.hunker.com/13409072/how-an-electric-water-pump-works, (Accessed 2021.07.15)
[11]. Patton E.W., Tissenbaum M., Harunani F., *MIT App Inventor: Objectives, Design, and Development*, Singapore: Computational Thinking Education, Kong SC., Abelson H., (2019), E-book (Accessed 2021.07.15)
[12]. Bradley L. J., Introduction to firebase, *Database Journal*, (2020), https://www.databasejournal.com /features/mysql/introduction-to-firebase.html, (Accessed 2021.07.15)

Proc. Annual Symposium on Research & Industrial Training, 08(2021) 88-96
Department of Electronics – Wayamba University of Sri Lanka

DESIGN AND IMPLEMENTATION OF FUZZY LOGIC CONTROLLER FOR BALANCING THE PALM OF A SERVICE ROBOT

M.S.A Mohamed*, W.A.S Wijesinghe

Department of Electronics, Wayamba University of Sri Lanka, Kuliyapitiya, Sri Lanka

**amsunfer922@gmail.com*

ABSTRACT

In this paper, we describe a fuzzy logic controller for balancing a palm targeting a service robot of a restaurant. The tilt angle of the palm is measured using an MPU6050 sensor module and the prototype system is implemented on an Arduino Uno R3 board. The noise in the angle measurements is reduced by applying a complementary filter. The fuzzy controller is designed with 11 input rules and 11 output rules. The results of the prototype system indicate that it has potential applications in controlling the palm of a service robot.

Keywords: Balancing robot palm, Fuzzy logic, MPU 6050 tilt angle

1.0 INTRODUCTION

Robotics technology is receiving special attention from researchers nowadays, particularly in humanoid robots [1]. For example, humanoid robots are becoming popular in restaurants to provide services. There are many studies reported on humanoid robots that have been developed aiming applications in restaurants as well as other places [2]. However, there are certain areas that still need proper solutions for humanoid robots. One such is the balancing palms of a service robot employed in a restaurant. This paper describes the study of balancing of a robot palm with the intention to be used in service robotic application

Many studies have been reported which used the MPU 6050 module for balancing purposes in the field of robotics. Among them, two-wheel balancing robots are special [3]. They have considered tilt angle as feedback for the robot prototype. In these studies, the MPU 6050 module has been used as the sensor module to measure the tilt angle. The controller system of some studies has been based on Proportional-Integral-Derivative (PID) controllers and some of the other has been based on Fuzzy logic controllers. Sensor fusion techniques have been adopted to reduce the sensing noise of these systems. These prototypes have the ability to stabilize the robot's upright position with 0 angle error [3, 4]. Further, studies have been done to develop control systems to balance a single spherical robot prototype's upright position. These control systems are also based on PID controllers [5]. An automated robot arm balancing system has been developed with a potentiometer-based balancing platform. This system has the ability to attain the balance position after four seconds [6].

In this work, we aim to develop a fuzzy logic based controller to balance the palm of a robot. In this prototype model, the MPU sensor module is used to measure angles which are fed to the fuzzy logic controller to balance the palm by adjusting angle parameters. Finally, we analyze the results of the prototype development.

2.0 MATERIALS AND METHODS

We used an MPU 6050 sensor module used as the measuring device of tilt angle. It is a 6-axis Motion Tracking Device. It combines 3-axis MEMS Gyroscope, 3-axis MEMS Accelerometer, and Digital Motion Processor all in a small package [7]. Data received from the angle sensor were processed and used as inputs to a Fuzzy logic controller. A Fuzzy logic controller is an artificial intelligence system that is different from crisp logic [8].

2.1 3-Axis MEMS Accelerometer

An accelerometer is a device that measures the vibration, or acceleration of motion of a structure. The force is caused by the mass vibrating or change in motion [9].

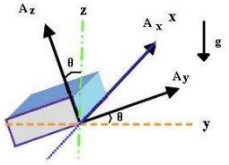

Figure2.1: Illustration of accelerometer inclination angle

$$\theta = \frac{Ay}{\sqrt{Ax^2+Az^2}} \quad (1)$$

Where,

Θ – Accelerometer inclination angle

Ax, Ay, Az – X, Y, Z axle readings

2.2 Complementary filter

The accelerometer can use to measure the tilt angle of an object. When measuring the movement of the object, there is noise on tilt value measured. Therefore the measurement of tilt angles must be filtered using a low pass filter to reduce the noise. Gyroscope rotation angle is incorporated with accelerometer measurements to obtain a smoother value. However, the gyroscope has a drift effect when it used for a prolonged period. Therefore, the gyroscope output value must also be filtered with a high pass filter. Therefore a complementary filter was used to reduce the noise of sensor readings and combine the accelerometer tilt angle and gyroscope rotation angle [10].

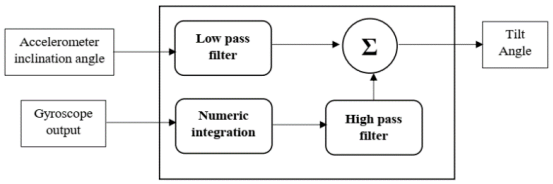

Figure 2.2: Block diagram of complementary filter

The complementary filtering process was done with a formula given in equation (2).

$$Tilt\ Angle = a \times (Angle\ +\ \omega\ \times dt\ ) + (1 - a) \times \theta \quad (2)$$

Where,

a – filter coefficient, Angle – tilt angle of complementary filter calculation before, ω - Gyroscope raw angle, θ - Accelerometer inclination angle, dt – sampling time

2.3 General description of the system

Fig. 2.3 shows the block diagram of the prototype system. The MPU 6050 sensor module is attached to the palm and the data was sent by the sensor module to the microcontroller as the tilt of the palm changes. The microcontroller was an Arduino Uno R3 board where the Fuzzy logic controller was programed. The servo motors received the control signals from the microcontroller which generated based on the Fuzzy logic controller, to adjust the palm. The controlling flow chart is given in Fig. 2.4.

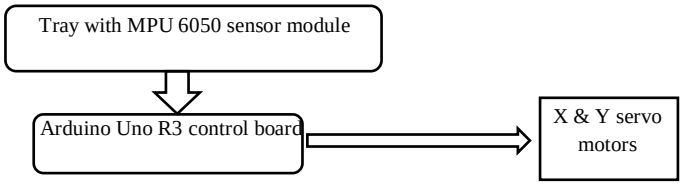

Figure 2.3: Block diagram of the system.

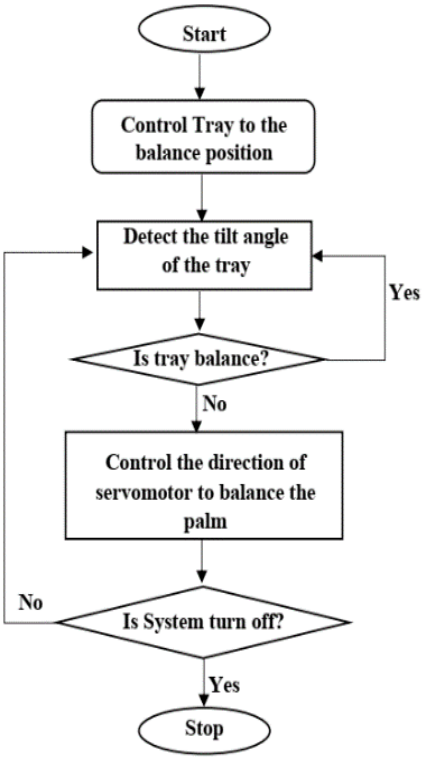

Figure 2.4: Flow chart of system process

We designed a robot forearm and the robot palm as shown in Fig.2.5, to mimic the robot arm. The palm has 2-degrees of freedom. This system is fixed to a stand.

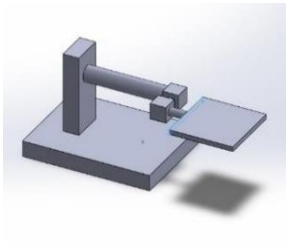

Figure 2.5: Proposed hardware design

The system uses 12v external power supply for the power.

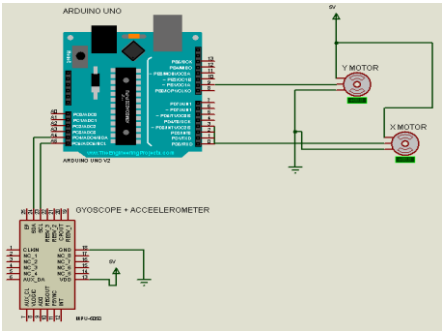

Figure 2.6: Circuit diagram of the system

2.4 Software design

The software was designed with Arduino IDE (Integrated development environment) programmed using C language. The fuzzy logic controller was design by using Matlab software. Then Matlab fuzzy code converted it into Arduino code with the help of MakeProto Matlab fuzzy interface system.

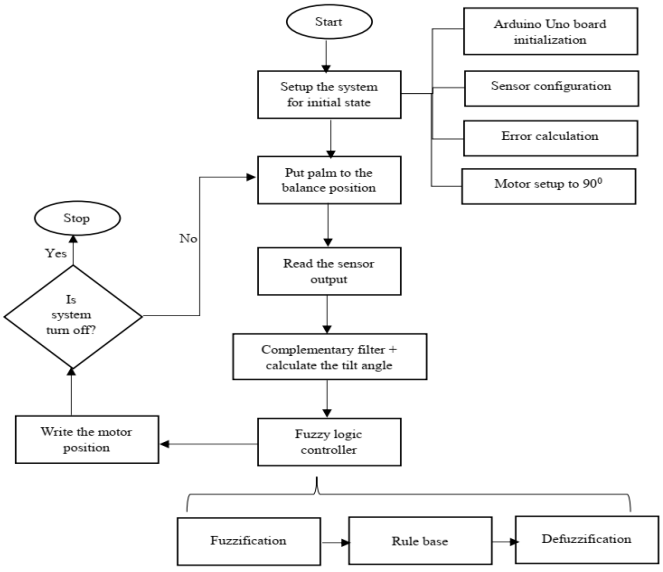

Figure 2.7: Flow chart of software process

2.5 Tilt angle calculation

Complementary filter formula formed to combine the gyroscope angle and accelerometer inclination angle.

Gyroscope raw angle calculated by output reading and scale factor according to sensor calibration.

$$Gyroscope\ raw\ Angle = Gyroscope\ output\ value\ \div Sensitivity\ scale\ factor \quad (3)$$

According to equation 3

Gyroscope raw angle (x, y) = (Gyroscope output / 32.8) – gyroscope raw error (x, y)

Gyroscope rotation angle calculated by raw angle and elapsed time for sample

$$Gyroscope\ Angle = Gyroscope\ raw\ angle\ \times sampling\ time \quad (4)$$

According to equation 4

$$Gyroscope\ Angle(X,Y) = Gyroscope\ raw\ angle(x,y)\ \times\ Elapsed\ time \quad (5)$$

Accelerometer raw angles calculated by sensor output and sensitivity scale factor according to sensor calibration.

$$Accelerometer\ raw\ angle\ = Accelerometer\ output\ value\ \div\ Sensitivity\ Scale \quad (6)$$

Accelerometer inclination angle according to equation 1 and equation 6

$$Accelerometer\ Angle\ (X) = \left(\frac{Invert \times rawX}{\sqrt{rawY^2 + rawZ^2}}\right) \times \frac{180}{\pi} \quad (7)$$

$$Accelerometer\ Angle\ (Y) = \left(\frac{Invert \times rawY}{\sqrt{rawX^2 + rawZ^2}}\right) \times \frac{180}{\pi} \quad (8)$$

Where,

rawY, rawX, rawZ - raw accelerometer angels

Invert = ± 1 ; depend on gyroscope angle direction

According to equations 2, 5, 6, 7, and 8 complimentary filter final formula in system software

$$Tilt\ angle\ X = 0.98\ \times (Tilt\ angle\ X + GyroAngle\ X\ ) + 0.02 \times AccelAngle\ X \quad (9)$$

$$Tilt\ angle\ Y = 0.98 \times (Tilt\ angle\ Y + GyroAngleY) + 0.02 \times AccelAngleY \quad (10)$$

3.0 RESULTS AND DISCUSSION

3.1 Design of fuzzy logic controller

The system used the Mamdani fuzzy inference system to design the fuzzy logic controller [11]. Fuzzification uses two inputs, are Tilt angle X (calculate by equation 9) and Tilt angle Y (calculate by equation 10) which is converted into the linguistic variable of XLN, LN, MN, SN, XSN, OK, XSP, SP, MP, LP, and XLP. Defuzzification outputs a one-output corrected angle value, which is converted into the linguistic variable of XLN, LN, MN, SN, XSN, OK, XSP, SP, MP, LP, and XLP. Membership functions of input and output are shown in Fig.3.1 (a) and (b) respectively.

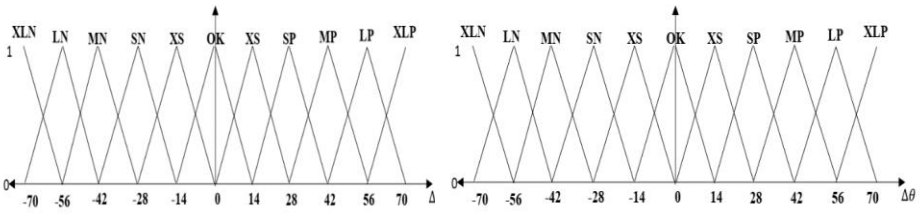

(a) (b)

Figure 3.1: Membership functions of input tilt angles and corrected output angles

Where,

$\Delta\theta$: Tilt angle, XLN: Extra Large Negative, LN: Large Negative, MN: Medium Negative, SN: Small Negative, XSN: Extra Small Negative, XSP: Extra Small Positive, SP: Small Positive, MP: Medium Positive, LP: Large Positive, XLP: Extra Large Positive.

For fuzzy inference process systems, uses if-then rule base rules to convert input into output.

If the input angle is positive range then convert it into corresponding negative range value, If the input angle is negative range then convert it into a corresponding positive range value.

3.2 Testing the tilt angle measuring

Tilt angle of the robot palm was measured by using Accelerometer and Gyroscope. Tilt angle is a combination of Accelerometer angle and Gyro angle. This value was checked manually. To check the tilt angle use a protractor and tilt angle reading shows in the serial monitor in Arduino IDE. Check the X and Y axis values separately. For each axis checked 15 angles for each direction (negative and positive).

$$Average\ Error\ angle = \frac{\sum\ \ angle\ errors\ (differences)}{Number\ of\ samples} \tag{11}$$

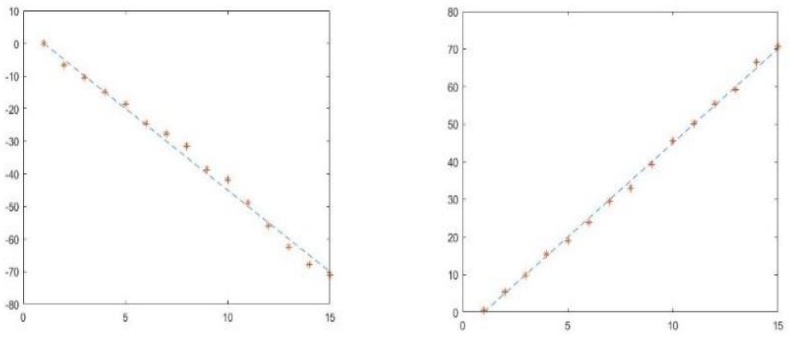

Figure 3.2: X-axis negative and positive sensor reading and manual reading angle values

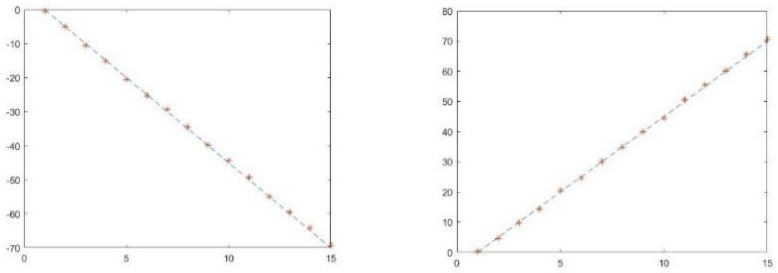

Figure 3.3: Y-axis negative and positive sensor reading and manual reading angle values

Where,

(-) Manual reading, (*) sensor reading

X-axis average angle error = 0.045

Y axis average angle error = 0.075

According to above-average values, sensor read tilt angles are probably correct.

3.3 Testing fuzzy logic controller

Fuzzy logic controller builds and tests in Matlab Simulink software. Manually enter some angle values and check the output angle values.

Table 3.1: Testing results of fuzzy logic controller

Manually entered angle value	Fuzzy controller output angle
35^0	-35^0
-56^0	56^0
24.3^0	-23.77^0
-2.78^0	3.36^0
75^0	0^0
-83.76^0	0^0

When the input angle is larger than $+70.00^0$ or less than -70.00^0 fuzzy controller output angle value is 0^0. If the input angle value is in range fuzzy controller outputs nearly exact opposite direction angle value.

3.3 Testing System performance

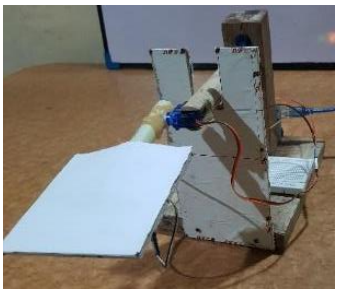

Figure 3.4: An image of the prototype system.

System performance was checked by directly changing the tilt of the arm with movement to eight directions. When the arms tilt was getting different, the palm was going to balance position. In here add some delay to motors to get the balance position, because in this paper used two servo motors to handle the balance position servo motors cant respond to frequently changing angles. It is not good for servo performance.

4.0 CONCLUSION

The fuzzy logic controller mechanism has been presented for balancing the robot palm targeting an application of a waiter robot. The controller has been implemented on Arduino Uno and tested with a prototype of a robot palm with a tray. A set of measurements were taken and analyzed to measure the accuracy of the system. Error percentages of X-axis and Y-axis sensor reading angles are 4.5% and 7.5% respectively. Further development is needed to use the system in service robotic applications.

REFERENCES

[1]. Maulana, R., Kurniawan, W. & Fahmi, H.Z., Noise reduction on the tilt sensor for the humanoid Robot balancing system USING Complementary Filter, *MATEC Web of Conferences*, 220, (2018)06002.
[2]. Seyitoglu, F. & Ivanov, S.H., Understanding the robotic restaurant experience: A multiple case study, (2020), doi: 10.31235/osf.io/e6rfa.
[3]. Sayidmarie, O.K. et al., Design and real-time implementation of a fuzzy logic control system for a two-wheeled robot, *2012 17th International Conference on Methods & Models in Automation & Robotics (MMAR)*, 2012
[4]. Shekhawat, A.S. & Rohilla, Y.,Design and control of Two-wheeled SELF-BALANCING robot using Arduino, *International Conference on Smart Electronics and Communication (ICOSEC)*,2020
[5]. Wyrwał, D. & Lindner, T., Control algorithm for holonomic robot that balances on single spherical wheel. *MATEC Web of Conferences*, 2019, 02005.
[6]. Deep, A. et al., Robotic arm controlling using automated balancing platform, *Communication, Control and Intelligent Systems (CCIS)*, 2015
[7]. Wikimedia foundation, Robotics, Wikipedia, 2021.07.11, https://en.wikipedia.org/wiki/Robotics, 2021.07.13.
[8]. Elmer p. Dadios (eds.), *Fuzzy logic - controls, concepts,theories and appliactions*, intechopen,jneza trdine 9,51000 Rijeka, Crotia, 2012. E-book
[9]. Wikimedia foundation, Robot, Wikipedia, 2021.07.10, https://en.wikipedia.org/wiki/Robot, 2021.07.12

[10]. Sholihin & Susanti, E., Humanoid robot control system BALANCE Dance Indonesia and Reader filters USING COMPLEMENTARY ANGLE VALUES. *E3S Web of Conferences*, 31, 2018, 10003.
[11]. Researchhubs.com, *Mamdan fussy Model*.,http://researchhubs.com/post /engineering/fuzzy-system/mamdani-fuzzy-model.html, (Accesse-2021.08.25.)

Proc. Annual Symposium on Research & Industrial Training, 08(2021) 97-103
Department of Electronics – Wayamba University of Sri Lanka

FORECASTING WIND POWER GENERATION OF A WIND FARM IN SRI LANKA BY USING ARTIFICIAL NEURAL NETWORK

D.A.T. Peiris[1*], J.M.J.W. Jayasinghe[1], Upaka Rathnayake[2]

[1]Department of Electronics, Wayamba University of Sri Lanka, Kuliyapitiya, Sri Lanka.
[2] Department of Civil Engineering, Faculty of Engineering, Sri Lanka Institute of Information Technology, Sri Lanka.

[*]amilatharangaac@gmail.com

ABSTRACT

Wind is one of the main renewable sources that the world is depending on to generate electricity. Most of the countries already use wind to generate power, while some of them including Sri Lanka are still in the early ages. Awareness of the wind power generation plays a very important role in the field since power generation highly impacts human beings and industries. Particularly, there is a need of high accurate forecasting techniques for power generation. Some statistical and non-statistical methods have been used to forecast the power generation. However, there is a research gap in using Artificial Neural Network (ANN) for forecasting wind power generation in the Sri Lankan context. Past data of "Pawan Danavi" wind farm was used in this study. It is located in Kalpitiya, North-Western province in Sri Lanka, which has identified as one of the best potential regions for wind farm installation in the island. Average wind speed, average wind direction and average ambient temperature from the year 2015 to 2019 have used as independent variables for the model while average power output used as the dependent variable. A prediction model has been developed by using ANN training algorithm of Levenberg-Marquardt. Study results showed lower MSE values and R values around 1, which concludes that the developed model accurately forecast the power generation.

Keywords: Renewable Energy, Wind Power, Artificial Neural Network

1.0 INTRODUCTION

An energy crisis is one of the main issues that the entire world is facing throughout a few decades. As a solution for that, the world has used more options to generate power. Increasing the use of renewable sources is one of the promising and effective ways since they are freely available and environmental friendly than the use of some other ways like fossil fuels. Among renewable sources like solar power, hydropower and a few more, use of the wind power has increased in recent times.

Wind is an eco-friendly energy source. Therefore it can be identified as one of the best alternatives for power generation rather than burning fossil fuels [1]. On the other hand, it is a productive source when comparing with the cost of fossil fuel and other non-renewable energy sources [2]. Now the world has passed the traditional age of burning fossil fuels and has encouraged the use of renewable sources. In that case, wind has a higher concern in the power generation sector and it is supposed to expand much more in the future [3].
Wind speed should touch the pivotal level to establish a wind plant and necessary conditions should be satisfied [2]. It is very important to forecast the wind power for system credibility and

cost-minimizing purposes and also for unit commitment, power system operations and economic dispatch [3,4]. Forecasting accuracy is essential to control and balance the power output [5]. Wind speed and direction are not constant parameters. They are volatile and continuously change with time, which affects the safety of the power grid. When the electric power which is supplied by the wind farm to the power grid, violate a certain unique value, it will affect the smooth operation of the power grid. An accurate forecast of the power output of the wind farm, can prevent those ill-effects to a large extent and increases the safety of the grid [6].

Artificial Neural Network (ANN) has developed to imitate the human brain. It has the qualities of strong thinking, remembering and problem-solving abilities of the normal human brain. ANN consists with processing units called 'neurons', which are highly interconnected. Basically, these neurons aggregate inputs from outside sources and create output from those inputs [1]. A basic ANN model has three layers. They are input, hidden and output. There may be one or a few hidden layers while only one input and output layers each. The input layer consists of non-aligned variables which have gathered from the external. They are connected to one or few hidden layers. The processing parts are happening in those hidden layers. It includes activation functions and calculations are done inside the hidden layers to achieve the output. The process is finished at the output layer and displays the results. If the final outcome is known, the process is called supervised training and if the outcome is unknown, it is called unsupervised training [7]. ANN is very useful for the occasions where the process is too complex for manual proceedings [8].

2.0 EXPERIMENTAL

As per the recent statistics of the center for climate and energy solutions, 26.2% of global electricity generation in 2018 was covered by renewable energy sources [9]. It is expected that it will increase by at least 40% at the end of 2040 and the major contribution will be from solar, hydropower and wind. When it comes to the numbers of Sri Lanka, as of the Ceylon Electricity Board (CEB) [10], which has the authority power of distributed electricity in the country, 67.02% of total electricity is generated by using thermal oil and thermal coal, 30.16% by using hydropower and 2.55% by wind power. On the other hand, generally Sri Lanka spent thousands of million dollars to import crude oil which is nearly 25% of total imports and equals 45% of total exports [11,12].

2.1 Forecasting techniques

As Hui Liu *et al*. mentioned in their work, wind speed forecasting is important for the safety of the system [13]. Basically, wind speed forecasting methods can be categorized into three types as statistical methods, physical methods and intelligent methods [13]. Sometimes hybrid methods are also used for forecasting by combining two or more techniques. Physical methods are more suitable in long-term works while statistical methods for short-term purposes. Hybrid methods are built to overcome difficulties and increase accuracy. Kavasseri and Seetharaman had introduced fractional-ARIMA models to ascertain the wind speed forecasting [14]. They have concluded that these models had highly acceptable outcomes in forecasting wind speed. ARIMA models also use to build and enhance the performance of other models. Numerical Weather

Prediction (NWP), which is a physical method, and statistical methods have been used in many works to forecast wind speed and wind energy [4].

2.2 ANN for forecasting wind power

Some of the intelligent and hybrid methods are also used for the same purpose. Bhaskar *et al.* indicate that ANN models can present a complex non-linear relationship and extract the dependence between variables through the training and learning process [15]. Hui Lui *et al.* has introduced a hybrid technique using the consolidation of the Wavelet Packet Decomposition algorithm and Elman neural networks to multi-step wind speed forecasting [13]. Alberto Pliego Marugan *et al*. have discussed the use of ANNs in the field of wind power plants to ensure the efficiency of the full system [8]. A.K Mishra and L. Ramesh have mentioned in their work that the wind speed can forecast with only the use of past data of the wind speed [1]. They have used regression analysis methods and ANN in their work. They have suggested a standard method to forecasting renewable energy using ANN in their study. In a study carried out in Portugal, Catalao *et al.* has proposed an ANN approach for short-term wind power forecasting which has resulted in a good trade-off between forecasting accuracy and computational time [16].

2.3 Levenberg-Marquardt (LM) training algorithm.

In ANNs, the LM training algorithm is one of the frequently used and it has been identified as the efficient and ideal algorithm for medium size networks [17]. LM is a standard technique for non-linear least square problems. It is a combination of the steepest descent and Gauss-Newton method [17]. It is an iterative technique that locates the minimum of a multivariate function expressed as the sum of squares of non-linear real-valued functions [18]. LM can use only for the small-sized neural networks due to its memory limitations [19].

2.4 Case study

The present study was carried out with the aim of forecasting wind power generation in a wind farm. For this work, past data of average wind speed (m/s), average wind direction (^{o}), average ambient temperature (^{0}c) and average power output (MWh) of the "Pawan Danavi" wind farm, which is located in Kalpitiya, has used. The related time period for data is from January 2015 to December 2019. The first three data sets have been used as inputs in the training process while the final set as the output. That means the first three are the independent variables of the function while the remaining one is the dependent variable. Mathematical expression for the above function which is a non-linear function between input and output variables can express as follows.

Average power output = f (average wind speed, average wind direction, average ambient temperature)

The neural net fitting framework of MATLAB R2014b version is used to analyze the data. To obtain the best results, the parameters of the number of hidden neurons and training and testing percentages are changed step by step. Here, training and testing percentages are depending on the length of the period of the data. For this study, validation percentage has changed from 5% to

25% with the step size of 5% while keeping the training percentage at 70%. In that case, the testing percentage is automatically changes with respect to the other changes. In the present work, the performance of the training algorithms are evaluated by using mean squared error (MSE) and coefficient of correlation (R) values. Smaller MSE values and R values around 1, leads to the best results [20].

$$MSE = \frac{\sum_{i=1}^{n}(O_i - E_i)^2}{n} \quad (1)$$

$$R = \frac{\sum_{i=1}^{n}(O_i - \bar{O})(E_i - \bar{E})}{\sqrt{\sum_{i=1}^{n}(O_i - \bar{O})^2 . \sum(E_i - \bar{E})^2}} \quad (2)$$

Here, O is the observed data values, E is predicted data values and n is the total number of observations.

3.0 RESULTS AND DISCUSSION

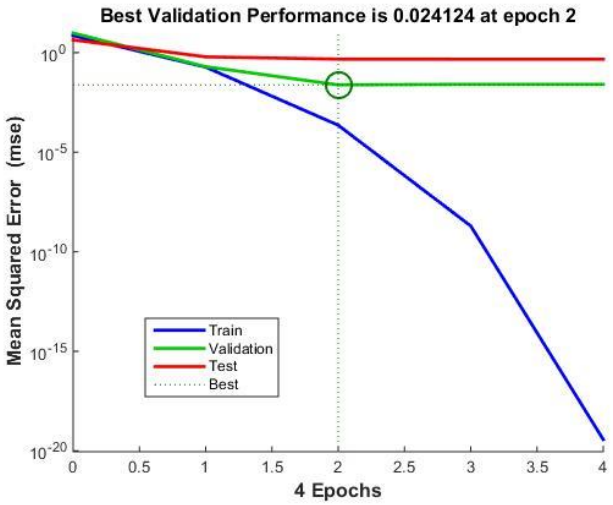

Figure 3.1: MSE value performance at 5% validation.

When comparing the training results of the Levenberg-Marquardt algorithm, at 5% validation percentage, the MSE value is the smallest among the five which was shown as 0.024 and it came at epoch 2. At the same time, the overall R value of 5% validation percentage was showed as 0.943, which was hanging almost equally with the results of the other four percentage values. At the 5% validation percentage, R values for training, validation and test are 0.999, 0.983 and 0.903 respectively, which were spread around 1 and gave reasonable good values for the coefficient of correlation.

Figure 3.1 shows the performance of mean square value and figure 3.2 shows the coefficient of correlation of predicted vs. actual power output.

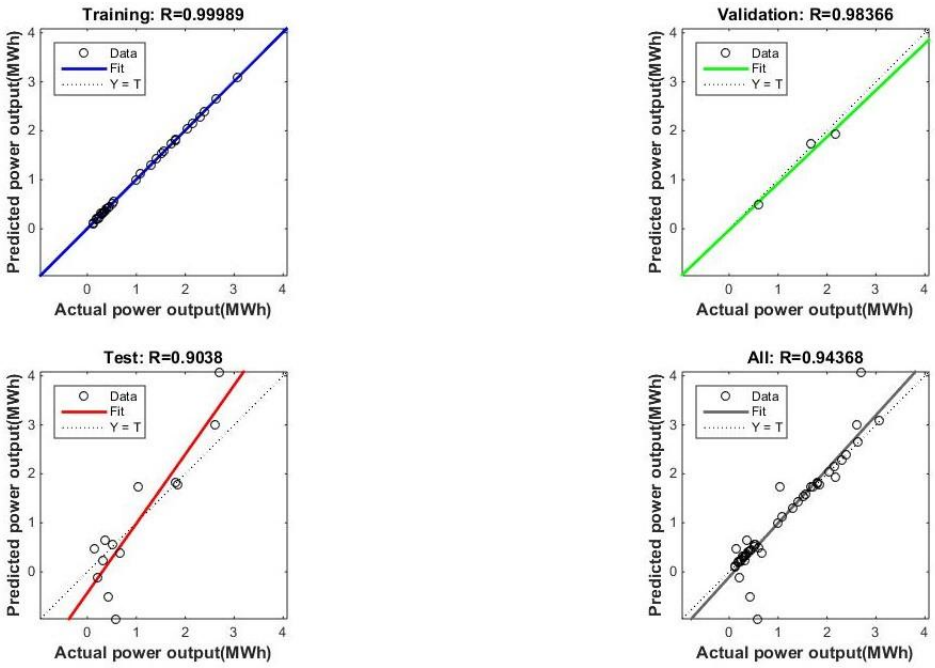

Figure 3.2: R value performance at 5% validation

When the LM algorithm is trained for all validation percentages, the following results which summarized in table 3.1 were obtained. The results of the training show that there is a strong correlation between input parameters and power output at all five validation percentages. All the five validation percentages gave a similar kind of results neglecting the difference of the validation percentage. The change of the validation percentage did not affect the results. These results show that the LM algorithm of the ANN is suitable for forecasting wind power generation.

Table 3.1: Summary of the results

Validation Percentage (%)	MSE value	Number of epochs	R value			
			Training	Validation	Test	All
5	0.024	2	0.999	0.983	0.903	0.943
10	0.114	4	1.000	0.911	0.358	0.913
15	0.114	2	0.990	0.917	0.958	0.967
20	0.127	2	0.994	0.937	0.900	0.968
25	0.147	2	0.999	0.920	0.950	0.966

4.0 CONCLUSION

This study shows that the input parameters (average wind speed, average wind direction and average ambient temperature) strongly impact the average power generated by the wind farm. LM algorithm gives acceptable results with smaller MSE values and coefficient of correlation values around one for different validation percentages. MSE values are slight increases with the increasing of validation percentages. Since all the MSE values are very smaller and all the R

values are hanging around one, it can be stated that the changes of the validation percentage does not affect the results. LM algorithm has higher accuracy and efficiency, despite the change of percentage. Hence, it can be concluded that LM model is suitable for the forecasting of the power output of the wind farm since it provides acceptable results.

ACKNOWLEDGEMENT

Authors would like to appreciate Mr. M.J.M.N. Marikkar, Deputy chief executive officer at LTL Holdings and Mr. Chathuranga Fernando, Electrical engineer/business development manager at LTL Holdings for the support that they extended to carry out this study.

REFERENCES

[1]. Mishra, A. K., Ramesh L., Application of neural networks in wind power (generation) prediction, *International Conference on Sustainable Power Generation and Supply*, (2009), 1-5, doi:10.1109/ supergen.2009.5348160
[2]. Awan, A. B., Khan, Z. A., Recent progress in renewable energy – Remedy of energy crisis in Pakistan, *Renewable and Sustainable Energy Reviews*, vol.33, (2014), 236–253, doi: 10.1016/j.rser. 2014.01.089
[3]. Zhang, Y., Chan, K. W., The impact of wind forecasting in power system reliability, *Third International Conference on Electric Utility Deregulation and Restructuring and Power Technologies* , (2008), 278
[4]. Chandra, D. R., Kumari, M. S., Sydulu, M., A detailed literature review on wind forecasting, *International Conference on Power, Energy and Control (ICPEC)*, (2013), 630-634, doi: 10.1109/ icpec.2013.6527734
[5]. Narayana, M., Witharana, S., Adaptive prediction of power fluctuations from a wind turbine at Kalpitiya area in Sri Lanka, *IEEE 6th International Conference on Information and Automation for Sustainability*, (2012), 262-265, doi: 10.1109/iciafs.2012.6419914
[6]. Guo, S., Yansong Li, Xiao, S., Wind speed forecasting of genetic neural model based on rough set theory, *5th International Conference on Critical Infrastructure (CRIS)*, (2010), 1
[7]. Kidong L., David B., Pervaiz A., A comparison of supervised and unsupervised neural networks in predicting bankruptcy of Korean firms, *Expert Systems with Applications*, 29, (2005), 1
[8]. Alberto P. M., Fausto P. G. M., Jesus M. P. P., Diego R.H., A survey of artificial neural network in wind energy systems, *Applied Energy*, 228, (2018), 1822, doi: 10.1016/j.apenergy.2018.07.084
[9]. Center for climate and energy solutions, https://www.c2es.org/content/renewable-energy/ (Accessed 2020-12-26)
[10]. Ceylon Electricity Board website, https://www.ceb.lk/ (Accessed 2020-12-27)
[11]. Samaratunga, R.H.S., Sri Lanka's petroleum industry: Policy, Organization and Challenges, *Sri Lanka Journal of Development Administration*, Vol.4, (2014), 39
[12]. Sri Lanka sustainable Energy Authority, http://www.energy.gov.lk/en/renewable-energy/ technologies/wind-power (Accessed 2020-12-30)
[13]. Hui L., Hong-qi T., Xi-feng L., Yan-fei L., Wind speed forecasting approach using secondary decomposition algorithm and Elman neural networks, *Applied Energy*, 157, (2015), 183, doi: 10.1016/j.apenergy.2015.08.014
[14]. Kavasseri, R. G., Seetharaman, K., Day-ahead wind speed forecasting using f-ARIMA models. *Renewable Energy*, *34*(5), (2009), 1388, doi: 10.1016/j.renene.2008.09.006
[15]. Bhaskar, M., Jain, A., Srinath, V., Wind speed forecasting: Present status, *International Conference on Power System Technology*, (2010), 1, doi: 10.1109/powercon.2010.5666623

[16]. Catalo, J. P. S., Pousinho, H. M. I., Mandes, V. M. F., An Artificial Neural Network Approach for Short-Term Wind Power Forecasting in Portugal, *15th International Conference on Intelligent System Applications to Power Systems*, IEEE, (2009), 1, doi: 10.1109/ISAP.2009.5352853
[17]. Hongwei Liu, On the Levenberg-Marquardt Training Method for Feed-Forward Neural Networks, *Sixth International Conference on Natural Computation*, IEEE, (2010), 456, doi: 10.1109/ICNC.2010.5583151
[18]. Levenberg, K., A Method for the Solution of Certain Non-linear Problems in Least Squares, *Quarterly of Applied Mathematics*, 2, (1944), 164
[19]. Bogdan M. W.,Yixin C., Efficient Algorithm for Training Neural Networks with one Hidden Layer, *International Joint Conference on Neural Networks*, IEEE, (1999), 1725, doi: 10.1109/ IJCNN.1999.832636
[20]. Erasmo C., Wilfrido R., Short term wind speed forecasting in La Venta, Oaxaca, Me´xico, using artificial neural networks., *Renewable Energy*, 34,(2009), 274, doi: 10.1016/j.renene.2008.03.014

Proc. Annual Symposium on Research & Industrial Training, 08(2021) 104-110
Department of Electronics – Wayamba University of Sri Lanka

DESIGNING A PROTECTION SYSTEM FOR SINGLE PHASE INDUCTION MOTOR BASED DEVICES

B.P. Sankalpa*, L.D.R.D. Perera

Department of Electronics, Wayamba University of Sri Lanka, Kuliyapitiya, Sri Lanka

*pramodh2009@gmail.com

ABSTRACT

The single-phase induction motor is the most frequently used motor for domestic applications. It is essential to diagnose its faults for trouble free longer use. The reported design introduces an automatic system to detect malfunctions of the motor capacitor and protect the coil (rotor) with minimum damage to induction motor used devices. The system is based on Arduino NANO and a current sensor, and it continuously detects current through the starter capacitor to identify the quality of the capacitor. The faults of the capacitor are indicated through LEDs. This system automatically cuts-off power to the motor when there is a fault in the capacitor to protect the coil from high currents. A prototype system was successfully designed, developed and integrated into a domestic ceiling fan.

Keywords: Induction Motor, Protection Circuit, Arduino NANO

1. INTRODUCTION

1.1 Overview

A single-phase induction motor is not self-starting. It should be supported by a starting capacitor. In this work, the focus is on permanent split capacitor motor-based devices which do not require high starting torques, such as ceiling fans. Many parts of the motor (rotor shaft, bearings, stator, and rotor circuits) wear out depending on operating stress and operation time. Degraded parts of a rotating motor can cause power and energy wastage, serious damages to the application, and accidents to those who are using them. It is better to repair the system with necessary parts, rather than condemning it or replacing it with a new motor system because the failure could be related only to a specific part and it may also save money. There are many different approaches for detecting faults of single-phase induction motors. For example, measurement of thermal images can be used for the analysis of fault detection. However, thermal imaging camera is very expensive.

Regarding ceiling fans, they can commonly experience the following situations;

- Fan rotates slowly or not at all on all speeds.
- Fan will not start but will rotate if started by a little push.
- Certain speeds are slow or do not work.
- The motor hums and turns freely by hand but will not spin [1].

These can happen mostly due to capacitor failures. If there is a bearing failure, the system is much nosier than usual. Therefore, the induction motor coil core is heated with time. It may also consume a higher current than in the normal operating mode, which leads to power and energy wastage while damaging the coil (rotor) of the system. Also, the coil repairing process is expensive and time consuming, if it is damaged due to a capacitor failure. But replacing the capacitor with a new one by identifying the fault at an early stage can save money and time.

1.2 Literature Review

A research project that monitors and controls the consumption current due to various domestic loads or short circuit has been reported [2]. That project was mainly based on Arduino and it compared the threshold values with the emergency states to make proper decisions to protect the system from damages/fire with the help of respective sensors. Raksha et al have reported a microcontroller based energy metering system [3], and Ahmed et al have reported an Arduino based alternating current monitoring multi-meter system that is used to send notifications about overload, under/over voltage, and low/ high frequencies conditions of a three-phase synchronous generator [4].

1.3 Research Objective

The aim of the reported project was to design and develop an automatic system to detect malfunctions of the starter capacitor and protect the coil (rotor) of a single-phase induction motor with minimum damage to the motor used device. The system was to be based on Arduino NANO to detect current through the starter capacitor and to identify the quality of the capacitor.

2. THEORY

A capacitor acts as a different phase generator for a single-phase motor. It splits the current into different phases so there can be sufficient phase difference to generate magnetic torque. There must be a revolving magnetic field or rotating magnetic field to create torque for rotating the rotor. So, in an induction motor, a two-phase supply has been created from a single-phase supply with the help of additional starting windings or auxiliary winding along with a capacitor [5]. The schematic representation of a single-phase induction motor circuit is shown in Figure 2.1.

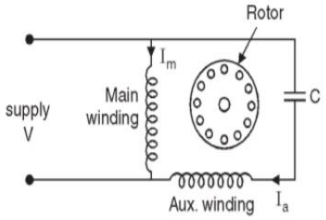

Figure 2.1: Schematic representation of a single-phase induction motor

Current sensors operate as the sealed secondary of a current transformer while the conductor carrying the current to be measured functions as a one-turn primary. Measurement accuracy can be improved by increasing the number of primary turns. The proposed design uses a ZMCT103C IC based current sensor as shown in Figure 2.2, which can measure 5A alternating current with a corresponding analog output of 5 mA [6].

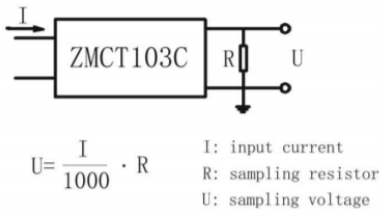

Figure 2.2: Schematic representation of ZMCT103C current sensor

3. EXPERIMENTAL

The proposed system consists of three parts: Power supply, Microcontroller, and Current Sensor unit. The Arduino NANO is powered with 110V-230V to 5V USB power supply. The block diagram of the circuit is shown in Figure 3.1.

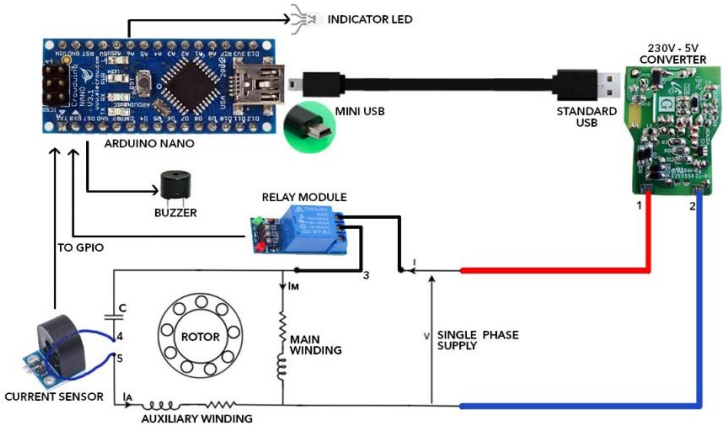

Figure 3.1: Block diagram of the proposed system

The whole system is designed to start when the main power switch is turned ON for the motor system. A single channel relay module is used as an emergency switch to cut-off mains supply when abnormal reading is detected by the current sensor. Flow chart of the system is shown in Figure 3.2.

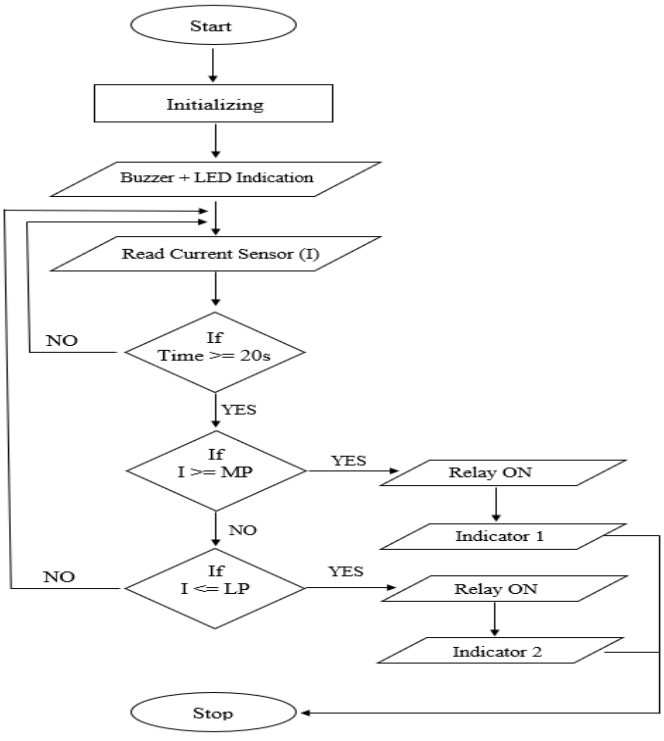

Figure 3.2: Flow chart of the system

The proposed circuit diagram and its connections to the microcontroller are shown in Figure 3.3.

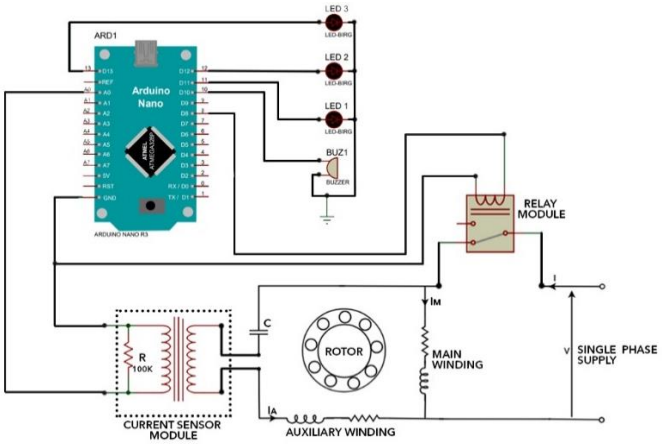

Figure 3.3: Circuit diagram of the proposed Protection System

The test subject for the proposed system is a ceiling fan as it is the most common household single phase induction motor-based device in which a weak capacitor failure affects most. Therefore, to define the threshold current values two ceiling fans were used from "Richsonic RCF-459" model which uses a starter-capacitor with a marked capacitance of 2.25µF.

- Standard starter-capacitor (C1) (marked value 2.25µF) → Measured value = 2.22 µF
- Weak starter-capacitor (C2) (marked value 2.25µF) → Measured value = 0.906 µF

Another standard starter-capacitor (C3) with marked capacitance of 2.5µF was also used. It had a measured value of 2.45µF. Here the term "standard" is used for the capacitors which are in brand new condition. All the capacitors were used in the starter-capacitor position which is marked as "C" in the circuit diagrams of Figure 3.1 and Figure 3.3.

4. RESULTS AND DISCUSSION

From the C1 capacitor, the standard working conditions were identified for this model. The measured current readings through the C1 capacitor as shown in Figure 4.1.

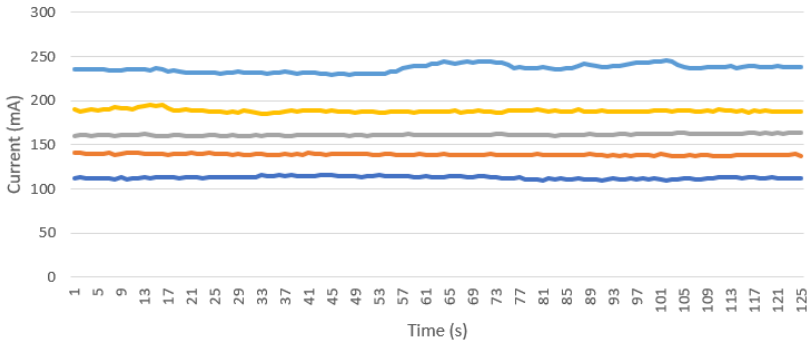

Figure 4.1: Current through standard starter-capacitor C1

After identifying the normal conditions, the weak capacitor, C2 was tested under the same conditions and the currents through a weak capacitor also measured. In the plots, each 5 different lines are for the 5 speed levels on the fan regulator. The current through the starter capacitor rises with an increasing speed level.

In Figure 4.2, the lower set of lines is related to the C2 capacitor and the upper set of lines is related to the C1 capacitor. The current comparison of both C1 and C2 is shown below.

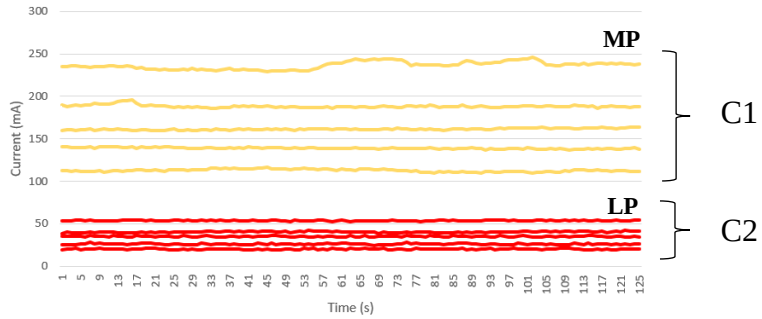

Figure 4.2: Current comparison of standard starter-capacitor (C1) and weak starter-capacitor (C2).

In Figure 4.3, the lower set of lines is related to the C2 capacitor and the upper set of lines is related to the C3 capacitor. The current comparison of both C3 and C2 is shown below.

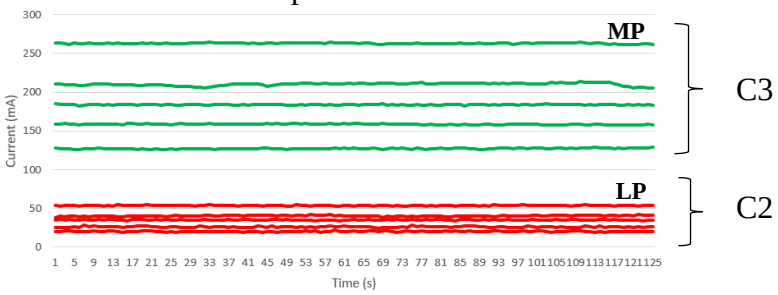

Figure 4.3: Current comparison of standard starter-capacitor (C3) and weak starter-capacitor (C2)

From the above observations, the Lowest threshold point (LP) was identified by observing the abnormal conditions of the 2.25µF weak starter-capacitor (C2) which are marked in RED color as shown in Figures 4.2 and 4.3. LP is the maximum abnormal current determined from the 2.25µF weak starter-capacitor. Maximum threshold point (MP) is the highest recorded current values for both standard starter-capacitors C1 and C3.

Therefore, when an induction motor-based device is working under normal conditions, capacitor current should vary between LP and MP. Further, if the current measured through starter capacitor shows a value lower than LP it means that the used capacitor is weak like the capacitor C2. Also, if the current measured through starter capacitor shows a value higher than MP, it could mean that the capacitor is under short-circuited condition or the starter capacitor terminals are short circuited. The protection logic is mainly based on these two points. The Arduino algorithm is programmed to detect the current levels through starter capacitor and to take further actions if there are any abnormal conditions.

The described protection system is fully autonomous. The main outcome of this product is to detect as well as to protect an induction motor-based system from severe damages. A specific algorithm has been developed as part of the system which can identify the relevant fault and notify with unique indications.

The system generates four notifications through indicating LEDs.

- GREEN Color Blink (With Buzzer) – When the system is initializing and starting.
- BLUE Color Blink (Without Buzzer) – Normal operating condition.
- RED Color Blink (With Buzzer) – High current through starter capacitor.
- YELLOW Color Blink (With Buzzer) – Low or no current through starter capacitor.

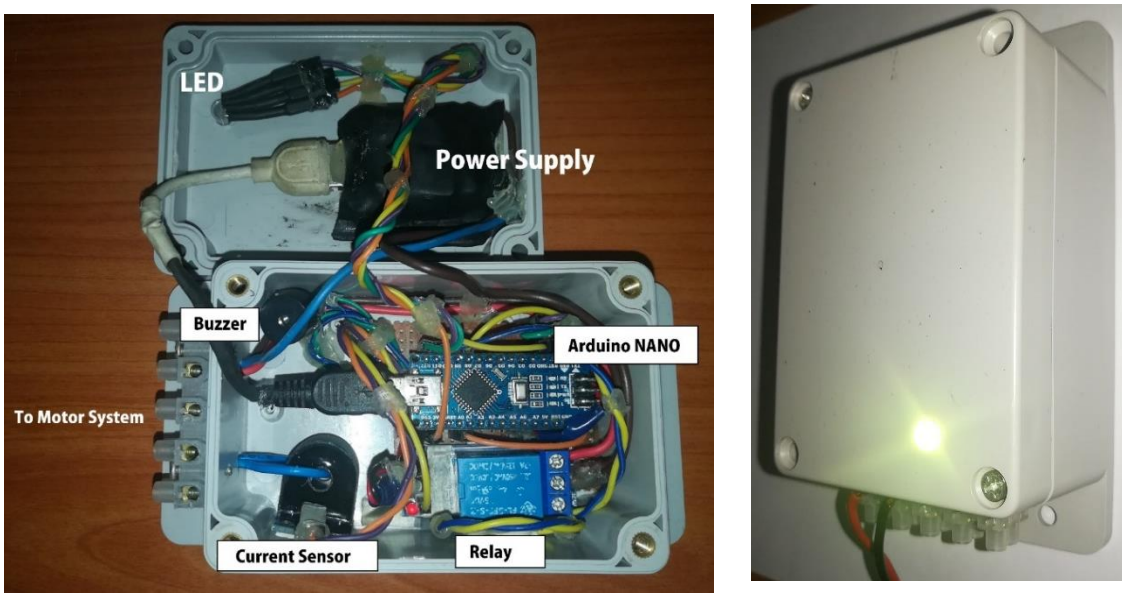

Figure 4.4: The Protection System-Final Product

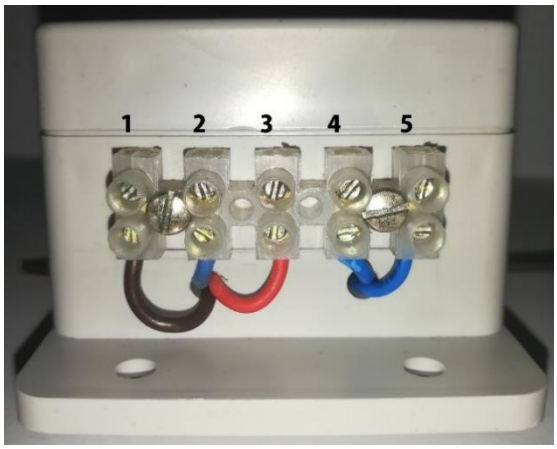

Figure 4.5: Connection Lines to the System

Where;
1 - 230V Input
2 - Neutral line
3 - Relay Out
4 - Capacitor In
5 - Capacitor Out

5. CONCLUSIONS

This research paper describes the design and development process of an Arduino-based protection system for Single Phase Induction Motor-based devices, from its idea generation stage to testing and functioning level. The main objective of this project was to protect the induction motor rotor (coil) from high currents and extend the lifetime as well as to reduce unnecessary repairing costs. It includes all the important steps; to detect the error, protect the system and notify the error to the user. The designed system was successfully integrated into a

domestic ceiling fan. Therefore, this introduced system is expected to be a potential solution for a major issue with induction motors. The developed system has further potentials for design upgrades and is expected to have an adequate market segment in the Single-Phase Induction Motor Industry.

ACKNOWLEDGEMENTS

Authors would like to sincerely thank all the staff of the Department of Electronics, WUSL, for the valuable advice and support for successful completion of this research project.

REFERENCES

[1]. Cinco Electronics, Troubleshooting of a ceiling fan capacitor, https://www.cincocapacitor.com /troubleshooting-of-ceiling-fan-capacitor.html (Accessed 2020-09-19)
[2]. Marhoon Hamzah and Taha Ihsan, Design and implementation of intelligent-circuit breaker for electrical current sensing and monitoring, *International Journal of Core Engineering and Management*,4/11, (2018), 39-40.
[3]. Raksha R. Sharma, Kalyani P. Wath and Yogesh P. Bawangade, Design a talking energy meter based on microcontroller, *International Research Journal of Engineering and Technology (IRJET)*,5/1,(2018),1-3.
[4]. Ahmed J. Ali, Ahmed M. T., and Omar T. Mahmood, Design of a smart control and protection system for three phase generator using Arduino, https://www.researchgate.net /publication/338357983_Design_of_a_Smart_Control_and_Protection_System_for_Three_Phase _Generator_Using_Arduino (Accessed 2020-09-19)
[5]. Ahmed M. T. and Ibraheem Alnaib, Single-phase induction motors, https://www. researchgate.net/publication/332835297_Single-Phase_Induction_Motors (Accessed 2021-06-10)
[6]. DatasheetsPDF, ZMCT103C current sensor data sheet. https://datasheetspdf.com /datasheet/ZMCT103C.html (Accessed 2021-05-25)

Proc. Annual Symposium on Research & Industrial Training, 08(2021) 111-118
Department of Electronics – Wayamba University of Sri Lanka

ROLL OVER TRAFFIC ACCIDENT DETECTING AND REPORTING SYSTEM

M.D.M. Perera*, G.A.K.S. Perera

Department of Electronics, Wayamba University of Sri Lanka, Kuliyapitiya, Sri Lanka

*dilinimadhushani622@gmail.com

ABSTRACT

Nowadays, the number of deaths and injuries due to traffic accidents is increasing rapidly. Even though traffic accidents happen in different ways, rollover accidents are among the most dangerous types of vehicular crashes. The risk of loss of life due to these types of accidents is also very high. To prevent these issues, this paper aims to introduce a rollover traffic accident detecting and reporting system using Global Positioning System (GPS) and Global System for Mobile communication (GSM) technologies. In this system, a MPU6050 – accelerometer and gyroscope sensor is used as an input to the system and corresponding response is analysed by the Arduino. If a rollover accident occurs, MPU6050 sensor readings exceeded the conditions (the angles related to the rollover), it takes the appropriate action. The current location coordinate is identified from GPS module and an alert message will be sent automatically to the relevant parties through the GSM module with geographical coordinate as a link for immediate help to the victims.

Keywords: Rollover traffic accident, GPS, GSM

1.0 INTRODUCTION

A traffic accident, also called as a motor vehicle collision or a motor vehicle crash occurs when a vehicle collides with another vehicle, pedestrian, animal, road debris, or other stationary obstruction, such as a tree, a pole or a building. The main cause for traffic accidents is found to be due to extensive speed. In addition, drunk and drive, diverting minds, over stress and mechanical and electrical failures are also considered as reasons for traffic accidents. Due to those reasons, different types of traffic accidents may take place including head on collisions, skidding, side impact collision, roll over. Among them, roll over is very dreadful because sometimes it is very difficult to trace the accident quickly. When such an accident occurs in night time at a lonely place, situation is very pathetic. However, risk of loss of life due to rollover accidents is comparatively very high [1].

There are several efforts, applications, approaches projected to produce security and safety to prevent these types of accidents. Many applications are developed using smartphones. The ability to detect traffic accidents using smartphones has only recently become possible because of the advances in the processing power and sensors deployed on smartphones [2]. An accelerometer can be used in a car alarm application so that dangerous driving can be detected. It can be used as a crash or rollover detector of the vehicle during and after a crash [3]. Also, the accident can be detected by a vibration sensor which is used as major module in the system. Vibration sensor will be activated when the accident occurs and the information is transferred to the registered number through GSM module [4]. In 2018, Arsalan Khan implemented an accident detection and smart rescue system by utilizing onboard sensors of the smartphone to detect vehicular accidents and to report it to the nearest emergency responder available and provide real-time location tracking for responders [5].

In 2014, Nitin Thakre implemented a design to detect and localize automatic vehicle accident using Bluetooth technology [6]. It used a vibration sensor to detect an accident. If an accident happens, the device will send an alert message with location data from the GPS module to the control station using the GSM network. In 2017, R. Saranya and R. Arun Kumar introduced an alert system which is called vehicle accident prevention using sensors [7]. This system used an IR sensor, eye blink sensor, Intel Galileo kit, vibration sensor. If an accident occurs due to sleepy and lethargic/half-sleep or otherwise intoxicated persons while in driving mode, an alert will be sent to the nearest hospital from this system.

Although the above methods can eliminate the rollover phenomenon, there are some issues with those systems. Other sensors and three axes accelerometers are embedded in smartphones. Nevertheless, smartphone data is hard to analyze due to calibration, noise and rotation issues. In addition, it is not clear the optimal frequency for acceleration samples and the time window width to record. Also in many situations, relying only on acceleration and vibration data may lead to false predictions: street bumps, holes and bad street conditions trigger false positives whereas external collisions coming from a vehicle while standing still may be classified as normal accelerations. To address these issues, a roll over traffic accident detecting and reporting system has been proposed and implemented.

2.0 EXPERIMENTAL

This system is not only effective but also feasible to implement. Accident detection and reporting systems can be installed in the vehicle and they will notify of unwanted incidents while traveling. Execution of the accident detection and reporting system is simple as the system makes use of GSM and GPS technologies. The below Figure 2.1 shows the block diagram of the system.

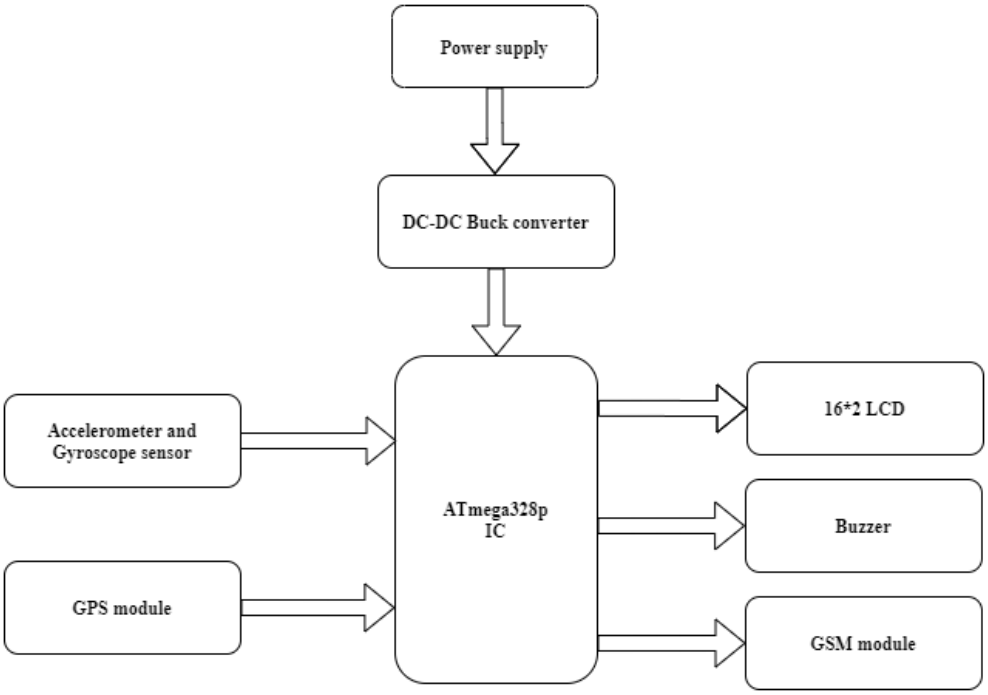

Figure 2.1: Block diagram of the system

In this system, a 12 V power supply was used. That power was directed to DC-DC buck converter to reduce to 5 V and to direct to the ATmega328p IC. Here, it was used an accelerometer and a

gyroscope sensor with the GPS module. The angles related to the rollover were provided by the accelerometer and the gyroscope sensor. That data were directed to the ATmega328p IC. The coordinates of the current location were provided by the GPS module and it was directed to the ATmega328p IC. If the data sent by the accelerometer and gyroscope sensor were satisfied with the conditions to occur a rollover, the coordinates of the current location were sent through the ATmega328p IC to the relevant parties using GSM module. After the process, it was displayed a message of "Message sent" on LCD. At that time, buzzer also switched ON. It will help the person who faces with an accident to know that relevant parties have been informed about the accident. The below Figure 2.2 shows the flow chart of the system.

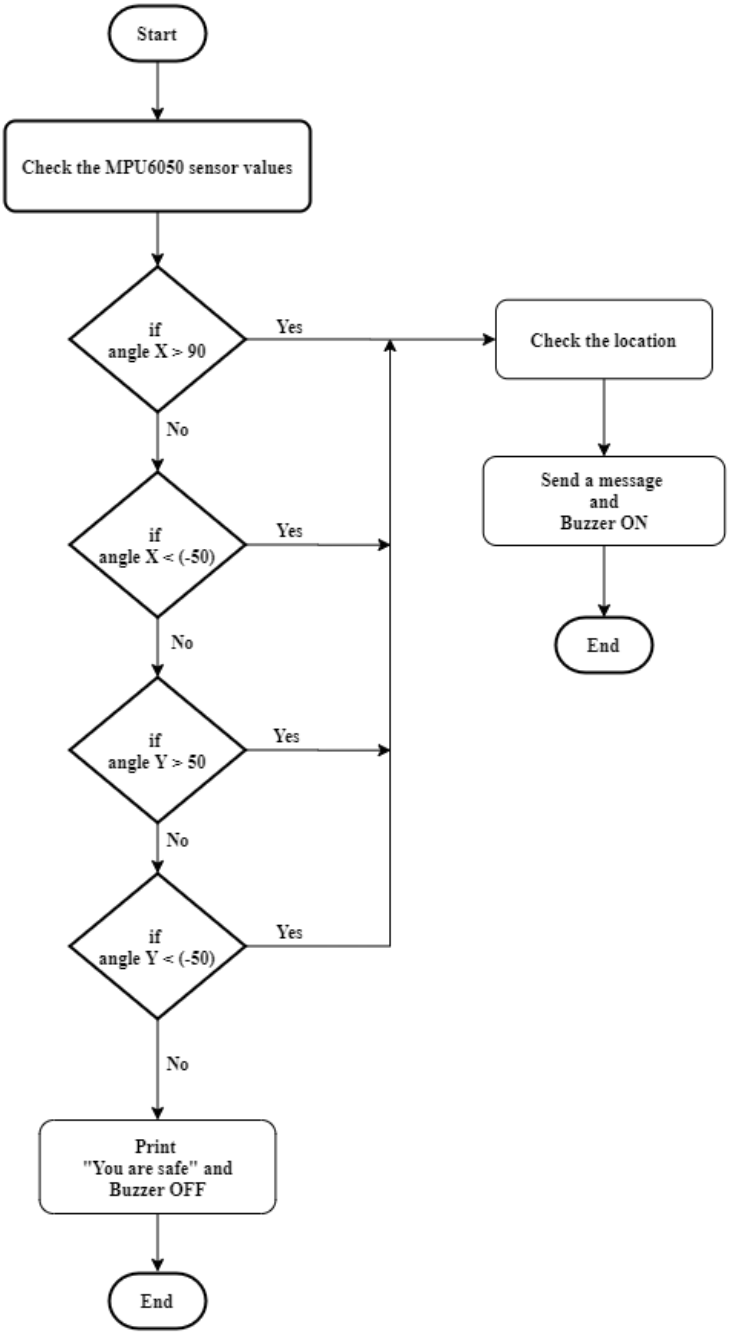

Figure 2.2: Flow chart for the system

2.1 ATmega328P IC

The ATmega328P is a high and feature-rich microcontroller. The internal circuits of the ATmega328P are designed with low power consumption characteristics [8]. It was used to store the code. Other sensors and modules are connected to it and it was used to exchange relevant data and signals.

2.2 MPU6050 – Accelerometer and Gyroscope sensors

The MPU 6050 is 6 degrees of freedom (DOF) or six-axis inertial measurement unit (IMU) sensor. It is used to measure speed, orientation, acceleration, displacement and other motor-like functions. It is more advanced than the speedometer. It can measure the tilt and lateral orientation of objects while the accelerometer can only measure linear motion [9]. Therefore, it was used to measure the angles related to the rollover. It always measures the angles corresponding to each direction. Those are x, y and z, which represent the angles from the rear bumper to the front bumper, from right side to left side and perpendicular to the ground respectively.

2.3 NEO-6M GPS Module

The NEO-6 fitting series is a family of independent GPS receivers equipped with high-performance u-bloc 6 positioning machines. NEO-6 GPS receivers provide excellent navigation performance even in the harshest environments [10]. Therefore, in this system it was used to provide the exact time of the accident and the coordinates related to the scene of the accident.

2.4 SIM900A GSM Module

The SIM900A modem is built with SIMCOM's GSM Dual band-based SIM900A modem. It works at 900 MHz. This module supports two modes, text mode and protocol data unit (PDU) mode [11]. Therefore, it was used to send the SMS to the relevant parties. This module was provided 1.5 A current to work properly in this system.

2.5 LM2596 DC-DC Buck converter

The buck converter is a DC-DC power converter that reduces the voltage from the input to the output. DC-DC Buck Converter Step-Down Module LM2596 power supply is a step-by-step switch, capable of driving 3 A loads with excellent line and load control [12]. Here it was supplied 12V and it reduced the voltage from 12 V to 5 V.

2.5 16*2 LCD Display

An LCD is an electronic display module that uses liquid crystals to create a visible image. This LCD display shows each character in a 5x7 pixel matrix [12]. It was used to display the signal messages and error messages in this system.

2.6 I2C module

The I2C module has a built-in I2C PCF8574 chip that converts I2C serial data into parallel data for the LCD monitor. The unit has a potentiometer to adjust the contrast in the lower part of the screen. It is needed to adjust the screen to display the text correctly [14]. This could be used to

change the contrast of the LCD display and the LCD could be easily connected to the circuit using only four pins of the I2C module. Therefore, the LCD was connected to this module.

3.0 RESULTS AND DISCUSSION

The complete picture of the circuit diagram is shown in Figure 3.1 (a), (b). All the components of this system are connected to ATmega328p IC via PCB.

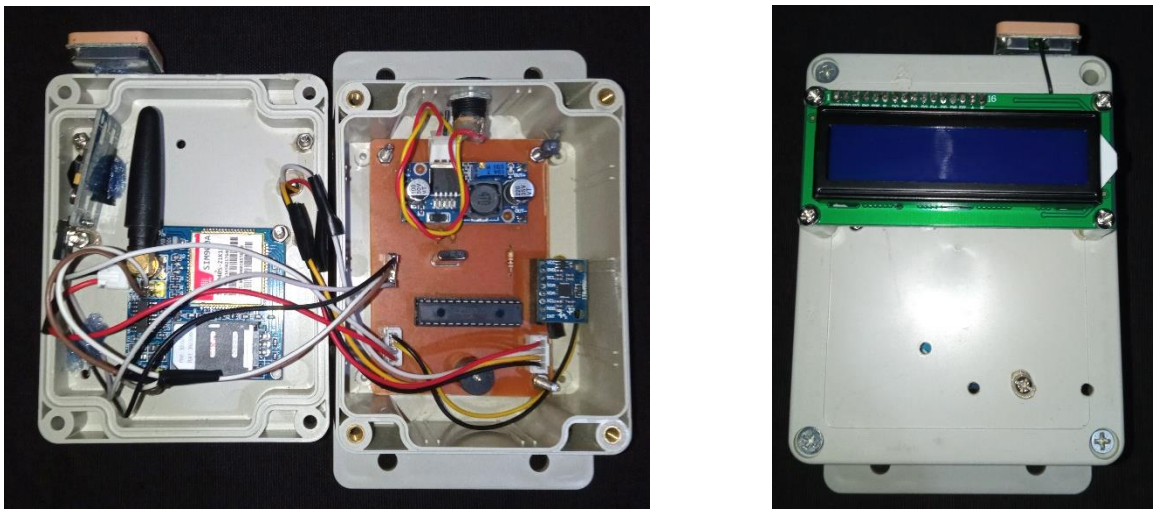

(a) (b)

Figure 3.1 (a), (b): Illustration of the inside and the top view of the implemented system

This system works at 5 V, but if the current is less than 1 A, the GSM module would not work. Therefore, to get a current of greater than 1 A, it has to be powered directly by a 12 V car battery. In this system, a buck converter is used to supply any voltage between 5 V to 30 V. The output of the buck converter is 5 V and the current is greater than 1 A. Further, it can be supplied by any type of vehicle battery between 5 V to 30 V.

As an additional feature, it is added a buzzer which is switched on after the message sent by the system. It helps the people who met with an accident to get to know that relevant parties have been informed.

The important part of this system is when an accident occurs, relevant parties are informed about the accident by sending a message that includes the time, date and the link which directly loads the location of the vehicle on google map.

A screenshot of a message that is sent to the relevant parties is shown in the below Figure 3.2. It displays the exact time, date and direct link with coordinates of the current location to access the google map. The Figure 3.3 shows the loaded google map for the exact location which has opened the link in the test message.

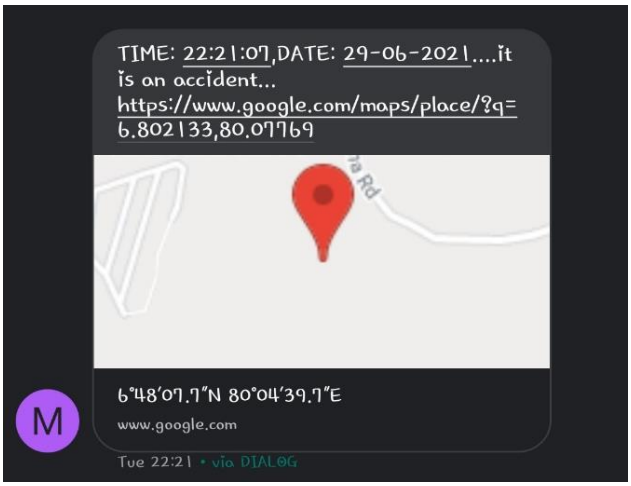

Figure 3.2: The screenshot of the received message

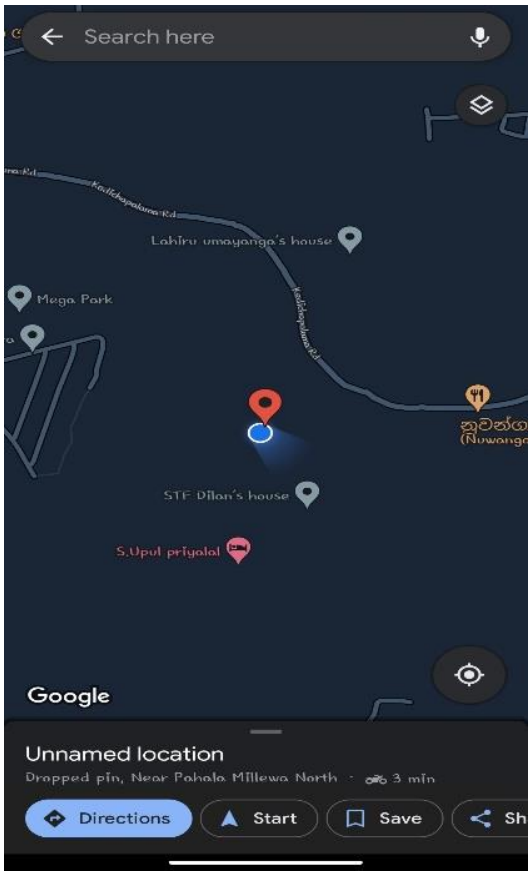

Figure 3.3: The screenshot of the loaded google map

This system was modified for cars. But this system can be developed for any kind of road vehicles. For that, it is needed the rollover angles of each and every vehicle model. Using those values, it can be modified for other vehicle models too.

This prototype system was built inside a plastic box enclosure. But it is better to use a metal and a waterproof box enclosure instead of plastic box enclosure because when an accident occurs, plastic box can be easily damaged. It is better to have a rechargeable battery for the system to avoid the power issues.

When GSM and GPS modules are connected to Atmega328p, serial data pins cannot be initialized separately. It is needed to be initialized together. Otherwise, the GPS module is not able to respond properly. Also, it is needed to connect the TX and RX of the GSM module to the RX and TX of the ATmega328p IC to communicate properly.

4.0 CONCLUSION

Roll over traffic accident detecting and reporting system with MPU6050 – Accelerometer and Gyroscope sensor was successfully implemented and tested using Arduino. The obtained results were accurate, reliable and easily operable. More importantly, it was possible to get exact location using the link which contained the current location coordinates. Therefore, this system can be used to reach the scene of the accident very easily and quickly. As a further work, this system can be extended using a wireless webcam which will help in providing driver's assistance. By using image processing technique, it will be able to avoid rollover accidents by providing an alert system that can stop the vehicle to overcome the accidents. In this project, it was used 6 modules with a PCB layout. Therefore, the cost of this whole project is around Rs. 7500.

AKNOWLEDGEMENT

I would like to express my gratitude to everyone who helped me in so many ways to carry out this project.

REFERENCES

[1]. Traffic collision - Wikipedia, *En.wikipedia.org*, (2021), https://en.wikipedia.org/wiki/Traffic_ collision , (Accessed 2021-05-10)
[2]. Hamid, M.A., Zainab, S.A., Car Accident and Notification System Using Smartphone, *International Journal of Computer Science and Mobile Computing*, 4, (2015), 620-635
[3]. Varsha, G., Padmaja V., Vehicle Accident Automatic Detection and Remote Alarm Device, *International Journal of Reconfigurable and Embedded Systems*, 1, (2012), 49-54, doi: 10.11591/ ijres.v1i2.493
[4]. Kalyani, T., Monika S., Naresh B., Mahendra, V., Accident Detection and Alert System, *International Journal of Innovative Technology and Exploring Engineering*, 8, (2019), 227-229
[5]. Viral, M.V., Viraj, C., Alcohol sensing and Accident Alert System for Car Based on Internet of Things (IoT), *International Journal for Research in Applied Science & Engineering Technology (IJRASET)*, 6, (2018), 2947, doi: http://doi.org/10.22214/ijraset.2018.4491
[6]. Tushar, S., Nilima, R., Accident detection System using Black Box System, *International Journal of Engineering Science and Computing*, 7, (2017), 5648
[7]. Saranya, R., Arun, K.R., Vehicle Accident Prevention Using Sensors, *International Research Journal of Engineering and Technology*, 4, (2017), 921-924
[8]. ATmega328 – Wikipedia, *En.wikipedia.org*, (2021), https://en.wikipedia.org/wiki/ATmega328, (Accessed 2021-05-15)
[9]. MPU6050 Pinout, Configuration, Features, Arduino Interfacing & Datasheet, *Components101*, (2021), https://components101.com/sensors/mpu6050-module, (Accessed 2021-05-15)
[10]. *U-blox.com*, (2021), https://www.u-blox.com/sites/default/files/products/documents/NEO6_ DataSheet_(GPS.G6-HW-09005).pdf,(Accessed 2021-05-18)
[11]. Hatti, M., *Smart Energy Empowerment in Smart and Resilient Cities: Renewable Energy for Smart and Sustainable Cities*, Springer Nature, 2019, E-book
[12]. Buck converter - Wikipedia, *En.wikipedia.org*, (2021), https://en.wikipedia.org/wiki/Buck_ converter, (Accessed 2021-05-21)
[13]. 16x2 LCD Pinout Diagram | Interfacing 16x2 LCD with Arduino, *Electronics For You*, (2018), https://www.electronicsforu.com/resources/learn-electronics/16x2-lcd-pinout-diagram, (Accessed 2020-09-12)

[14]. *Lastminuteengineers.com*, (2021), https://lastminuteengineers.com/i2c-lcd-arduino-tutorial/, (Accessed 2021-05-21)

Proc. Annual Symposium on Research & Industrial Training, 08(2021) 119-125
Department of Electronics – Wayamba University of Sri Lanka

DESIGNING A SMART PLANT CARING POT WITH HYDROPONICS

Y.B.E.S.K.K. Bandara*, U.A.D.N. Anuradha

Department of Electronics, Wayamba University of Sri Lanka, Kuliyapitiya, Sri Lanka

*eshani9544@gmail.com

ABSTRACT

In the modern days, the urbanization process has raised a question on sustainable development and growth of urban population. The recent changes with COVID 19 pandemic showed the ill preparedness to grow own food. The rise in global urbanization is escalating the growth of the smart indoor gardening system market due to the increase in consumer preference for enhancing the aesthetics of residential and commercial spaces, and due to the increasing demand for exotic construction modes. The usage of smart indoor gardening systems has increased as they provide smart data, smart nutrition, smart light, and allow to plant of fresh herbs, greens in less space. Based on development, the smart indoor gardening systems are segmented into self-watering, smart sensing, smart pest management, etc. Moreover, these indoor plant systems are again segmented according to the end-user as residential and commercial. This paper proposes a low-cost, flexible design of a smart indoor plant caring pot with the combination of sensor technology, hydroponics technology, and the Internet of Things. The design is consists of smart water level detection, optimum pH regulation in nutrient solution, smart lighting, and smart data monitoring capabilities.

Key words: Low-cost smart indoor plant pot, Optimum pH range adjusting, Residential end user

1.0 INTRODUCTION

Growing plants is a wonderful experience for people who face problems in life. Under the influence of urbanization, the physical connection between humans and nature gradually decreased. In order to strengthen the nature experience in everyday life and work, designers have developed various forms of designs, and smart plant products such as virtual cultivated plants, smart flower pots, voice flower pots, smart gardening systems. Today people are trying to make these pots not only as a solution for the care and maintenance of plants, but also to protect valuable limiting environmental factors such as water and land [1].

Lan Da Van et al. proposed an IoT (Internet of Things) based intelligent hydroponic plant factory solution called “Plant Talk” that built on an arbitrary smartphone. The “Plant Talk” can flexibly configure the connections of various plant sensors and actuators through the smartphone [2]. Yeong- Keun Lee et al. proposed a smart plant pot system using a USB plug-in sensor that provides the security function of detecting a fire, a trespasser, and monitoring the smooth growth of plants with the use of various sensors [3].

As mentioned, people are trying to find new designs and innovations to strengthen the connection between humans and nature, though most of the existing flowerpots and products are primarily design-focused. However, due to several reasons, such as the high cost of existing smart plant-pots, the unpopularity of production, the lack of awareness of modern innovation, the lack of ease of use and flexibility, and the lack of environmental factors needed for growth further, research is required to improve the sense of connection between humans and nature.

In order to meet the specified requirements of a hydroponic technology, a pH balancing system has been introduced. This system maintains the pH of the nutrient solution in an optimum range for

the root system of the plant. The main purpose of Smart plant pots is to provide sustainable solutions for caring for plants in order to help people and conserve limited resources for the future. According to the current World Population Clock, the world population as of February 2021 is 7.8 billion. The world's population will reach 10 billion by 2057, and land is becoming increasingly scarce. Currently, 2.2 billion people in the world do not have access to safely manage sanitary water. Researchers have shown that people consume a lot of water during outdoor activities such as gardening. In a world of depleted land, water, and increasingly unstable environments, smart plant pots can provide nutritious greens without considering limited resources, making people aware of plant health at ease and can participate in the care of plants in various ways. In addition, this design is a smart way to enhance the connection between humans and nature, thereby improving the natural connection of the indoor environment.

2.0 EXPERIMENTAL

Smart indoor gardening systems are self-growing gardening solution which enables the user to grow fresh plants, herbs, and flowers with higher nutritional content. A survey was done in order to identify different experiences, behaviors related to gardening, and to identify the preferences to a smart indoor plant caring system. According to the responses, for a low-cost, reusable, time saving, durable smart plant caring solution was preferred by the most of consumers. Further, several facilities had been expected by most of the consumers such as, temperature & humidity monitoring, water level monitoring, pest and weed controlling, light level adjusting and automatic fertigation. Lack of time, pest & weed, lack of space, and climate and weather control were identified as the major problems in soil based gardening. Hydroponics technology was used to overcome these problems.

Hydroponics is a high-tech method of growing plants in water rich minerals instead of soil. Absolutely, the need of soil and pest & weed problems could have been cut off by hydroponics. Therefore, available space, lighting, budget, and time constraints were considered when designing the smart plant caring solution. Kratky hydroponic method was used since the most of growers required a low cost and less space consuming solution. As the very first step of this experiment a capsicum plant was grown for 3 weeks by using Kratky method. Optimum water temperature, optimum pH range, optimum nutrient mixed water level, optimum air temperature, and optimum humidity were the identified critical parameters that affect the plant growth. According to that experiment, this solution was further need to develop with the expected features such as pH level adjusting, water level sensing, weather controlling, temperature and humidity monitoring. Therefore this hydroponic smart plant pot was built by combining three separate sections; pH up and down tanks, nutrient mixed water tank and the sensor based controller unit.

This smart plant pot was integrated with several sensors and was accompanied by a mobile app which was built on the Blynk platform to track the real time health status of the plants. Arduino Uno microcontroller and Nodemcu were taken as the processors and both were used to control the processes of each sensor. Sensors were selected according to the requirements of a hydroponic plant. The below figure illustrates the functional block diagram of the smart indoor plant caring pot. In this figure, plant sensors sends the captured data to the Arduino Uno from the input pins of the Arduino. Then, the captured data were parsed to the Nodemcu via the RX, TX serial communication pins. After that, the data was pushed to the Blynk server through Wi-Fi. Then the real time information about the pH level, air temperature, humidity, light intensity, water level, and water temperature was displayed on the widgets on the mobile app.

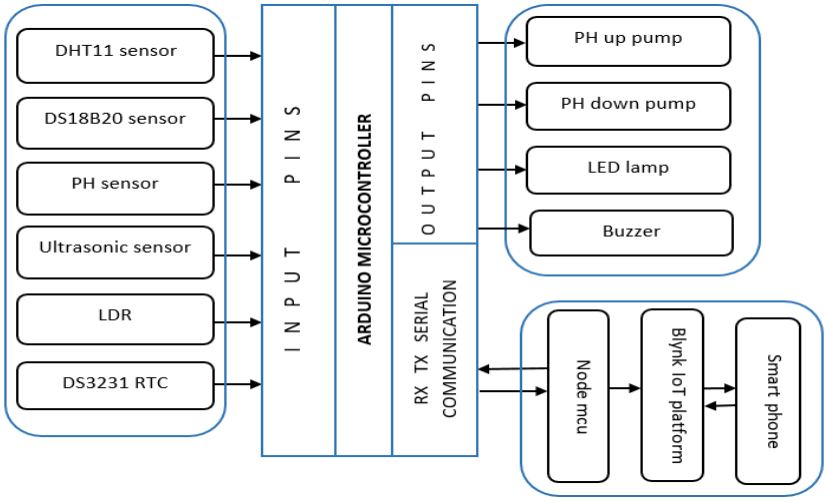

Figure 2.1: Functional block diagram of the smart hydroponic plant pot

The following tasks were taken place with the combination of sensors and actuators.

- The nutrient mixed water level of the tank was indicated by the ultrasonic sensor which was placed on the lid of the nutrient mixed water tank. If the detected water level was less than 3.6cm, the plant pot was notified the user by generating a tone via the buzzer.
- Temperature, humidity and water temperature effect on a growth of hydroponic plants. Therefore the temperature and humidity in the air were detected by the DHT11 temperature and humidity sensor and the water temperature in the nutrient mixed water tank was detected by the DS18B20 one wire temperature probe.
- The pH sensor probe was placed in a nutrient mixture tank and checked to see if the pH value was in the optimum range of 5.5 to 6.6. The pump in the pH up tank was turned on by the Arduino microcontroller when the pH value was less than 5.8. When the pH value was greater than 5.8, the pH down solution was added to the nutrient tank.
- This plant pot has the ability to adjust the light level to provide a sufficient amount of light.
- The light intensity values were taken by Light Dependent Resistor (LDR). If the light intensity level is below 200 lux, the low power LED lamp was turned ON and if the light intensity level is above 600 lux, the lamp was turned OFF.

3.0 RESULTS AND DISCUSSION

3.1 Identifying the problems encountered while gardening

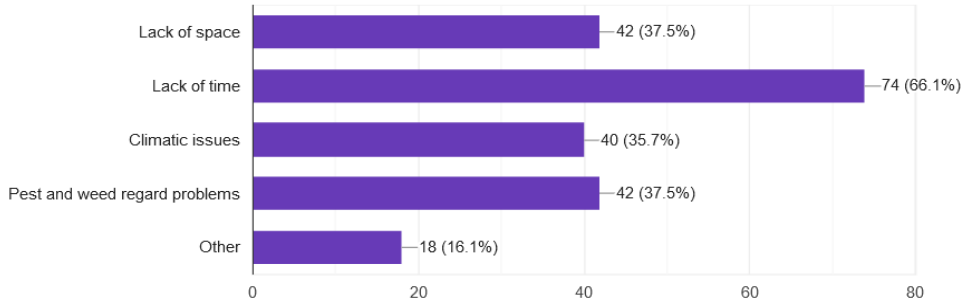

Figure 3.1: Graphical representation for current gardening problems

This graph represents the results for encountered problems while gardening. The smart plant pot was developed by considering the above problems while gardening. Following sections show the results of testing, and developed smart plant caring pot.

3.2 Determining the Accuracy of the pH Sensor Probe

Since the only reliable way to determine whether the pH sensor probe is accurate or not is to test the pH sensor probe in standard solutions. A pH sensor probe is considered accurate and in good condition if the error pH value (the reading difference between the pH measurement and the standard pH value) is less than or equal to ±0.01.

Table 3.1: The results of pH buffer solutions

pH value of buffer solution at 30^0 C	Measured voltage for the pH buffer solution	Measured pH value of the buffer solution at 30^0 C	|Error pH value|
4.01	2.998V	4.0	0.01
9.14	2.110V	9.146	0.006

According to the observations, the error pH value for 4.01 standard buffer solution was equal to 0.01 and error pH value for 9.14 standard buffer solution was less than 0.01. Therefore, the pH sensor probe was accurate and in good condition to measure pH values of solutions.

3.3 Determining the pH value of the Albert's solution

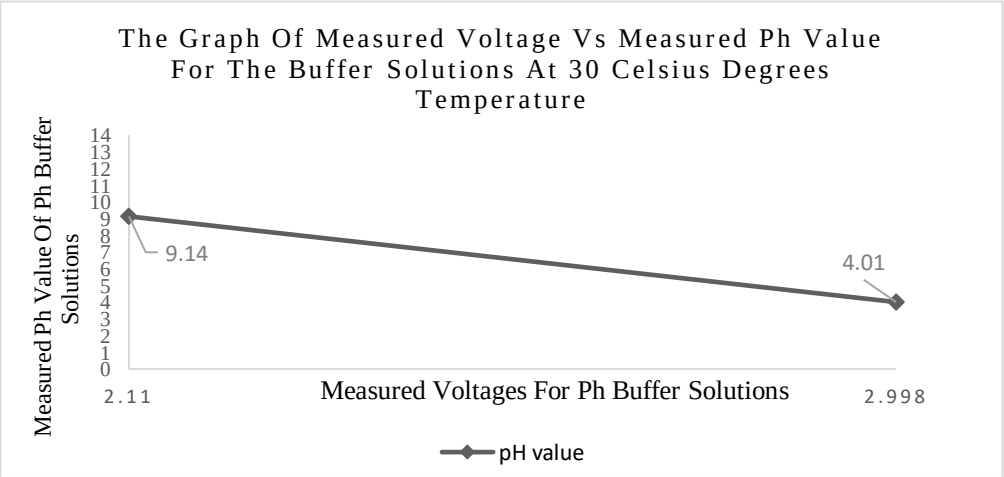

Figure 3.2: The graph of measured pH values vs measured voltages for the buffer solutions at 30^0 C temperature

The measured voltage for Albert's solution was 2.728V.

$$The\ gradient\ of\ the\ graph\ = \frac{(pH_{9.18} - pH_{4.01})}{(VpH_{9.18} - VpH_{4.01})} = \frac{(9.14 - 4.0)}{(2.110 - 2.998)} = -5.788$$

The pH value for Albert's solution was calculated by using the gradient of the graph. Therefore, the pH value of the Albert's solution was 5.849.

3.4 Design and position of the sensors

Figure 3.3: Design of the smart plant pot and the positions of sensors.

The concept was sketched and designed with AutoCAD to preview a better understanding of the plant pot and the positions of sensors and tanks.

In following Figure 3.3, figure A represents the design of the smart pot with the positions of a nutrient tank (right side) and pH up and down solution bottles (left side). The top view of the smart pot is represented by figure B. Figure C represents the pH up and pH down solution tanks. Figure D represents the positions of DS18B20 temperature sensor probe, ultrasonic sensor, and pH sensor probe (opposite direction of the pH up and down tank). Figure E represents the position of LDR sensor. Figure F represents the position of DHT11 sensor at a side of the circuit box. Figure G represents the final design of the smart plant caring pot model. Figure H represents the prototype of the first testing.

3.5 Mobile application on the Blynk platform

Figure 3.4: Testing the mobile app with sensors

The Arduino microcontroller sends the captured data from the sensors to Nodemcu via serial communication. Blynk server is responsible for all communications with smartphones and the hardware. The Nodemcu enables communication with the Blynk server and processes all the incoming and outgoing commands. This app allows the user to monitor the status of the smart plant pot regularly. It was successfully displayed sensor data, update data and visualize them. Furthermore, it notifies the user when the device is offline and online.

3.6 Discussion

The major problem encountered while growing plants with this smart pot were controlling the growth of Algae. Though the nutrient-mixed water is placed in a dark container, the environmental condition in the nutrient-mixed water tank allows growing Algae. Therefore the nutrient-mixed water was exchanged in 30 days. The growth of Algae was able to impact the pH level of the nutrient mixed water solution.

This smart pot is a low-cost, time-saving solution to grow plants indoors. Further, there is no need to concern about balancing pH level in the nutrient solution, the plant pot notifies the owner when the nutrient solution level is not sufficient to care for the plant and assembles the lamp when it requires additional light.

4.0 CONCLUSION

Smart connected innovations in plant pots and systems offer exponentially expanding opportunities for new functionality, far greater reliability, and capabilities to cut across and transcend the traditional boundaries in taking care of plants and strengthen the connection between nature and humans. However, due to some reasons like high cost, low popularity, lack of awareness of modern

innovations, less flexibility and less user-friendliness in the existing innovations, further research and development of innovation is required.

Therefore this research was conducted to design a smart plant caring pot with hydroponic technology. According to the results of this study, the pH adjusting system works properly and keeps the optimum pH range. Moreover, it can monitor data regularly and is able to update the data in the mobile application on the Blynk platform regularly. The user should add the water to the water tank when the water level of the water tank is low, moreover, the plant pot generates a tone when it requires water. The plants were grown in a sponge with a gravel container. Algae growth is the major problem encountered when growing plants in this pot. Therefore the water in the tank was changed in 30 days.

Furthermore, this system can be modified by introducing an automated algae controlling system and with a way of measuring and controlling the electric conductivity of the nutrient solution.

ACKNOWLEDGEMENTS

Author would like to express the sincere gratitude to the supervisor's stimulating suggestions and encouragement throughout this research project. Appreciation is also extended to the Final Research Project Coordinator and the staff at the Department of Electronics, WUSL, for their coordination and careful monitoring throughout the research project.

REFERENCES

[1]. Adam Dunkels, Plants-as-a- Service: Office Plants Made Greener with the IoT, https://www.things quare. com/ blog/articles/interior-landscapes/ (2021.01.25)
[2]. Lan-Da-Van, Yi-Bing Lin, Tsung-Han Wu, Yun-Wei Lin, Syuan-Ru Peng, Lin-Hang Kao, Chun-Hao Chang, PlantTalk: A Smartphone-Based Intelligent Hydroponic Plant Box. *Sensors* 19/8, (2019),1763, doi:10.3390/s19081763
[3]. Yeong-Keun Lee, Koo-Rack Park, Dong-Hyun-Kim, Implementation of Smart Pot System using USB Plug-in Sensors(Basel). *International Journal of recent Technology and Engineering (IJRTE)* 8/2S6, (2019),245-250, doi:10.35940/*ijrte*.B1046.0782S619

Proc. Annual Symposium on Research & Industrial Training, 08(2021) 126-130
Department of Electronics – Wayamba University of Sri Lanka

DESIGNING AN AUTOMATED OIL MEASURING DISPENSER UNIT

G.K.H. Madushan*, L.D.R.D. Perera

Department of Electronics, Wayamba University of Sri Lanka, Kuliyapitiya

*harshamadushan4422@gmail.com

ABSTRACT

Measuring liquids is an important and essential process in our day to day life. A seller must measure correctly as the customer wishes. Doses of liquid medicine to a patient must be measured very accurately. Some of the liquid measuring processes are crude, have no accuracy and consume time. It is therefore necessary to produce a simple and accurate Liquid Measuring Dispenser to ease this process. The designed system consists of a Flow-rate sensor, arduino board, solenoid valve, display and a keyboard. For low cost, light weight and also for reliability, aluminum box bars and aluminum boards were used for assembling the system. The fabricated system can measure any liquid with any quantity without changing settings. The designed dispenser system is easy to operate. When the required liquid amount is entered in milliliters and the "Enter" button is pressed, a solenoid valve opens and oil flows through the PVC pipe line. Flow rate sensor senses the liquid volume and the Arduino board does the calculation part. The fabricated dispenser is small in size and easy to operate. The dispenser could be further improved to be controlled by a mobile phone.

Keywords: Liquid dispenser, Flow-rate sensor, Solenoid valve

1.0 INTRODUCTION

For years, the manufacturers of planes, trains, vehicles, and consumer goods have frequently been dispensing oils onto various parts during the fabrication process. The modern large-scale industries incorporate oil dispensing systems to provide oil to different elements during assembly regularly to keep them lubricated. Apart from oil, grease is also distributed onto machine parts [1].

The inefficient transfer of oil at production facilities can lead to serious safety issues and costly downtimes. Companies cannot afford to use low-quality bulk oil dispensers as it would only lead to increased costs both in terms of factory shutdown and maintenance costs. For this reason, investments are made to obtain high-quality oil dispensing systems to reduce the inefficient transfer of oil [2].

In this study, an oil dispenser was designed to deliver a measured volume of oil at the press of a button. In normal use, the operator selects a volume, presses a button and the dispenser delivers the required volume without further operator intervention.

2.0 EXPERIMENTAL

In the process of designing the liquid measuring dispenser, collecting data was a major activity. Therefore, as the first step basic study was carried out on the oil measuring machines operation, mechanism and technology, and their auxiliaries [3]. The designed machine is electrically operated with electro-mechanical actuators. Some types of machines are controlled based on the PLC system and it is a very complex controlling system. All the machines are operated by

electrical, electronic and mechanical combinations. Therefore all the above mentioned systems, operations and requirements of this machine were studied in detail [4].

2.1 Arduino based Flow Rate Sensor

This sensor sits in line with the oil line and contains a pinwheel sensor to measure how much liquid has moved through it. There is an integrated magnetic Hall Effect sensor that outputs an electrical pulse with every revolution. The Hall Effect sensor is sealed from the oil pipe and allows the sensor to stay safe and dry [5].

Figure 2.1: Arduino based Flow Rate Sensor

2.2 Block diagram of the designed system

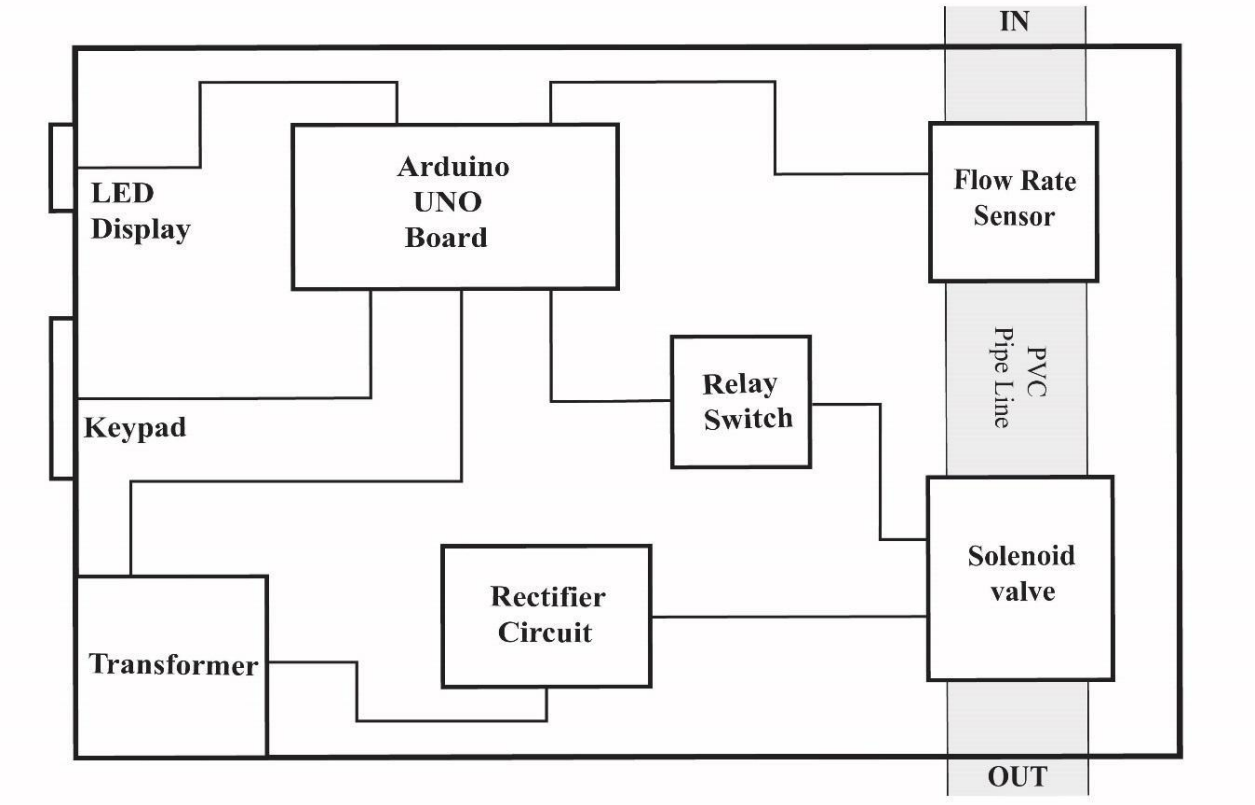

Figure 2.2: Block diagram of the dispenser Unit

2.3 Mechanism of the dispenser system

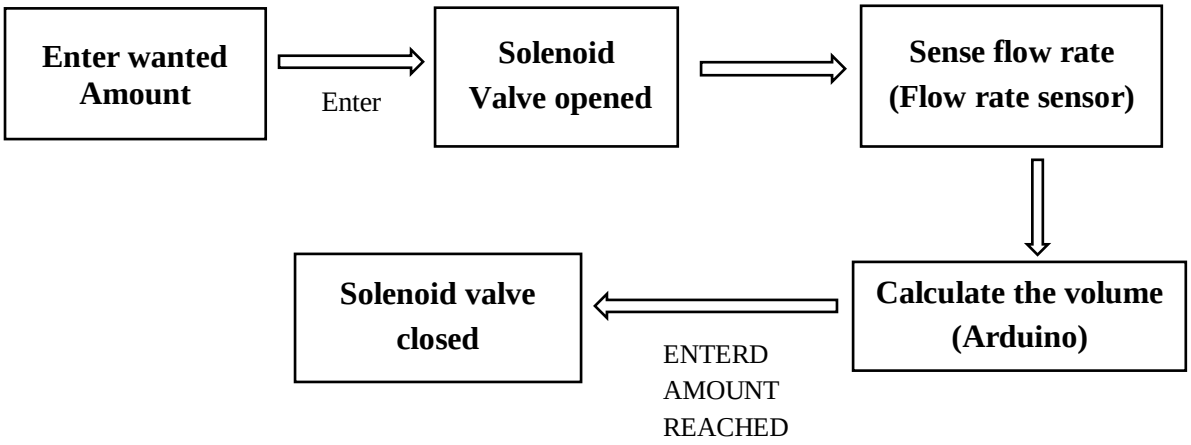

Figure 2.3: Flow chart of the dispenser mechanism

When the required volume of the oil (in ml) is entered through the key pad and press the enter button ("#" button), solenoid valve will open. Then oil will flow through the PVC pipe line and the flow rate sensor will sense the rate of flow. When the required amount of liquid is reached solenoid valve will be closed.

Solenoid valve is used for controlling the oil flow. At the beginning solenoid valve is closed and there will be no oil flow. When the required volume is entered, valve will open and oil flows through the PVC pipe line. 12V relay switch was used to interface the solenoid valve with Arduino because solenoid valve is a 12V component. Flow rate sensor was used to measure the oil volume. The oil flowing through the flow rate sensor is sensed by the flow rate sensor and the volume is calculated by the Arduino.

3.0 RESULTS AND DISCUSSION

3.1 Designed system

Figure 3.1: Front view of the dispenser unit

The designed system has an LED display (16*2) and a keypad on the front panel. User can easily enter the required amount of oil and press Enter ("#") button and fulfill the requirement. LCD displays oil amount in milliliters. The final product was small in size (16 cm * 18 cm * 25cm), hence it can be easily handled.

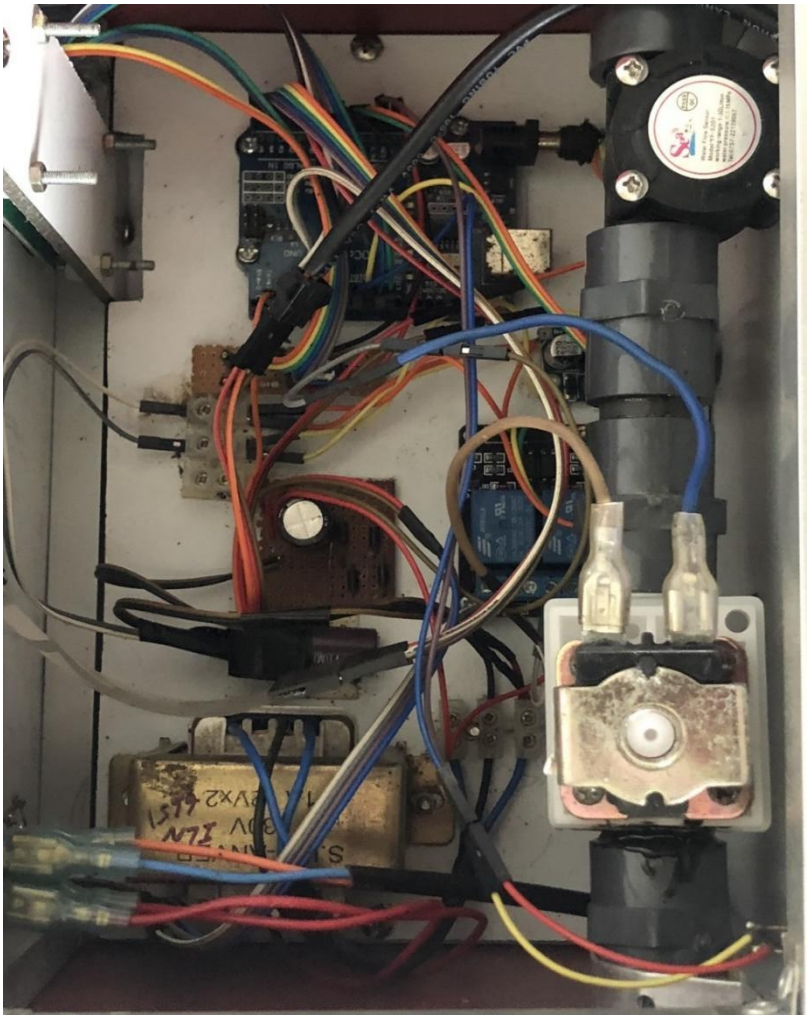

Figure 3.2: Inside view of the dispenser unit

3.2 Performance of the designed system

The designed system gives fast feedback and accomplishes our requirement within minimum time. The LED displays the amount required. This system can be used for measuring any liquid. Special feature of the system is that it has a simple operating method, hence any persons can use this dispenser system.

Table 3.1: Time required for dispensing various liquids

Type of liquid	Required Time in Seconds to dispense		
	250 ml	500 ml	1000 ml
Water	12	25	55
Coconut Oil	24	52	112
Petrol	13	28	62

When designing this machine the target was to achieve some objectives like, making the machine size smaller by packing all the components and mounting the right components to right dimensions. Another main barrier encountered was that the solenoid valve did not open without required pressure. At the beginning of the design, it was planned to use a pump. But due to the unavailability of a suitable pump, first design used gravity pressure but it was not suitable. Then it was decided to use water line pressure to this machine. It worked but the pressure was always changing. This pressure change affects the measurements and it was difficult to calibrate the machine. But performance should improve when a pump is connected to apply a constant pressure.

4.0 CONCLUSIONS

The main objective of the project was to design an Oil measuring dispenser machine to measure and dispense oil easily, and to save time and wastages in measuring. The fabricated dispenser is small, easy to use and quick. It can dispense a specified amount of an oil by pressing the keys.

The designed machine can be improved further. It can be designed to be controlled using a mobile phone via Bluetooth. Then it will be very easy for the user to operate this machine without touching it.

ACKNOWLEDGEMENTS

Authors wish to extend their gratitude to the academic and nonacademic staff at the Department of Electronics, Faculty of Applied Sciences, Wayamba University of Sri Lanka, for their support to make this project a success.

REFERENCES

[1]. Advantages of using Efficient Oil Dispensing Systems, https://www.micro-lube.com/blog/post/advantages-using-efficient-oil-dispensing-systems/ (Accessed 2021-06-28).

[2]. Sadique, S.K., Vanalkar, A.V., Design Consideration of Oil Measuring & Dispensing Machine, *IJIRST –International Journal for Innovative Research in Science & Technology*, 2, (2), July 2015, ISSN: 2349-6010

[3]. Li, B., Wu, L., Li, L., Seeger, S., Zhang, J., & Wang, A., Superwetting double-layer polyester materials for effective removal of both insoluble oils and soluble dyes in water. *ACS applied materials & interfaces*, *6*(14) (2014), 11581-11588, doi: 10.1021/am502313h.

[4]. Wang, Q., Yu, Y., Yang, J., & Liu, J., Fast fabrication of flexible functional circuits based on liquid metal dual-trans printing. *Advanced Materials*, *27*(44), (2015), 7109-7116.

[5]. Rahmat, R. F., Satria, I. S., Siregar, B., Budiarto, Water pipeline monitoring and leak detection using flow liquid meter sensor, In *IOP Conference Series: Materials Science and Engineering*, 190, (1) (2017), p. 012036

Proc. Annual Symposium on Research & Industrial Training, 08(2021) 131-134
Department of Electronics – Wayamba University of Sri Lanka

DIGITALLY CONTROLLED SAMPLE EVAPORATION SYSTEM TO DETECT ALPHA PARTICLES

W.A.A. Dilshan[1*], M.A.A. Karunarathne[1], M. Mahakumara[2]

[1]*Department of Electronics, Wayamba University of Sri Lanka, Kuliyapitiya, Sri Lanka*
[2]*Radiation Protection and Technical Services Division, Sri Lanka Atomic Energy Board, Orugodawatte, Sri Lanka*

[*]arunadilshanfernando@gmail.com

ABSTRACT

There are many radioactive detectors to detect radiations in a water sample, but the alpha radiations or particles, in the water cannot be measured with those detectors. Therefore, the water sample is mixed with the liquid scintillation cocktail and its data are used to detect the presence of alpha particles. But this sample evaporation system clear the road to detect the alpha particles in the water sample by evaporating the water in the sample. This is because alpha particles travel quite a distance with water vapor. The detectors then detect the alpha particles. This system is a step used to identify alpha particles, which cause water to fall to the surface of the plate and evaporate the water by heating the plate. Depending on the amount of water evaporating, the temperature of the heater which attached to the plate is controlled and the rate of evaporation is accelerated by reducing the humidity in the surrounding area. The system can also measure the time it takes to evaporate. The detector can easily detect alpha particles as the system evaporates water more efficiently.

Keywords: Evaporation, Radiation

1.0 INTRODUCTION

Radiation is energy in the form of waves or streams of particles. There are many kinds of radiation all around us. When people hear the word radiation, they often think of atomic energy, nuclear power and radioactivity, but radiation has many other forms. Sound and visible light are familiar forms of radiation; other types include ultraviolet radiation (that produces a suntan), infrared radiation (a form of heat energy), and radio and television signals. Radiation can be categorized as ionizing radiation and non-ionizing radiation. It is depending on the energy of radiated particles. Ionizing radiation can emit electrons out of the atoms by either direct interaction with the atoms or by other methods. A common source of ionizing radiation is radioactive materials that emit α, β, or γ radiation [1].

Alpha particles are composite particles consisting of two protons and two neutrons tightly bound together. They are emitted from the nucleus of some radionuclide during a form of radioactive decay, called alpha-decay. An Alpha particle is identical to the nucleus of a normal (atomic mass four) helium atom i.e. a doubly ionized helium atom. Alpha radiation can be stopped by a piece of paper or the dead outer layer of the skin. Consequently, Alpha radiation from nuclear substances outside the body does not present a radiation hazard. However, when Alpha-radiation-emitting nuclear substances are taken into the body (for example, by breathing them in or by ingesting them), the energy of the Alpha radiation is completely absorbed into bodily tissues. For this reason, Alpha radiation is only an internal hazard. An example of a nuclear substance that undergoes Alpha decay is radon-222, which decays to Polonium-218 [2].

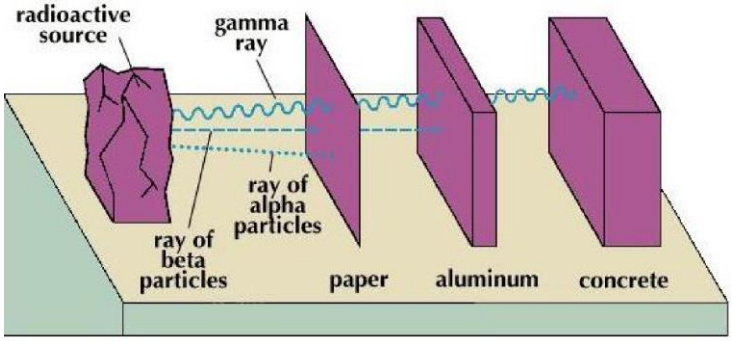

Figure 1.1: Penetration power of three types of radiation

According to the above description Alpha radiation can be a hazard to the human when Alpha particles are taken into the body. Also uncontrolled use of man-made radiation carries a potential risk to the health and safety of workers and the public. Alpha particles can be mixed with river water, underground water, etc. because of human or nature activities. So the drinking water which contains Alpha particles is the easiest way for Alpha particles to get into the human body. Therefore it is important to recognize that kind of water sources which mixed with Alpha radiations for health safety.

Most radiation detectors are used to measure radiation on a surface or in an area. Gamma and Beta particles are going through the water and those can be measured with detectors but Alpha which is in the water is not. So Alpha particles that dissolve in the water must be taken on to a surface to measure the radioactivity. Also the water sample is mixed with the liquid scintillation cocktail and its data are used to detect the presence of alpha particles. The radioactive detectors detect the alpha particles in the water sample by evaporating the water sample. This is because alpha particles travel quite a distance with water vapor. The detector then detects the alpha particles. Then a special evaporation system is needed to evaporate Alpha particles concentration of the water, which cause water to fall to the surface of the plate and evaporate the water by heating the plate. So in this project a Digitally Controlled Sample Evaporation System is produced to solve the above problem.

2.0 EXPERIMENTAL

The “Liquid scintillation cocktail” solution to find alpha particles, alpha particles in a water sample should be found at low cost. With this study to solve the above problems, a digitally controlled sample evaporation system was developed to find the presence of the alpha particles in the water sample. This system evaporates to some extent which can evaporate water samples and then detect the concentration of alpha particles of the water sample.

This digital evaporation system had a Water container, Surface temperatures sensor, Thermo-cooling peltier, DC fan, Humidity and temperature sensor, LCD module, RTC module and Microcontroller. The water container was used to hold the water sample and it was gradually dropped in to the hotplate. Thermo-cooling peltier was used as a heater and it was controlled with PWM techniques. The temperature of the hotplate was measured from the surface temperature sensor. The DC fan was used to change the evaporation rate and to remove the evaporating water vapor from the air. The fan was controlled using PWM techniques. DHT11 humidity and Temperature sensor were used to measure humidity and temperature of the hotplate environment and those values could be shown in the LCD display. The RTC module was used to display the real-time clock and date. The start time and the end time were recorded in the microcontroller

using this module. As well as if the system was stopped the process due to the power failure, the time of the particular moment is recorded. This Reading can be shown in the LCD module. The microcontroller was the brain of the system and it was used to receive data from a surface temperature sensor, DHT 11 sensor, and RCT module and send data to the thermo-cooling peltier, LCD module and DC fan. All of the controlling activities of the system are done by the microcontroller.

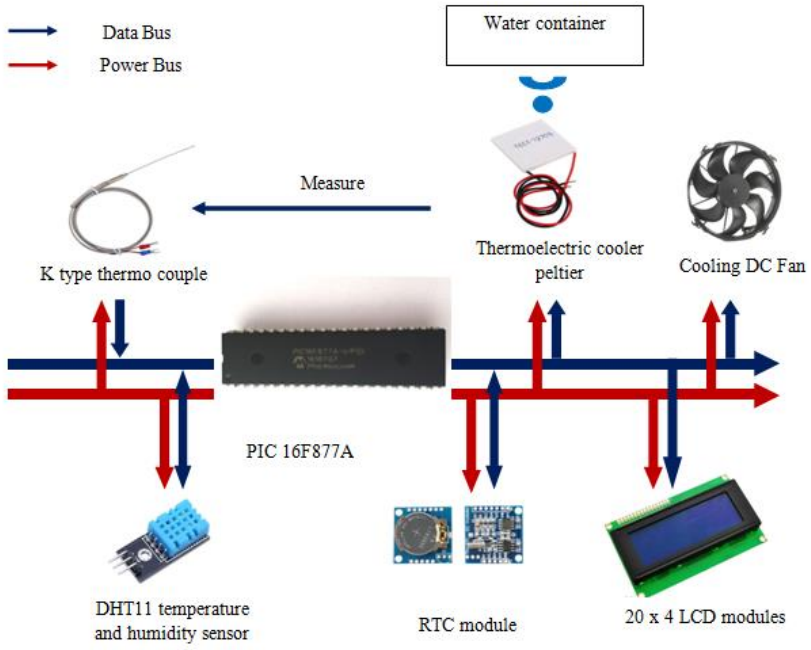

Figure 2.1: Block diagram for the digital evaporating system

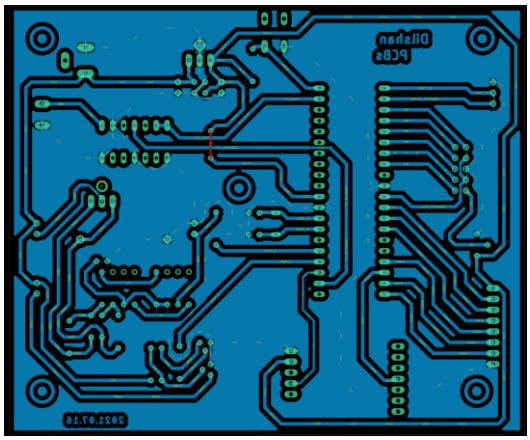

Figure 2.2: PCB layout for the digital evaporate system

3.0 RESULTS AND DISCUSSION

Water evaporation was done by a digital evaporation system developed as a prestep to detect alpha particles. This system is used to check whether there are alpha particles or not in the water sample which is not detected by detectors in water.

A DC heater was used in the design of this system and this heater is controlled by PWM. It is not possible to control the current through the heater directly from the PWM. As a solution to this, a

circuit was created to control the current by PWM. The circuit components were overheated and the problem was solved by using a heat sink and a tiny cooling fan. The current was measured by changing the voltage values to check the accuracy of the variation of the current according to the voltage.

The current corona pandemic situation was a big problem while designing this system and it made a lot of difficulties to design a water container because it could not be tested in the institute. Also it was difficult to obtain components, however it was possible to successfully create the main components of the system.

External EEROM can be used as a recommendation for the internal EEPROM of the microcontroller of the system. Then this system can store data when evaporation is starting, is stopping, is resuming and time it started to evaporate, and at the power on, and off time.

4.0 CONCLUSION

Digital evaporate system was a low cost solution for checking steps when finding the alpha radiation particles of the water sample. This system can measure the temperature of the hotplate and monitor the real time clock. Also it was designed as a prototype system. Finally the system could be created by covering the system objectives precipitating the Alpha (α) particles which are dissolved in water by using water evaporation, measuring the radioactivity of Alpha (α) particles using precipitated sample, identifying the aquatic source areal which consisted with harmful Alpha (α) radiations by using data analysis.

ACKNOWLEDGEMENT

Authors would like to thank all the staff of Department of Electronics, Faculty of Applied science, Wayamba University of Sri Lanka. Sincerely gratitude is also extended to the staff members at the General Scientific Services Division in Sri Lanka Atomic Energy Board.

REFERENCES

[1]. What are different type's radiations, *letstalkscience*, https://letstalkscience.ca/educational-resources/backgrounders/what-are-different-types-radiation, (Accessed 2021-03-25)
[2]. Alpha particles, *arpansa*, https://www.arpansa.gov.au/ understanding-radiation/what-is-radiation/ionising-radiation/alpha-particles, (Accessed 2021-05-30)

Proc. Annual Symposium on Research & Industrial Training, 08(2021) 135-140
Department of Electronics – Wayamba University of Sri Lanka

TRACER STUDY ON USAGE OF FIBRE OPTIC TECHNOLOGY FOR BROADBAND SERVICE IN SELECTED AREAS IN SRI LANKA

T.G.S. Lakshith*, P. M. Senadeera

Department of Electronics, Wayamba University of Sri Lanka, Kuliyapitiya, Sri Lanka

*Sahanlakshithgamage1995@gmail.com

ABSTRACT

This paper describes study on the evaluation of the usage of fibre optic technology in selected areas in Sri Lanka. Here, the usage of fibre optic technology in present society in Sri Lanka and also the willingness of the people to adopt for the fibre optic technology was investigated. Data collection was done by distributing a google form among the people. The questionnaire was pre-tested to clarify misunderstandings by using 10 respondents from Gampaha region and the necessary changes were made to upgrade the questionnaire. Sample size of 107 respondents have been used and these respondents were selected by using the simple random sampling technique in order to increase the reliability of the findings, since the respondents have to be identified as fibre optic technology users (14 respondents) and non-users (93 respondents). Descriptive analysis was done to analyze the demographic factors and the other collected data via google form. According to the results obtained from selected areas of the country, 93 respondents have used 4G and ADSL technology to have internet connection around the country whereas only 14 respondents have used fibre optic technology to obtain internet connection. As a result, the internet speed of the non-users was in the range of about 1-10 Mbps whereas the internet speed of the users of fibre technology was between 30 and 100 Mbps. It was concluded that most of the users and non-users prefer to enhance the technology with fibre to have a better connection.

Keywords: Descriptive analysis, Fiber optic technology, Internet speed

1.0 INTRODUCTION

1.1. Overview

The world is constantly adopting to the new technology creating with them new career opportunities. As the world-wide demand for broadband increases, the need for high-speed data transmission is apparent, hence creating a market for fibre optic technology is essential. When considering the internet usage in Sri Lanka, it is increasing day by day. But the speed of data transmission is low due to the high usage and network traffic [1]. To minimize those barriers, fibre optic technology was emerged. Fibre was not used widely in Sri Lanka and the majority of the fibre networks in the country were used only for the purpose of transporting backhaul traffic.

1.2.Literature Review

Fiber optic is the technology used to transmit information as pulses of light through elements of fiber made of glass or plastic over long distances. A fiber-optic cable contains anywhere from a few to hundreds of optical fibers within a plastic casing. Fiber optic cables are also known as optic cables or optical fiber cables. They transfer data signals in the form of light [2-6]. In addition, data signals via fiber optic cables travel hundreds of miles significantly faster than traditional electrical cables. Fiber optic cables are not affected by electromagnetic interference that reduces the speed of transmission. Because the fiber-optic cables are non-metallic [7 -10]. In addition, fiber cables are safe because they do not carry a current and not generate a spark. When considering the traditional technologies, copper media has limited

speed, capacity and data transmission. Traditional Digital Subscriber Line systems consist of few Mbps and is unable to supply fast accurate services. Copper cable' limitations hustled the service providers to explore new technologies. As a result, fiber optic technology was recognized as the most convenient technology due to its great bandwidth and fast service that uses light impulses instead of electrical signals for transmission [11-14]. Similarly, fiber optics is frequently used in broadcasting and electronics to provide better connections and performance.

1.3.Research Objective

Evaluation of the usage of fibre optic technology in Sri Lanka by conducting a survey via distributing the google form among the people in the society was suggested. Estimation of the usage of fibre optic technology in present society by using selected areas in Sri Lanka and the estimation of the willingness of the people to adopt for the fibre optic technology were carried out. This was carried out by collecting the data related to the data usage, internet speed, preference to enhance the technology with fibre and demographic factors of the respondents.

2.0 EXPERIMENTAL

2.1. Research design

Total of 107 respondents were used for the study and these respondents were selected using the simple random sampling technique in order to increase the reliability of the findings.

2.2. Data collection

Data collection was conducted randomly by selecting a particular area in Sri Lanka like Rathnapura, Gampaha, Colombo, Galle, Kurunegala, Kandy, Matara, Badulla, Hambantota, Kalutara, Kegalle, Matale, Puttalam, Jaffna and Anuradhapura. It was done by using a google form due to the COVID 19 pandemic situation. The sampling procedure for the research was the simple random sampling method. Every member of the population has an equal chance of being selected to the sample. In the groups of users and non-users of fibre technology, simple random sampling method was used to interview respondents. The questionnaire was pre-tested to clarify misunderstandings by using 10 respondents from Gampaha region and the necessary changes were made to upgrade the questionnaire.

2.3. Data analysis

Data analysis was done by using SPSS statistical software. It was done to achieve the main objectives of the study. Descriptive statistics are used to describe the basic features of the data in a study. They provide simple summaries about the sample and the measures. Together with simple graphics analysis, they form the basis of virtually every quantitative analysis of data. Descriptive statistics were brief descriptive coefficients that summarized a given data set, which can be either a representation of the entire population or a sample of a population.

3.0 RESULTS AND DISCUSSION

The data gathered with respect to the samples selected from users and non-users of fibre optic technology was analysed here with descriptive statistics. The sample represented attitudes of 107 respondents towards the fibre optic technology. Out of 107 respondents, current fibre optic technology users and non-users according to the collected data could be classified as follows. Table 3.1 shows the percentage values of the users and non-users of fibre optic technology.

Table 3.1. Percentages of respondents who are users and non-users of fibre technology

	Users	Non-Users	Total
No of respondents	14	93	107
No of respondents%	13.1%	86.9%	100%

Among the respondents most have not used fibre optic technology facilities to get internet connection. According to the results obtained from selected areas of the country, 93 respondents have used 4G and ADSL technology to have internet connection around the country whereas only 14 respondents have used fibre optic technology to obtain internet connection.

3.1. Analysis of demographic factors of the respondents

Table 3.2. Profile of the respondents

	Users		**Non-users**	
	n	**%**	**n**	**%**
TOTAL	14	13.1%	93	86.9%
GENDER				
Male	7	50%	65	69.9%
Female	7	50%	28	30.1%
AGE GROUP				
<30	7	50%	55	59.1%
31-40	5	35.7%	20	21.5%
41-50	2	14.3%	13	14%
51-60	-	-	5	5.4%
>60	-	-	-	-
PROFESSION				
Government	4	28.6%	20	21.5%
Non - Government	5	35.7%	45	48.4%
Self - employee	5	35.7%	28	30.1%
EDUCATION LEVEL				
O/L	-	-	1	1.1%
A/L	3	21.4%	6	6.5%
Technical/Vocational	1	7.1%	13	14%
Degree or above	10	71.4%	73	78.5%
MONTHLY INCOME (Rs.)				
<10000	5	35.7%	35	37.6%
10000-50000	3	21.4%	41	44.1%
50000-100000	4	28.6%	13	14%
100000-300000	1	7.1%	4	4.3%
300000-500000	1	7.1%	-	-
MARITAL STATUS				
Single	5	35.7%	55	59.1%
Married	9	64.3%	38	40.9%

3.2. Frequency of currently used technology

The frequency of currently used technology as percentage was shown Figure 3.1. Out of 107 respondents, most of them (79%) use 4G technology for getting internet facilities. 13% of the respondents have used fibre connection as current technology. Another 8% of the sample used

ADSL for internet connection. Figure 3.1 shows the frequency of the respondents who have used 4G, ADSL and fibre technology.

Main objective of this study was to estimate the usage of fibre optic technology among the data collected from the respondents. According to these obtained results, fibre optic technology usage was lower than the 4G technology among respondents. Sometimes, there was not enough facilities to develop fibre optic technology around the country due to the high cost.

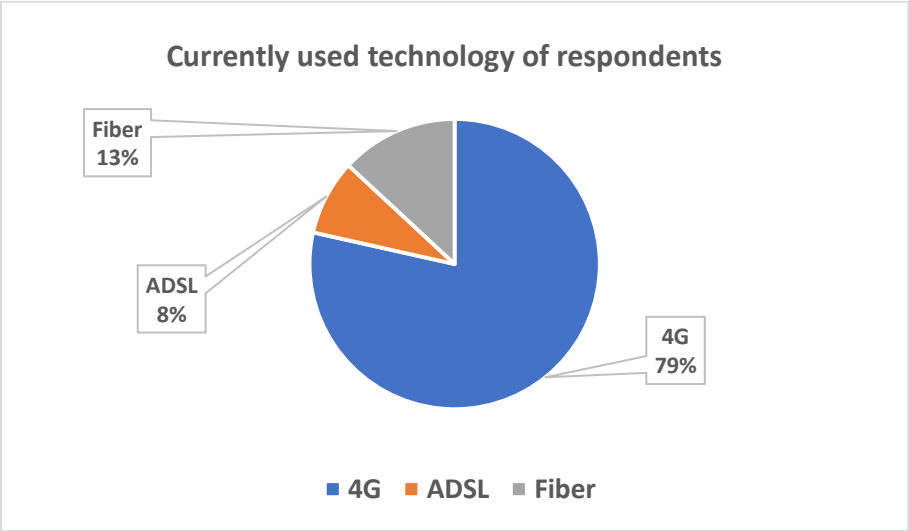

Figure 3.1: Currently used technologies of respondents to access internet

3.3. Comparison of speed of internet between fibre users and non-users

When comparing the graph of internet speed between the users and non-users of fibre optic technology, most of the respondents have the internet speed from 1-10 Mb/ps among the non-users of fibre optic technology. In the same time among the users of fibre optic technology, most of the respondents have the internet speed between 30-100 Mb/ps. It was depicted that the fibre optic technology can be used to increase the internet speed. Therefore, it has also influenced to avoid the traffic of the usage of internet among the internet users. As a result of that, most of the consumers prefer to adopt the fibre optic technology.

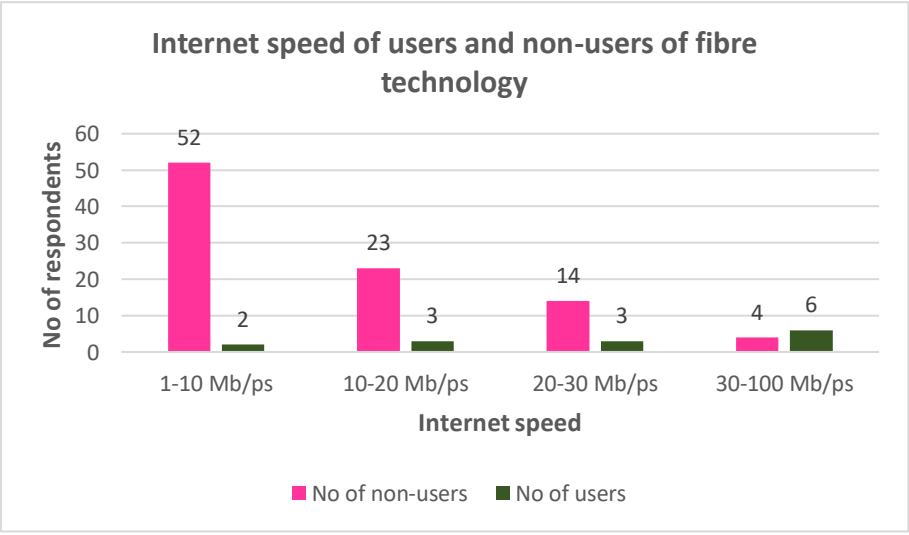

Figure 3.2: Level of the internet speed of the non-users and users of fibre technology

3.4. Comparison of satisfaction related to the currently used technology between fibre users and non-users

The satisfaction of fibre users was good according to the results obtained from the survey. But the satisfaction of the non-users of fibre optic technology was poor due to the improper internet facilities. It depicts that most of the people prefer to adopt the fibre optic technology to have a better connection.

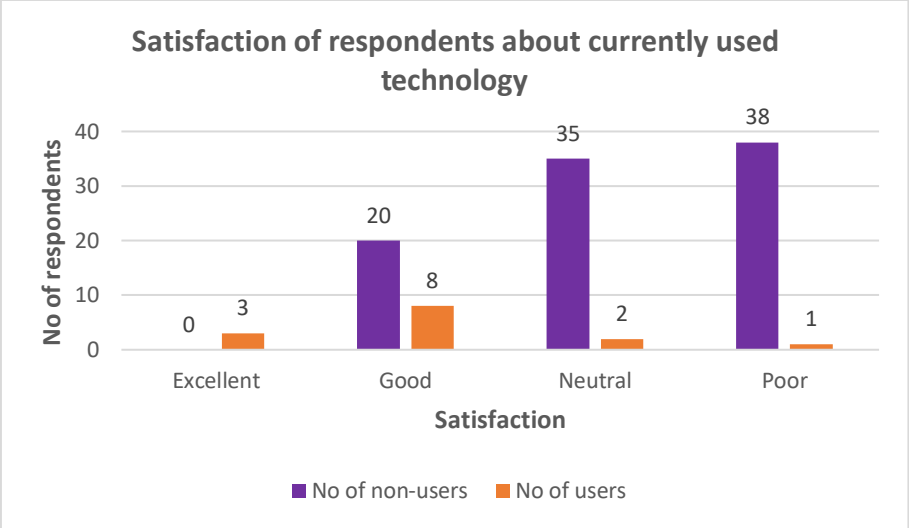

Figure 3.3: Satisfaction level of the non-users and users of fibre technology

3.5. Comparison of preference to enhance the technology with fibre between users and non-users

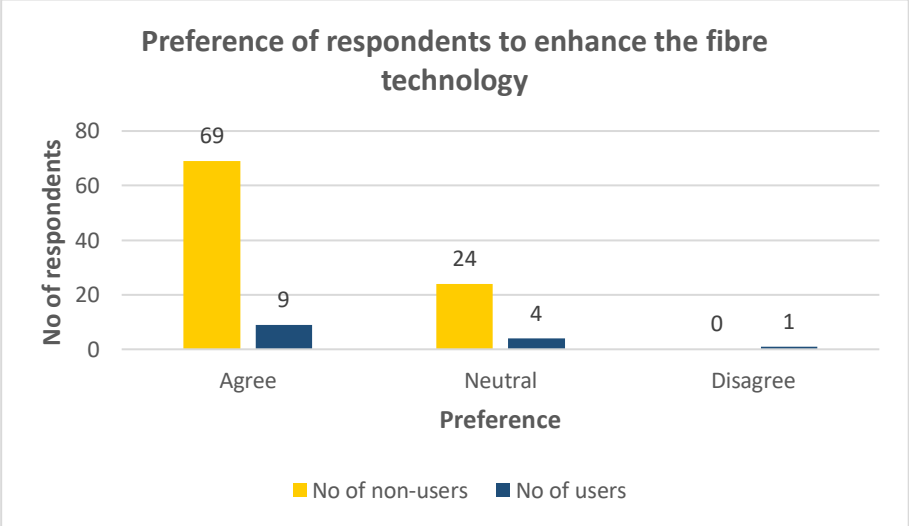

Figure 3.4. Level of the preference to enhance the fibre technology among the non-users and the users

According to the results obtained from the preference to enhance the technology with fibre, Most of the users and non-users prefer to enhance the technology with fibre optic technology. A total of 69 respondents among the non-users prefer to enhance the technology with fibre as well as 9 respondents among the users prefer to enhance the technology with fibre.

4.0 CONCLUSION

Some facts for the evaluation of the development of fibre optic technology in some parts of the Sri Lanka was concluded in this study. In addition, the usage of fibre optic technology in present society in Sri Lanka and also the willingness of the people to adopt for the fibre optic technology were estimated in this study. Data collection was carried out by distributing the google form among the people. It was found that the internet speed of the non-users was in the range of about 1-10 Mb/ps whereas the internet speed of the users of fibre technology was between 30 and 100 Mb/ps. It can be concluded that most of the users and non-users prefer to enhance the technology with fibre to have a better connection.

ACKNOWLEDGEMENTS

The authors wish to express their gratitude to all academic and non-academic staff members of Department of Electronics, Faculty of Applied Sciences, Wayamba University of Sri Lanka.

REFERENCES

[1]. Caka, N. & Hulaj, A., The analysis of different FTTH architectures and possibilities of their implementation in Kosovo, *11th WSEAS International Conference on Applied Informations and Communications*, 23 – 25.
[2]. Blog-Four-Advantages-of-Fibre-Optic-Communications, https://www.antaira.com/ (Accessed 2021-05-03)
[3]. Optical-fibre-technology-how-it-works, https://www.nai-group.com/
(Accessed 2021-05-02)
[4]. Daniel, C. and Rodney, S, Optical Fibre in Telecommunications, Sixth Edition, 324 – 367
[5]. Definition/fibre-optics-optical-fibre, https://www.searchnetworking.techtarget.com/ (Accessed 2021-05-02)
[6]. Definitions/fibre-optics, https://www.verizon.com/info/ (Accessed 2021-05-02)
[7]. Lafir Naveeth, Dewmini, Capacity Expansion of Fibre Optic Network in Sri Lanka, *International Symposium South Eastern University of Sri Lanka*, (2019)
[8]. Vaiano, P., Carotenuto, B., Pisco, M., Ricciardi, A., Quero, G., Consales, M., Crescitelli, A., Esposito, E. and Cusano, A., Lab on Fibre Technology for biological sensing applications, *Laser & Photonics Reviews*, 10(6), (2016). 922-961.
[9]. Oh, K. and Paek, U.C., Silica optical fibre technology for devices and components. *Design, fabrication, and international standards*, (2012), 240.
[10]. Bennett, P.J., Monro, T.M. and Richardson, D.J., Toward practical holey fibre technology: fabrication, splicing, modeling, and characterization, *Optics letters*, 24(17), (1999), 1203-1205.
[11]. Nishii, J., Morimoto, S., Inagawa, I., Iizuka, R., Yamashita, T. and Yamagishi, T., Recent advances and trends in chalcogenide glass fibre technology: a review, *non-crystalline solids*, 140, (1992), 199-208.
[12]. Debord, B., Amrani, F., Vincetti, L., Gérôme, F. and Benabid, F., Hollow-core fibre technology: The rising of "gas photonics", *Fibres*, 7(2), (2019), 16.
[13]. Cusano, A., Consales, M., Crescitelli, A., Ricciardi, A., Lab-on-fibre technology. *Springer International Publishing*, (2015), 532.
[14]. Kim, W.H., Nguyen, V.Q., Shaw, L.B., Busse, L.E., Florea, C., Gibson, D.J., Gattass, R.R., Bayya, S.S., Kung, F.H., Chin, G.D. and Miklos, R.E., Recent progress in chalcogenide fibre technology at NRL. *Non-Crystalline Solids*, 431, (2016), 8-15.

Proc. Annual Symposium on Research & Industrial Training, 08(2021) 141-145
Department of Electronics – Wayamba University of Sri Lanka

AUTOMATION OF THE TEA WITHERING PROCESS

T.A.R.N. Thenuwara[1*], W.A.S. Wijesinghe[1], P.D.S. Pushpakumara[2]

[1]*Department of Electronics, Wayamba University of Sri Lanka, Kuliyapitiya, Sri Lanka*
[2]*Communication Division of Arthur C Clarke Institute for Modern Technologies, Katubedda, Moratuwa, Sri Lanka*

[*]rnisansalathenuwara@gmail.com

ABSTRACT

Withering is the first process in tea manufacture. The main purpose of withering tea is to reduce the moisture content of the leaf and soften it. The tea leaves are withered manually in the tea factories. Also, properly withered or not it can be determined through organoleptic properties such as hand scenes. As a result, the tea leaves are more damaged and the quality of the tea can be reduced. Automating the tea withering process could minimize these damages and improve the quality of the product. This paper describes a development of a prototype for the automation of the tea withering process. It mainly consists of sensors to measure moisture and temperature, and controlling of a fan.

Keywords: Tea withering, Automation

1.0 INTRODUCTION

The tea plant, species of evergreen (*Camellia sinensis*), is valued for its young leaves and leaf buds, from which the tea beverage is produced. [1] Tea is a non-alcoholic aromatic beverage and it is generally accepted that, next to the water, it is the most frequently consumed beverage in the world [2]. In order to get a quality product the time taken for each process of tea, production must be carefully judged. This is because the exact time depends on the moisture content of the harvested leaf, the temperature and humidity present during the production period and various other factors.

The main processes of tea production are plucking, withering, rolling, fermenting, drying, and sorting [3]. Withering is the first process in tea manufacture. The main purpose of withering tea is to reduce the moisture content of the leaf and soften it. As a result, it is flexible and can withstand the subsequent process of rolling, without breaking into flakes. The withering process increases the hydrolytic activity due to water loss, which increases hydrolysis and tea extract activity. Withering brings about biochemical changes in tea leaves. The improved aroma, flavor and other benefits of tea can be obtained from the process of withering tea [4].
In the past, tea leaves were withered in "Chung House" and that what we called "Natural Withering". In this type of withering, leaves were spread over the hessian cloth in the "Chung house" overnight to wither the leaves [4]. Normally, Tea leaves are withered in an artificial method. Tea leaves are packed in trucks which used for withering tea leaves. On average, about 04 Kg – 05 Kg of tea leaves is planted per square foot. The tea leaf trucks vary according to the rpm value of the motor in it. The withering process usually takes about 06 hours and it is important to maintain an average temperature of 60 ^{0}C – 50 ^{0}C and moisture of 48% – 50% for tea leaves to wither. It is very important to roll the tea leaves while the tea process is ongoing. This is done every 20 minutes or so. Properly withered tea leaves do not crumble when rolling. It just happens to be crushed into a pattern. Properly withered tea leaves retain their aroma, taste and quality. Usually tea leaves are withering at night. Because the tea leaves must be withered without too much heat.

Currently, tea withering in tea factories in Sri Lanka is done manually. This withering process was made to do this process automatically. In the process of withering, the tea leaves are spread on the truck's net. There are a fan and two kinds of louvers are controlled according to the temperature and humidity of the room. The fan is powered on while the tea leaves are being withered and when tea leaves are withered properly the fan is powered off. However the tea leaves are properly withered or not can be determined through organoleptic properties such as hand sens. This method will not only increase the damages of the tea leaves but also decrease the quality of the tea leaves. Automation of the tea withering process was developed to solve the above problems. Furthermore, in next the section, the method and materials, results and discussion and conclusion will be explained sequentially in detail.

2.0 MATERIALS AND METHODS

Data of moisture and temperature content of the tea leaves for properly withered tea were got to mobile phone via GSM SIM800L module. DHT11 sensor was used to get the temperature and humidity of the room temperature and moisture and temperature content of the tea leaves. LCD 16*2 display was used to displayed moisture, temperature and humidity values. DC motor was used as the fan and servo motor was used as the louvers. PIC 16F877A microcontroller was used as the on board in the implementing stage of the project. CP2102 UART module was used to send data to the computer and the real-time data was plotted.

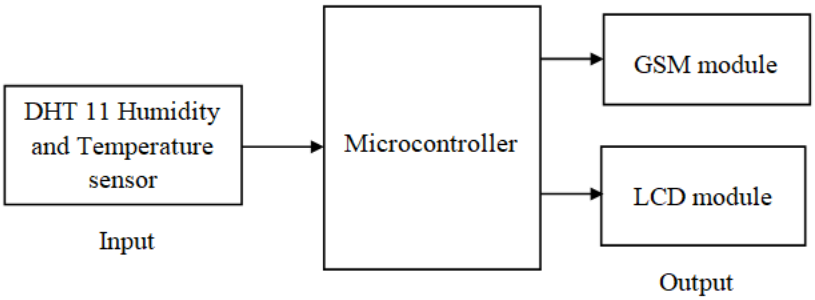

Figure 2.1: Block diagram for the analysis section

A microcontroller was used to receive data from the surface DHT11 sensor and send data to the Phone. This data was stored to develop the system. DHT11 sensor was used to measure the temperature and the moisture content of the tea leaves. These temperature and moisture data are sent to a phone via the GSM module. That data was received by phone as an SMS. This device was used to display sensor data as an SMS.

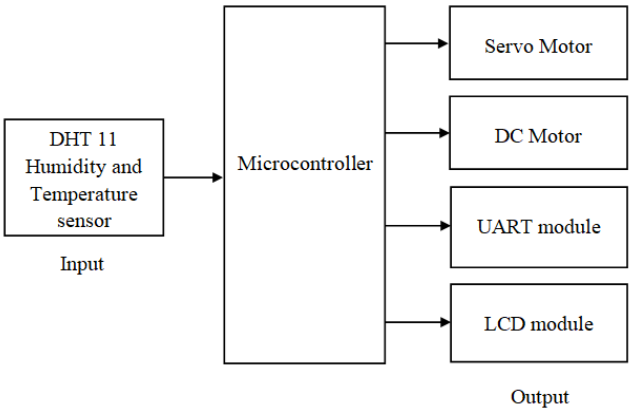

Figure 2.2: Block diagram for the Tea withering system section

The Fan was controlled depending on the moistures and temperature content of the tea leaves also the louvers were controlled according to the room temperature and humidity. The DHT 11 sensor sends data in to the laptop through the UART module and these real-time data were plotted to display the data.

3.0 RESULTS AND DISCUSSION

The automation of the tea withering process prototype system was designed to retain the flavor and quality of the tea, and obtain the requirement that the temperature and relative humidity at which the tea leaves withered properly. So the first system was created and it was expected to get data on to the phone for a month. Although the data were expected to be used to analyze the best temperature and humidity for tea leaves to wither, the system was unable to install in the factory because of the country's corona pandemic situation.

But the approximate temperature and humidity at which the tea leaves wither were discovered by the tea factory and the second section were designed accordingly. Here the louvers were controlled according to the room temperature and humidity, and the fan was controlled according to the humidity and temperature of the tea leaves. The PCB fabrication was not done at this time. Also there is needed to calibrate the temperature and humidity value to find the real values of humidity and temperature. But the Hygrometer was not found because of the corona pandemic situation. But the temperature values were calibrated using a thermometer.

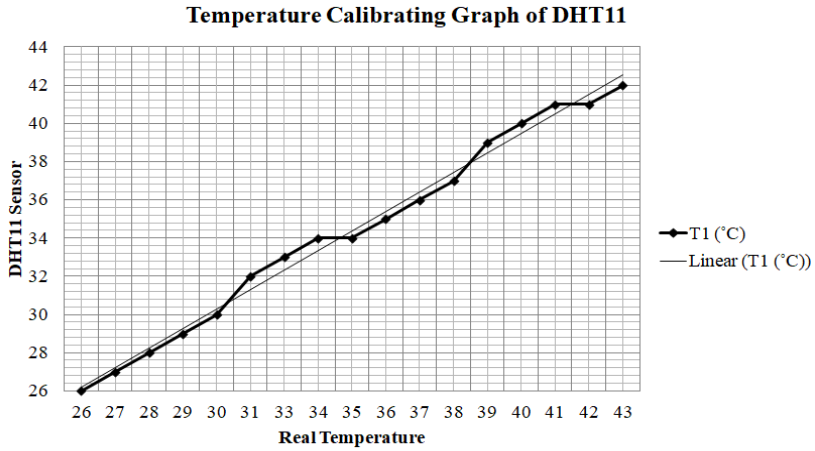

Figure 3.1: Graphs for the calibrate the temperature value of the DHT Sensor

$$Y = mX + C \quad (1)$$

Where; Y, X, m and C are autonomous variable, dependency variable, gradient and course respectively. Consider the Equation 1 for the Figure 3.2;

$$Y_1 = m_1X_1 + C_1 \quad (2)$$

gradient of the graph,

$m_1 = 0.94$ and $C_1 = 1.81$

Consider the Equation 1 for the DHT11 sensor

$$Y_2 = m_2X_2 + C_2 \quad (3)$$

$$Y_2 = m_2m_1X_1 + m_2C_1 + C_2$$

$m_2 = 1.06$ and $C_2 = -1.92$

Hence DHT11 sensor equation is,

$$Y_2 = 1.06X_2 - 1.92 \quad (4)$$

Using Equation 4 it is possible to obtain real values for the temperature of the sensor.
The system also showed a graph of the temperature and humidity of the tea leaves with the time. Although hoped to use the Bluetooth module for data transmission between pc and microcontroller, however the UART module was used due to the problem of obtaining components and testing.

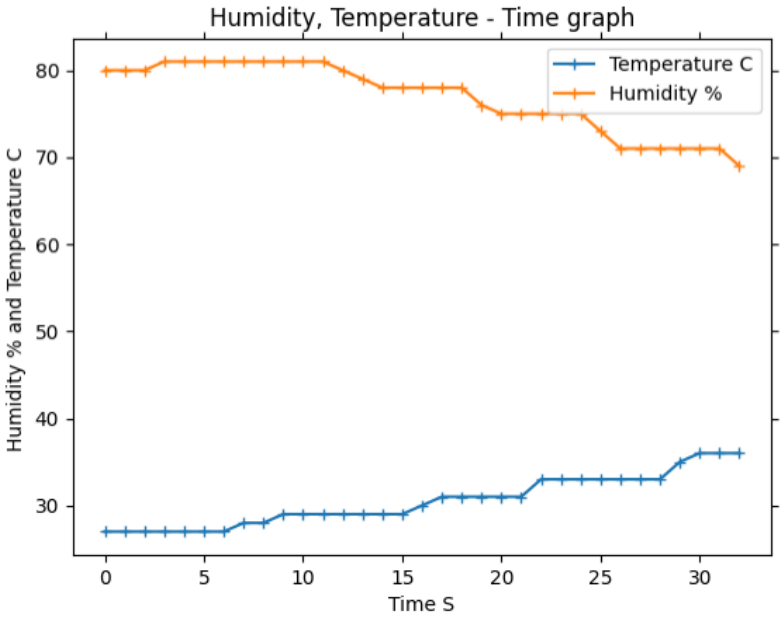

Figure 3.2: The graphs of the humidity and temperature

Also 12v, 240v motors can be suggested for this system as a recommendation and therefore it can be used not only as a prototype system but also in the tea factories.
There are many advantages to using automation of the tea withering process system and that solves all the problems. The improved aroma, flavor and other benefits of tea depend on the moisture content of the harvested leaf, the temperature and the humidity present. The percentage of damaged tea leaves of the manual process is high. But automating the tea withering process would minimize this damage due to over fire.

4.0 CONCLUSION

This paper described a development of a prototype system for the tea withering process. The prototype system demonstrates the measurement of moisture and temperature of tea leaves and control of louvers and fan while displaying relevent information on the LCD panel. This prototype system could be extended to automate the real tea withering process to minimize the damage and enhance the quality of the tea product.

ACKNOWLEDGEMENT

Authors would like to thank all the staff of Department of Electronics, Faculty of Applied science, Wayamba University of Sri Lanka. Since gratitude is also extended to the staff members at the communication division in Arthur C Clarke Institute for Modern Technologies.

REFERENCES

[1]. Harler, C.R, Adviser on tea to the Central Treaty Organization, *The Culture and Marketing of Tea*, (2013), https://www.britannica.com/plant/Camellia (Accessed 2021.03.21)
[2]. Deb, C., Pou, K.R.J., A Review of Withering in the Processing of Black Tea, *Bio System Engineering*, 41(4), (2016), 365 – 37
[3]. Amar, AlmarTeas, *Ceylon the Tea History*,(2010), http://www.almarteas.com/ tea_history.html (Accessed 2021.03.31)
[4]. Sri Lanka Tea Board, (2014), http://www.srilankateaboard.lk/index.php/features/fine-ceylon-tea (Accessed 2021.04.01)

Proc. Annual Symposium on Research & Industrial Training, 08(2021) 146-151
Department of Electronics – Wayamba University of Sri Lanka

DESIGN OF A 12V PORTABLE MINI UPS FOR WIFI ROUTER

G.S.A.Fernando*, U.A.D.N. Anuradha

Department of Electronics, Wayamba University of Sri Lanka, Kuliyapitiya, Sri Lanka.

*thushariakalanka@gmail.com

ABSTRACT

In recent years, the use of routers has increased rapidly, and in many cases, routers cannot operate properly due to power outages. The service providers are committed to maintaining the connectivity of the routers, repair and restore any faults as soon as possible. The main problem during maintenance was that if there was no proper way to power the router during maintenance, the technician could not reset the router, it wasting the effort and time of the technicians. In addition, during maintenance, when need to check the quality of the copper wire worn on the road, the ADSL (Asymmetric Digital Subscriber Line) value is checked from the phone via the router's wifi. It also demonstrated the importance of having a safe and proper way to power the router during maintenance. Therefore, these routers require an uninterruptible power supply. However, the main problem is the limited capacity of the battery. The usage time provided by the battery is often far from ideal. Many technicians face the problem of not being able to power all portable routers without getting in the way of powering the router at the critical moments needed. However, a typical backup power supply can solve this problem. UPS typically performs two functions: It charges the built-in battery and powers external electronic devices. Considering all the methods needed to design a UPS, this buck-boost converter-based model was designed as a solution to the above problem.
The UPS consisted of a variety of features that met almost all the specifications needed to activate the router by connecting batteries in series or in parallel within the UPS, depending on the requirements.

Keywords: Lithium Battery, Buck Converter, Boost Converter.

1.0 INTRODUCTION

1.1 Battery Technologies - Overview

A “battery” is the generic term for an electrochemical source of electricity, which stores energy in a chemically bound form until converting it directly into electric power. A battery may either be a single cell or multiple cells connected in a series or parallel configurations [01].
Batteries are categorized as being either primary or secondary systems. For instance, primary batteries are commonly known as disposable batteries and are not engineered for recharging (For example, primary batteries are commonly known as disposable batteries and are not designed for charging. There is a risk of explosion if anyone tries to charge it.) Conversely, secondary batteries are designed to be safely recharged. This is because the anode-cathode discharge reaction is reversible. A properly designed secondary battery can be recharged hundreds or thousands of times [01].
Conversely, secondary batteries are engineered so they can be safely recharged. This is owed to the fact that the anode and cathode discharge reactions are reversible. Properly designed, a secondary battery can be recharged hundreds or thousands of times [01].

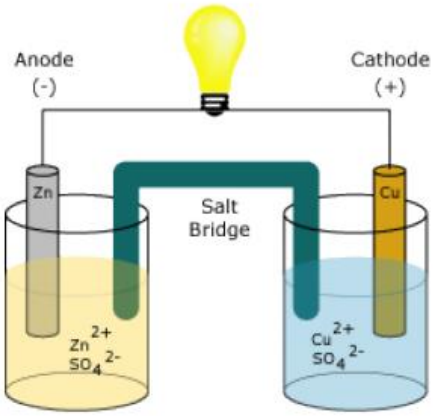

Figure 1.1: Daniel cell

1.2 Mini UPS (Mini Uninterruptible Power Supply)

A mini UPS is a small-sized UPS system that provides an uninterrupted power supply to electronic devices in case of a power failure or voltage drop/surge to an unacceptable level. It avoids any interruptions in the functioning of connected electronic devices as it maintains its power supply. Unlike a generator, a UPS immediately supplies power to the devices without any lag. A mini UPS consists of a battery that stores DC power and supplies AC power to the devices in the event of a power outage or surge.

1.3 Problem Statement and Research Objective

One of the problems encountered was cutting the copper wires to check the quality of the wire worn on the road, attaching a router, and checking the ADSL values from the phone via the wifi of the router. However, it is impossible to do this even if the router is connected due to there is no way to get the power to the router.

Moreover, if a technician goes to repair the router in the customer's home, it will not be possible to repair it properly if the home does not have electricity. This wastes time as well as organization costs and is unable to provide efficient customer service. Considering the above, the main objective of this project is to create a portable mini USB that can provide the power required to operate a 12 v router. It can be used to power a router on the road, in a customer's home, or anywhere without electricity, and allows repairs to be made without any interruption.

2.0 EXPERIMENTAL

2.1 Equipment and Apparatus

18650 Lithium Battery

A 18650 Battery is a lithium-ion rechargeable battery. The first 4 digits of the designation “18650” indicate the physical dimensions while the 5th digit indicates it is a cylinder cell. The standard 18650 battery is 18mm around 65mm long. This type of battery is very common in applications such as laptop battery packs, flashlights, electric vehicles, cordless tools, and various other devices that require portable power.

Some types of 18650 have been modified adding either a button top and/or internal protection circuit. This can increase the physical length of a “18650” battery from 65mm to 70mm or in certain cases even longer [02].

2S BMS Board

BMS (Battery Management System) – a battery management system is designed to monitor the status of batteries, control the process of charging/discharging the battery, etc.

This module is perfect for making a 2S battery pack using a 18650 Li-ion Battery. HX-2S-JH10 is a 2 Series (2S) Lithium-Ion Battery Management System (BMS) Module with an 8 Ampere continuous Li-ion protection board [03].

XL 4015 Module

The XL4015 power module is a DC to DC step-down (BUCK) power module that operates at a switching frequency of 180 kHz. In such high frequency, it provides smaller-sized filter components compared with low frequency switching regulators [04].

This DC-DC switching buck converter is capable of driving a 5A load with excellent line and load regulation. The main switching component is XL4015, an adjustable output version switching regulator. It is an efficient switching regulator and the output efficiency is significantly higher in comparison with the popular boost regulators. At higher input voltages, the regulator operates at a switching frequency of 180 kHz, thus allowing the overall board size to be smaller and space-saving. It is a high-power switching module with a toroidal ring inductor [04].

XL 6019 Module

XL6019 module is a DC-DC boost switching power supply module, uses the conventional topology fully integrated constant pressure boost output, and the output voltage can change within 5 to 40 V. Its conversion efficiency is up to 90%. This module is based on the XL-Semi XL6019IC. The XL6019 regulator is a wide input range, current mode, DC/DC converter which is capable of generating either positive or negative output voltages. It can be configured as either a boost, flyback, SEPIC, or inverting converter. The XL6019 built-in N-channel power MOSFET and fixed-frequency oscillator, current-mode architecture results in stable operation over a wide range of supply and output voltages [05].

1N5822 Diode

1n5822 is a Schottky diode, also known as a hot-carrier diode, mainly used in fast-clamp diode switching applications. It is made up of semiconductor material and carries low forward drop voltage [06].

Fuse

Fuses are safety devices that are used to protect the home appliances like televisions, refrigerators, computers from damage by high voltage. The fuse is made up of a thin strip or strand of metal, whenever a heavy amount of current or an excessive current flow is there in an electrical circuit, the fuse melts and it opens the circuit and disconnects it from the power supply. Also, it works as a circuit breaker or stabilizer which protects the device from damage. In the market, many types, features, and designs of fuses are available nowadays. Their strips are made up of aluminium, copper, zinc & it is always connected in series with the circuit to protect from overcurrent in the running cables [07].

2.2 Procedure

18650 two batteries were connected in parallel and then two pairs of such batteries were connected in series to form a battery pack. This package allows the UPS to power the router for longer periods. A lithium-ion battery holder was used to make the battery pack. Therefore, it is easy to replace that battery from the pack when there was a problem occur in one of battery. The positive

terminal and negative terminal of the battery pack were connected to the B+ and B- of the 2S BMS board respectively. The middle point of the battery pack was connected with the BM of the BMS board. 2S BMS board is designed to monitor the status of batteries, control the process of charging and discharging the battery. This allows charging the UPS without damaging the battery.

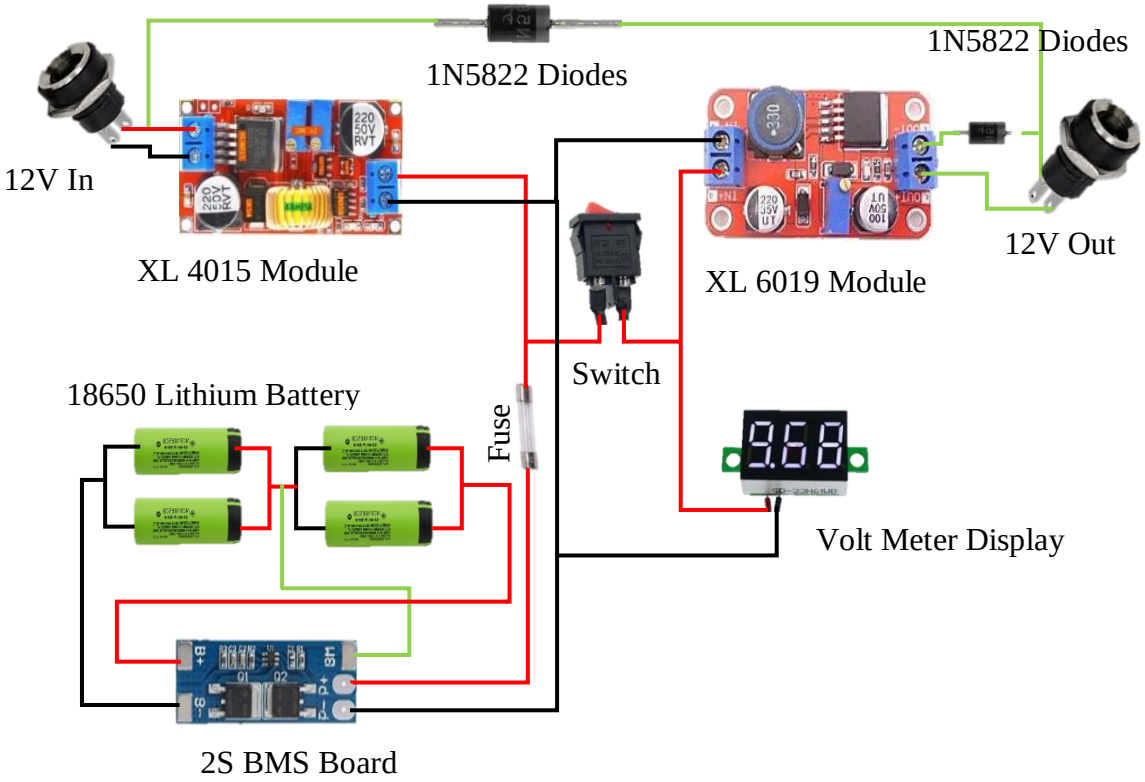

Figure 2.1: Block diagram of the 12V Portable Mini UPS for Wi-Fi Router.

XL 4015 DC to DC step down buck converter was used to charge the battery pack and the initial current and voltage values were given. The voltage of the XL 40I5 module was set to 7.6V. This is because the voltage across the 18650 battery pair is also 7.6V. Since the current in the ADSL router is 2A, the current of the XL 40I5 module was set to 2A. The fuse was connected to the P+ of the 2S BMS board and the positive terminal of the XL 4015 buck converter. It was worked as a safety device that was used to protect the device from damage by high voltage and made of a thin strip of a metal strip. When there is an overcurrent in the electrical circuit, the metal strip was melted, opened the circuit, and disconnecting the power supply. This protects some devices from overcurrent.

Voltmeter display input terminals were connected to the input terminals of the boost converter and P - terminal of the 2S BMS board. The output voltage of the boost converter was adjusted to 12V, the voltage of the router was 12V. Therefore, the output voltage given by the USP was 12 V. The XL 6019 converter is boosted the low voltages. The negative terminals of two diodes (D1 and D2) were connected and it was attached to the positive terminal of the 12V DC Jack. The positive terminals of the D1 and D2 diodes were connected to the input positive terminal of the buck converter and output positive terminal of the boost converter respectively.

The negative terminal of the DC Jack was connected with the output negative terminal of the boost converter. Two heat sinks were connected to refrain the heating of the buck converter and boost converter. These two devices were provided safety for the system. When a current flows through the system, and sometimes the microcontroller in it heats up and the code inserted in it can be destroyed. By using a heat sink, could be prevented from overheating the microcontroller.

Figure 2.2: inside the 12V Portable Mini UPS for Wi-Fi Router

3.0 RESULTS AND DISCUSSION

The most impressive feature of this UPS was the ability to provide power backup for up to 4 hours. It was equipped with four 4300mAh Li-ion battery and it is provided a long battery backup. XL 4015 module is supplied battery overcharging protection in place for the safety of the device. The intelligent battery management system in the UPS automatically switched to charging mode when it is plugged in and it is switched to power backup mode automatically when the mainline power was cut off. The designed UPS is supported by 12V and 2A powered wifi routers. The USP was extremely lightweight due to weighing in at 300 grams. It was portable easily because of the lightness. Since the UPS has consisted of a quality casing, is more secure. The whole USP system could be designed at a low price.

3.1 Features of designed mini USP

1. Light Weight ($\leq$ 300 grams)
2. Output: 12V / 2A
3. Back up time up to 4 Hours
4. Uses 4 x 4300mAh 18650 Battery
5. Battery Voltage Display

Figure 3.1: 12v Portable Mini Ups for Wifi Router.

4.0 CONCLUSION

The designed mini USP could be operated by a 12V and 2A WIFI router. It can provide uninterrupted power for up to 4 hours to a router. It has consisted of 4300 mAH lithium-ion rechargeable batteries and a battery charger to protect the device**.** As the name, it is a lightweight and portable mini-device that weighing a mere 300 grams.

ACKNOWLEDGEMENT

Authors would like to express their sincere gratitude to everyone who helped to carry out this project successfully.

REFERENCES

[1]. DNK POWER COMPANY LIMITED, Handbook On Lithium Battery Pack Design, 3
[2]. 18650 Batteries, 18650 Batteries - Rechargeable 3.7V Li-Ion Cells - 18650 Battery Store – 18650BatteryStore.com, (Accessed 2021-02-26)
[3]. LITHIUM ION 2S 15A 7.4V BMS CHARGE PROTECTION CIRCUIT, Lithium ion 2S 15A 7.4V BMS Charge Protection Circuit [RKI-4739] - ₹120.00 : Robokits India, Easy to use, Versatile Robotics & DIY kits, (Accessed 2021-02-26)
[4]. XL4015 DC-DC Step Down Module, https://components101.com/modules/xl4015-dc-dc-converter-module, (Accessed 2021-02-26)
[5]. XL6019 DC-DC Step Up Boost Module, https://www.dnatechindia.com/xl-6019-dc-dc-boost-step-up-module-buy-india.html, (Accessed 2021-02-26)
[6]. Mia, 1N5822 Schottky Diode: A Detailed Introduction, 2 Feb 2021, 1N5822 Schottky Diode: A Detailed Introduction (apogeeweb.net), (Accessed 2021-02-26)
[7]. Tamanna Sharma, What is Fuse: Types and Working, Jan 05, 2018, What is Fuse? Different Types of Fuses and Working (circuitdigest.com), (Accessed 2021-02-26)

Proc. Annual Symposium on Research & Industrial Training, 08(2021) 152-159
Department of Electronics – Wayamba University of Sri Lanka

DESIGN OF A SYSTEM FOR OUTDOOR M-SAN TO DETECT POWER FAILURES AND LOCATION

H.W.E. Madushani[1*], J.M.J.W. Jayasinghe[1], S.R. Palliyaguru[2], K.L.S.S. Chandrasiri[2]

[1]*Department of Electronics, Wayamba University of Sri Lanka, Kuliyapitiya, Sri Lanka*
[2]*Sri Lanka Telecom PLC, Matara, Sri Lanka*

[*]erangimadhushani@gmail.com

ABSTRACT

Power failures of MSAN (Multi Service Access Node) are occurred due to lightning or power outage. Sri Lanka Telecom (SLT) has an issue related to power failures of MSAN. In the current system, there is no clear update about power failures, whether the trip switch is OFF or power outage occurred in that area. Further, the location of the power failure cannot be identified. Hence, it is difficult for amateur technicians of SLT to locate the MSAN where the power failure has occurred. This paper presents a design of a system based on Arduino to avoid these issues. The circuit was designed on Proteus design software. The circuits convert 230V AC that coming from commercial power to 5V DC voltage. If there is a power failure, the designed system clearly detects whether the trip switch is OFF or power outage occurred in that area by comparing the signals that are coming from circuits. Further, the location of the power failure is identified via Global Positioning System (GPS) and the message is displayed on Liquid Crystal Display (LCD). Then, the message is sent to the phone via Global System for Mobile communications (GSM) with MSAN location code and MSAN location. Further, if there is a power outage in any area, it can be reported to the Ceylon Electricity Board immediately. In this context, the proposed system is very useful for SLT to manage their time and resources.

Keywords: Power failure, GSM, GPS

1.0 INTRODUCTION

A multiservice access node is a broader term that refers to a group of commonly used aggregation devices. These devices include digital subscriber line access multiplexers (DSLAMs) used in xDSL networks, optical line termination (OLT) for PON/FTTx networks, and Ethernet switches Active Ethernet connections. Modern MSANs often support all of these connections, as well as providing for additional circuits such as plain old telephone services (referred to as POTS) or Digital Signal. All the MSANs in Sri Lanka are connected with each other in a two ring through IP Multimedia System (IMS) for the safety precautions. In addition, there were two types of MSAN due to their placement used – indoor MSAN and outdoor MSAN [01].
They currently have an NMS (Network Management System) to monitor MSANs at the Colombo head office. Also they have a separate NMS to monitor the alarms in MSANs. When there is a power failure in the MSAN for whatever reasons, NMS update that as a power outage alarm with MSAN location code. Then having monitored alarms in the NMS, power team have to go to the relevant MSANs. But before they go there they don't know if it's tripped OFF or a power outage in that area. Therefore, if it has power outage in that area, they have go there to check whether the trip switch is OFF or not. They have to go to the location of the relevant MSAN to turn it on if the trip switch is OFF.

Because there is no update about it they have to go there even when there is no electricity. But if the technician of the power team gets updates of that, it is very useful for them to manage the time and their resources. Also if it has power outage in that area, they report about that to the electricity board. This update also makes it easier for them.
Another problem with the existing system is that it is difficult to find the location of the MSANs on the MSAN location code. It is not too difficult to experienced technicians but it is difficult to amateur technicians. Therefore, the proposed system gives the location of relevant MSANs.

1.1 Literature review
Several systems have been developed using different ways and ideas. In 2020 Janet Nanyangwe Sinkala, Jackson Phiri, implemented an Automatic Power Failure Sensing Based On Lte (4G) And Solar Charged Battery as Backup Supply using Google API and SIM7600E 4G/GPS module. This study proposed the use of Arduino microcontroller, SIM7600E 4G/GPS module, cloud application, Google API (application programming interfaces), solar panel, MPPT (maximum power point tracker) solar charge controller and battery to enable automation of the distribution network and thus reduce on the duration of the power failures [02].

In 2017, A Power Notification System was implemented for Network Operation Centers which is based on GSM. This system was implemented on an Android device capable of sending SMS text messages and force vibrating the phone of the ICT personnel on duty based on an incorporated shift timetable arrangement. The smartphone device is connected permanently to the power source through a wall socket and any power outage is detected [03].

2.0 EXPERIMENTAL

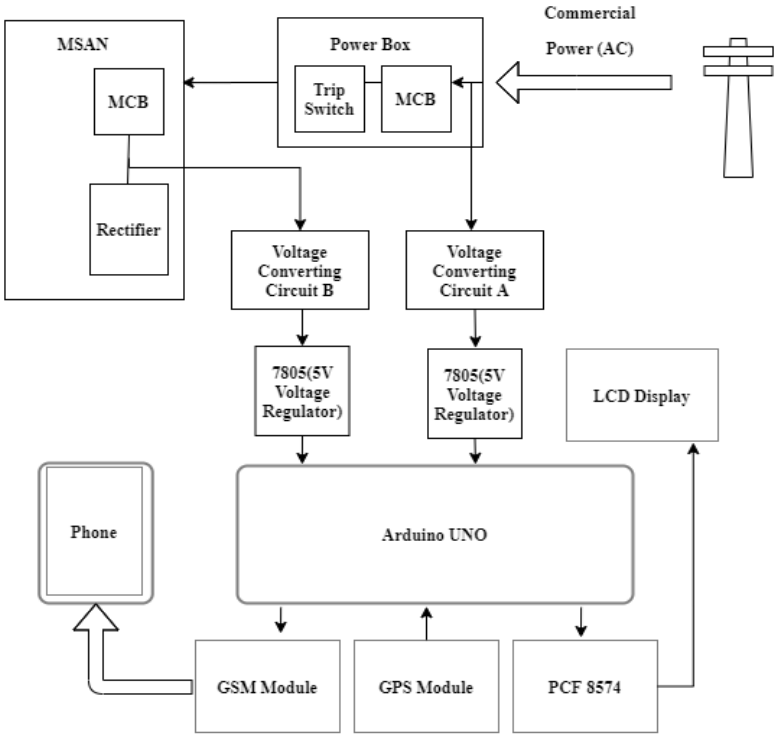

Figure 2.1: Block diagram of the design

As illustrated in the block diagram, the commercial power comes to the MSAN via the trip switch and MCBs (Miniature Circuit Breaker). There is a voltage of 230V on either side of the trip switch. Hence, voltage converting circuits were needed to sense the voltages on both sides.

The circuit A and circuit B were designed to convert the 230V AC to 5V DC voltage as shown in Figure 2.2. A step down transformer is a type of transformer that has the ability to transform high alternating voltage to a low alternating voltage [06]. Two step down transformers were connected to the both sides to convert 230V AC to 20V AC. Four 1N4007 diodes were connected to the circuits to convert the alternating voltage to a direct voltage. Then, two voltage regulators (7805 voltage regulator) were connected to the circuit. It provides a constant +5V output voltage for a variable input voltage supply [04]. Output pin of voltage regulators was connected to digital pins 2 and 3 of the Arduino board to receive the signals from the circuits A and B which sense the voltages.

The code uploaded to the Arduino board as hex file was written to detect power failures and pass those output to 12 and 13 pin of Arduino and display about power failure on the Liquid Crystal Display (LCD). Blue and yellow (light emitting diode**)** LEDs were connected to those pins. Blue LED for the signals coming from circuit A and Yellow for circuit B. The LEDs are used to make it easier for the user to identify the power failure. If there is a power outage in that area, the two LEDs light OFF. If the trip switch is OFF, only blue LED lights up. The LCD also shows about that the trip switch is OFF.

The LCD was connected to the Arduino board to display outputs. 16×2 LCD is named because it has 13 columns and 2 rows [10]. Generally, to be able to use an LCD display, need at least 6 free pins, but the number of pins can be minimized with the help of external components like PCF8574 12C expander, that's allows us to use only 2 pins from microcontroller [09].

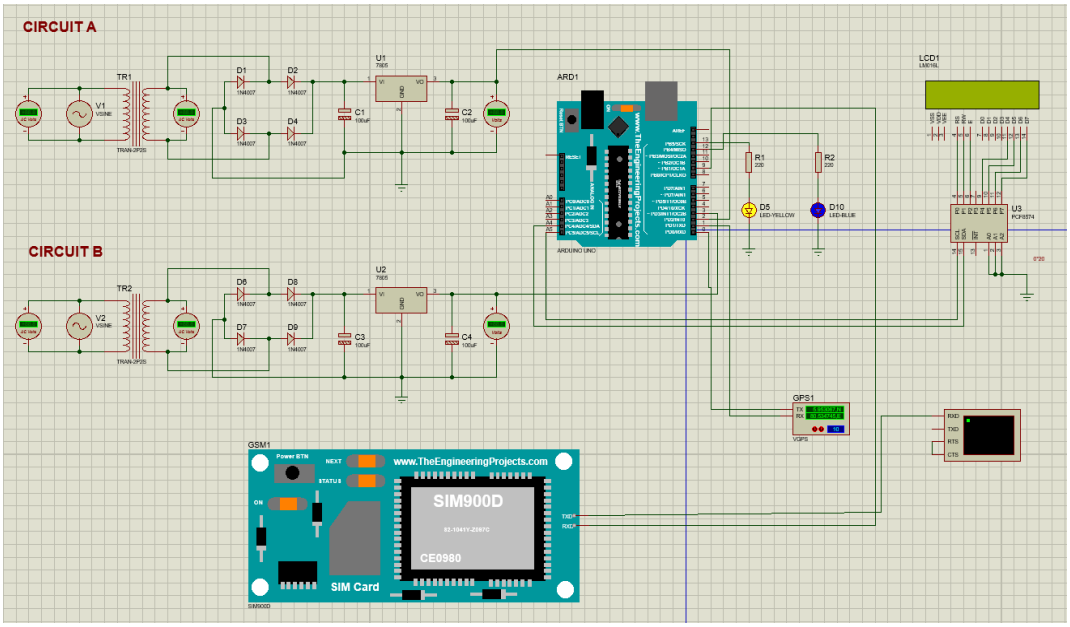

Figure 2.2: Circuit Diagram

The Global Positioning System (GPS) was connected to the Arduino board to identify the location of the relevant MSAN where the power failure occurred. GPS receiver calculates its position by precisely timing the signals sent by GPS satellites [08]. The location of the power failure can be found using the coordinates provided by the GPS.

The Global System for Mobile communications (GSM) was connected to the Arduino board to send the message about the power failure with MSAN location code (Name of MSAN used in SLT) and MSAN location. That message can be seen on virtual terminal in Proteus with the time that the power failure occurred. The SIM900A is a Dual-band GSM in a SMT (Surface-mount technology) module which is an industry-standard interface, the SIM900A delivers GSM/GPRS 900/1800 MHz performance capabilities for voice call, SMS, Data surfing [07].

Arduino is an open source microcontroller which can be easily programmed, erased and reprogrammed at any instant of time [05]. The Arduino integrated development environment (IDE) is open source software which is written in Java and supports to variety of platforms such as Windows, Mac and Linux [11].

3.0 RESULTS AND DISCUSSION

As illustrated by the block diagram, 230V AC power is received to circuit A and circuit B when connected to either side of the trip switch named the circuit A and circuit B respectively in this circuit. Circuit A and circuit B are connected before and after MSAN's trip switch respectively. It converts 230V AC to 5V DC voltage that coming from commercial power.

When there is a power failure in the MSAN, the system gets the signals of both sides. After comparing the signals by receiving Circuit A and Circuit B, the system is identified the power failure whether the trip switch is OFF or power outage occurred in that area. The message is displayed on the LCD screen and sent to the phone via GSM module with the MSAN location code and MSAN location.

In verifying the results of this designed system, a voltage of 230V was first applied to circuit A and circuit B that is there is power supply on both sides of the trip switch. The result is displayed on the LCD screen, as there is no power failure in the MSAN.

In the event of a power outage, since there is no power supply on either side of the trip switch, 0V is applied to circuits A and B to monitor the results. By the designed system sends information to the phone via the GSM module that MSAN has occurred a power outage, along with the time, name of MSAN, and location. The message can be viewed on the virtual terminal. It also displays on LCD. Result is shown in Figure 3.1.

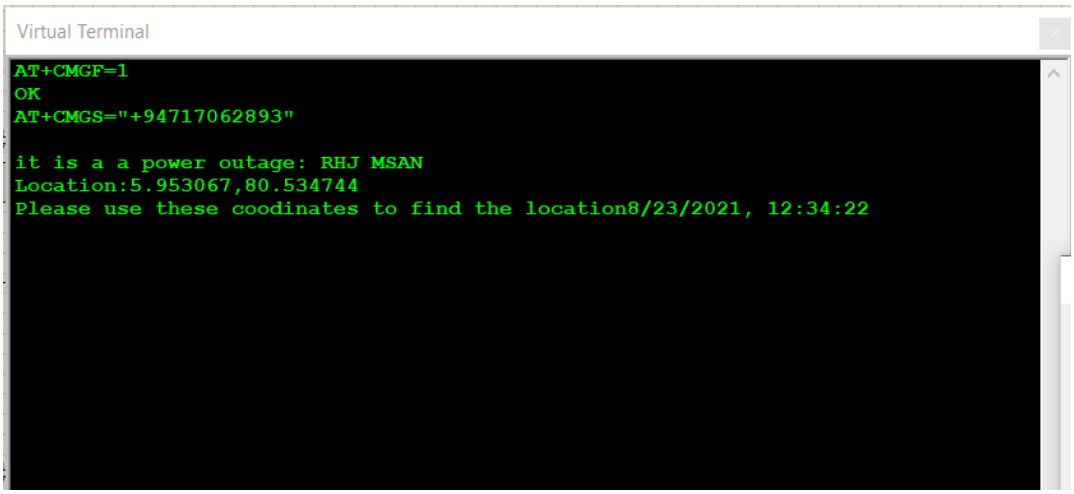

Figure 3.1: The screenshot of message sent by GSM when power outage in that area

When the trip switch is OFF, the circuit after the trip switch does not receive power, so the results are monitored by applying a voltage of 0V to circuit B and voltage of 230V to circuit A. The results are shown in Figure 3.2 and figure 3.3.

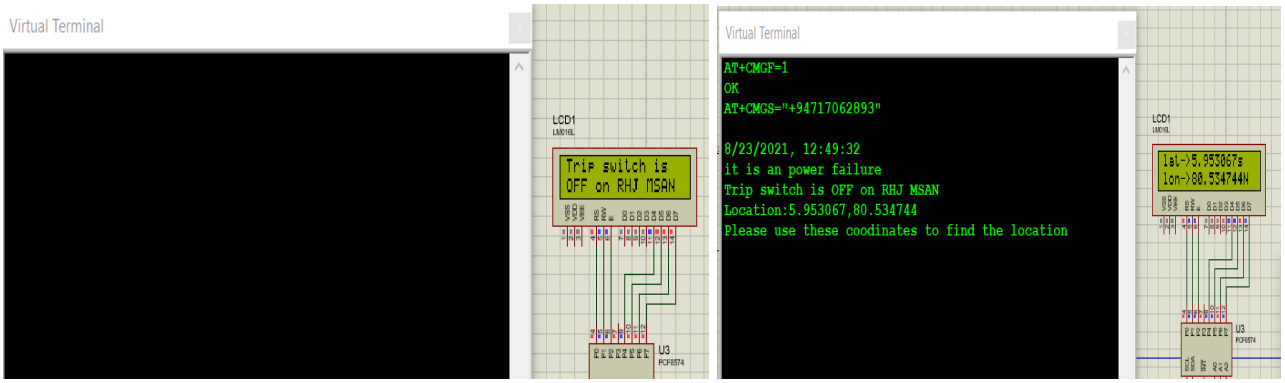

Figure 3.2: Message on LCD and Virtual Terminal that send by GSM

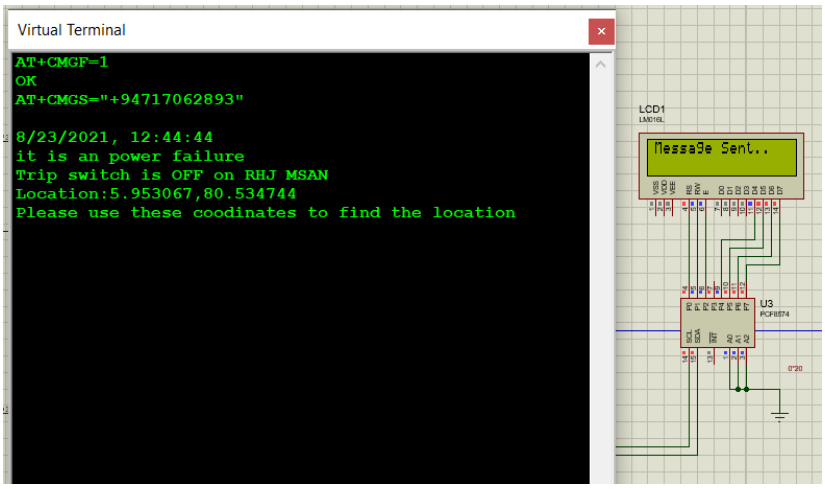

Figure 3.3: After sent the message from GSM

Using these location coordinates, power team can be found relevant MSANs. Details of MSAN (Location code: RHJ MSAN) at Rahula junction are illustrated here.

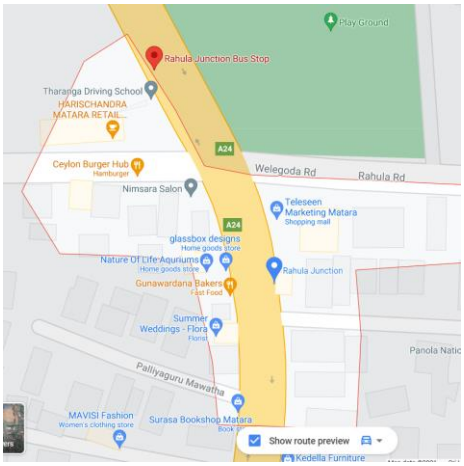

Figure 3.4: Screenshot of google map according to coordinates by GPS

In the proposed system, a voltage module was proposed to measure the voltage on both sides, but it was possible to measure those voltages by coding the Arduino during system implementation. Also a RTC module was proposed to give the time of power outage, but it is not essential because the time and date can be obtained by coding the GPS module using Arduino.

4.0 CONCLUSION

This research study was conducted to detect power failures and location of outdoor MSANs. When there is a power failure in the MSAN for whatever reasons, NMS update that there is a power outage alarm with MSAN location code. Then having monitored alarms in the NMS, power team has to go to the relevant MSANs. However, these is no proper mechanism to identify whether there is a tripped OFF or a power outage in that area.
The Proteus simulation was successfully completed but the development of hardware couldn't be completed with Covid 19 pandemic situation. By downloading the required libraries, the circuit was designed on Proteus design software. If there is a power failure, the designed system clearly detects whether the trip switch is OFF or power outage occurred in that area, identify the location that power failure occurred and the message is displayed on LCD. Then, the message is sent to the phone via GSM with MSAN location code (Name of MSAN used in SLT) and MSAN location. That message can be seen on virtual terminal in Proteus with the time that the power failure occurred. A simple circuit like this can detect a power failure of MSAN and get all the desired results.

ACKNOWLEDGEMENTS

Authors would like to express their sincere gratitude to the staff members at Sri Lanka Telecom who helped to carry out this project successfully.

REFERENCES

[1]. Sri Lanka Telecom Internal Source: Matara
[2]. Janet Nanyangwe Sinkala, Jackson Phiri, Automatic Power Failure Sensing Based On Lte (4g) And Solar Charged Battery As Backup Supply, *International Journal Of Advanced Studies*, 09, (2020), 1. (Accessed 2021-05-06)
[3]. Ayodeji Olalekan Salau, Adekunle Olugbenga Ejidokun, Implementation of agriculture automation system using web & GSM technology A GSM-Based SMS Power Notification System for Network Operation Centers, *International Journal of Scientific & Engineering Research*, 08 (2017), 830-831 (Accessed 2021-05-10)
[4]. 7805 Voltage Regulator IC, *Components101*, 2021, https://components101.com/ics/ 7805-voltage-regulator -ic-pinout-datasheet, (Accessed 2021.07.06)
[5]. Leo Louis, Working Principle of Arduino and using IT as a tool for study and research, *International Journal of Control, Automation, Communication and Systems*, 2 (2016), 21.
[6]. Stepdown transformer in proteus – How to simulate AC voltage, *Ettron*, 2021, https://ettron.com how-to-simulate-ac-voltage-step-down-transformer-with-proteus/, (Accessed 2021.08.16)
[7]. Rabindranath Bera, ,Prashant Chandra PradhanChuan-Ming Liu, Advances in Communication, Devices and Networking, Springer Nature, (2019), E-book
[8]. Haseeb Jamal, GPS Constellation and Characteristics of GPS Constellation, *about civil.com*, 2017, https://www.aboutcivil.org/gps-constellation-characteristics, (Accessed 2021.08.21)
[9]. How to connect PCF8574 I2C LCD with Arduino, *Electronic Hub*, 2019, https://www.electronicshub.org/pcf8574-i2c-lcd-with-arduino, (Accessed 2021.08.22)
[10]. 16x2 LCD Module, *Components101*, 2021, https://components101.com/ displays/ 16x2-lcd-pinout-datasheet, (Accessed 2021.08.22)
[11]. What is Arduino, 2021, https://www.arduino.cc/en/guide/introduction, (Accessed 2021.08.22)

Proc. Annual Symposium on Research & Industrial Training, 08(2021) 160-167
Department of Electronics – Wayamba University of Sri Lanka

DEVELOPING 3D MODEL FOR A FOLLOW-UP OF THE RADIATION EXPOSURE TO CARDIAC CATHETERIZATION LABORATORY STAFFS DURING INVESTIGATION

M.S.A. Mohamed[1*], Y.A.A. Kumarayapa[1], T.V.A. Ruwansiri [2]

[1]*Department of Electronics, Wayamba University of Sri Lanka, Kuliyapitiya, Sri Lanka*
[2]*Division of Bio-medical engineering services, Ministry of Health, Colombo 10, Sri Lanka*

*amsunfer922@gmail.com

ABSTRACT

The medical staff was exposed to scatter radiations during catheterized x-ray examinations and medical treatments since they were unaware of the density of the scatter radiation around the room. Ionizing radiation is potentially dangerous and can cause malignancy. This increases the prevalence of eye lens cataract and left side brain tumors in doctors. Using Lead aprons, collars and shielding are the safety precautions to protect staff in the Cath lab room. However, long-term use of heavy shields are causes for some injuries in staff members like back pain injuries. Therefore, it is critical to increase awareness about hazardous radiation areas in the room before entering. This research study focus to identify and demonstrate such hazardous locations using a 3D model. The proposed system is design to reduce the amount of scatter radiation that staff members are exposed during cardiac catheterization. Hypothetical dose level of this 3D hazard indication model was developed for the automation of the robot vehicle.

Keywords: Scatter radiation, 3D Automated Hazard indication model, Exposure dose limit

1.0 INTRODUCTION

In cardiac clinics, numerous x-ray methods are used daily for observing the insight of patients to save their lives. When the x-ray beam irradiates a patient, tissue interactions like Compton events occur and rays are scattered from the patient in all directions. Hence, the patient is a contributing factor for exposing scatter radiation to the working staff in X ray rooms. The daily staff exposure increases their risk of stochastic effects; the probability of cancer and heritable diseases and deterministic effects such as radiation induced tissue damages [1].

Interventional cardiologists and Cath lab staff facing high risk at their workplace due to daily exposure to ionizing radiation from the angiographic X-ray systems that are central to their procedures. Hence, they face threats of increased cancer risks and developing cataracts. Over the past decade, the concern has risen sharply as older interventionists began showing high rates of cataracts, left-side brain cancers and chronic orthopedic back problems. For this reason, the younger generations of new interventional cardiologists are actively looking for ways to reduce their radiation exposure and eliminate the need to wear lead aprons, or at least to reduce the weight [2]. This research study was done for finding hazed spots and illustrating on- site acceptable warning solutions using robot model. That is for protecting the staff from over-exposure due to their ignorance to invisible leakage radiation at the work place. Hence, the main aims of this research are to identify high-risk areas before entering the cardiac catheterization laboratory and prevent doctors and nurses from exposing those areas during surgery using a 3D automated display system.

1.1. Theoretical aspects and existing techniques

Figure 1.1: Example of a C-arm setup used in angiographic x-ray interventions [1]

Parameters used for research study

- Distance from bed to staff.
- Average height of staff employees.
- Places where staff members are located during the operation.
- Location of the cat-lab operator.
- Dose limits recommended by International Commission on Radiological Protection
- (ICRP) and National Council on Radiation Protection and Measurements (NCRP).

1.2. Scatter radiation

When x-rays interact with a material, such as inside the patient during x-ray procedures, scatter radiation is produced. The radiation exposure to staff in the x-ray intervention rooms are due to Compton scatter events in the patient, hence the patient is the source of the scatter radiation. The energies of typical diagnostic x-rays (26 - 140keV) that enter the patient will be distributed into three types of possible processes. One part of the incoming x-ray energy will be absorbed as a result of the photoelectric effect, another part will travel through the patient to the image detector that gives rise to an image and the rest will be scattered as a result of Compton scatter events. Compton scatter is the dominant interaction in tissue at diagnostic x-ray energies [1].

1.3.Inverse square law

From the laws of physics, the rays from a point source form a divergent beam. The fluence φ; the number of photons passing per unit area perpendicular to the direction of motion, decreases with the squared distance. The fluency in a point source in a vacuum behaves according to equation 1 [1].

$$\varphi 2 = \varphi 1\left(\frac{r^2}{R^2}\right) \quad \ldots\ldots\ldots\ldots\ldots\ldots\ldots\ldots\ldots\ldots\ldots\ldots\ldots (1)$$

$\varphi 1$ is the fluence at the initial point, r is its distance to source, $\varphi 2$ is the fluence in the point of interest, and R is its distance to the source [1].

1.4. X2 Ray safe survey meter

The versatile X2 Survey sensor is primarily used to perform leakage and scatter measurements in diagnostic X-ray applications. It is based on an energy compensated silicon diode array. Unlike a pressurized ion-chamber, a silicon-based sensor can be shipped via air or ground without any special considerations or arrangements [3].

1.5. Recommended dose limits of the ICRP and NCRP

Table 1.1: Recommended dose limits for ionizing radiation (mSv in a year). [4]

Type of limit	ICRP	NCRP
Occupational exposure Stochastic effects Effective dose limit (cumulative)	20 mSv/yr. averaged over 5 years, not to exceed 50 mSv in any one year	10 mSv × age
Annual	50 mSv/yr.	50 mSvr/yr.
Deterministic effects Dose equivalent limits for tissues and organs (annual) Lens of eye Skin, hands, and feet	150 mSv/yr.	150 mSv/yr.
	500 mSv/yr.	500 mSv/yr.
Embryo/fetus exposure Effective dose limit after pregnancy is declared	0.5 mSv/month	Total of 1 mSv to abdomen surface
Public exposure (annual) Effective dose limit, continuous or frequent exposure Effective dose limits, infrequent exposure Dose equivalent limits Lens of eye Skin and extremities	No distinction between frequent and infrequent - 1 mSv/yr.	1 mSv/yr.
		5 mSv/yr.
	15 mSv/yr.	15 mSv/yr.
	50 mSv/yr.	50 mSv/yr.
Negligible individual dose (annual)	No statement	0.01 mSv/yr.

Table 1.2: Radiation exposure reduction with various protection equipment [5]

Protective equipment	Reduction in radiation
Radio absorbent surgical caps	3.3%
Leaded glasses	35–90%
Gloves	20–50%
Thyroid collar	>95%
Lead apron	>95%

2.0 EXPERIMENTAL

2.1. The field studies

The real situation was observed from field studies at cardiac catheterization laboratory in national hospital Colombo. X2 ray safe survey meter was used to obtain the exposure strengths Division of biomedical engineering services, Colombo.

2.2.Average height of staff members

The mean height of males and females was 163.6±6.9cm and 151.4±6.4cm respectively. Mean height showed a significant negative correlation with age ($p<0.001$, $r=-0.207$). The highest mean height in females 154.0±5.9cm and males 165.6±6.9cm were observed in those born after 1977 [6].

2.3.The proposed robot hardware

The robot chassis is developed by an aluminum frame and aluminum bar, it consists vertical arm and four DC motors with a driving board that drives the robot which is attached to the aluminum frame. The motor shaft is attached to the wheels. Wheels are controlling individually. The robot consists five ultrasonic sensors to measure distance in the X, Y, and Z-axes. Four ultrasonic sensors are attached to an aluminum frame from four sides and the other sensor is fixed to the robot arm to measure the distance from the ground to the survey meter. Arduino board and ray safe survey machine attached to the aluminum frame. The robot arm consists with one stepper motor, end stop switch and a rubber belt for moments.

2.4.The functionality of the proposed automated robot

Here we proposed to develop an automated robot. It contains a robot arm and a robot car. This robot is developing for self-working. Robot arm for moving the survey meter in vertical plane positions and robot car for moving the robot arm in horizontal plane positions. Automatically survey meter moves other height levels after 30 seconds when all height levels are completed. Also it passes messages to the robot car instructing to move to the next horizontal position. The car always keeps a constant distance range for one circle between the X-Ray bed and robot arm. For keeping this constant distance range, it moves in an ellipsoidal path around the X-Ray bed of the Cath lab. When the robot complete one turn, the robot car moves to the other distance range automatically.

The scatter radiation was measured at each measurement using X2 Ray safe survey meter. For a more accurate result, more readings should be obtained. It is intended to obtain nearly 120 readings vertically and horizontally in order to display in a 3D-plot.

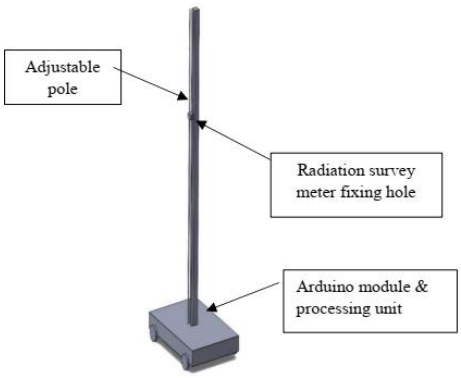

Figure 2.1: Hardware design of the proposed system

2.5.Horizontal and vertical radiation density measuring points

The horizontal measurement points are located at ten radial directions (0^o, 30^o, 60^o, 120^o, 150^o, 180^o, 210^o, 240^o, 300^o, 330^o,) and 20cm , 45cm, 75cm from the center. Additionally, operator position also including. Four vertical positions from the floor (75cm, 110cm, 150cm, 200cm) made up total 120 to 124 data points. Further illustrated by Figure 2.2.

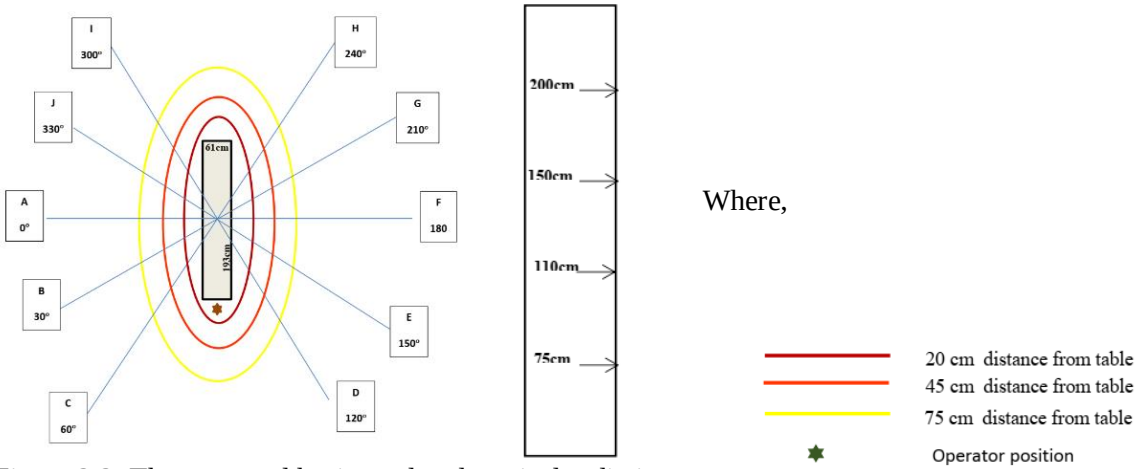

Figure 2.2: The proposed horizontal and vertical radiation density measuring points for data acquisition

2.6. The Proposed System working process

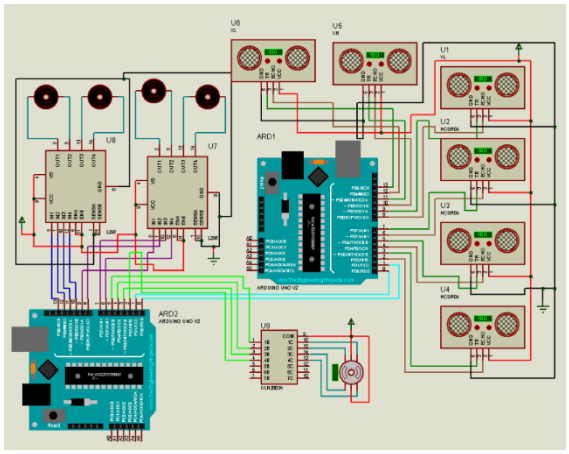

Figure 2.3: Circuit diagram of the proposed system

When the system starts its process always identify survey meter's current location and verifies the location by it self, if the location is in correct system moves the survey meter into correct position. The system identifies the survey meters location by ultrasonic sensor readings and verifies it by internal calculation in the microcontroller. Then system pass commands to dc motors (direct-current) and stepper motors to fix the position. Then the microcontroller pass the x, y, z positions of the survey meter to the Personal Computer (PC) via bluetooth. At the same time survey meter pass the readings to the PC via bluetooth. PC receive all the values from robot module and plot the 3D graph in real time.

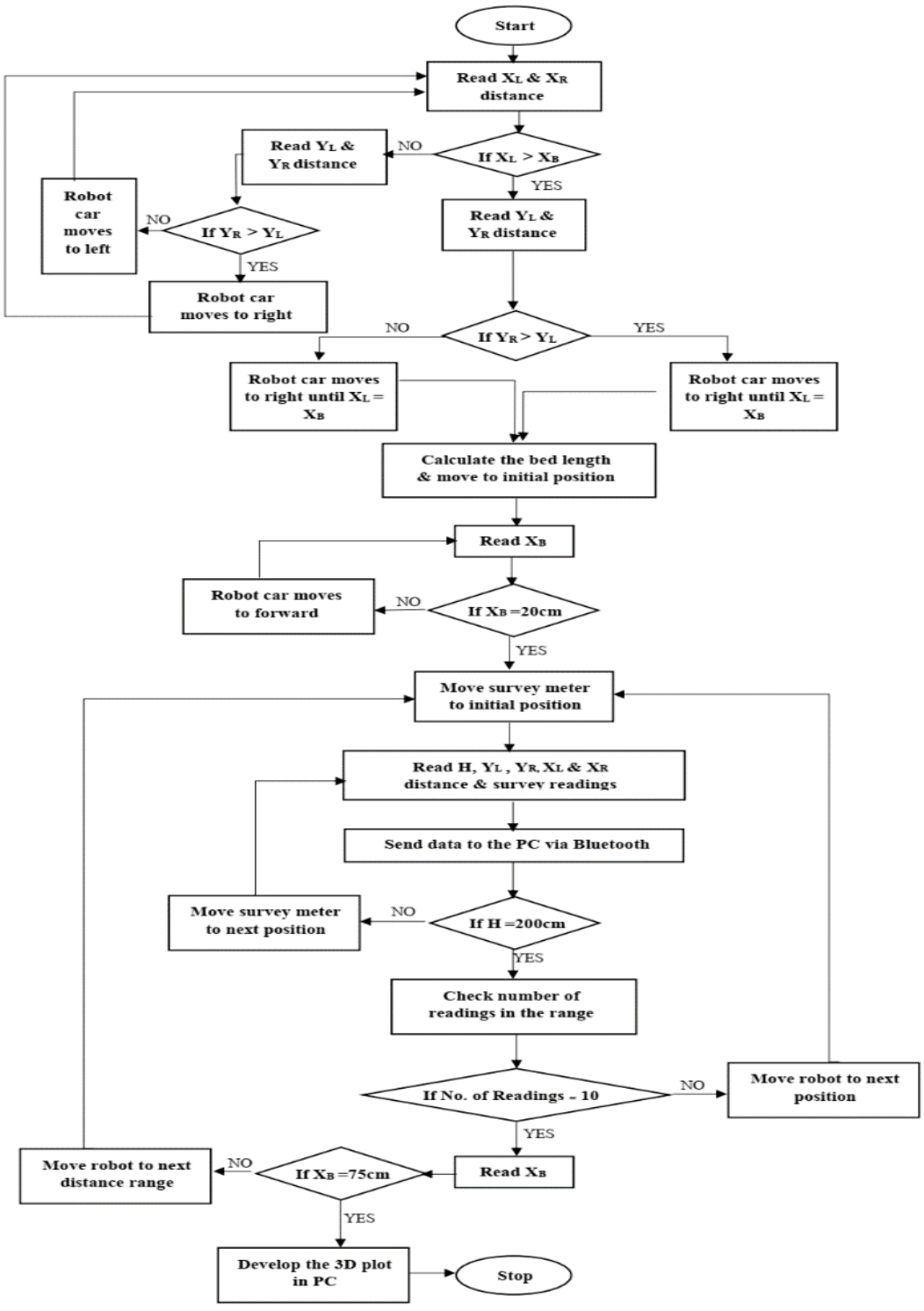

Figure 2.4: Flow chart of the proposed system process

3.0 RESULTS AND DISCUSSION

The following radiation density graph was developed considering standard & predicted outputs.

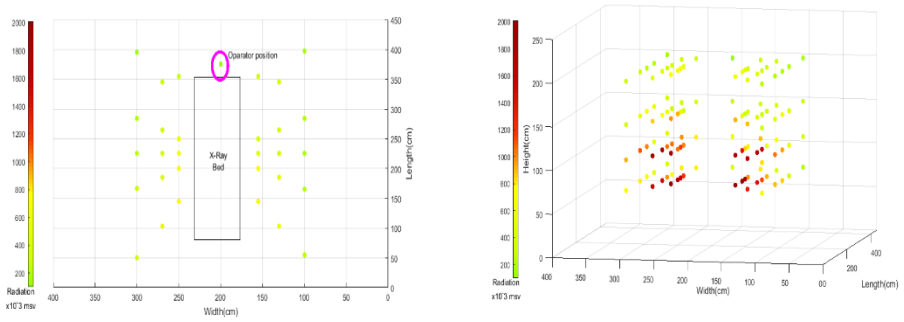

Figure 3.1: The data collecting positions and the Predicted output 3D graph

3.1.The advantages of the proposed system

This system avoids exposing individuals to X-rays during the patient examining period as the proposed robot operates automatically. In addition, the proposed system result illustrating a different color scheme on a three-dimensional plane can be used to give a clear understanding of the risk in the cardiac catheterization laboratory. This system is proposed to design the robot at a low cost. Because the data transferring is done via Bluetooth technology, the final 3D model result can be easily viewed through a laptop.

The result can be illustrated as shown in the Figure 3.1. It can be obtained in three-dimensional plot using our proposed system so that high-risk areas can be identified clearly.

3.2.Discussion

Exposure to scatter radiation during cardiac catheterization can have contrary health effects on the operator and working staff. Advancements in the technology have reduced scatter radiation dose on operator and working staff, but due to the long-term damage occur on their body, the operator and other staff members are reluctant to use them.

This proposed system is designed to shows the intensity of the impact of the scatter radiation on the site in real time. So that workers who are operating in high-risk areas have the ability to bypass, those areas hence reduce their over-exposure.

Previous studies have done with personal dosimeters. Dosimeters measure the total accumulated amount of radiation to which it exposed. Survey meters' measure exposure rate or the intensity of radiation at a location at some point in time.

The system proposed to use survey meter so that user can easily get to know the dose limit per year in that location. Dosimeters are like badges, to measure radiation from dosimeter someone want to wear it and enter to the laboratory. In this proposed system, a robot vehicle will be built with arm to hold the survey meter. Hence, no one need to enter to laboratory for measurements as it is a fully automated robot. This system minimizes potential hazards to the humans.

In general, the working staff using lead aprons and shields. The system allows practicing the behavior of how to place the lead shielding for protections. The shielding is positioned by staff members, their positions cannot be predicted and need to be dynamically changed. However, this automated exposure evaluating system helps to get a good and accurate idea about the place where they want to fix the shielding.

As the actual exposure was higher than predicted from inverse square law, it is therefore not a fully reliable and safe estimation technique of scatter radiation for this purpose.

4.0 CONCLUSION

The proposed robot vehicle positioning can be identified using HC-SR04 Ultrasonic sensors. But it's not practically suitable for this robot, because maximum range of this sensor is up to 200cm but the dimension on catheterization laboratory is nearly 600 cm × 1000 cm. so the readings of this sensor is not practical for this proposed robot. This system used Ray Safe X2 survey meter for measuring the radiation and it can be used to send data easily to the PC via Bluetooth. The proposed robot can be constructed with an Arduino Uno board so system always need a PC or laptop to show the output because output is to be processed using Matlab software. Output is predicted by using only 124 measuring points. To obtain an accurate output result it is necessary to increase the number of measuring points. For further development of this robot system, it has been planned to use URM06- Analog ultrasonic sensor. Moreover, for further developments of this robot system it has been planned to use image-processing techniques in order to increase reliability of the proposed 3D exposure indicating system.

ACKNOWLEDGEMENT

First and foremost, praises and thanks goes to the Almighty Allah, for his showers of blessing throughout my research work to complete the research successfully.
I would like to express my deep and sincere gratitude to my supervisors and research coordinator for giving me the opportunity to do research and providing invaluable guidance throughout. Finally, I would like to express my love and heartiest gratitude to my family for being my backbone for my life. Moreover, I would like to express my heartiest appreciation for my friends and colleagues to their support.

REFERENCES

[1]. Rehn, E., 2015. *Modeling of scatter radiation during interventional x-ray procedures*. Thesis. Linköping: Linköping University.
[2]. Defining the Cath lab workplace radiation safety hazard. *DAIC*. https://www.dicardiology.com/content/blogs/defining-cath-lab-workplace-radiation-safety-hazard (Accessed 2021.08.26).
[3]. Products. *Fluke Biomedical*. https://www.flukebiomedical.com/products/radiation-measurement/x-ray-qa-instruments/raysafe-x2-x-ray-measurement-system (Accessed 2021.08.26).
[4]. Gupta R.C., McClella, R.O., Health effects of nuclear weapons and releases of radioactive materials. In *Handbook of toxicology of chemical warfare agents*. London: Academic Press, (2020), 707–743.
[5]. Ranasinghe, Priyanga, Jayawardana, Naveen & Constantine, Godwin & Sheriff, M.H.R & Matthews, David & Katulanda, Prasad, Patterns and correlates of adult height in Sri Lanka. Economics and human biology. 9, (2011), 23-9, doi: 10.1016/j.ehb.2010.09.005.
[6]. Biso, Sylvia Marie R, Mladen I Vidovich, "Radiation protection in the cardiac catheterization laboratory." *Journal of thoracic disease* ,12,4(2020):1648-1655. doi:10.21037/jtd.2019.12.86

Proc. Annual Symposium on Research & Industrial Training, 08(2021) 168-174
Department of Electronics – Wayamba University of Sri Lanka

INSTALLATION AND EVALUATION OF DIRUI CS-400 BIOCHEMISTRY ANALYZER

D.A.T. Peiris*, U.A.D.N. Anuradha

[1]*Department of Electronics, Wayamba University of Sri Lanka, Kuliyapitiya, Sri Lanka.*

*amilatharangaac@gmail.com

ABSTRACT

As science and technology grew rapidly in the past few decades, many sectors and areas have developed rapidly in parallel to technology. The biomedical healthcare sector is one of the main fields that developed rapidly with time [1]. This sector has evolved step by step to the current stage from its primary stages. Bio-medical healthcare sector has been subdivided into various categories as it has to cover a wide area. Medical laboratory service is one of the main sub-sector. It is related to all the medical tests that do for all types of medical problems in every condition. When it comes to laboratory services, it is also divided into sub-sectors according to the methodology or type of the test. Many companies all around the world are involved in biomedical laboratory services and most of them are involved in the invention and development of laboratory machines. CS-400 Auto chemistry analyzer is one such machine that is widely used inside the field. This work includes details about the DIRUI CS-400 biochemistry analyzer and a comparison between other analyzers in the field, and also the installation procedure. Study results concluded that DIRUI CS 400 analyzer has higher test rate efficiency when compared with other medium range analyzers. It's unique reagent adding mechanism which has two reagent disks and two probes and sample disk with higher number of sample positions direct to this higher test rate.

Keywords: Biomedical healthcare sector, Biochemistry analyzer, Software installation

1.0 INTRODUCTION

Applying engineering principles and problem-solving techniques to biology and medicine has improved the biomedical engineering section throughout the past few decades continuously. These principles are further combined with the principles of medical sciences aiming to streamline the healthcare services in the world. Therefore, biomedical engineering has become one of the niche engineering branches in the world and its continuous development benefited special medical equipment, analyzers, and components with the highest technology which can enhance the medical security of the living beings in the world [1]. On the other hand, it causes the enhancement of the efficiency and eases the functionality of the analyzer to the end-user.

When it comes to laboratory analyzers, we can mainly identify a few products such as biochemistry analyzers, hematology analyzers, blood gas analyzers, electrolyte analyzers and many more in the field. From those products, biochemistry analyzers are in the frontline [2]. A biochemistry analyzer is one of the essential analyzers in a laboratory since it performs tests that have an essential demand in every type of hospital [3]. Hospital or the laboratory, considers the sample rate and the type of tests when they select a biochemistry analyzer. An analyzer becomes unique and special when it can perform more tests than the others. Generally, rural hospitals or laboratories select a test rate less than 200 per hour, and others who have a higher sample load, select an analyzer that has a

medium test rate like 400-500 tests per hour. There are some special occasions that a hospital has a heavy sample load and they select an analyzer with a higher sample test rate.

1.1 DIRUI auto chemistry analyzer

DIRUI Auto-Chemistry Analyzer (Model: CS-400) is a medium test rate analyzer with a discrete system, emergency priority function as well as an external computer. The analyzer can automatically realize sampling, reagent injection, anti-interference, mixture, pre-temperature, reaction measurement, rinse, calculation, display, and print function. The analyzer is composed of an optical system, mechanical system, flow path system, electronic control system, and software system where the first four systems built up the analysis section and the software system built up the operating system. The analyzer section and operating system are connected through a RS-232 serial port cable. At most 88 colorimetric test items and 3 ISE test items; K, Cl, and Na, can be performed by the analyzer. Four test methods are used for measurements; 1-point end assay, 2-point end assay, 2-point rate assay, rate-A assay. The analyzer uses primary and secondary wavelengths for its measurements and they are a total of 12 in the number; 340 nm, 380 nm, 405 nm, 450 nm, 480 nm, 505 nm, 546 nm, 570 nm, 600 nm, 660 nm, 700 nm, and 800 nm. This biochemistry analyzer can maintain a constant rate of 400 test items per hour without ISE tests. The maximum rate is 800 test items per hour with ISE tests. The analyzer uses two reagents for its purposes. Hence it has two reagent disks with a refrigeration function. There are 45 reagent positions per disk and a total number of 90 positions in two disks. The total number of 115 sample positions in the sample disk. They are divided into 50 routine positions, 34 calibrator positions, 20 stat positions, 8 control positions, and 3 detergent positions while 8 control positions and 17 calibrator positions have refrigeration functions. Serum, urine, plasma, gastric juice, CSF, and ascites can be used as the sample types for the analyzer. 20W/12V quartz halogen lamp is positioned inside the analyzer as the light source, absorbance range in between 0 to 3.3. Six sets of cuvettes, which contain 20 cuvettes in each, are used as the reaction positions. The analytic system is composed of a sample disk, two reagent disks, a reaction disk, a cooling system, and an optical system. Sample adding mechanism, reagent adding mechanism, stirring mechanism, rinsing mechanism, cooling mechanism and sample analyzing mechanism are included in the analytic system [4].

2.0 EXPERIMENTAL

In this work, a CS-400 analyzer was compared with two other analyzers in the field. Analyzer structure, technology, analyzer software, test rate and efficiency have been used as the comparison parameters. Installation procedure of the analyzer also mentioned.

2.1 Analyzer requirements

The analyzer should position inside a safe room which has enough space to perform its activities. There should be a minimum of 50 cm for the nearest wall (barrier) from the analyzer and a proper place for waste draining. Analyzer needs an ambient temperature between 15^0C to 32^0C, relative humidity in between 30% to 75%, and atmospheric pressure in between 75kPa ~ 106kPa. The analyzer should be placed in a well-ventilated room without dust, mechanical vibration, noise sources, and power interference and also should be avoided from direct sunlight. The power supply requirement of the analyzer is 220/230V, 50/60Hz [4].

2.2 Hardware installation

The analyzer installation procedure is divided into two main sections; analyzer installation and software installation. After matching all the pre-requirements, the analyzer was adjusted to a horizontal level. Reagent probes and sample probes were fixed. 500mL of pure water was added into the incubation bath. Reaction cuvettes were installed. Front door of the analyzer was opened; CS-Alkaline Detergent was added to the detergent box. A Reagent bottle of CS-Anti-Bacterial Phosphor-Free Detergent was placed in Position 45 of R1 and R2. Pure water supply pipe was used to connect the outlet of the pure water equipment and "pure water inlet" on the right rear plate of the analyzer.

Next step is to connect the waste liquid pipelines. One end of the concentrated waste pipeline was connected with the concentrated waste liquid outlet connector and one end of the diluted waste pipeline with the diluted waste liquid outlet connector in the analyzer. Other ends were placed into the waste liquid collector or draining system. One end of the concentrated waste liquid level sensor was connected to the concentrated waste liquid level sensor connector on the right rear cover plate of the analyzer. Other end was placed into the concentrated waste liquid tank. Two screws on the right were removed, fixing the ISE waste liquid collector onto the right side of the rear panel of the analyzer. ISE waste liquid pipe was inserted into the ISE waste liquid collector and the lower waste liquid pipe of the ISE waste liquid collector was connected to the waste liquid discharge device. The ISE cover plate of the analytic unit was opened. Nuts of Potassium (K), Chloride (Cl), Sodium (Na) and Na REF (Reference) on the flow cell were unscrewed and took out each seal plug and ring. Electrodes of Cl, K, Na and Na REF (same to Na electrode) were fixed onto the flow cell. Front left cover plate was removed. A container was placed in front of the analyzer, and then the rubber plugs at the end of hoses were removed. Then the hoses were inserted into the container. Purified water was injected into hoses with supplied funnels until water flows out from the hoses. Front left cover plate was fixed.

2.3 Software installation

Computer and printer were connected. Then printer software was installed on the computer. One end of the accompanying communication cable was connected to the "RS-232" port on the left rear cover plate of the analyzer; the other end to the main case serial port of the computer. The Relevant power connection was applied as per the power requirements. Power cable for the analyzer in the left rear panel. The CD rom which came with the software accessories was used to install the analyzer software to the computer. Normal software installation methods can be used for installing the software application. After the successful installation of the analyzer and the software, it has to set up the analyzer for use before handing it to the customer. Hence has to set up system login, debug the analyzer, reagent set up, calibration and quality control checking and report format setting. Analyzer was powered on. Software icon on the desktop was double clicked. "User Login " window appeared. After successful login, the interface shows the offline state, indicating that the software is not connected to the analyzer. Hence the online status button in the first appeared menu was clicked to set the analyzer into the online status.

2.4 Analyzer debugging and quality checking

After the installation, the analyzer was operated in the "System Maintenance" interface to guarantee that the analyzer works properly. It is necessary to following analyzer debugging setups were executed to confirm the proper analyzer functionality; exhaust-syringe pump exhaust, reagent and sample probe horizontal check, mechanism operation check, rinse ISE and reaction cuvettes, light intensity check, cuvette blank test, ISE checkup. After setting up the analyzer it has to check the credibility of the results of the analyzer. For that purpose I have to do calibration and quality control checking. The goal of quality control in the laboratory is to guarantee test result reliability for each sample. Single-click "calibration" key was used to carry out the registration of calibration information and the check of calibration result. Calibration can be divided into two sub keys; colorimetric calibration and ISE calibration. Colorimetric calibration interface allows doing the colorimetric calibration and checking the calibration results. The ISE calibration interface also allows the same. After only the calibration results show success, Quality control (QC) should start. Otherwise QC results may be out of the range. QC chart is a kind of graph with a quality control limit. QC limit is a controllable analysis method in which a known specimen (QC sample) carries out a repetitious test to get the mean value (X) and standard deviation (SD). X±2SD is the warning limit. X±3SD is out of control. Single click "QC register" in the Quality Control interface was allowed to register the QC samples. Before running QC samples, it is essential to register them. At most eight QC samples can be used simultaneously to carry out quality control. QC samples were placed in C positions in the sample disk. After QC registration, confirm whether control and calibrator are placed correctly. First calibration was done. Then the "QC Test" key was clicked to start QC tests. If the QC is out of control, it should check whether the input parameters and used control and reagent are correct, or operate according to the alarm information and related prompts.

3.0 RESULTS

3.1 Analyzer comparison results

When comparing this analyzer with the other analyzers in the field, the main specialty in this analyzer is its higher test rate. Other medium-range analyzers also provide around 400 constant tests per hour, but they could not reach the maximum test rate value of 800 tests per hour with ISE tests which this analyzer can achieve. When considering the higher workload of a laboratory, higher test rate is a must to manage workload. When the other analyzers are limited to around 90 cuvettes in the reaction disk, the DIRUI analyzer is operating with 120 cuvettes and it also enhances the efficiency of the analyzer. One of the other special features in the analyzer is its sample disk which has higher sample positions than the other analyzers. The total number of 115 sample positions with 20 specific positions for emergency samples in DIRUI analyzer while the numbers of others are less than this. It allows the user to perform tests from more samples in a single time. DIRUI analyzer has two independent reagent disks and two independent reagent probes to handle the reagent adding mechanism. The analyzer uses two reagents in two separate disks to enhance the efficiency of the mechanism. When considering the other analyzers, they have only one reagent disk with one probe. On some special occasions, two reagent probes are used for a single reagent disk. But it is not effective as using two independent reagent disks and reagent probes to reagent adding mechanism. Not only the number of reagent disks but also the number of reagent bottle positions in the DIRUI analyzer is also higher than other analyzers.

In DIRUI analyzer, digital level sensor, volume tracing, probe-blocking detection and probe collision-proof including in the reagent level sensor system while horizontal and vertical obstruct detection, level detection and tracking including mainly in other analyzers. Not only for the reagent mechanism but these sensor systems are also used for sample probes for sample level detection. When comparing the analyzer software system, every manufacturer uses their own unique system for their product. Hence the sample, calibration, and QC registration procedures are unique for the analyzer software. Analyzers use an RS-232 interface for communication between the analyzer and the computer. DIRUI analyzer supports the latest version of the operating system, Windows 10 while some of them are restricted to older versions.

3.2 Analyzer results

DIRUI CS-400 auto chemistry analyzer obtains different types of results for different types of tests and actions performed by the analyzer. Mainly, the analyzer obtains results for sample tests including colorimetric tests and ISE tests. Generally, these test results are obtained in the software interface. These results can convert into a printing format suitable for the report format formed in the installation procedure.

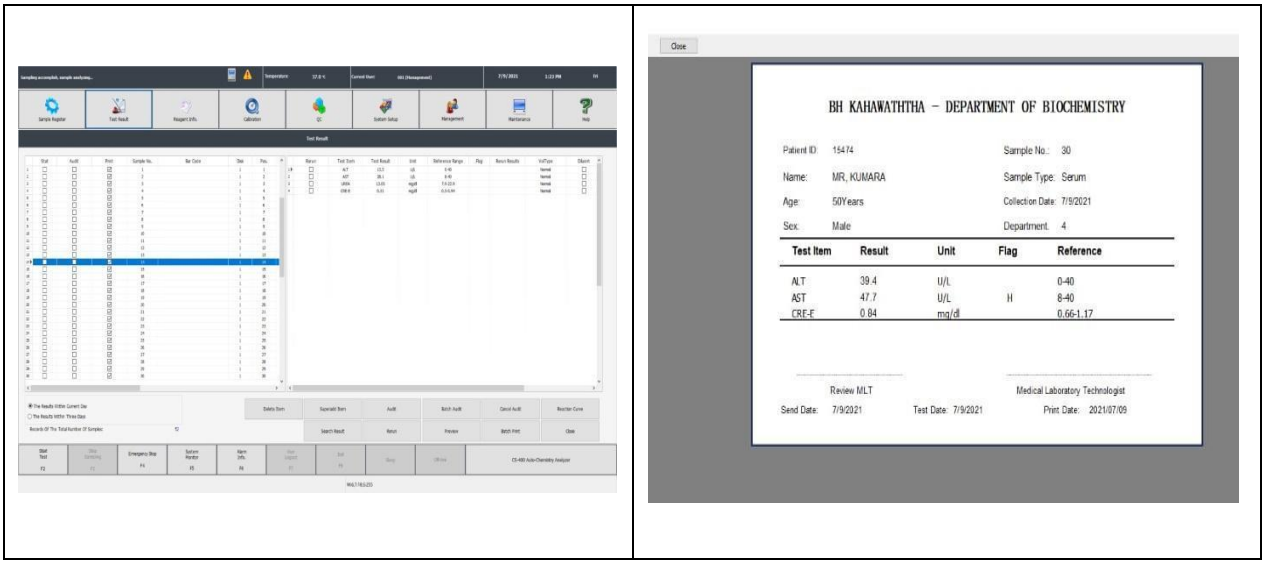

Figure 3.1: Test results of the interested analyzer

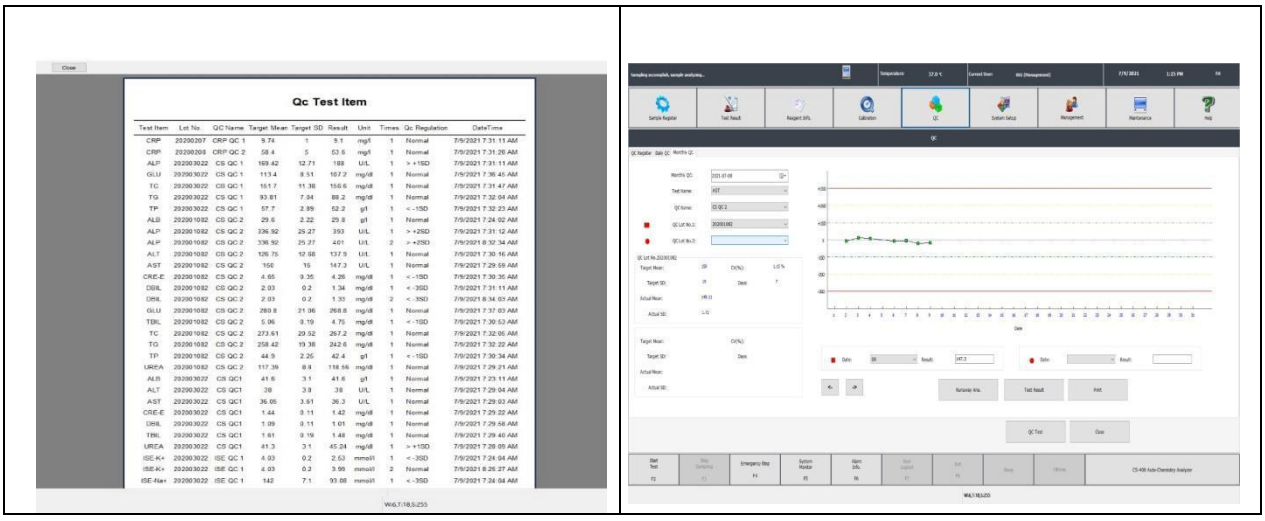

Figure 3.2: QC results of the interested analyzer

Calibration and QC results obtained for the colorimetric and ISE tests individually shown in figure 3.2. These results can be viewed as numbers and graphs. Apart from the test, calibration and QC results, the analyzer obtains results for system maintenance such as light quantity checkup, ISE checkup and cuvette blank test. These actions should be performed to confirm that the light source, cuvette sets and ISE units function accurately and the analyzer is ready to perform sample testing.

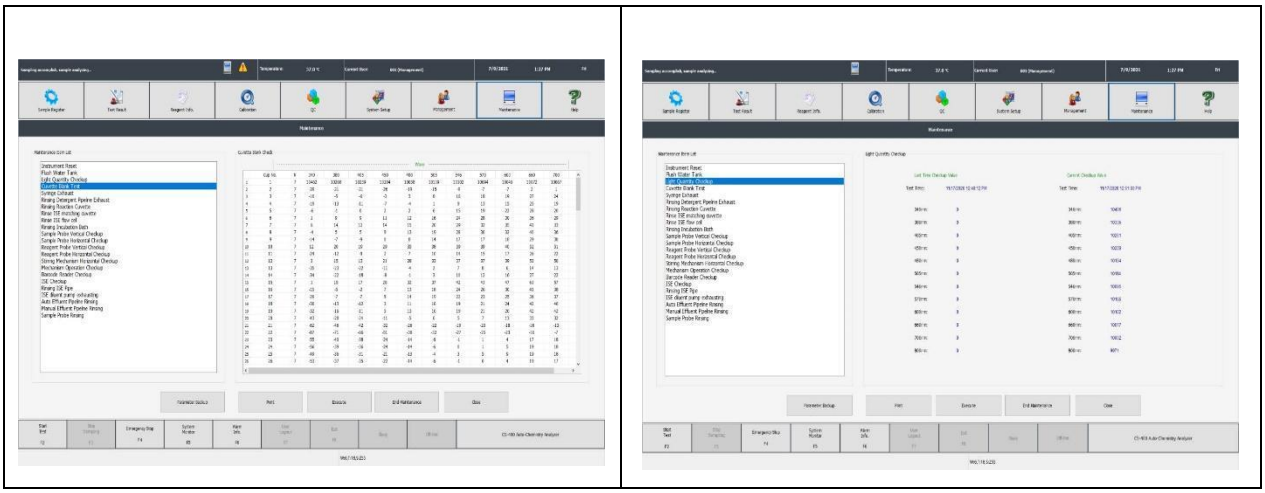

Figure 3.3: System maintenance results of the interested analyzer

4.0 CONCLUSION

A biochemistry analyzer is one of the essential analyzers in a laboratory since it can cover many test areas. Different routine biochemistry tests can be carried out by a biochemistry analyzer. Generally, the end-users consider two main points when they choose a biochemistry analyzer for their laboratory; test rate and the type of tests that run by the analyzer. When considering medium test rate analyzers, the DIRUI CS400 analyzer is more efficient than the others. Its higher test rate, more sample positions in the sample rack, more sample positions for emergency tests, two independent reagent disks and two independent reagent probes adds value to the analyzer and are

highlighted from the other analyzers. The analyzer has come up with its own software system and it is very user-friendly and clear to handle. When considering all the above facts, the medium test rate biochemistry analyzer of DIRUI manufacturers is very much fit to a laboratory for its continuous, smooth and efficient work.

REFERENCES

[1]. Lantada, A.D., Morgado P.L., Rapid prototyping for biomedical engineering: current capabilities and challenges, *Annual review of biomedical en*, (2012),73,doi: org/10.1146/annurev-bioeng-071811-150112
[2]. Xu W., Kaizheng H., Bin X., Design for step motor control system of automatic biochemistry analyzer, *8th International Conference on Electronic Measurement and Instruments, (*2007), 607
[3]. Lv X., Luo Y., Deng M., Chen Y., The design of the semi-automated biochemistry analyzer, *International Conference on Information Acquisition*, (2004),164, doi: 10.1109/ICIA.2004.1373342
[4]. DIRUI Industrial co. Ltd, *Auto chemistry analyzer (CS-400) user manual*, 2017

Proc. Annual Symposium on Research & Industrial Training, 08(2021) 175-181
Department of Electronics – Wayamba University of Sri Lanka

RADIO FREQUENCY IDENTIFICATION BASED SMART CHECK-IN SYSTEM

B.P. Sankalpa*, J.W. Jayasinghe

Department of Electronics, Wayamba University of Sri Lanka, Kuliyapitiya, Sri Lanka

*pramodh2009@gmail.com

ABSTRACT

Guard-tour Patrolling Routing is a system used to check-in and assure the protection of relevant properties of an organization or any premises. It helps to ensure that the employees make the assigned visits at correct intervals and offers records for legal or insurance purposes. Amano Watchman's clock is a device that has been used for check-in purposes, which is based on a mechanically operated punching key system. This research paper describes how the old mechanical process is converted into a digitalized smart system, which is based on the RFID (Radio Frequency Identification) tag scanning method. Moreover, it describes how the old manual log-keeping process is digitalized to store scanned data into an electronic data sheet with a single board computer, namely Raspberry Pi Model 3B. The designed system consists of an RFID scanner, a log file storing server, and a desktop application which can be used to access the FTP log file server. Further, this device can operate for 8-9 hours after charging for about 2 hours. The external RTC (Real Time Clock) module system provides a backup timer that can be remotely operated with no internet connection. When compared to the existing manual system, the proposed system can increase security, reduce the processing time, and expenses for inspecting properties.

Keywords: RFID, Raspberry Pi, Watchman Clock, Check-in system, RC522 module

1.0 INTRODUCTION

1.1 Overview

If a land area of an organization or company is spread over a broad area, then its properties must be monitored verifying its security several times a day as per a patrolling routine. To maintain the quality of the patrolling routine, the security officers must be "Checked-in" at specific locations (properties) and they must visit/ inspect the area in specific time periods. Amano Watchman's Clock has been a popular device for many years to perform security patrolling checked-in routines. An old device is shown in Figure 1.1.

A major drawback of the current system is that most of the "Station Marking Keys" tend to wear out and they do not indicate clear marks on the carbon paper as shown in figures 1.3(a) and 1.3(b). Also, the carbon paper rolls are expensive and one pack of 10 rolls costs around LKR 6000. The latest model of the device costs around LKR 290,000 [1].

Figure 1.1(a): Amano Watchman's Clock 3d view

Figure 1.1(b):Amano Watchman's Clock front

Figure 1.2: Inside view from top

Figure 1.3(a): Punching Key

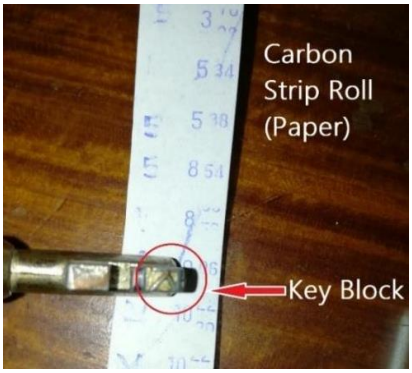

Figure 1.3(b): Carbon Paper Roll

Further, the relevant officer must check the time logs recorded on long papers as shown in Figure 1.3(b), which consume a lot of time. This research describes how the old mechanical process is upgraded into a high-accuracy digitalized system. The proposed design consists of an RFID-based scanning system with an electronic log-file saving database. Hence, it is low cost compared to the existing RFID-based scanning devices available in the market.

1.2 Literature Review

Many researchers have utilized RFID technology in developing access control systems. Reference [02] describes RFID Technology and gives a brief introduction on the classification of RFID tags and reader, frequencies used, current application, as well as advantages and limitations with the future scope of this technology. Reference [03] is about developing an RFID-based monitoring

and access control system consisting of an RFID terminal, a camera, a server, and an alert device. Upon detecting a transponder, the terminal captures a photo and transmits the data, including the UID and photo to the server through a TCP/IP connection. The server searches the database for this query and sends the results back to the terminal to allow or deny access. Reference [4] describes how handheld RFID reader units become increasingly important in the supply chain, warehouse, and retail store management. Also, it describes the importance of the design requirements for a handheld reader unit as size, sufficient battery life, and suitable read range for the desired applications.

2.0 EXPERIMENTAL

The proposed system comprises three sub-systems namely the power supply system, Raspberry Pi log file server, and sensor-indicator system.

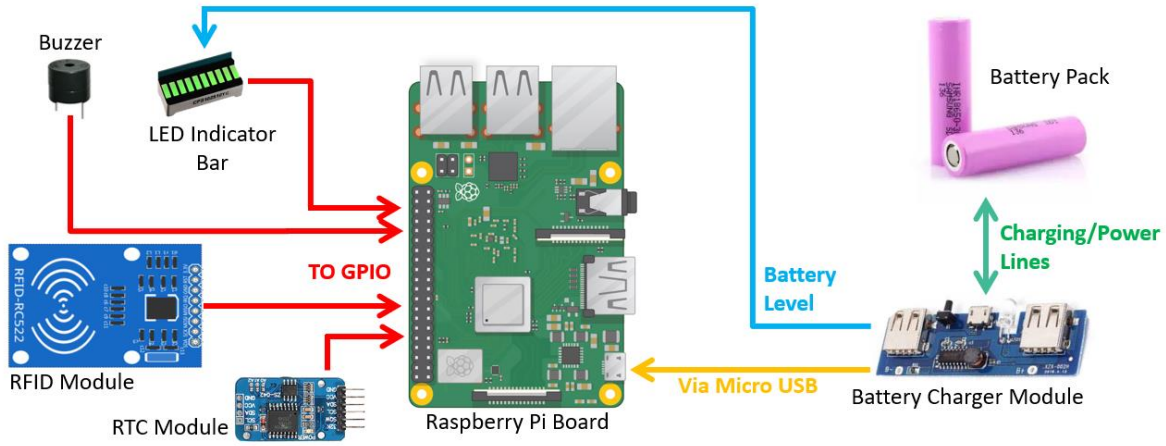

Figure 2.1: Block Diagram of the system

The power supply system is based on a Dual-USB power bank charger module along with a 7000mAh battery pack. The power bank module is used for charging the battery as well as powering up the Raspberry Pi board. The module indicates the battery level via 4 LED bars and when the batteries are being charged, the module cuts off the power line to the Raspberry Pi board as a precaution. The 1.2A USB output port is used to power up the Raspberry Pi board and the vacant port is completely disabled in the proposed system.

Indicator 1 is a one-second status LED blink with the buzzer and indicator 2 is a status LED blink twice with the buzzer beep for 0.1 second as shown in the Figure 2.3.

The time accuracy of the system is considered for measuring the accuracy of the new system. Here, the least counts of the two devices are compared. Along with that, log readings per unit time are also compared with the old process. The obtained results are shown in Table 3.1. The 18650 Lithium-Ion rechargeable battery pack can provide 3.7V and it is rated as 7000mAh. The Dual-USB power bank charger port is directly connected along with the battery pack for charging purposes. The micro USB power supply is connected through an ON/OFF switch to control the power supply to the Raspberry Pi board.

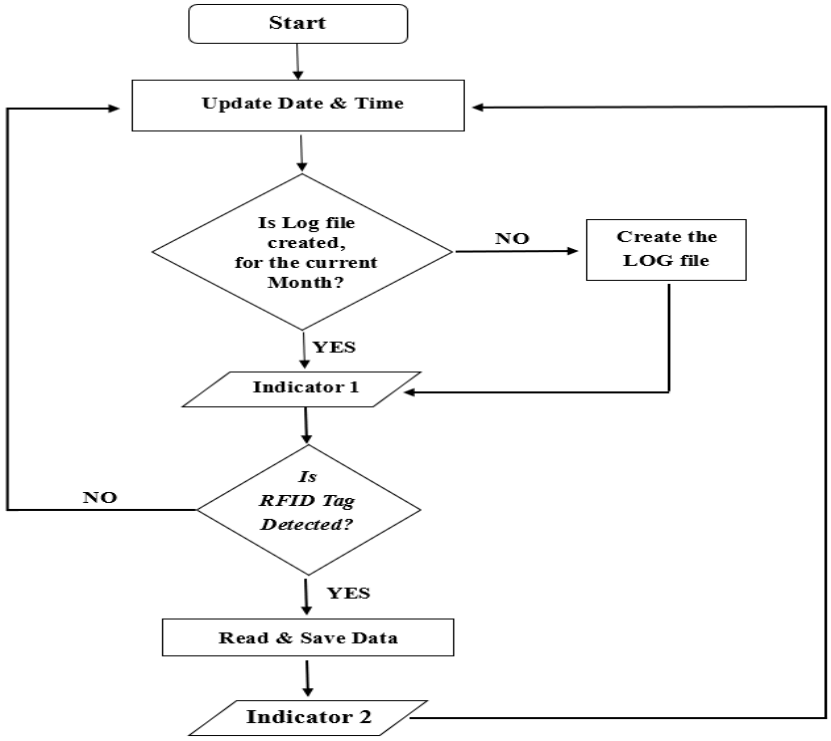

Figure 2.2: Flow chart of the system

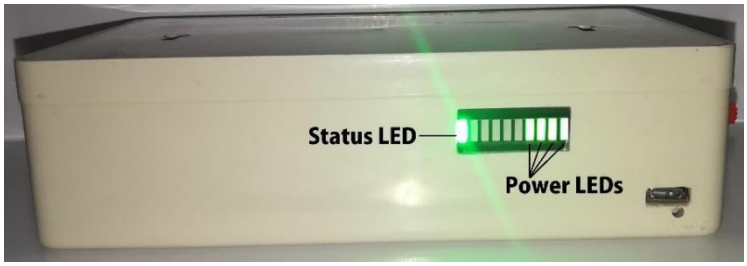

Figure 2.3: Indicator LEDs of the system

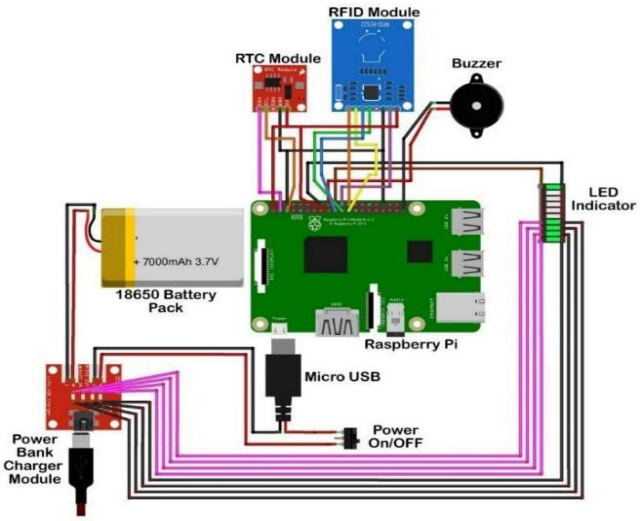

Figure 2.4: Circuit Diagram of the system

The RTC (Real Time Clock) module used here can update the time when the system power is OFF. Also, it helps the Raspberry Pi system to maintain accurate time when the device is operating in remote areas, where there is no internet connectivity to the device. The RTC module is powered by a CR2032 battery and it will last for about 10 years. [05] The FTP server created in the Raspberry pi internal storage saves log data files according to the relevant month. [06] Saved log data can be accessed by the following desktop application.

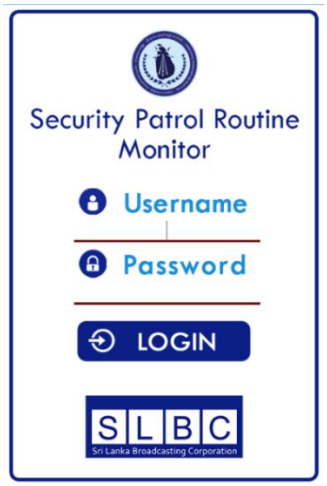

Figure 2.5: Desktop Application User Interface

The desktop application is programmed using Java language and it is developed using the Netbeans platform. The user interface is designed using Adobe Photoshop as shown in Figure 08. The application runs on a local server on the relevant desktop PC. The database is developed on the XAMPP platform using MySql. The standard operations are included in this application, such as; Exit Button, Exit confirmation message, Wrong password warning message, and Error notification on blank fields.

3.0 RESULTS AND DISCUSSION

The old mechanical device is digitized into a new system which can operate for about 8-9 hours, once fully charged and the charging time is about 2 hours. When the system is on stand-by mode, the battery life remains for 5 days. The system can be charged via any micro USB mobile phone charger. The system date and time are updated via WIFI while the system is turning ON. Once the time is updated via WIFI at the first system power-up, no internet connection is needed further on. Therefore, system time is precise and accurately up to date. Accordingly, the user does not need to consider system time as in the old device. In the old system, if the used battery is discharged, the clock machine stops and needs to re-adjust the time manually. The installed RTC module is added as a backup timer. Therefore, the device can be used in remote areas also. The old time-consuming and expensive Carbon-Ink paper-roll based log file is replaced by the Raspberry Pi FTP server-based log file. To access the scanned log data, the desktop application can be used, and it directs the user to the log file directory on the FTP server. The desktop application is password protected and only authorized officers can access the log data. The log files are organized according to the month name and a new file is created automatically when a new month is started. The log file saves and updates into a Microsoft Office Excel file (.xls).

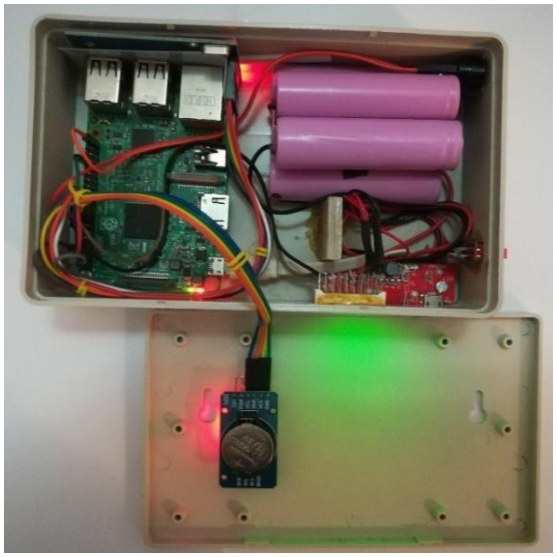

Figure 3.1: The Portable RFID Scanning Unit

Figure 3.2: Installed RFID tag at property

Rather than observing an un-organized physical log paper as shown in Figure 1.3(b), the proposed electronic log file is easy to read and there are no additional costs for ink and paper rolls compared to the old system. The punching keys are replaced by RFID tags as shown in Figure 3.2. Therefore, there will be no unclear or damaged log readings in the new system, compared with the old system.

In this system, accuracy can be measured by two methods: by logs per unit time and by the least count of the device. Hence, the old system updates time for every 2 minutes, a time-unit is declared as 120 seconds for calculating the accuracy.

Table 3.1: Accuracy Comparison of the Old device & New System

	Logs per unit time	**The least count of the device**
Old Device	1 log update per 120-seconds time unit. **Accuracy$_{Old}$** = 1/120% = 0.834 %	**Least count =** 2 minutes *(Ex: After 00:00:00, the next obtainable reading is 00:02:00)* *Time Format = hh:mm:ss*
New System	60 updates per 120 seconds time unit (Updates time every 2s) **Accuracy$_{New}$** = 60/120% = 50 %	**Least count =** 1 second *(Ex: After 00:00:00, the next obtainable reading is 00:00:01)* *Time Format = hh:mm:ss*
Increment	**Accuracy$_{New}$ - Accuracy$_{Old}$ =** = (50 – 0.834)% = 49.116 %	Least Count accuracy increment* = (120-1)/120% = 99.16%

*In the old device, only one reading can be obtained in a time interval of 120 seconds. In the new system, 120 points are available for reading within the same time interval.

4.0 CONCLUSION

This research paper describes the development of a portable RFID scanner model that digitalized the traditional log-keeping security patrolling routine. This smart check-in device is a complete alternative for the mechanical punching key-oriented, Amano Watchman's clock-based security patrolling routing. In the proposed system, the old station keys are replaced by the RFID tags installed at the property locations. The portable RFID scanner device is responsible for saving the scanned data into Microsoft Office Excel data sheets, which organize data as monthly log files. These log files are precise and well-structured as compared to the old Carbon-Ink paper roll-based punching key method. Using the desktop application, the authorized officer can access the FTP server to download the log sheets. Compared to the old device, the proposed system has indicators to notify new log entries as well as battery level indications to the user. This design costs about 7000 LKR. Compared to market prices, the proposed system is very cost-effective. Unlike the old device, this device does not incur any Carbon Ink Roll paper cost.

ACKNOWLEDGEMENTS

The authors would like to acknowledge the academic staff of the Department of Electronics, Faculty of Applied Sciences, Wayamba University of Sri Lanka.

REFERENCES

[1]. Amano PR-600 Model Price, https://www.desertcart.lk/products /27416250 -amano-pr-600-watchman-s-time-clock, (Accessed 2021-03-08)
[2]. Chechi, Davinder & Kundu, Twinkle & Kaur, Preet., The RFID Technology and Its Applications, *International Journal of Electronics, Communication & Instrumentation Engineering Research and Development (IJECIERD)*, (2012),1-2.
[3]. F. Lourenco and C. Almeida, "RFID based monitoring and access control system," in *Proc. INFORUM*, (2009).
[4]. Ukkonen, Leena & Sydänheimo, Lauri & Kivikoski, Markku., Read Range Performance Comparison of Compact Reader Antennas for a Handheld UHF RFID Reader., *IEEE Communications Magazine* (2007), 63 – 70.
[5]. CR2032 Battery lifetime, https://www.panasonic-batteries.com/en/specialty/lithium-coin/coin-lithium-cr2032, (Accessed 2021-08-09)
[6]. server on a Raspberry Pi, https://phoenixnap.com/kb/raspberry-pi-ftp-server, (Accessed 2021-08-01)

Proc. Annual Symposium on Research & Industrial Training, 08(2021) 182-187
Department of Electronics – Wayamba University of Sri Lanka

DESIGNING A BIO-MEDICAL INSTRUMENT TO MEASURE CHOLESTEROL LEVEL OF HUMAN BLOOD USING A COLOUR SENSOR

M.D.M. Perera[1*], W.A.S. Wijesinghe[1], and T.V.A. Ruwansiri[2]

[1]*Department of Electronics, Wayamba University of Sri Lanka, Kuliyapitiya, Sri Lanka*
[2]*Division of Biomedical Engineering Services, Ministry of Health, Sri Lanka*

[*]dilinimadhushani622@gmail.com

ABSTRACT

Cholesterol detection plays a vital role in prevention of heart diseases. The traditional lipid profile test for cholesterol detection is done using serum. There are several systems and models to detect the cholesterol level in the blood. Most of the systems use photodiode array detectors and wave filters to detect the intensity of the colour and measure the cholesterol level. In this designed cholesterol measuring system, RGB colour identification of the TCS3200 sensor was used to detect the intensity of the colour and determine the cholesterol level of the samples. Colour sensor's responses belong to the visible light range of the spectrum. Cholesterol level was calculated based on the amount of light absorbed by the sample in the test tube. The light wavelength range that absorbs cholesterol is around 500-550 nm, that is the green colour in the visible range. It was able to measure the total cholesterol level of the human blood by using this technique.

Keywords: Cholesterol level, Colour sensor, RGB colour identification

1.0 INTRODUCTION

Cholesterol is a fatty substance (lipid), which is essential to healthy life. Cholesterol travels through the blood in particles called lipoproteins. The three common lipoproteins are low density lipoproteins (LDL), high density lipoproteins (HDL), and very low-density lipoproteins (VLDL). Therefore, total cholesterol consists of LDL, HDL and VLDL. Medical research has shown that elevated LDL cholesterol levels are associated with an increased risk of coronary artery occlusion, while elevated HDL cholesterol levels reduce this risk. Thus, doctors sometimes refer to LDL as "bad cholesterol" and HDL as "good cholesterol"[01]. The human can be categorised as a healthy person or not based on cholesterol level in the blood. If the cholesterol level is less than 200 mg/dL, then the person is a healthy person. If the cholesterol level is between (200-239) mg/dL, it is the moderate level. If the cholesterol level is greater than 240mg/dL, it is the risky level [02]. Therefore, high cholesterol levels may cause heart disease and stroke.

There are several systems and models to detect the cholesterol level in the blood. Many systems are implemented using image processing techniques, photodiode array detectors and wave filters [03]. The cholesterol measuring device uses a photodiode array detector that detects the intensity of the colour. Also, it uses a wave filter to filter the light rays. Then cholesterol level is calculated using intensity of the light rays. In 2015, Kumara Ganapati Adi introduced the analysis and detection of cholesterol using waves and ANN classification. The proposed work focused on development based on level segmentation, wave filters, and artificial neural network (ANN) architecture for real-time detection of cholesterol with biomedical imaging using MATLAB [03].

The existing method for checking blood cholesterol levels uses an invasive technique of collecting blood samples. A simple tool is needed to measure blood cholesterol levels, which can be done

without collecting blood samples. In 2020, Usman Umar introduced a real-time, non-invasive cholesterol monitoring system. It uses an infrared sensor with a wavelength of 940 nm IR LED as a transmitter. A photodiode was used as a detector with a wavelength range of 400-1100 nm and a microcontroller as a minimum system to monitor the value of the output voltage in the form of digital data and then convert it to whole blood cholesterol levels [04].

Although the above systems can detect the cholesterol level, there are some issues with those systems and models. In most of systems, image processing technique was used to measure the cholesterol level using MATLAB. Also, RGB values can be calculated using image processing technique. The accuracy of the RGB values depend on the quality of the capture image that insert to the MATLAB, therefore low pixel density camera may cause some wrong calculations. The image processing technique also use of the above mentioned systems, to have a clear image with more details it must need at least a 16-bit camera instead of a 8-bit camera, it is costly use that kind of camera for the project. Some current systems use photodiode arrays to detect and wave filters to the process. Those photodiode array detector and wave filters are extremely high costly. Therefore, it is very difficult to replace those components in a breakdown. To address these issues, a bio medical instrument to measure cholesterol level of human blood using a colour sensor has been proposed and implemented.

2.0 MATERIALS AND METHODS

This system is an Arduino based system which uses one sensor module. In this system it mainly uses a colour sensor (TCS 3200) to read the RGB values of the output colours. The whole system consists of an optical system and an Arduino based system. Figure 2.1 shows the block diagrams of the optical system.

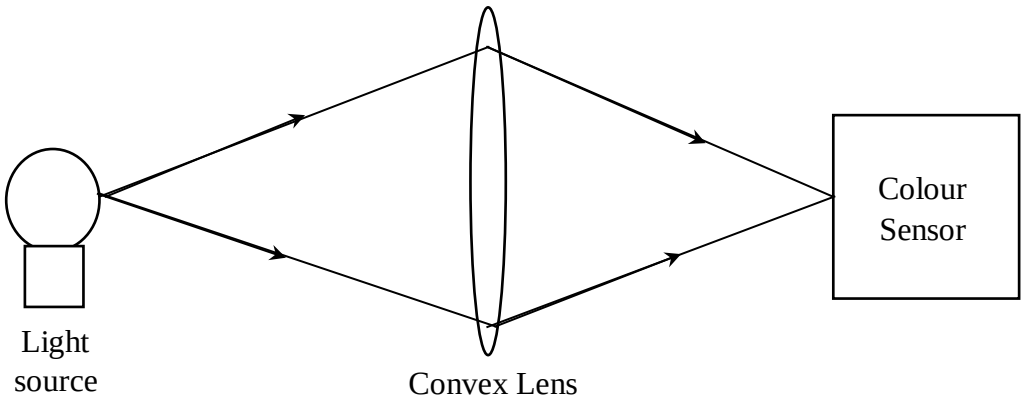

Figure 2.1: Block diagram for the optical system

`

According to Figure 2.1, the optical system consists of a light source, a convex lens and a test tube. Here it was needed to use a light source with high intensity and for that a dual-filament bulb had been used. The light rays of the light source are focused on the sensor by using a convex lens. Also, those light rays are passed through the test tube. By focusing the light beam on the colour sensor, the readings related to the absorption can be obtained. Figure 2.2 illustrates the arduino based system. It consists of a power supply, colour sensor and LCD display. The colour sensor (TCS3200) is the main part of this system. TCS3200 is a light-to-frequency converter. This module can detect colour using a microcontroller. It can recognize a wide variety of colours based on their

wavelength, such as red, blue and green. Frequency scaling optimizes the sensor reading [05]. Therefore, this sensor can easily obtain readings related to the green colour. Finally, it can be displayed on the LCD display.

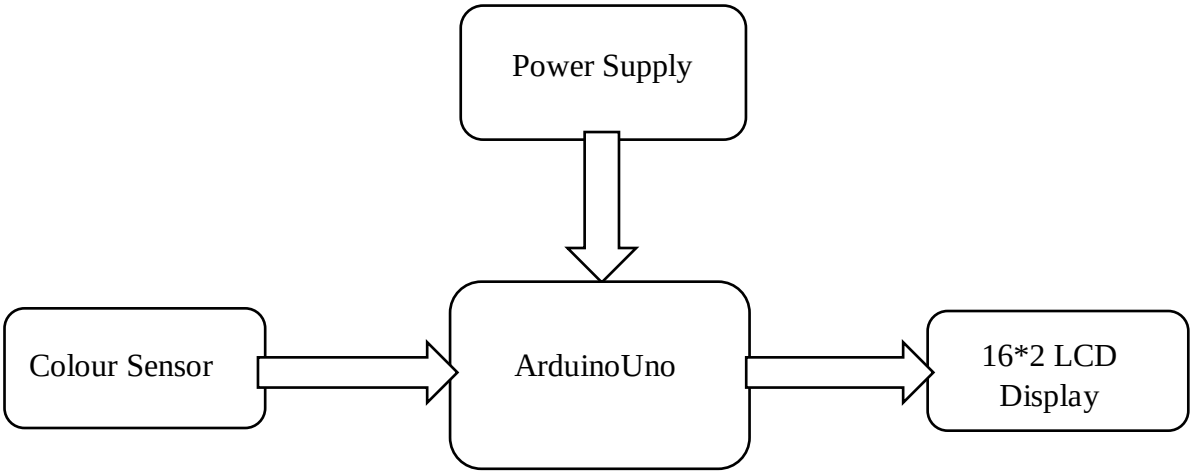

Figure 2.2: Block diagram for the Arduino based system

There are several key steps in the experimental process of the proposed technique. For this system, blood serum is needed to use. Firstly, the blood serum was filtered from the blood sample. But it has to be done in a laboratory using a laboratory centrifuge. In this manner a prepared serum sample was obtained from a laboratory and used this system. Also, the blood serum sample, reagent and standard samples should be stored at 2 ^{0}C - 8 ^{0}C temperature. After the blood serum was obtained, blood serum (10 µml) was mixed with the reagent (10 ml) prepared beforehand. The standard sample (10 µml) was also mixed with the reagent. Also, 10 ml of reagent was taken separately as a sample. Those three samples were stored for 5 min in the heater block, until the reaction was complete at the temperature of 37 ^{0}C. For that, a DS18B20 temperature sensor was used to measure the temperature [06]. Then the test tube with reagent sample was inserted into the compartment so as to take measurements of the reagent. The lens focuses light onto the test tube and the colour sensor detects the RGB value of the reagent sample in the test tube. Same procedure was done to the standard and blood serum sample. The Arduino program stores parameters to calculate cholesterol level of the blood sample according to the RGB factor using Beer-Lambert law as shown in Figure 2.3.

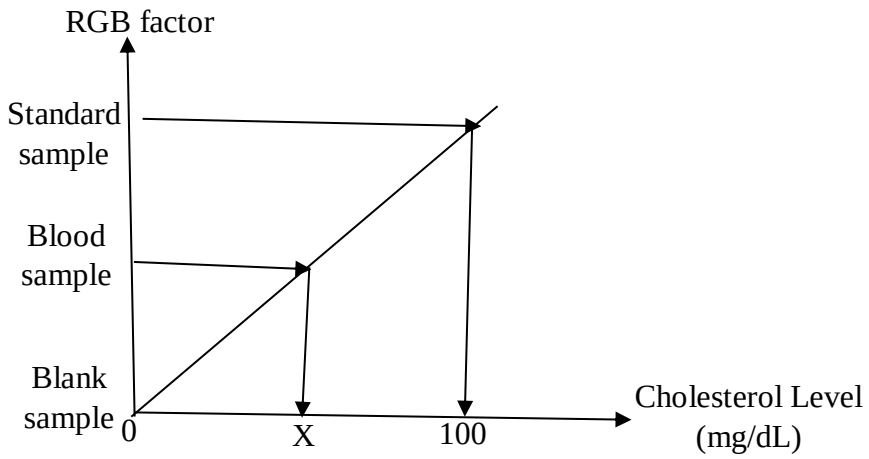

Figure 2.3: Calculation method of cholesterol level

Where; 0 = Blank sample cholesterol level

100 = Standard sample cholesterol level

X = Unknown blood sample cholesterol level

When developing the system, an important factor was identified. In this case, in addition to the light rays from the light source, other light rays from the external environment may be directed to the sensor. Due to this reason, there may be some errors in the readings. To prevent stray light from entering the system, a specially designed enclosure was used. The Figure 04 below shows the designed enclosure for this system.

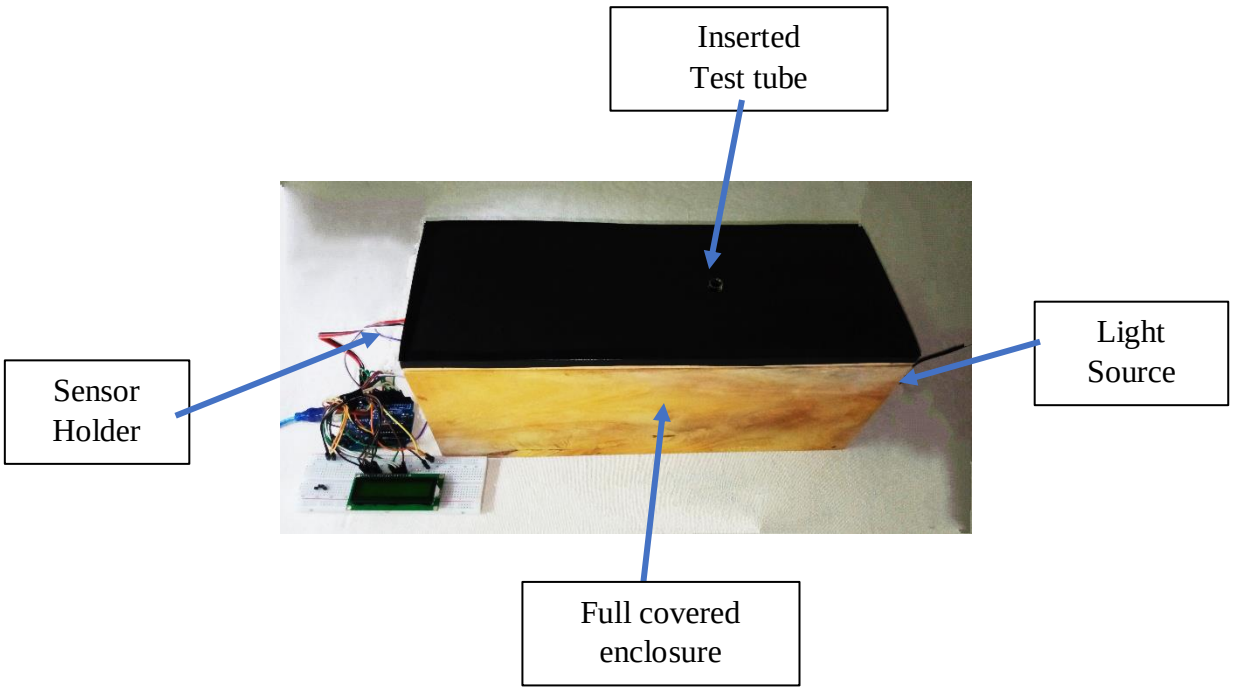

Figure 2.4: Designed enclosure for the system

3.0 RESULTS AND DISCUSSION

Figures 3.1 shows the data of blank, standard and blood samples respectively.

R= 150	G= 97	B= 163
R= 156	G= 97	B= 169
R= 150	G= 97	B= 163
R= 164	G= 97	B= 163

(a)

R= 202	G= 177	B= 208
R= 202	G= 177	B= 207
R= 202	G= 177	B= 208
R= 202	G= 177	B= 208

(b)

R= 198	G= 156	B= 195
R= 200	G= 156	B= 195
R= 189	G= 156	B= 195
R= 188	G= 156	B= 195

(c)

Figure 3.1: Data of (a) blank, (b) standard and (c) unknown samples

The values of R, G, B in Figure 3.1 represent the RGB values of red, green and blue respectively. Also, it is proportional to the intensity. The following graph is plotted using the above data.

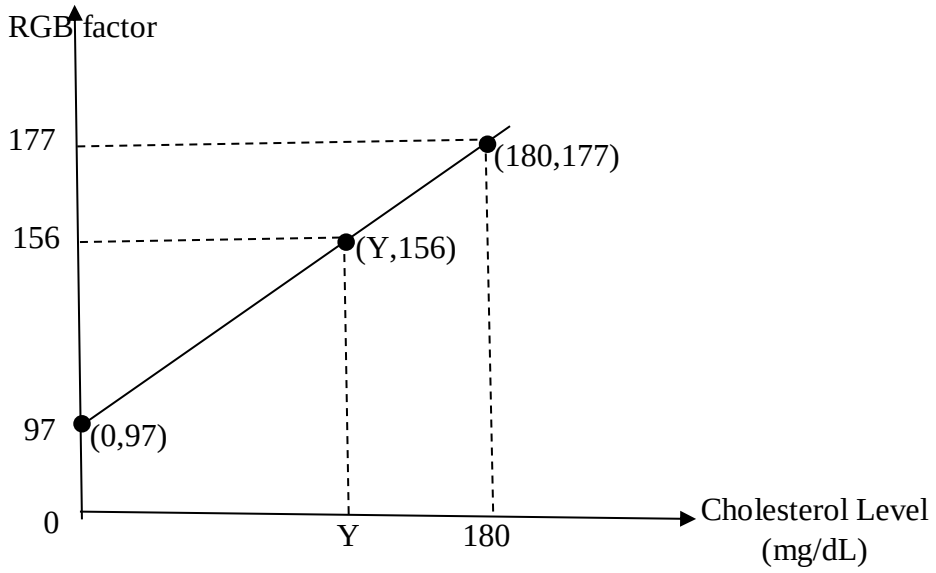

Figure 3.2: The graph for observed data

Where;

Reagent = (0, 97)
Standard Sample = (180, 177)
Blood Sample = (Y, 156)

According to those values, Y = 133 mg/dL.

But the actual value of the given sample was 135 mg/dL.

According to that, there is slight difference between observed and actual values due to following points;

A Halogen lamp is the ideal light, but it needs 6 V to switch ON the bulb. Therefore, it is difficult to use without a power supply unit. We decided to use the dual-filament bulb instead of the halogen lamp bulb. The intensity of the bulb is considered, it may also cause the result as well. Further when the samples were prepared, it should be taken 1 ml reagent sample, 10 µl standard and serum samples. To fill the sample, a pipette with microliter range was used. But to measure 1 ml, it had been used 10 times for that. Some errors also may occur due to bubble formation in the disposable pipette tip.

After preparing three samples, it had to be kept 5 min under 37 ºC. A hot water bath was used to keep the sample at 37 ºC. It was really difficult to keep samples at the temperature due to less facilities to keep the temperature as constant. This also affects the readings as well.
It was really difficult to operate this practical without lab facilities. This reason causes the major impact of the output results. Also, it was difficult to keep the samples and reagent at home. Because a refrigerator is needed to keep those safe. But temperature variations could happen due to using a normal refrigerator at home, most likely in a situation of power cut.
All above mentioned reasons may cause errors in this system.

4.0 CONCLUSION

The biomedical instrument to measure cholesterol level of human blood using a colour sensor was implemented and tested using Arduino. The obtained results were reliable. But it could be able to get more accurate results under lab facilities. As a further work, this system can be extended using a halogen lamp. By using halogen lamps, it will be able to measure cholesterol level with more accuracy than this system. The designed system is a low-cost solution for measuring cholesterol level.

ACKNOWLEDGEMENT

I would like to express my gratitude to the staff at the Division of Biomedical Engineering Services, Ministry of Health who helped me in so many ways to carry out this project.

REFERENCES

[1]. Cholesterol Levels: MedlinePlus Medical Test, *Medlineplus.gov*, 2021, https://medlineplus.gov/ lab-tests/cholesterol-levels/ , (Accessed 2021-03-03).
[2]. Understanding Cholesterol Numbers, *WebMD*, 2021, https://www.webmd.com/choleste rol-management/guide/understanding-numbers , (Accessed 2021-03-03).
[3]. Kumara Ganapathi Adi, Dr.P.V.Rao, Dr.Veena K Adi, Analysis and detection of Cholesterol by Wavelets based and ANN Classification, Procedia Materials Science, *2nd International Conference on Nanomaterials and Technologies*, 2014.
[4]. Usman Umar, Syafruddin Syarif, A real time non-invasive cholesterol monitoring system, *MATEC Web of Conferences*, *2020*, 331.
[5]. TCS3200 Colour Sensor Module, *Elecrow*, https://www.elecrow.com/wiki/index.php?title=TCS 3200_Colour_Sensor_Module, (Accessed 2021-03-15).Bhalla S., Bhateja V., Chandavale A., Hiwale A. and S. Chandra, *Intelligent Computing and Information and Communication: Proceedings of 2nd International Conference, ICICC*. Springer, (2018), 572, E-book

Proc. Annual Symposium on Research & Industrial Training, 08(2021) 188-194
Department of Electronics – Wayamba University of Sri Lanka

THE EFFECT OF LEDs FOR GROWTH OF PLANTS

Y.B.E.S.K.K. Bandara[1*], L.D.R.D. Perera[1], J.P.D.S. Athuraliya[2]

[1]*Department of Electronics, Wayamba University of Sri Lanka, Kuliyapitiya, Sri Lanka*
[2]*Arthur C Clarke Institute for Modern Technologies, Katubedda, Moratuwa*

[*]eshani9544@gmail.com

ABSTRACT

Though regular LEDs have long lifetime, low maintenance costs and less environmental hazards, regular LEDs have not been considered for horticultural LED lights. Therefore, this research was conducted to identify the effectiveness of using 5mm regular LEDs for horticultural lighting. For this study, 18W SMD 5730 high power LED Grow Lights and 12V regular red and blue LEDs were used. The study was conducted in a dark poly tunnel using two identical Chilli plants. Both LED lights were placed at 12-inch hanging height above the plants for 15 days and then placed at 6-inch height for another 15 days. After the 30 days both lights were again placed at 12-inch hanging height for another 11 days. At 12-inch hanging height period the measured average light intensities were in the ranges of 730-850 lux and 530-650 lux for LED Grow Light and Regular LED light, respectively. The spectral range was measured with a handheld spectrometer. Both light sources had close values for peak wave lengths for red and blue colours. Arduino Uno based circuit was used to maintain a constant photoperiod of 7 hours throughout this study. Both plants showed better growth and health status when the lights were placed at 12-inch hanging height. The average plant growth rate under regular LED (0.256 $cmday^{-1}$) was higher than the growth rate under high power LED grow light (0.097 $cmday^{-1}$). The limited study showed the potential to use regular LEDs instead of expensive LED Grow Lights for horticultural lighting. Further work with a larger sample of plants is recommended to confirm the effectiveness of regular LEDs as a substitute for LED Grow Lights.

Key words: LED Grow light, Horticultural lighting, Arduino Uno

1.0 INTRODUCTION

When growing plants indoors or in protected agriculture, replicating the effect of sunlight is the biggest problem. As indoor cultivation has become more popular, those facilities have discovered that LED lighting is the best option for optimum plant growth because of its potential to improve irradiance efficiency and to replace the traditionally used lamps which are power hungry and emit too much heat. The rate of growth and length of time a plant remains active is dependent on the amount of light the plant receives. When determining the effect of light on plant growth, there are three main factors to consider: light quantity (light intensity), light quality (spectral range) and photoperiod [1].

The amount of bright light or amount of energy in the forms of photons falling on the leaves determine the rate of photosynthesis. For photosynthesis, plants use light in Photosynthetic Active Region (PAR) of 400nm-700nm wavelengths [2]. Photoperiod is the duration that plant receives light.

An LED grow light is an electric light that helps plants grow. They work well when it comes to growing plants indoors. LED grow lights use less power and radiate less heat compared with traditional lamps such as High Intensity Discharge and High Pressure Sodium lamps [3].
Paucek et al. have discussed an updated status of current global horticulture LED industry and the present features and potentialities for LEDs' applications [4]. In this study a review of this industry

was integrated through a database compilation of 301 manufactures and 1473 LED lighting systems for plant growth. This study identified Europe (40%) and North America (29%) as the main regions of production. This study shows that the current LED luminaires' lifespans have 10 and 30% losses of light output after 45000 and 60000 working hours on average [4].
Gómez et al. have shown that the crop production efficiency could ultimately increase by preventing crop losses with the monochromatic nature of LEDs which help to prevent physiological disorders that are common in indoor environment and help to reduce pest and disease pressure in agriculture [5]. Furthermore, this study showed that by increasing canopy photon capture efficiency and/or precisely controlling light output in response to the environment or to certain physiological parameters, energy efficiency and plant productivity can be optimized with LEDs [5].

LED Grow lights are usually used for commercial horticulture and for indoor gardening. Commonly identified problems in high power LED Grow Lights are high cost, emission of unnecessary heat on to the plant canopy and relatively higher power consumption compared with regular LEDs. Regular LEDs are less popular as horticultural LEDs due to lower light intensities and less coverage area. Since regular LEDs are low cost, have less hazards, have long lifetime and are available with saturated colors, this study was carried out to identify the effectiveness of using regular LEDs for horticultural lighting. The experiment was carried out by comparing the absolute growth rates of two identical Chilli plants under 5mm regular LED (red and blue) lights and under 18W (SMD 5730) red and blue high power LED Grow Light which are available in the market.

2.0 EXPERIMENTAL

The light quality (wavelength), light quantity (light intensity), and photoperiod are the three main factors to consider when determining the effect of light on plant growth. Different types of LEDs have different wavelengths for same color. Therefore, the peak wavelength of each LED (SMD 5730 red and blue LEDs, regular red and blue LEDs) was determined by using PSR-1100F spectrometer.

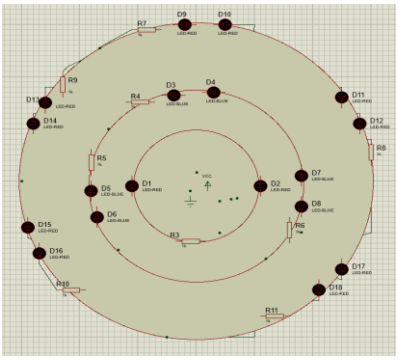

Figure 2.1: 12V LED Circuit- Schematic Layout

In order to design the regular LED light circuit (figure 2.1), several factors such as forward voltage of each LED, resistance of series limiting resistors, number of series LEDs in a path of circuit, number of series and parallel LED combinations in the circuit, the maximum voltage of the circuit, and maximum current of the circuit were considered.
The light temperature can affect the growth of plants. Therefore, the temperature of each LED source was measured with FLIR Thermal Imaging Camera. However, temperatures at various heights cannot be measured with FLIR Thermal Imaging Camera since it is a passive device. Therefore, LM35 temperature sensor was used to measure temperature of both lights (SMD

5730LED Grow Light and 12V LED light system) at12-inch height and at 6-inch height. This test was done in two separate chambers of the dark poly tunnel.

Light quantity (light intensity) and photoperiod are the other two main factors to consider when determining the effect of light on plant growth. In order to have a constant photoperiod, a light triggering circuit (figure 2.2) was designed with Arduino Uno microcontroller. This circuit was used to trigger the two light sources for specific time with 2 channel relay module, and DS3231 Real Time Clock (RTC) module. For this experiment 7 hour photoperiod was used. Both lights were turned ON at 9.15 am and turned OFF at 4.15 pm.

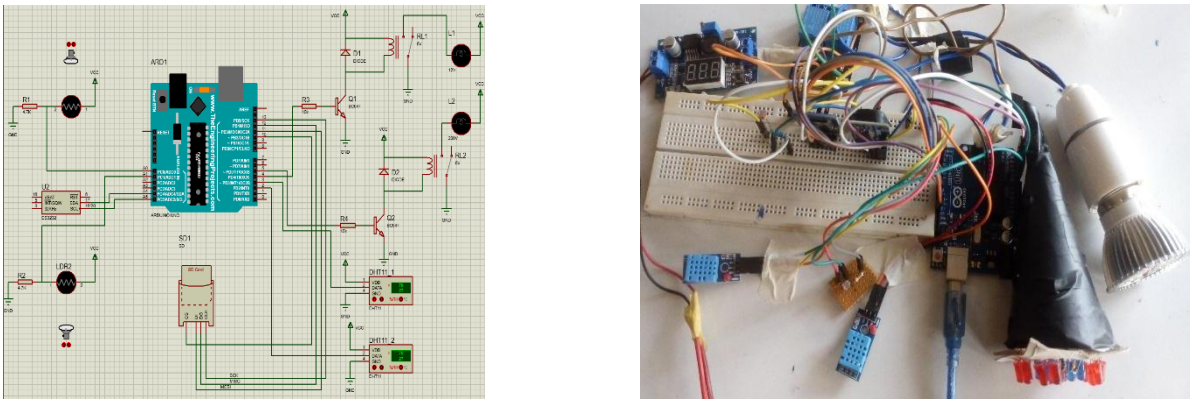

(A) (B)

Figure 2.2: (A) Schematic Layout of the Light Triggering Circuit (B) Circuit Developed for the Proposed System

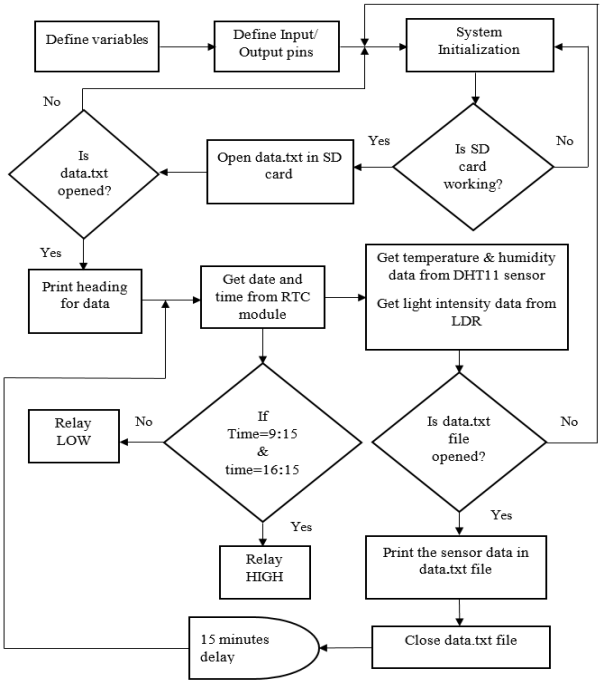

Figure 2.3: Flow Chart of the Arduino Programme

The humidity in each chamber can have a significant effect on the plants' health status. Therefore, humidity of each chamber was measured with DHT11 temperature and humidity sensor.

Figure 2.3 shows the flow of the Arduino programme. The inputs were taken from DHT11 sensors, and LDR sensors to the Arduino microcontroller. The time was taken with DS3231 Real Time Clock module. If the time was between 9.15 am and 16.15 pm both LED sources were in ON state, otherwise in OFF state. This specific triggering was used to maintain a constant photoperiod.

The temperature and humidity, and light intensity (at 6 or 12-inch height) of each chamber were stored in SD card module. This data recording was repeated every 15 minutes.
For this study two Chilli plants were selected from a sample and placed them separately in two chambers of the poly tunnel. One was placed under LED Grow Light and other was placed under 12V regular LED light chamber.

$$Light\ Intensity\ (I) = \frac{p}{4\pi R^2} \quad [2.1]$$

Where *P* is the power of the light wave, and *R* is the distance. For this study two Light Dependent Resistors (LDRs) were placed near the canopy of each plant and the light intensity was measured for every 15 minutes. Initially, both lights were placed at 12-inch height from each plant canopy for 15 days. Then both lights were placed at 6-inch height from each plant canopy for another 15 days. Since the plant in LED Grow Light chamber seemed to be burnt after the second 15-day period, possibly due to heat, both lights were re-placed at 12" hanging height for another 11 days.

Both plants were treated equally i.e. same amount of water and nutrients were added. (200ml water per day and nutrients per two weeks were added). The status of each plant was checked daily by counting number of leaves, measuring height, and by observing the symptoms of plants. After that Absolute Growth Rates (AGR) of both plants were obtained. AGR gives Absolute values of biomass between two intervals. It is mainly used for a single plant organ e.g. leaf growth, plant weight, etc. In this experiment, plant height was determined to obtain the AGR by using equation [2.2].

$$AGR = \frac{h_2 - h_1}{t_2 - t_1}\ cm\ day^{-1} \quad [2.2]$$

Where h_1 and h_2 represent the plant's initial height and final height at the beginning of the period (t_1) and end of the period (t_2), respectively.

3.0 RESULTS AND DISCUSSION

Since different types of LEDs have different wavelengths for the same color, peak wavelength of each LED (for 6 and 12 inch height) was determined using PSR-1100F spectrometer. According to figures 3.1 (A) and (B) both 5 mm blue LEDs and SMD 5730 blue LEDs had the same peak wave length of 456nm. SMD 5730 red LED had 633nm peak wave length and 5mm red LED had 661nm peak wave length.

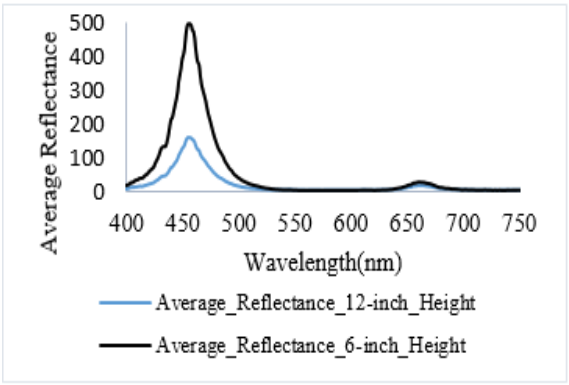

(A)

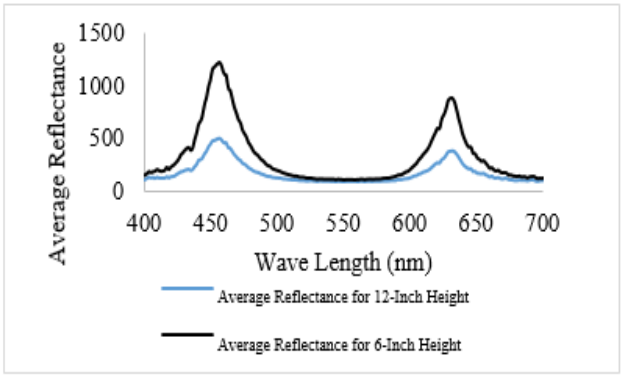

(B)

Figure 3.1: (A) Wavelength vs Average Reflectance for 5mm Red and Blue Combination for 6, and 12 Inch Height (B) Wavelength vs Reflectance for SMD 5730 Red and Blue LEDs for 6, and 12 Inch Height

Figures 3.2 shows the plant height variation with time and the average light intensity variation for both lights. The plants were kept under separate light sources for 41 days. In first 15 days, both light sources were placed at 12-inch height from the plant canopy. During that period the measured average light intensity of SMD 5730 LED Grow Light was in the 750-850lux range and the average light intensity of regular LED light was in the 530-650 lux range. During the next 15 days, both light sources were placed at 6-inch height from each plant canopy. In that period, the measured average light intensity of LED Grow Light was in the range 930-1020 lux while it was in the 750-870 lux range for regular LED light. At the end of this period the plant canopy under LED Grow Light was observed to be burnt, possibly due to higher light intensity.

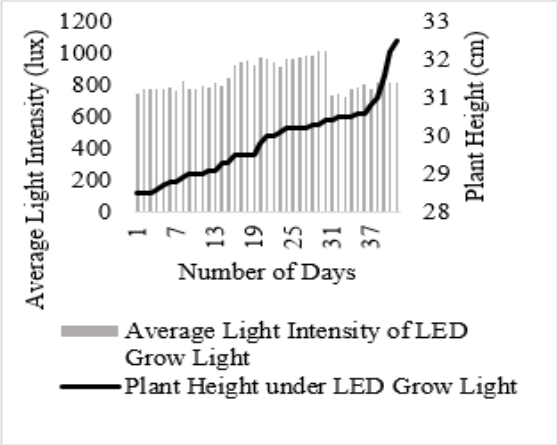

(A)

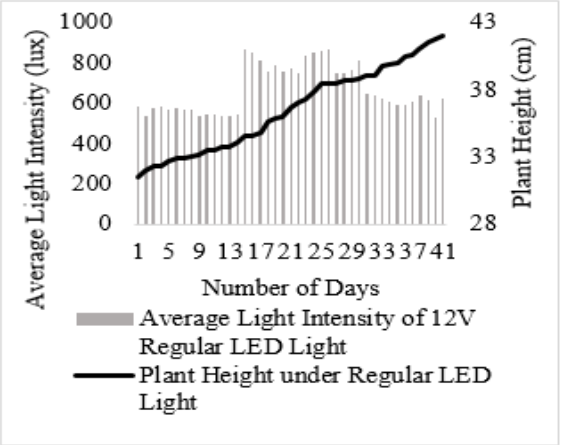

(B)

Figure 3.2: (A) Variation of Plant Height and Average Light Intensity of LED Grow Light Over 41 Days (B) Variation of Plant Height and Average Light Intensity of Regular LED Light over 41 Days

The AGR of a plant can be calculated using initial height, final height, and time interval details given in figures 3.2. The average AGR for the Chilli plant in regular LED light chamber was 0.256 $cmday^{-1}$ and that for the plant in LED Grow Light chamber was 0.097 $cmday^{-1}$.

Figures 3.3 represents the variation of average temperature at each hour for sources at 12-inch and 6-inch height, respectively. The average room temperature variation is also shown in the graphs to get a better idea about temperature difference. The average temperature of regular LED light was close to room temperature for both lamp heights whereas the average temperature of LED Grow light was higher than the average room temperature in both cases.

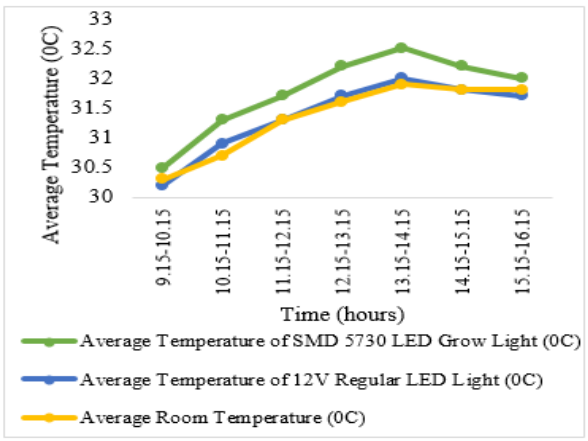

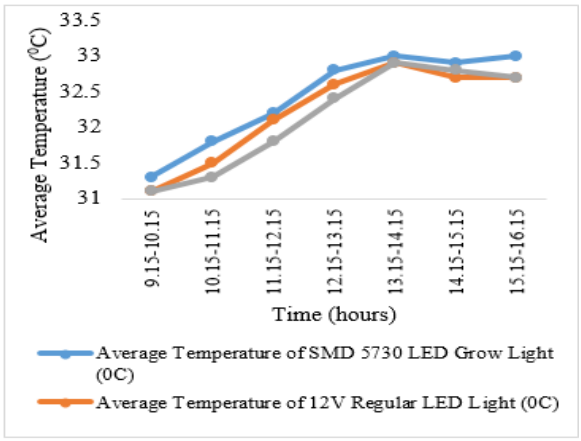

(A) (B)

Figure 3.3: (A) Average Temperature of Chilli Plants' Canopy (at 12 Inch Height) with Time (B) Average Temperature of Chilli Plants' Canopy (at 6 Inch Height) with Time

Figure 3.4 (A) represents the count of leaves of two plants during the 41-day period. During the second 15-day period the leaves of both plants were fallen. Moreover, the leaves and canopy of the plant under LED Grow Light seemed to be burnt at the end of this period.

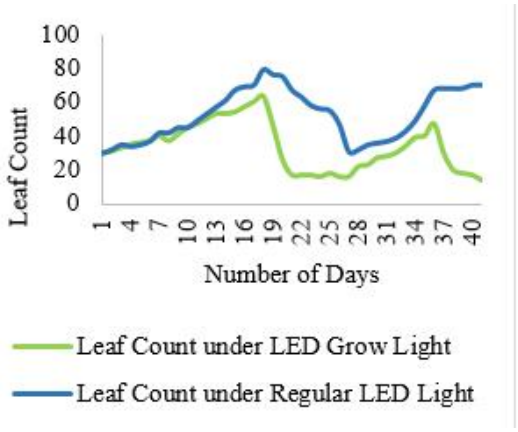

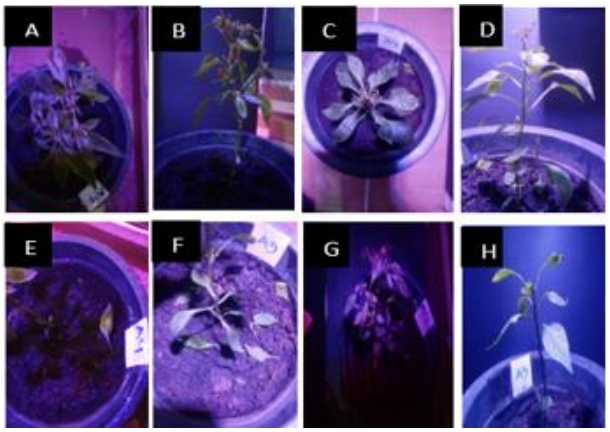

(A) (B)

Figure 3.4: (A) Leaf Count Variation with Time (B) Status of Chilli Plants during the Period

Figure 3.4 (B) shows each Chilli plants' status during this study period. Figures 3.4(A) and (B) indicates the top and front view of the Chilli plant under regular LED light at the beginning of the period. Figure 3.4(C) and (D) represent the top and front view of Chilli plant under LED Grow Light at the beginning of the study period. Photographs E and F were taken after 19 days period. Photographs E and F show the fallen leaves of the Chilli plant in regular LED light chamber and in the LED Grow Light chamber, respectively. Figures 3.4 (G) and (H) show the status of plants finally observed after 41 days in regular LED and in LED Grow Light chambers, respectively.

Before placing the plants under LED environments, both plants were in the same growth stage and in a better health status. But after placing them under LED light environments for 41 days they did not have the same healthy status. Though the plants had to be in flowering stage at the end of the study period, both plants under LED light environments resulted in delayed flowering.

4.0 CONCLUSIONS

This research was conducted to investigate whether 5mm regular LEDs can be used as a substitute for expensive horticultural LED Grow Lights, which are widely used in LED lighting. The measured average light intensity of LED Grow Light at 12-inch height was in the range of 730-850 lux and that of regular LED light at 12-inch height was in the 530-650 lux range. In that lower light intensity ranges at 12-inch hanging height, better growth and health status were observed in both plants. For both light sources, peak wave length of blue LEDs was 456nm. For red LEDs in regular LED light, peak wave length was 661nm while for red LEDs in LED Grow Light the peak wave length was 633nm. According to the results of the limited study, the average plant growth rate under regular LED was higher than the growth rate under high power LED grow light. Placing the plants under LED environments was observed to affect plant health. The study revealed the potential to use regular LED lights for horticultural lighting. This research needs to be carried out further with a larger sample of plants to confirm the effectiveness of using regular LEDs as a substitute for expensive horticultural LEDs.

ACKNOWLEDGEMENTS

Authors would like to express their sincere gratitude to all the staff at the ACCIMT for provision of research facilities, stimulating suggestions and encouragement throughout this research project. Appreciation is also extended to the staff at the Department of Electronics, WUSL, for their coordination, careful monitoring and feedback throughout the industrial training.

REFERENCES

[1]. Light, Temperature and Humidity - Ornamental Production. https://aggiehorticulture.tamu.edu/ornamental/a-reference-guide-to-plant-care-handling-and-merchandising/light-temperature-and-humidity (Accessed 2021-06-22)
[2]. CANNA Research, LEDs for plant production. https://www.cannagardening.com/leds_plant_production (Accessed 2021-06-24)
[3]. Max, Top 10 Full Spectrum LED Grow Lights- Buyer's Guide and Reviews. https://www.trees.com/gardening-and-landscaping/best-led-grow-lights (Accessed 2021-06-24)
[4]. Paucek, I., Appolloni, E., Pennisi, G., Quaini, S., Gianquinto, G., Orsini, F., LED Lighting Systems for Horticulture: Business Growth and Global Distribution. *Sustainability*, *12*, (2020), 7516, doi: 10.3390/su12187516
[5]. Gómez, C., Gennaro Izzo, L., Increasing efficiency of crop production with LEDs. *AIMS Agriculture and Food* 3/2, (2018), 135-153, doi: 10.3934/agrfood.2018.2.135

Proc. Annual Symposium on Research & Industrial Training, 08(2021) 195-201
Department of Electronics – Wayamba University of Sri Lanka

DESIGNING OF AUTOMATED UV DISINFECTION CHAMBER FOR COVID 19 RELATED MEDICAL EQUIPMENT USING IMAGE PROSESSING TECHNIQUE

G.K.H. Madushan[1*], Y.A.A. Kumarayapa[1], T.V.A. Ruwansiri[2]

[1]*Department of Electronics,* Wayamba *University of Sri Lanka, Kuliyapitiya*
[2]*Division of Biomedical Engineering Services, Ministry of Health, No 27, Colombo 10*

[*]harshamadushan4422@gmail.com

ABSTRACT

With the increasing use of complex medical equipment in the healthcare settings, the challenge of ensuring adequate cleaning and disinfection of instruments is increasing [1]. Evaluation of the applicability and relative contribution of Ultraviolet Germicidal irradiation (UVGI) to disinfecting of air in health care facilities as well for environmental surfaces are important for today's public and private health services. The balance of scientific evidence indicates that UVGI should be only considered as a health equipment disinfection application with compare to other stranded methods such as appropriate heating, ventilating, and other optoelectronic source based systems [2]. This disinfection chamber room for the division of Biomedical Engineering Services in ministry of health and it may help to avoid the spread of COVID- 19 virus. Proposed chamber consist of UVGI lights to kill the virus on surfaces of the medical equipment and goods. Authorize persons of the Biomedical unit in Ministry of Health can access the chamber room and place the disinfection needed medical equipment inside the chamber room. After specified period of exposer, they can get their medical equipment without virus. Image processing technique use for identify the person before entering the chamber. Hence, the healthcare staff (technician officers, biomedical engineers, minor employees etc.) can be protected from the UV as well from the virus including present corona epidemic.

Keywords: UVGI, Disinfection chamber, Optoelectronic devices

1.0 INTRODUCTION

The COVID 19 pandemic has drastically affected the overburdened public health systems in many countries. This has the challenged their safety. This pandemic has highlighted a strong need for sustainable investment in healthcare systems and how crucial it is to develop resilient healthcare systems. Additionally, enforcing the critical role both in crisis response and in building a future that is prepared for health emergencies [3].

Proposed disinfection chamber is a navel low cost design. For the division of biomedical engineering Services in Ministry of Health this will be useful to avoid the spread of the virus among the related health care workers and society. Also this method more beneficial and accurate than the other disinfection methods, because some methods are more harmful for the PCB boards and sensors in the medical equipment.

1.1 Important of using UVGI lights

The ultraviolet germicidal radiation (UVGI) is used for disinfecting the virus in schools, restaurants and other public places. Using this method, ultraviolet (UV) lights would be able to disinfect contaminated public spaces to stop the transmission of the virus. UV light from the sun has shorter wavelengths than visible light and, therefore, is not visible to the naked eye. The full

spectrum of UV radiation is sourced from the sun and can be subdivided into UV-A, UV-B and UV-C rays. In this spectrum, UV-C rays are the most harmful and are completely absorbed by the Earth's atmosphere. Further, while both UV-A and UV-B rays are harmful, exposure to UV-B rays can cause DNA and cellular damage in living organisms. Therefore, it is important to design and construct the proposed optoelectronic device for disinfecting the virus [4].

1.2 How germicidal UV does kills virus?

Germicidal UV products can actually change the DNA and RNA of bacteria and viruses, destroying their ability to reproduce. Most UV-C products can inactivate up to 99.9% of pathogens including viruses, bacteria, mold spores, and fungus. Viruses are not technically living organisms, germicidal UV technically "inactivates" viruses [5].

Since COVID-19 can live on certain surfaces for up to three days and can travel through the air, germicidal UV is a great tool to disinfect air and surfaces.

2.0 METHODOLOGY

The proposed chamber mainly focused on automated disinfection system for ensuring the safety of health workers and avoid the spread of virus among the workers. Image processing technique will be used for capturing the persons' accidental entry and control the UVGI lights. And use micro switch for the safety of the person who entering in to the chamber room. Table inside the room and Ultra Sound sensor use to identify the medical equipment on the table before exposer.

2.1 The proposed Chamber Room block diagram

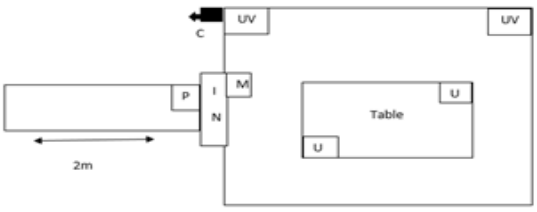

Figure 2.1: Block Diagram of the proposed Disinfection Chamber

UV - Ultraviolet Lights, P – PIR Sensor, U – Ultra Sound Sensor
C – Camera, M – Micro Switch

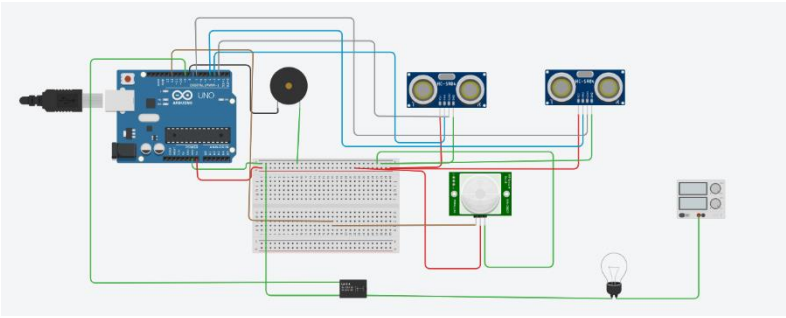

Figure 2.2: Circuit diagram of the proposed Disinfection Chamber automation

2.2 The working principle of the proposed chamber room

Before disinfecting equipment are put in the chamber all, UVGI lights in the chamber make OFF mode and authorize person can enter the room safely. After that person put in the equipment on the table, he leaves the room and close the room door, the only the UVGI light became ON mode. UVGI lights are control by Ultra Sound Sensors, Micro Switch and PIR sensor. Main purpose of the using Ultra Sound Sensor is to identify whether the equipment on the table placed or not. Authorize person come out the room and close the door then UVGI lights became ON mood as the result of micro switch and PIR sensor. PIR sensors are used for identify the person is there or not. After disinfection process, when authorize persons reach the direction of the room door to the get the equipment, the camera and PIR Sensor detect the person and give the signal to OFF the UVGI light. Therefore, person can enter the room and he should keep the door open. Because UVGI lights were not became ON mode until the door is open as the results of the micro switch.

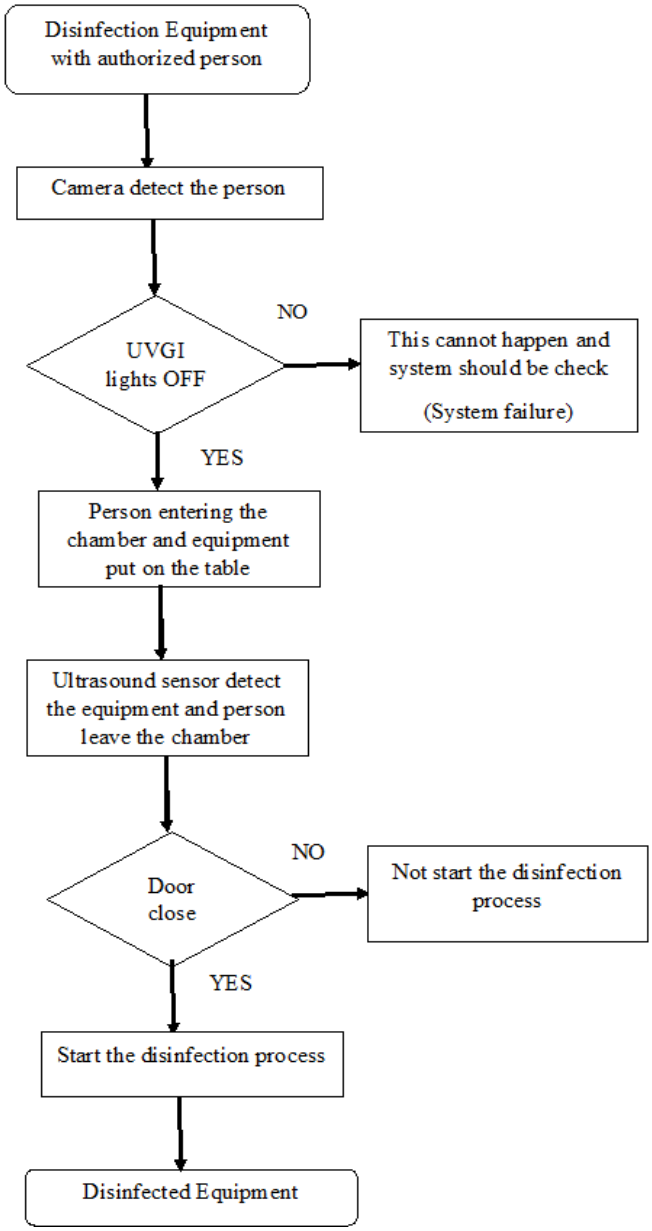

Figure 2.3: Data flow diagram for placing equipment in the chamber

3.0 RESULTS AND DISCUSSION

The UV lamps is a kind of low- pressure lamp. The lamp tube is made of pure quartz glass. This is excited by two- pressure steam (< 10~2 pa) and emits ultraviolet rays of 253.7nm and 185nm wavelength. Quartz glass has a very high transmission rate of ultraviolet rays. Reaching more than 90% UVC with enough strength energy can be used for disinfection and sterilization various fields.

Table 3.1: 100% disinfection time for various fields of bacteria, viruses, mold spores and algae

Category	Name	100 % kill Required time(s)	Name	100 % kill Required time(s)
Bacteria	Escherichia coli	0.51s	Mycobacterium tuberculosis	0.30s
	Bacillus diphtheriens	0.41s	Cholera bacillus	0.15s
	Tetanus bacilli	0.53s	Pseudomonas	0.80s
	Bacillus anthracic	0.28s	Salmonella	0.20s
	Shigatia dysenterians	1.23s	Enterobater bacteria	0.20s
	Botulinum	0.45s	Salmonella typhimurium	0.40s
	Leptospira	0.36s	Shigella	0.41s
	Legionella pneumophila	0.25s	Staphylococcus	0.64s
			Streptococcus	0.37s
	Micrococcus	0.33s		
Viruses	Adenovirus	0.10s	Influenza virus	0.23s
	Phagocytic cell virus	0.20s	Poliovirus	0.80s
	Coxsackie virus	0.80s	Rotavirus	0.52s
	ECHO virus	0.75s	Tobacco mosaic virus	0.16s
			Hepatitis virus	0.73s
Mold spores	Aspergillus niger	6.67s	Soft spore	0.33s
	Aspergillus	8.80s	Penicillium	0.80s
	Dung fungi	8.00s	Torsn producing penicillium	3.33s
	Raspberry	4.67s	Other penicillium species	0.87s
			Corona Virus	Yet to be decided
Algae	Blue – green algae	40.0s	Grass worm	7.30s
	Chlorella	0.93s	Pralonium	6.70s
	Nematode eggs	3.40s	Green algae	1.22s

The following data analysis graphs interpret the exposure duration with respect to each germ.

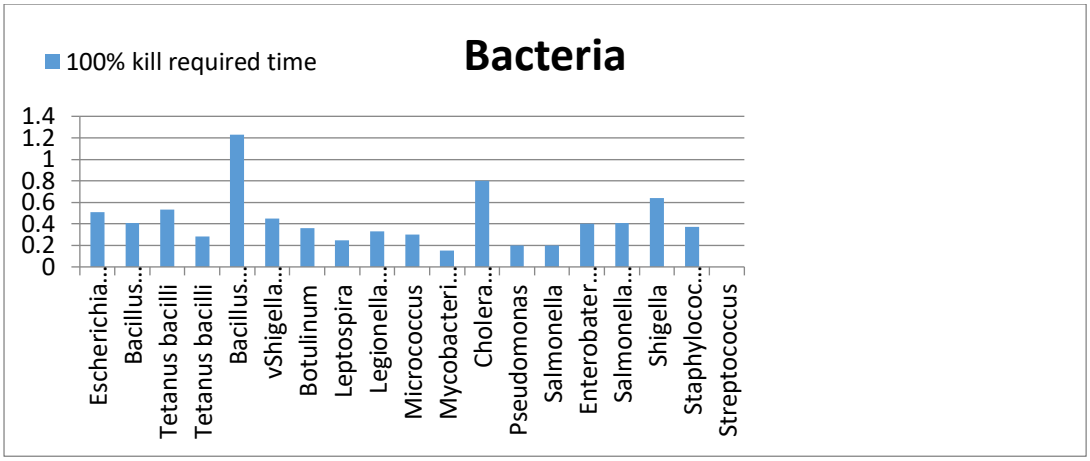

Figure 3.1: Bacteria vs 100% kill required time (s)

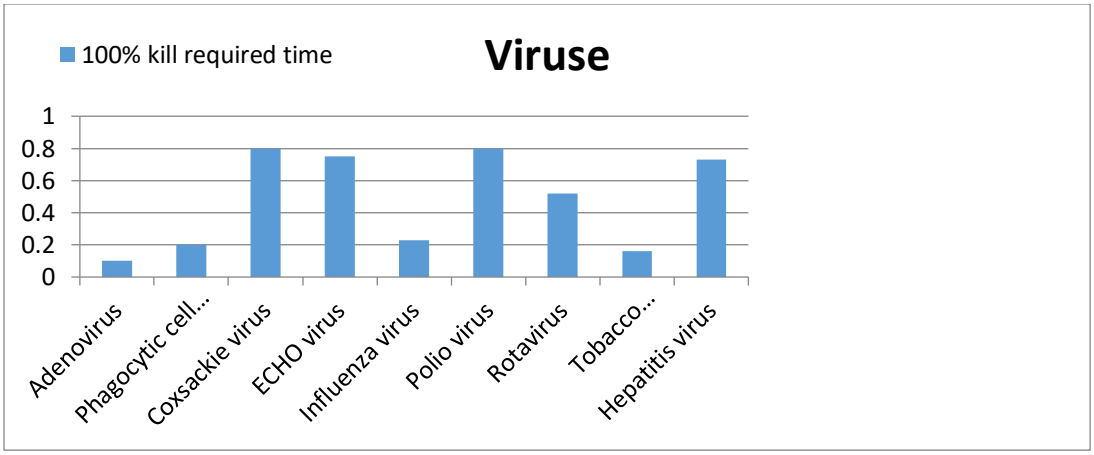

Figure 3.2: Viruses vs 100% kill required time (s)

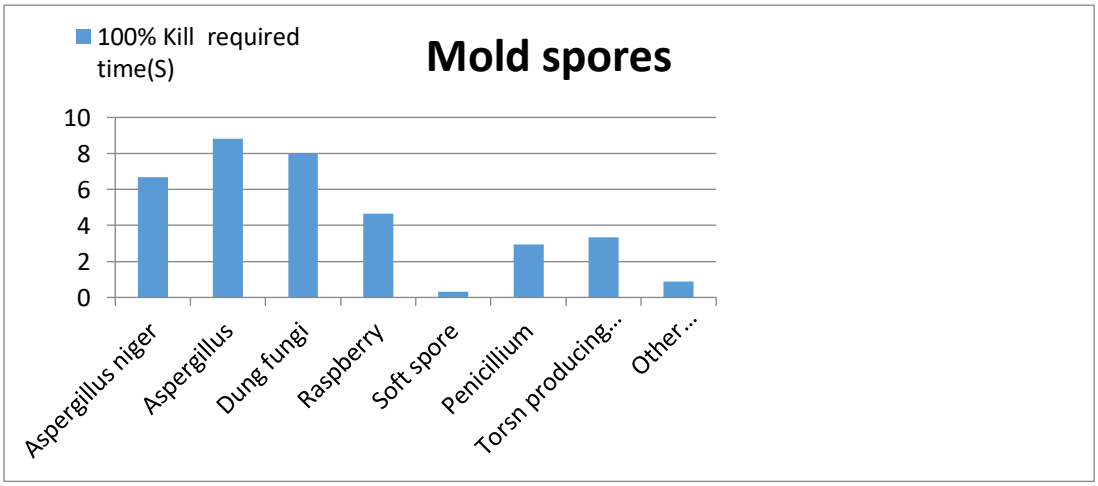

Figure 3.3: Mold spores vs 100% kill required time (s)

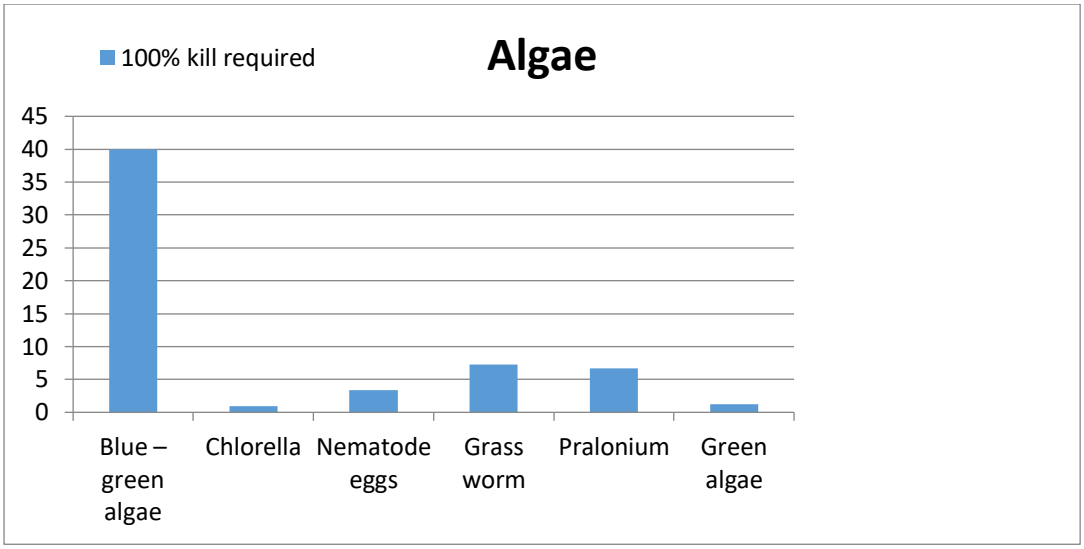

Figure 3.4: Algae vs 100% kill required time (s)

According to above data and the graphs tabulation, it can be observed that all the viruses can be destroyed, if use maximum expose time 0.8s. Bacteria can be destroyed maximum expose time 1.23s and also Mold spores and Algae can be destroyed maximum expose time 8.80s and 40.0s.

4.0 CONCLUSION

Designing of such disinfection chamber during six-month training period is helpful for the division of biomedical engineering services (BMES) because of the current COVID -19 pandemic situation. This proposed chamber mainly helpful for the health workers and Foreman to prevent from the viruses, other germs hence ensuring their safety at the services. Using this system, main purposes is to kill COVID – 19 viruses according to the above analysis and table 3.1. All the viruses can be destroyed by exposure to UVGI lights.

BMES received large number of broken medical equipment from government hospitals and private biomedical engineering companies. Without disinfecting, such used equipment is highly risky for technician and related staff. Therefore, in feature the utilization of such disinfection chamber will be beneficial for saving life of the patient and health sector employees. On the other hand, proposed technique is more beneficial than other available disinfection methods because it protect the sensitive PCB boards, sensors an inner parts of such expensive medical equipment.

Also this method is time efficient process and trustworthy. According to our analysis, although the exposure time 0.08 s is convenient for killing all the known viruses and Jerome, but in the case of Corona, it is yet to be experimentally proved.

ACKNOWLEDGEMENT

Authors wish to extend their gratitude to the academic and nonacademic staff at the Department of Electronics, Faculty of Applied Sciences, Wayamba University of Sri Lanka. Sincere gratitude is also extended to the staff members at the Division of Biomedical Engineering Services.

REFERENCES

[1]. Klaiber, P., Wen, J.H., DeLongis, A., The ups and downs of daily life during COVID-19, age differences in affect, stress, and positive events, *The Journals of Gerontology, Series B*, 76(2), (2021), 30-37.

[2]. Memarzadeh, F., Olmsted, R.N., Bartley, J.M., Applications of ultraviolet germicidal irradiation disinfection in health care facilities, effective adjunct, but not stand-alone technology, *American journal of infection control*, 38(5), (2010), 13-24.

[3]. Miller, S.L., Linnes, J., & Luongo, J., Ultraviolet germicidal irradiation: future directions for air disinfection and building applications. *Photochemistry and photobiology*, 89(4), (2013), 777-781.

[4]. Ilyas, S., Srivastava, R.R., Kim, H., Disinfection technology and strategies for COVID-19 hospital and bio-medical waste management. *Science of the Total Environment*, 749, (2020), 141652.

[5]. Cortés, A. M., Galvis, J.H., Comparison of the biological activity of high-level disinfection and sterilization in medical devices and biomedical equipment. *J Health Hyg*, 1(1), (2017), 5.

ISSN 2362-0560